ol. 113 No. 2, January 15, 1980
mpleting Vol. 113

ISSN 0003-2670

ANALYTICA CHIMICA ACTA

International journal devoted to all branches of analytical chemistry

ELSEVIER SCIENTIFIC PUBLISHING COMPANY

ANALYTICA CHIMICA ACTA

International journal devoted to all branches of analytical chemistry
Revue internationale consacrée à tous les domaines de la chimie analytique
Internationale Zeitschrift für alle Gebiete der analytischen Chemie

PUBLICATION SCHEDULE FOR 1980 (incorporating the section on Computer Techniques and Optimization).

	J	F	M	A	M	J	J	A	S	O	N	D
Analytica Chimica Acta	113/1 113/2	114	115	116/1	116/2	117	118/1	118/2	119	120/1	120/2	121
Section on Computer Techniques and Optimization			122/1			122/2			122/3			122/4

Scope. *Analytica Chimica Acta* publishes original papers, short communications, and reviews dealing with every aspect of modern chemical analysis, both fundamental and applied. The section on *Computer Techniques and Optimization* is devoted to new developments in chemical analysis by the application of computer techniques and by interdisciplinary approaches, including statistics, systems theory and operation research. The section deals with the following topics: Computerized acquisition, processing and evaluation of data. Computerized methods for the interpretation of analytical data including chemometrics, cluster analysis, and pattern recognition. Storage and retrieval systems. Optimization procedures and their application. Automated analysis for industrial processes and quality control. Organizational problems.

Submission of Papers. Manuscripts (three copies) should be submitted as designated below for rapid and efficient handling:

Papers from the Americas to: Professor Harry L. Pardue, Department of Chemistry, Purdue University, West Lafayette, IN 47090, U.S.A.

Papers from all other countries to: Dr. A. M. G. Macdonald, Department of Chemistry, The University, P.O. Box 363, Birmingham B15 2TT, England.

For the section on *Computer Techniques and Optimization:* Dr. J. T. Clerc, Universität Bern, Pharmazeutisches Institut, Sahlistrasse 10, CH-3012 Bern, Switzerland.

American authors are recommended to send manuscripts and proofs by INTERNATIONAL AIRMAIL.

Information for Authors. Papers in English, French and German are published. There are no page charges. Manuscripts should conform in layout and style to the papers published in this Volume. Authors should consult Vol. 111, p. 343 for detailed information. Reprints of this information are available from the Editors or from: Elsevier Editorial Services Ltd., Mayfield House, 256 Banbury Road, Oxford OX2 7DE (Great Britain).

Reprints. Fifty reprints will be supplied free of charge. Additional reprints (minimum 100) can be ordered. An order form containing price quotations will be sent to the authors together with the proofs of their article.

Advertisements. Advertisement rates are available from the publisher.

Subscriptions. Subscriptions should be sent to: Elsevier Scientific Publishing Company, P.O. Box 211, 1000 AE Amsterdam, The Netherlands. The section on *Computer Techniques and Optimization* can be subscribed to separately.

Publication. *Analytica Chimica Acta* (including the section on *Computer Techniques and Optimization*) appears in 10 volumes in 1980. The subscription for 1980 (Vols. 113–122) is Dfl. 1390.00 plus Dfl. 160.00 (postage) (total approx. U.S. $756.00). The subscription for the *Computer Techniques and Optimization* section only (Vol. 122) is Dfl. 139.00 plus Dfl. 16.00 (postage) (total approx. U.S. $75.50). Journals are sent automatically by airmail to the U.S.A. and Canada at no extra cost and to Japan, Australia and New Zealand for a small additional postal charge. All earlier volumes (Vols. 1–112) except Vols. 23 and 23 are available at Dfl. 150.00 (U.S. $73.00), plus Dfl. 10.00 (U.S. $5.00) postage and handling, per volume.

Claims for issues not received should be made within three months of publication of the issue, otherwise they cannot be honoured free of charge.

Customers in the U.S.A. and Canada who wish to obtain additional bibliographic information on this and other Elsevier journals should contact Elsevier/North Holland Inc., Journal Information Center, 52 Vanderbilt Avenue, New York, NY 10017. Tel: (212) 867-9040.

Analytica Chimica Acta, 113 (1980) 205—220

A COMPARISON OF ARGON-COOLED AND NITROGEN-COOLED PLASMA TORCHES UNDER OPTIMISED CONDITIONS BASED ON THE CONCEPT OF INTRINSIC MERIT‡

S. GREENFIELD*

Albright and Wilson Ltd., P.O. Box 80, Trinity Street, Warley, West Midlands, B69 4LN (Gt. Britain)

D. THORBURN BURNS

Department of Analytical Chemistry, The Queen's University of Belfast, Belfast, BT9 5AG (Northern Ireland)

(Received 11th September 1979)

SUMMARY

A comparison is made of argon-cooled and nitrogen-cooled systems under strictly optimised conditions where possible, and on one spectrometer. The basis of the comparison, the method of optimisation, and the effects of the nebulisation system on the optimisation and on the results are discussed. The differences found suggest that the mode of excitation may be different in argon- and in nitrogen-containing systems. A more reliable estimate than was available hitherto is given of the power which is required for general analysis by plasma spectrometry.

Although analytical spectroscopists are beginning to recognise that high-frequency inductively coupled plasma torches constitute excitation sources for emission spectroscopy with quite exceptional properties, there is by no means universal agreement on such matters as equipment, operating parameters and excitation mechanisms. Two such problem areas are the question of the power necessary for useful analytical work and its optimum value, and the question of torch size. This paper is an account of work carried out in an attempt to resolve these questions.

Whilst it is obvious that any resolution of these problems must involve a comparison of torches over a range of powers, it is not at all obvious what figure of merit should be used to make this comparison. Detection limits are subject to some controversy, as their measurement is not independent of the spectrometer [1]. However, it has been shown that the ratio of the spectral radiances (the energies emitted in watts per cm^2 per steradian per Ångstrom) of the net signal and net background emitted by the plasma is

‡The work reported in this paper forms part of a thesis submitted by S. Greenfield to Loughborough University of Technology in partial fulfilment of the requirements for the degree of Doctor of Philosophy.

independent of the spectrometer and hence may be regarded as a figure of intrinsic merit. Unfortunately, this ratio involves quantities which are not easily measured but it has been shown [1] that the intrinsic merit of two or more plasmas can be compared on a single spectrometer by comparing their easily measured net signal to background ratios. The plasma with the highest net signal to background ratio will be the best plasma on any spectrometer. A given plasma may give different values for this ratio on different spectrometers but the merit order of two plasmas will remain unchanged. Moreover, if two plasmas are examined at the same gain on any spectrometer, the better plasma will give the better detection limit provided that it also gives the greater net signal [1]. If different gains are used, simple criteria involving the gains can be applied similarly. If these criteria are not satisfied, the better plasma may or may not give the better detection limit at the gains used.

The quantities involved in the measurement of net signal to background ratio are: x, the gross or total signal; b, the gross background; and a, the dark current. Thus, the net signal is $x - b$, the net background $b - a$ and the net signal to background ratio $(x - b)/(b - a)$.

At the commencement of this work, it was known that the measured emission from a plasma source depends on the height of viewing and the power (temperature) of the plasma. Furthermore, these parameters were known to be inter-active, as shown by the data illustrated in Fig. 1, obtained

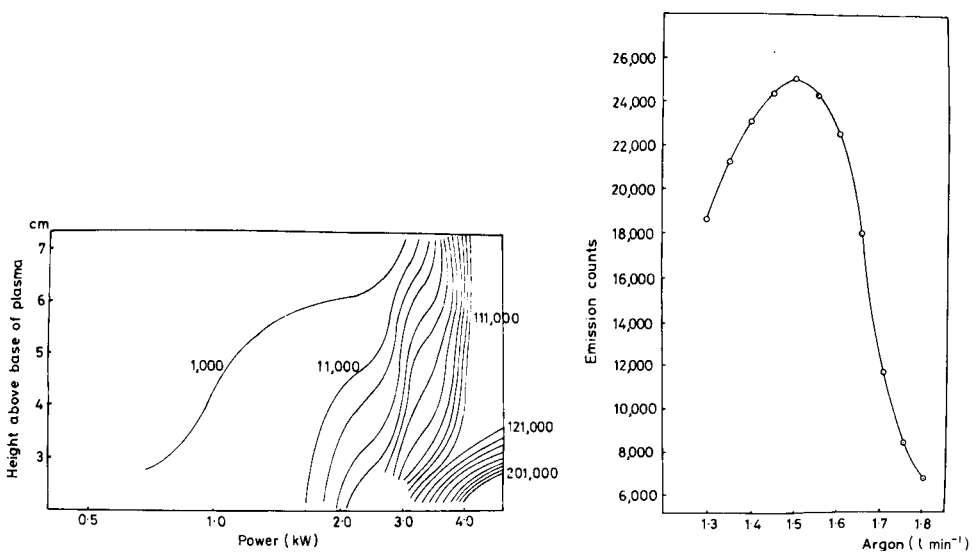

Fig. 1. Height–power–emission relationships. Boron 249.7 nm; 1000 ppm. Contours of emission at intervals of 10,000 counts.

Fig. 2. Effect of nebuliser gas flow rate on the emission from 100 ppm of calcium at 396.8 nm.

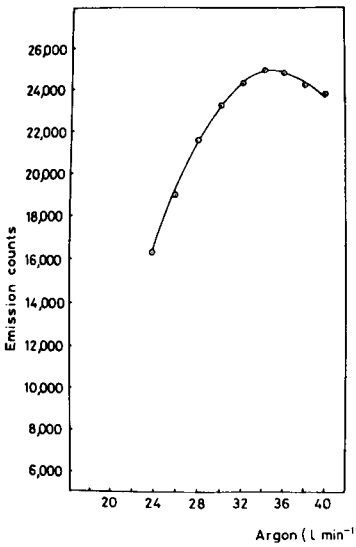

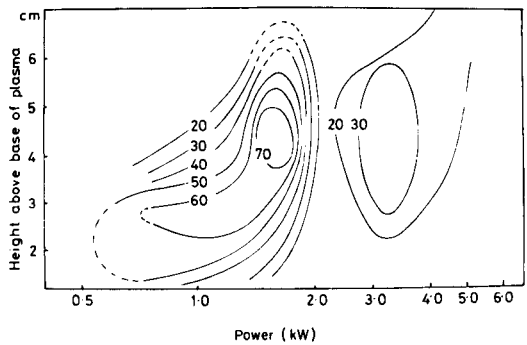

Fig. 3. Effect of plasma gas flow rate on the emission from 100 ppm of calcium at 396.8 nm.

Fig. 4. Height—power—emission relationships. Boron 249.7 nm; 1000 ppm. Contours of $(x - b)/(b - a)$ at intervals of 10 units, where x is the gross signal, b the gross background, and a the dark current.

by using the equipment described in this paper. It was also known that the emission was dependent on the nebuliser gas flow, as shown by the data in Fig. 2. A similar dependence occurs with the plasma gas flow; data illustrating this effect are shown in Fig. 3.

In the light of these data, the question arose whether or not all these parameters were interactive one on the other. If they were, then before any comparison could be made between plasma torch systems it would clearly be necessary to ensure that each system was operated under the optimum conditions. The necessity for careful optimisation can be seen by reference to the height, power and emission data shown in Fig. 4. At small heights above the base of the plasma the ratio $(x - b)/(b - a)$ passes through a maximum at low powers; it will also have a low value. Any further increase in power at this height causes the ratio to decrease. However, at greater heights the maximum value of $(x - b)/(b - a)$ is much larger and occurs at a higher power. Further increase in the observation height again gives a lower ratio. Thus it can be seen from Fig. 4 how easy it is to be misled in the absence of detailed information, which in the case illustrated is further complicated by the presence of two maxima.

The variables which it was necessary to optimise were power, height of observation, and the three gas flows, plasma, nebuliser and coolant.

Initially a factorial design [2] was used in an attempt to optimise the variables and when this was unsuccessful, a simplex method [3] was used;

this too was unsuccessful. One difficulty with both these methods is that two discrete levels of each variable have to be chosen. If the difference between the two levels is small, the effect may be swamped by errors of measurement, while if it is too high, the points may lie on slopes on either side of the maximum. Both cases can and did give rise to apparently capricious results.

It was found that the alternating variable search method [3] was more successful and so was subsequently used. This method maximises the ratio when one variable at a time is changed. This programme was repeated until no change occurred when a cycle of variables was altered. Under some circumstances the optimisation converged quite quickly, although when diagonal ridges occurred, as in Fig. 4, the convergence was slow and required many cycles. The real advantage of this method was that the variables could be changed quickly and continuously over a wide range, and the effect was seen quickly so that the problem of choosing discrete levels did not occur.

EXPERIMENTAL

Equipment

Generators. (a) Radyne, S.C.15., free running with capacitive tuning for control of power; the output is a nominal 2.5 kW, with a frequency of 36 MHz. (b) Radyne, R.D.150., free running, with power control by varying the H.T. on the oscillator valve; the output is a nominal 15 kW, with a frequency of 7 MHz. (The above power refers to the rating of the generator; henceforth the power will refer to the actual wattage in the cell, which was determined from calorimetric calibrations [4]).

Torch and work coil. Three torch systems were used, the Scott torch [5] operated solely on argon and the Greenfield torch [6] operated with both argon and nitrogen coolant gas flows. The Scott torch was provided with an extra tangential inlet tube so that it could be run with both plasma and coolant gases. It was not found practicable, because of instability, to run this torch with a nitrogen coolant so that only argon was used. Both these torches have been illustrated, with full dimensions, elsewhere [7] as has the work coil for the Greenfield torch. A similar work coil, but with a smaller diameter, was used for the Scott torch.

Nebuliser. A Meinhard T-230-A2 nebuliser was used with a backing pressure of 150 psi (ca. 10 atm.).

Spray chamber. A Scott spray chamber [5] and the cyclone chamber illustrated in Fig. 5 were used as discussed below.

Spectrometer. The F.A.19 Polychromator was as previously described [6]. The optical arrangements whereby the two generators and torches could be used on the same spectrometer are shown in Fig. 6.

Ancillary equipment included a Bryans X—Y Auto Plotter Model 21001 with an operational amplifier on each of the two inputs, and an Analog

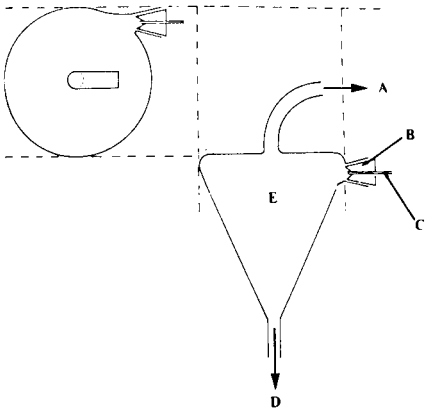

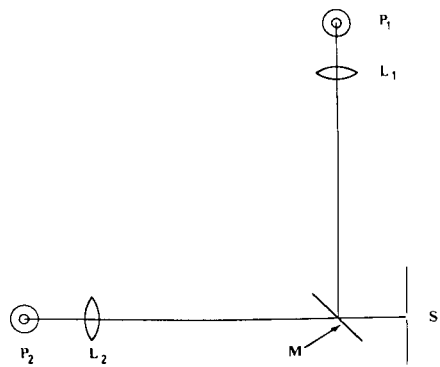

Fig. 5. Cyclone spray chamber. A, aerosol to plasma; B, teflon plug; C, nebuliser; D, drain; E, 750 ml conical flask.

Fig. 6. Entrance optics. P_1 and P_2, tail flames from plasmas of SC 15 generator and RD 150 generator, respectively; L_1 and L_2, positions of 13.2-cm focal length lens; M, mirror used for SC 15; S, entrance slit of spectrometer.

Devices Integrated Circuit A.D.530L operated in the divide mode. For the latter, each input had an operational amplifier, and output meters indicating the quantities $x - a$, $b - a$ and $(x - a)/(b - a)$ were incorporated.

Optimisation procedure

After the equipment had been set up, the signals from each of the 30 channels of the direct-reading spectrometer were compared, one with another, when a plasma through which pure water was nebulised was viewed at different heights of observation to provide a range of intensities. By choosing two channels where these signals moved together, it was possible to estimate the relative value of the background at a given wavelength simultaneously with the intensity of the spectral line of an analyte at that wavelength, thereby obtaining a relative value of the signal-to-background ratio. The two channels chosen were sufficiently far apart in wavelength for the analyte signal in one not to affect the background signal in the other. The signals were displayed either on the X—Y recorder or on the meters of the signal-divider, in each case with the dark current offset. The ratio measured is proportional to $(x - a)/(b - a)$ rather than the ratio $(x - b)/(b - a)$ which is required, but the ratios are very simply connected: $(x - a)/(b - a) = (x - b + b - a)/(b - a) = (x - b)/(b - a) + 1$.

After the optimisation was completed, the signal and the background were measured digitally, by integration, on the same channel.

Initially the optimisation was carried out by using the X—Y recorder. Figure 7 shows the plots obtained in one complete cycle of a search for the

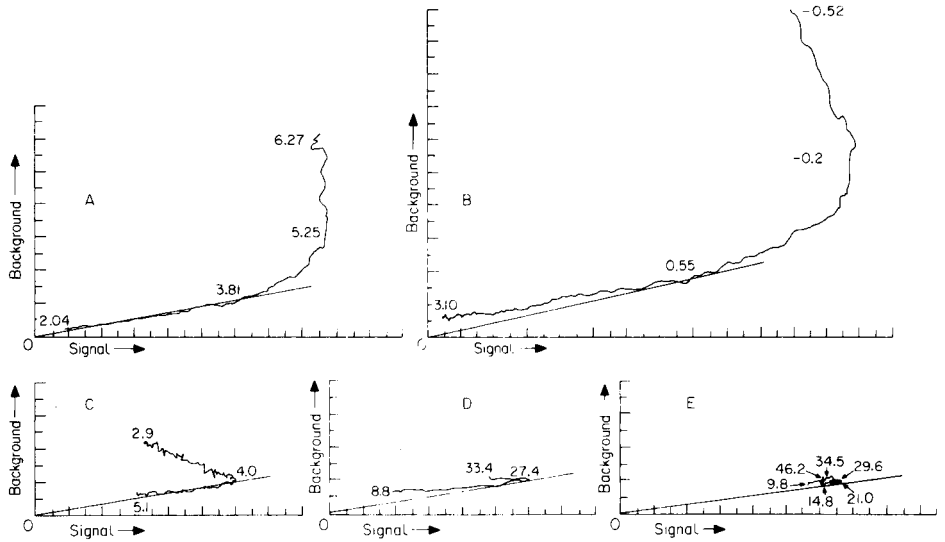

Fig. 7. A complete optimisation cycle for the boron 249.8-nm line. In all cases, the variations of signal and background, corrected for dark current, were measured. (A) Variation with power (kW) in the plasma; (B) variation with height of observation, measured (in cm) from the top of the plasma; (C) variation with nebuliser gas flow (argon, 1 min^{-1}); (D) variation with plasma gas flow (argon, 1 min^{-1}); (E) variation with coolant gas flow (nitrogen, 1 min^{-1}).

optimum values for the boron line 249.8 nm. The first variable to be altered was power (Fig. 7A). The horizontal coordinate is the signal from the boron channel at 249.77 nm and the vertical coordinate the estimate of the background at 254.24 nm. The ratio $(x-b)/(b-a)$ has its maximum value when the slope of the vector from the origin is smallest. This ratio is almost constant between 2 and 3.8 kW: this illustrates the presence of long ridges. At a power somewhat above 3.8 kW, the ratio deteriorated very dramatically. The power was, therefore, set to 3.8 kW where the signal is highest, and the next variable altered. This value of 3.8 is not necessarily the final value; it is the optimum value of power at the settings used for the other variables. In the next cycle of optimisation, when all the other variables may have new values, it may be replaced by a higher or a lower value.

The next variable altered (Fig. 7B) was the height of observation, here measured from the top of the plasma. The ratio improved modestly as the plasma was approached until the distance was 5—6 mm. Thereafter it worsened until, when the plasma was entered, there was a striking deterioration.

The effect of varying the nebuliser flow is shown in Fig. 7(C). Here again there existed a ridge with a constant ratio of $(x-a)/(b-a)$ between 5.1 and 4.0 l min^{-1}. The ratio and the signal both decreased at lower values. The effect of varying the plasma gas flow is shown in Fig. 7(D); in this case there were large variations in the signal but only small changes in the

background. The effect of varying the coolant gas flow is shown in Fig. 7(E), which shows that, for boron, the ratio does not depend very strongly on the coolant gas flow, but that, nevertheless, the range 20—30 l min^{-1} is preferable.

The data illustrated in Fig. 7 show one cycle of the optimisation process and this was repeated until no further inprovement was achieved. It is possible, when diagonal ridges occur (cf. Fig. 4), that this procedure would not lead to the true maximum but to a position on the ridge which is a maximum with respect to each variable separately but not when they are varied together. Accordingly, it was checked that altering the variables two at a time did not lead to any improvement.

The above account of the preliminary work is given to illustrate the procedure and the effects on signals when variables were altered. In later work, the X—Y recorder was replaced by the signal-divider and the signals were read directly from the meters; this proved a faster approach to experiments which were both difficult and tedious.

One difficulty was the destruction of torches through overheating when unusual values of operating parameters were being examined. It is emphasised, therefore, that in the experiments reported later only one torch of each kind was used.

Mention has been made of the ridges and plateaus which occur in these optimisation experiments. The presence of plateaux makes accurate measurement essential, and while this could be done in cases where both net signal and net background were reasonably large, it often happened that the gross background was very small. In these cases the net background was not well defined, so that the ratio had poor accuracy. In fact if the background becomes very small, not only does its accurate measurement become very tedious, but the whole idea of signal-to-background ratio becomes rather artificial. In principle, if the background is indistinguishable from zero, the amplification should be increased until the background has a measurable non-zero value. In practice this may require a major re-design of the apparatus.

In these experiments every effort was made to ensure the accuracy of the results, mainly by averaging, but the problem remains and some of the ratios measured are poorly defined.

RESULTS AND DISCUSSION

Effect of spray chamber

Since the Scott torch is normally used with the Scott spray chamber [5] and the Greenfield torch with the cyclone spray chamber shown in Fig. 5, the extent to which the spray chamber affected the signals from the plasma was investigated with a view to using one spray chamber for all the plasma systems. The results obtained were surprising and totally unexpected.

The Scott torch was first mounted directly above the Scott chamber

as is the normal practice. The operating conditions were optimised and the spectrometer signals measured. The Scott torch was then connected to the cyclone chamber by 35 cm of plastic tubing (1.2 cm i.d.), as is the normal practice with this chamber and the signals were obtained again after optimisation of the operating conditions. For comparison purposes, the Scott torch was also connected to the Scott chamber by the 35-cm length of tubing and the procedure repeated. The detailed results are given in Table 1. It is seen that the addition of the plastic tube made no significant difference to the value of the ratio $(x - b)/(b - a)$ obtained for the Scott chamber, but that the cyclone chamber gave a value about twice as large.

It was difficult to understand why the signal-to-background ratio was influenced by the shape of the spray chamber, so this effect was further investigated. Table 2 shows the uptake rate, transfer efficiency and flow in ml min^{-1} arriving at the injector tip for the two chambers. It was known that the uptake rate is affected by temperature, and so all measurements were taken in a temperature-controlled room. The quantity arriving at the injector was found from the difference of the uptake rate and the quantity going to the drain.

It can be seen from Table 2 that although the uptake rate is less when the cyclone chamber is used, the transfer efficiency is greater and a similar, or a larger, amount of material is carried at a slower, or similar, rate; therefore there is a similar, or larger, amount of material in the plasma for a longer or similar time. There is no obvious reason why the uptake rates, when nebulising into free air and into the chambers, should be different, or why they should be different for different chambers. Back-pressure, or cooling effects from adiabatic expansion, are factors which might be involved in attempts to explain this feature but such explanations are not entirely convincing. The

TABLE 1

Optimised operating conditions and values of x, b and a with different spray chambers (1 ppm sodium; 589.6-nm line.)

Spray chamber	Scott	Scott with tube	Cyclone
Power (kW)	1.0	0.93	1.0
Plasma gas flow (l min^{-1})	>0.0[a]	1.0	>0.0[a]
Nebuliser gas (l min^{-1})	2.7	2.5	2.2
Coolant gas (l min^{-1})	15—24[b]	22.0	22.0
Viewing height above base of plasma (cm)	5.8	6.3	5.6
x (cts/10 s)	917	636	1614
b (cts/10 s)	17.7	14	17.4
a (cts/10 s)	8.7	9.2	9.6
$(x - b)/(b - a)$	100 ± 12	130 ± 18	205 ± 12

[a]Not measurable but greater than zero.
[b]No change in ratio from 15 to 24 l min^{-1}.

TABLE 2

An examination of the parameters involved in the comparison of the two spray chambers

	Scott chamber + Scott torch	Cyclone chamber + Scott torch
	(1) *Optimised conditions*	(3) *Optimised conditions*
Nebuliser flow-rate (l min^{-1})	2.7	2.2
Liquid uptake (ml min^{-1})	7.48	5.89
Transfer efficiency (%)	1.6	2.0
Flow at injector (ml min^{-1})	0.12	0.118
	(2) *Non-optimised conditions*	(4) *Non-optimised conditions*
Nebuliser flow-rate (l min^{-1})	2.2	2.7
Liquid uptake (ml min^{-1})	6.71	7.06
Transfer efficiency (%)	1.3	2.0
Flow at injector (ml min^{-1})	0.087	0.141
Nebulisation into free air without chamber		
Nebuliser flow-rate (l min^{-1})	2.2	2.7
Liquid uptake (ml min^{-1})	5.8	7.31

different transfer efficiencies are probably explained by the greatly different surface-to-volume ratios of the chambers. The cyclone chamber has the smaller ratio and it might be expected that less material would be deposited on its surface than is the case for the Scott chamber. In these tests, 2.4% (w/v) magnesium sulphate solution was sprayed through the nebuliser and the droplets were collected on microscope slides and examined under the microscope; no difference in particle size or distribution could be detected between the two systems. However, the collection of the particles was not complete, and in particular it was noticed that much of the fine mist was carried round the slide without impinging on it. Little, therefore, can be said about the distribution of the finest particles.

Effect of nebuliser

Half-way through the experiments it became apparent that the Meinhard nebuliser was no longer working properly. For a given pressure the gas flow had risen and the solution uptake rate had fallen; the series was therefore started again with a new nebuliser. This mishap was not without its compensations as it was possible to examine the effects of different nebulisers on the optimised conditions. Table 3 shows an example for the barium 455.4-nm line on the Scott torch. It is noticeable that the second nebuliser gives values for the plasma gas flow and the injector gas flow which are much more in line with those reported by regular users of the Scott torch, namely zero plasma gas flow and up to 1 l min^{-1} for the nebuliser [5].

TABLE 3

Effect of different nebulisers on optimum conditions

	Nebuliser No. 1	Nebuliser No. 2
Power (kW)	0.81	0.66
Plasma gas flow (l min^{-1})	1.3	0.0
Nebuliser gas flow (l min^{-1})	1.7	0.95
Coolant gas flow (l min^{-1})	22.0	20.0
Viewing height above base of plasma (cm)	3.2	3.3
$(x - b)/(b - a)$	110	232

TABLE 4

Optimisation cycles for 1 ppm aluminium at the 396.1-nm line

Cycle No.	1	2	3	4	5
Plasma gas flow (l min^{-1})	3.0	2.0	2.0	0.5	0.0
Nebuliser gas flow (l min^{-1})	2.5	2.7	1.7	1.75	1.75
Viewing height above base of plasma (cm)	3.6	4.6	4.8	4.9	4.8
Power (kW)	1.11	1.34	1.12	1.12	1.12
Coolant gas flow (l min^{-1})	24.0	24.5	26.0	26.0	26.0
x (cts/10 s)	179	333	658	750	768
b (cts/10 s)	162	162	133	105	104
a (cts/10 s)	65.1	65.1	65.1	65.1	65.1
$(x - b)/(b - a)$	0.2	1.8	7.7	16.2	17.0

Example of optimisation

Table 4 shows an example of the optimisation process for the Scott torch and the aluminium 396.1-nm line. The first set of conditions, in column 1, was obtained from a previous optimisation with the faulty nebuliser. It can be seen that the plasma gas flow was reduced from 3.0 l min^{-1} to zero after four cycles. The nebuliser gas flow started high, went higher and then was reduced, although its final value was still unusually high for the Scott torch. The observation height approached its final value quickly. The power increased and then returned practically to its initial value. The coolant flow showed only small changes.

Some of these changes, such as the increase and subsequent reduction in power, may appear unconvincing. However, if the consistent increase in the ratio at each stage is noted, it is clear that an apparently irrational pattern in any one variable is probably the result of interaction between the variables. It is a pity that it is so difficult to visualise 5-dimensional space.

Comparison of the Greenfield and Scott torches

Once a working optimisation technique had been achieved a comparison

was made of the three torch systems mentioned earlier. The lines used together with their physical data and the concentrations of the elements studied are shown in Table 5. These lines were chosen to give a range of difficulty of excitation and it was thought that any pattern established for these eight lines would be repeated many times over for the thousands of useful analytical lines.

The results obtained on the three systems are shown in Tables 6—8; the results are for atomic lines except for the final three columns (Ba, V, Al) which pertain to ionic lines.

Although not rigorously correct, the excitation potential and the sum of the excitation potential and the ionisation potentials were used as indicators of how difficult it was to excite the neutral and the ionic lines, respectively. Although the quantity optimised was the ratio $(x - b)/(b - a)$ and not the net signal $x - b$, it was to be expected that the optimum ratio would be

TABLE 5

Lines employed in the comparison of torches

Element	State	Wavelength (nm)	Transition prob. 10^8 s^{-1}	Ex. pot. (eV)	Ion pot. (eV)	Conc. (ppm)
Na	U_1	589.6	1.8	2.10	5.14	1000
Na	U_1	589.6	1.8	2.10	5.14	1
Cs	U_3	455.5	1.4	2.70	3.90	1000
Ba	V_1	455.4	0.9	2.71	5.20	1
Al	U_1	396.1	1.3	3.10	6.00	1
Al	U_1	396.1	1.3	3.10	6.00	1000
V	V_1	309.3	4.3	4.38	6.74	1000
Zn	U	307.6	.013	4.01	9.40	1000
Zn	U	307.2	2.0	8.01	9.40	1000
Al	V_2	281.6	1.2	11.71	5.99	1000

TABLE 6

Optimised operating conditions for the Scott torch together with the signals obtained

Element	Na	Cs	Al	Zn	Zn	Ba	V	Al
Conc. (ppm)	1	1000	1	1000	1000	1	1000	1000
Wavelength (nm)	589.6	455.5	396.1	307.6	307.2	455.4	309.3	281.6
Plasma gas (l min^{-1})	0.2	0.0	0.0	0.0	0.0	0.0	0.25	1.0
Nebul. gas (l min^{-1})	2.2	1.7	1.75	1.0	0.5	0.95	0.75	1.0
Ht. above base (cm)	5.6	3.7	4.8	3.3	2.0	3.3	2.3	3.5
Power (kW)	1.0	0.66	1.12	0.89	0.53	0.66	0.65	1.16
Coolant gas (l min^{-1})	22.0	20.0	26.0	19.0	19.0	20.0	19.0	22.0
x (cts.)	1614	998	768	481	147	4452	27228	100.8
b (cts.)	17.4	14.9	104	52.1	83	26.1	32.5	61.4
a (cts.)	9.6	7.3	65.1	24.7	24.3	7.0	12.2	5.2
$(x - b)/(b - a)$	20.5	129	17	15.6	1.09	232	1340	0.7

TABLE 7

Optimised operating conditions for the Greenfield torch, with argon coolant, together with the signals obtained

Element	Na	Cs	Al	Zn	Zn	Ba	V	Al
Conc. (ppm)	1	1000	1	1000	1000	1	1000	1000
Wavelength (nm)	589.6	455.5	396.1	307.6	307.2	455.4	309.3	281.6
Plasma gas (l min^{-1})	0.5	0.0	2.0	0.0	8.5	2.0	0.0	3.0
Nebul. gas (l min^{-1})	2.2	2.7	1.5	1.2	1.3	1.2	1.0	2.1
Ht. above base (cm)	5.1	6.2	4.3	3.5	3.6	4.8	3.3	3.4
Power (kW)	1.39[a]	1.42[a]	1.39[a]	1.44[a]	1.86	1.41[a]	1.46[a]	3.92
Coolant gas (l min^{-1})	24	22	16	26	33	20	24	40
x (cts.)	499.6	698	237.9	1950	2201	4358	23524	4793
b (cts.)	22	17.1	34.9	129.4	1152	38.9	24.4	3030
a (cts.)	12.5	9.9	23.6	26.8	30.6	9.3	6.0	5.4
$(x-b)/(b-a)$	50	95	18	17.7	0.94	146	1277	0.58

[a]Not truly optimised as under the conditions set the variable required to go lower than was practicable.

TABLE 8

Optimised operating conditions for the Greenfield torch, with nitrogen coolant, together with the signals obtained

Element	Na	Cs	Al	Zn	Zn	Ba	V	Al
Conc. (ppm)	1	1000	1	1000	1000	1	1000	1000
Wavelength (nm)	589.6	455.5	396.1	307.6	307.2	455.4	309.3	281.6
Plasma gas (l min^{-1})	7.0[a]	4.5[a]	6.0	9.0	18	5.0	5.0	32
Nebul. gas (l min^{-1})	2.2	2.8[b]	2.7	1.5	1.8	1.7	2.1	1.8
Ht. above base (cm)	3.8	4.4	4.4	2.9	2.8	3.2	3.5	3.2
Power (kW)	0.8[a]	0.91[a]	1.15	1.19	2.6	0.95	1.66	2.6
Coolant gas (l min^{-1})	7.0	8.0	15	14	36	12	30	40
x (cts.)	538	974	320	1011	4449	6232	12800	2838
b (cts.)	17.7	12.7	27.1	107	1912	27.3	21.9	1249
a (cts.)	12.3	9.9	24.4	28.1	33.5	9	5.2	5.3
$(x-b)/(b-a)$	96	343	108	11.5	1.35	339	765	1.28

[ab]Not truly optimised as under the conditions set the variable required to go lower (a) or higher (b) than was practicable.

obtained at a higher power for lines difficult to excite. If it is assumed that the system is in local thermodynamic equilibrium, so that one temperature governs all the relevant processes through the equilibrium laws of Boltzmann and Saha, then the background from the continuum arising from free electrons will increase with temperature and so will the intensity of the line until the norm temperature is reached. It therefore seems reasonable to expect the signal-to-background ratio for a given element to increase until the sensitivity curve begins to flatten out near the norm temperature. Thus it would be expected that higher temperatures would be required for the more difficult lines and that this will be achieved with higher power.

The data in Fig. 8(A) show that for the Greenfield torch with a nitrogen

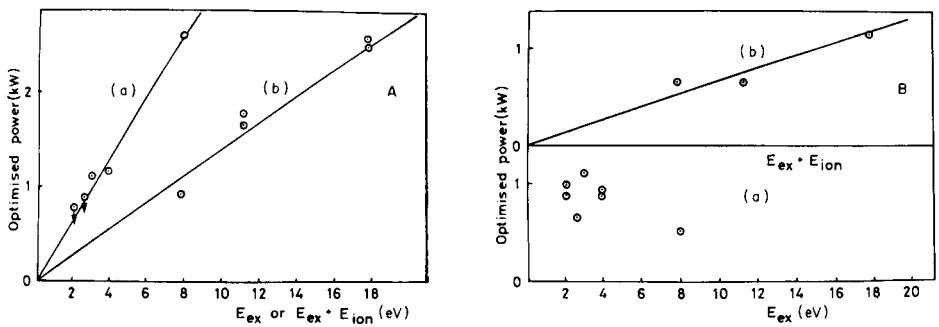

Fig. 8. Plot of optimum power against E_{ex} or $E_{ex} + E_{ion}$ for (A) the Greenfield torch with nitrogen coolant and (B) the Scott torch with argon coolant. (a) Atoms; (b) ions.

coolant, convincing linear correlations between optimum power and difficulty of excitation were obtained. At this stage, no reasons can be given why the correlation should be linear. Two different lines are obviously required for neutral atoms and ions. The two lowest points, marked with arrows, correspond to the lowest settings of the generator; the indications were that the optimum powers were lower than this. The range of optimum powers thus lies between something less than 0.8 kW for sodium to 2.6 kW for the Zn 307.2-nm and Al 281.6-nm lines.

Figure 8(B) shows the corresponding results with the Scott torch. Here there is no obvious correlation for the neutral atoms and a possible correlation for the ion lines. Thus there is a difference between results for the Greenfield torch with a nitrogen coolant and the Scott torch with an argon coolant.

It had been hoped that the set of optimisations which were carried out on the Greenfield torch with an argon coolant would allow a judgement to be made as to whether the difference was due to the nature of the coolant gas, or to the difference in torches. Unfortunately, six of the eight spectral lines required a lower power than could be reached. The only line which was strictly optimised with power was the Al 281.6-nm line, while the optimum power for Zn 307.2-nm line lay between 1.88 and 1.83 kW, these being respectively the lowest power on the large generator and the highest power on the small generator. These limits were close enough to be useful, but one point for each of the ion and atom results is inadequate to establish a correlation.

There is therefore no direct experimental evidence to show whether the cell design or the nature of the coolant gas is responsible for the difference in behaviour of the two systems. It is, however, tempting to speculate that the coolant gas is the determining feature. The results obtained with nitrogen are, at least qualitatively, consistent with thermal excitation, with the source in local thermodynamic equilibrium. This is implied in using excitation potentials or the sum of excitation and ionisa-

tion potentials as indicators of the difficulty of exciting a line. The failure of this approach with an argon coolant is perhaps paralleled by reports [8] that systems in which only argon is used seem not to be in local thermodynamic equilibrium and that other mechanisms of excitation may apply.

It has been postulated [8] that some excited argon atoms do not spontaneously return to the ground state through a radiative transition but remain in the metastable state. The excitation energy is then transferred by a process known as Penning ionisation [8]

$$Ar_{(meta)} + X \rightarrow \begin{matrix} Ar + X^{+}* + e \\ \searrow \\ Ar + X^{+} + e \end{matrix}$$

The argon metastables have excitation energies around 11 eV and can thus excite ion lines. This type of excitation may therefore increase the population of ions, excited or otherwise, and as a consequence perturb the equilibria between the excited levels and between the ionisation states. Thus less power would be required to excite some lines than would normally be expected.

The data in Table 9 allow the comparison of the net ratios obtained from the optimised conditions for the three systems. The asterisked values are not true optimisations in the sense that some variable had reached its limit before the ratio had peaked.

Although seven out of eight values for the Greenfield torch with an argon coolant suffer from these limitations, and hence have values which are strictly undetermined, it appears that better values are obtained with a nitrogen coolant than with argon. The two exceptions are the Zn 307.6-nm and the V 309.3-nm lines. This was probably caused by the second positive emission system from the N_2 molecule: spectra were photographed from plasmas with nitrogen and argon coolants and weak lines, possibly band heads, were visible at these wavelengths when nitrogen was used but absent

TABLE 9

Comparison of the values of the $(x - b)/(b - a)$ ratios for the three systems

Element	Wavelength (nm)	Concentration (ppm)	Scott Ar	Greenfield Ar	Greenfield N_2
Na I	589.6	1	205	50*	96*
Cs I	455.5	1000	129	95*	343*
Al I	396.1	1	17	18*	108
Zn I	307.6	1000	15.6	17.7*	11.5[a]
Zn I	307.2	1000	1.09	0.94*	1.35
Ba II	455.4	1	232	146*	339
V II	309.3	1000	1340	1277*	765[a]
Al II	281.6	1000	0.7	0.62	1.28

[a]Interference from N_2 bands.
*True optimisation not reached.

when argon was used. In this experiment no solution was aspirated, as the strong OH bands in this region might have masked the lines sought. Thus it seems justified to claim that unless there is interference from molecular emission, a plasma with a nitrogen coolant gives a better signal-to-background ratio than one with an argon coolant, at least with the Greenfield torch.

CONCLUSIONS

The eight lines studied were chosen to give a range of difficulty of excitation. Of these, five gave a better value for signal-to-background ratio when the Greenfield torch was used with a nitrogen coolant than when the Scott torch was employed. Two others suffered from molecular interference, and for these the Greenfield torch with argon coolant gave values which were not significantly worse than those with the Scott torch. The last case is sodium, for which it was not possible to reach a sufficiently low power to obtain a true optimisation with the particular generator used. Some of the differences in the ratios obtained with the two different torches are sizeable; for the Al 396.1-nm line there is a factor of 6, which is well worth having. Of the thousands of useful spectral lines, most would be expected to give better results with the Greenfield torch run with a nitrogen coolant.

The optimum powers found depend on the torch and on the coolant gas. On the Greenfield torch with a nitrogen coolant, the optimum powers lie in a range from < 0.8 kW to 2.6 kW. These are actual powers developed in the plasma. The range for the Scott torch was 0.53—1.16 kW. For elements difficult to excite, the Greenfield torch with argon does require quite high powers, as much as 3.92 kW, which are much greater than those required for the Scott torch.

This work has taken account of an intrinsic property of the plasma which is measured by the net signal-to-background ratio. No account has been taken of other properties of the plasma which are power-dependent such as efficiency of dissociation of molecules and ionisation. These dependencies are as yet little known and await rigorous investigation.

On the question of choice of torch, it was observed that the injector of the Scott torch, which is an integral part of the torch, was much more readily blocked by aerosols of high solute content, such as 1% (w/v) aluminium nitrate, than was the injector of the Greenfield torch. Browner [9] reported that a low-powered system with a Scott torch was easily blocked by carbon when organic solvents were nebulised. No such problem has ever been encountered with the large torch operating at high power.

Browner [9] also reported the presence of a green hue, denoting Swan bands, in his low-powered system. This hue is absent when high power is used, and the C—C bands are not visible in the spectra obtained from such a system. This has nothing to do with the type of torch, but is an example of the advantage of dissociation of molecules by the use of high power.

The answer to the question of the optimum wattage necessary for useful work depends on the type of torch used, which in turn depends on the analytical purpose. With the present state of the art and assuming that the full power of the technique is to be exploited, it would seem reasonable to specify a generator capable of producing a power in the plasma of 4—5 kW, but also operable at a tenth of this value. This power would give a reasonable expectancy that most eventualities could be dealt with.

The authors thank H. T. Searle, Chairman, Specialities Sector, Albright and Wilson Ltd., and Professor R. F. Phillips of Loughborough University of Technology for facilities and encouragement in post-graduate studies afforded to S. G., and H. McD. McGeachin and P. B. Smith for technical assistance and many hours of helpful discussion.

REFERENCES

1 S. Greenfield and D. Thorburn Burns, Spectrochim. Acta, in press.
2 O. L. Davies, The Design and Analysis of Experiments, 2nd edn., Oliver and Boyd, 1956.
3 M. J. Box, D. Davies and W. H. Swann, Non-linear Optimization Techniques, Oliver and Boyd, 1969.
4 S. Greenfield and H. McD. McGeachin, Anal. Chim. Acta, 100 (1978) 101.
5 R. H. Scott, V. A. Fassel, R. N. Kniseley and D. E. Nixon, Anal. Chem., 46 (1974) 75.
6 S. Greenfield, I. Ll. Jones, H. McD. McGeachin and P. B. Smith, Anal. Chim. Acta, 74 (1975) 231.
7 R. M. Barnes, I.C.P. Inf. Newsl., 1 (1975) 51.
8 J. Robin, Methodes Phys. Anal. (special issue), (1971) 3.
9 R. F. Browner, XXIst Colloquium Spectroscopium Internationale and 8th International Conference on Atomic Spectroscopy, Cambridge, U.K., July 1979, Abstract in I.C.P. Inf. Newsl., 5 (1979) 137.

Analytica Chimica Acta, 113 (1980) 221—226

ATOMIC AND IONIC FLUORESCENCE SPECTROMETRY WITH PULSED DYE LASER EXCITATION IN THE INDUCTIVELY-COUPLED PLASMA

M. S. EPSTEIN,** S. NIKDEL, J. D. BRADSHAW, M. A. KOSINSKI, J. N. BOWER and J. D. WINEFORDNER*

Department of Chemistry, University of Florida, Gainesville, FL 32611 (U.S.A.)

(Received 20th August 1979)

SUMMARY

The atomic and ionic fluorescences of iron, tin, barium and indium excited by flash-lamp- and nitrogen laser-pumped pulsed dye lasers in the inductively-coupled plasma (ICP) are studied. Noise sources are investigated and detection limits are compared to the techniques of ICP-emission and laser-excited atomic fluorescence spectrometry.

The advantages of the inductively-coupled plasma (ICP) as an atomic/ionic vapor cell for emission spectrometry have been well documented [1]. The high temperature (ca. 6000 K) [2] as well as long residence time experienced by the analyte makes the ICP extremely effective for vaporization, atomization, and/or ionization processes and also produces an extremely complex and intense spectrum with many analytically useful atomic and ionic emission lines. There are, however, inherent disadvantages to the ICP when used for atomic emission spectrometry (a.e.s.). A high-resolution monochromator is required to isolate the analyte emission from plasma background and matrix element emission. Background correction procedures are mandatory for accurate analytical determinations with the ICP for emission. Most significant, however, is that the detection limits of the present ICP—a.e.s. methods are fundamentally limited by the characteristics of the technique itself. Although some improvement may be expected from refinements in nebulizer design and increases in r.f. power applied to the plasma, only a major development similar to the development of electrothermal atomization for atomic absorption spectrometry will result in orders-of-magnitude improvement in ICP—a.e.s. detection limits.

One major advantage that atomic fluorescence spectrometry (a.f.s.) exhibits over other atomic spectrometric techniques is the direct dependence of sensitivity on the intensity of the excitation source (short of saturation of the spectral transition) [3]. Application of the ICP to a.f.s. measurements

**On leave from the Center for Analytical Chemistry, National Bureau of Standards, Washington D.C. 20234, U.S.A.

can therefore provide an extremely effective combination. The inert gas atmosphere provides a high quantum efficiency and the high temperature not only reduces chemical interferences, but also increases the number of analytically useful fluorescence transitions. Background correction in ICP—a.f.s. is less critical than in ICP—a.e.s. since matrix-induced changes in the plasma background are not observed or are easily corrected for by blocking the laser; moreover, spectrometers of moderate resolution are satisfactory. Most important, however, is the simplicity of improving detection limits by increasing source intensity.

Several investigators have used the ICP as an atomic/ionic vapor cell for a.f.s. Using electrodeless discharge lamps as the excitation source, Montaser and Fassel [4] reported atomic fluorescence in the ICP tail plume (3—5 cm above the coil). Better detection limits for fluorescence than emission were obtained for cadmium, zinc and mercury with a special torch configuration. Pollard et al. [5] investigated the application of a continuous-wave dye laser to a.f.s. in the ICP for barium, sodium, lithium and vanadium. They were restricted, however, by the limited wavelength range of their laser and found that a power level of 0.7 kW provided the best signal-to-noise (S/N) ratio.

The pulsed tunable dye laser is presently the most useful laser for the excitation of fluorescence in atomic vapor cells because of the wide wavelength range that can be covered. In this investigation, the application of two such lasers was studied; a flashlamp-pumped dye laser and a nitrogen laser-pumped dye laser were used for the excitation of atomic and ionic fluorescence in the ICP.

EXPERIMENTAL

A nitrogen laser-pumped dye laser (UV-14, Molectron Corp., Sunnyvale, CA.) [6] and a flashlamp-pumped dye laser (CMX-4, Chromatix Inc., Sunnyvale, CA.) [7, 8] were used as the excitation sources. The experimental system was similar to that described by Pollard et al. [5] with the following modifications. Experimental measurements with the flashlamp-pumped dye laser were made by using rhodamine 6G laser dye, frequency doubling, and narrowing of the spectral bandwidth of the laser to ca. 0.003 nm with a high finesse etalon. The laser radiation was focused by a lens (Spectrosil, 2.5-cm diameter, focal length 30 cm) to a spot 0.1—0.2 cm in diameter, 1.5—2.5 cm above the coil in the pencil region of the plasma. The resulting fluorescence was focused 1 : 1 on the 0.35-m monochromator which employed a 3-mm slit height and 0.5-mm slit width (spectral bandpass, ca. 1 nm). The photomultiplier was modified for pulsed, high-current operation [6] and synchronous gated (boxcar) detection was employed. A strip-chart recorder and integrator were used for readout. Experimental measurements with the nitrogen laser-pumped dye laser were as described by Weeks et al. [6] and Omenetto et al. [9] as were the detection and signal-processing systems for both lasers. The forward power to the ICP was 0.65 kW for the atomic lines and 1.1 kW for the ionic lines studied.

RESULTS AND DISCUSSION

Flashlamp-pumped dye laser

Detection limits for laser-excited ICP—atomic fluorescence spectrometry (LICP—a.f.s.), ICP—atomic emission spectrometry (ICP—a.e.s.), and laser-excited flame a.f.s. (LF—a.f.s.) are given in Table 1. For the two elements investigated (iron and tin), the detection limits for LICP—a.f.s. were approximately two orders of magnitude worse than the best ICP—a.e.s. detection limits reported in the literature for pneumatic nebulization, although they were almost identical to the best detection limits that were obtained with the present instrumentation by ICP—a.e.s. Furthermore, they are within an order of magnitude of the estimated detection limits for ICP—a.e.s. published by Winge et al. for the same lines [10].

Of more significance, however, since they were done with the same laser system, is a comparison of LF—a.f.s. with LICP—a.f.s. The LF—a.f.s. detection limits obtained with a nitrogen-separated air—acetylene flame are two to three orders of magnitude better than the LICP—a.f.s. detection limits. While a factor of 3 difference in laser power resulting from losses in reflective optics used to direct the laser beam into the ICP (3 mirrors and one lens compared to only one mirror for the LF—a.f.s. system) can account in a small part for the poorer LICP—a.f.s. detection limits, the greatest effect is undoubtedly due to the greater background emission (and noise) of the plasma. The LICP—a.f.s. and LF—a.f.s. detection limits were obtained under shot-noise limited conditions. In Fig. 1, the effect of r.f. power on

TABLE 1

Detection limits (ng ml^{-1})

Element	Fluorescence wavelength (nm) ($\lambda_{ex}/\lambda_{em}$)		LICP—a.f.s.		LF—a.f.s.	ICP—a.e.s.
			Pulsed[c]	c.w.[d]	Pulsed	
Iron[a]	Fe I	296.7/373.5	50	—	0.06[e]	26(4.3)[h], 0.2[i]
Tin[a]	Sn I	300.9/317.5	500	—	3[f]	200(111)[h], 6[i]
Barium[b]	Ba II	455.4/455.4	2	—	—	1(1.3)[h], 0.06[i]
	Ba II	614.2/455.4	30	6	—	—
Indium[b]	In I	410.2/410.2	300	—	0.8[g]	400(187)[h], 30[i]

[a]Flashlamp-pumped dye laser. [b]Nitrogen laser-pumped dye laser. [c]This work; detection limit defined as 3 × std. deviation of the noise for an observed time constant of 1 s. [d]Continuous-wave dye laser detection limit [5]. [e]Detection limit at the same transition as LICP—a.f.s. with a 10-s time constant and multi-pass cell [7]. [f]Detection limit at the same transitions as LICP—a.f.s. with a 1-s time constant and single-pass cell [8]. [g]Detection limit at the same transitions as LICP—a.f.s. with a time constant of 0.5—5 s and a single-pass cell [6]. [h]Best ICP—a.e.s. detection limits with the present monochromator/detection system and a 0.3-s time constant; estimated ICP—a.e.s. detection limits [10] for same lines in parentheses. [i]ICP—a.e.s. detection limits with pneumatic nebulization [11].

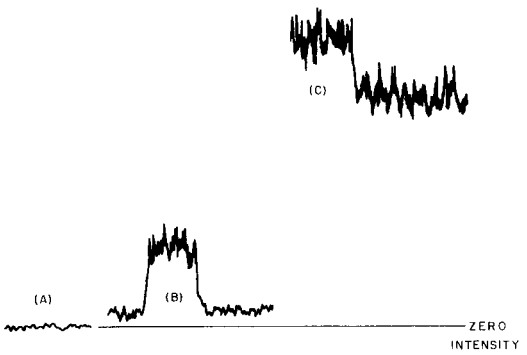

Fig. 1. Recorder tracings of laser-excited atomic fluorescence signals from 10 μg Fe ml^{-1} in the ICP. (A) Detector/electronic noise with photomultiplier shutter closed; (B) baseline and fluorescence signal at 0.65 kW forward power to the ICP; (C) baseline and fluorescence signal at 1.25 kW forward power to the ICP.

the S/N of the fluorescence signal for 10 μg Fe ml^{-1} at power levels of 0.65 kW and 1.25 kW is shown. While the background signal increases by a factor of ca. 18 with increasing power, the S/N ratio decreases approximately 4-fold, characteristic of a shot-noise limited system.

Factors influencing the signal and the S/N ratio for the LF—a.f.s. and LICP—a.f.s. methods include: efficiency and rate of atom production; quantum efficiency of the atomic transition; luminosity of the entrance optical—monochromator—detection system; and background emission of the atomization system. The efficiency and rate of atom production in the flame and ICP depend on the rate and efficiency of sample introduction. Although this parameter was not measured, it is assumed that the ICP is a much more efficient atomizer. Similarly, it is also assumed that the ICP is a much less efficient quencher of excited atoms than oxidizing flames. The luminosity (throughput) of the LF—a.f.s. system (16-nm spectral bandpass and an f 3.5 aperture) was much greater ($\approx$ 64 X) than that of the LICP—a.f.s. system (1-nm spectral bandpass and an f 6.8 aperture). Finally, the background emission of the ICP is several orders of magnitude greater than that of the nitrogen-separated air—acetylene flame.

As shown in Fig. 1, detector/electronic noise (the noise contributed by the detector and electronics in the absence of photons striking the detector) is a major noise source at low ICP power levels (0.65 kW), although the dominant noise is ICP background emission shot-noise. At the higher ICP power level used (1.25 kW), the ICP background emission flicker is the only major source of noise. The noise sources in an ICP analysis will therefore vary from detector/electronic noise at very low background emission intensities, through a region of moderate background emission intensity where background emission shot-noise is dominant, to a region of high back-

ground emission intensities, where background emission flicker is the major noise source. The best region for an analysis, based on signal-to-noise ratio consideration, is the background emission shot-noise limited region (where the background emission is essentially a continuum over the spectral bandpass of the wavelength-dispersive device). In the detector/electronic noise region, the noise is not a function of optical throughput, so that the *S/N* ratio (i.e., the signal component) may be increased by increasing the throughput. In the background emission flicker noise region (again, under conditions of a continuum background, which was observed for the elements investigated), the noise may be decreased at a rate faster than the signal by decreasing the spectral bandpass, thus again improving the *S/N* ratio. Thus, methods of improving the *S/N* ratio for the aforementioned noise regions require measurements to be made in the background emission shot-noise limited region. Here, an increase or decrease in spectral bandpass does not change the *S/N* ratio as long as the upper or lower noise regions, where new noise sources are added, are not too closely approached. The *S/N* ratio can be improved in the background emission shot-noise limited region by increasing the optical throughput by means other than increasing the spectral bandpass such as increasing the *f*-number of the optical system to match that of the spectrometer. This method will be effective until the background emission flicker region is reached, where further increases in throughput will not improve the *S/N* ratio.

As mentioned previously, the throughput (luminosity) of the LF—a.f.s. system is much greater ($\approx$ 64 ×) than the throughput of the LICP—a.f.s. system. Figure 1 illustrated the LICP—a.f.s. analysis to lie in the background emission shot-noise limited region (0.65 kW) close to the detector/electronic noise-limited region. The significantly lower background level of the separated flame would thus place the LF—a.f.s. analysis far into the detector/electronic noise region using the optical throughput of the LICP—a.f.s. system. Therefore, the increased throughput of the LF—a.f.s. system significantly improves detection limits using flames compared to the ICP for laser-excited AFS, as was illustrated in Table 1.

Nitrogen laser-pumped dye laser

Detection limits shown in Table 1 are similar to those observed for the flashlamp-pumped dye laser, relative to the other techniques listed. The limiting noise sources for LICP—a.f.s. (with the nitrogen laser-pumped dye laser) were a combination of r.f. interference noise from both the ICP and the nitrogen laser (with the 15-ns gate) and the background emission shot-noise from the plasma.

The expected improvements in LICP—a.f.s. detection limits arising from an improvement (compared to flames) in the quantum efficiency and in the restricted volume of the analyte in the plasma (which is optimal for laser excitation) are more than offset by the increase in the background intensity of the ICP compared to separated flames. The differences in detection limits

between LICP—a.f.s. and ICP—a.e.s. are largely due to the duty cycle differences in the measurement systems (continuous wave compared to 1-μs or 5-ns pulses times the repetition rate) under shot-noise limited conditions (flashlamp-pumped) or r.f. interference shot-noise limited conditions (nitrogen laser-pumped). Barium fluorescence, for example, is saturated when the nitrogen laser-pumped dye laser is used, so that the fluorescence intensity is significantly greater than the emission intensity when measured over the gatewidth of the boxcar averager used for signal processing. Nevertheless, the ICP—a.e.s. detection limit under continuous d.c. processing conditions is about the same as the LICP—a.f.s. detection limit. In such cases, improvement in a.f.s. detection limits can only be obtained by using lasers of greater duty cycle, assuming complete uniform illumination of the atomic vapor by the intense central (spatial) portion of the laser beam.

The major noise source at high concentrations in LICP—a.f.s. is flicker noise from pulse-to-pulse variations (intensity and spatial) of the laser; a similar noise component was observed in flame cells [7, 8]. Analytical calibration graphs for the elements studied were linear up to 1 mg ml^{-1}.

Conclusions

While the initial evaluation of laser-excited a.f.s. in the ICP has not indicated the technique to be superior to ICP—a.e.s. or to LF—a.f.s., the application of multipass optical cells to reflect the laser beam several times through the ICP [7], as well as the use of more powerful laser sources with higher repetition rates should improve detection limits enough so that the advantages inherent in the combination of a high-temperature atomic vapor cell with the atomic fluorescence method will be fully realized. Furthermore, laser-excited a.f.s. is still a very powerful tool for diagnostic studies of the ICP [9].

Research supported by AF-AFSOR-F44620-76C-0005 and by NSF-CHE-77-23138.

REFERENCES

1 V. A. Fassel and R. N. Kniseley, Anal. Chem., 46 (1974) 1110A.
2 D. J. Kalnicky, R. N. Kniseley and V. A. Fassel, Spectrochim. Acta, Part B, 30 (1975) 511.
3 N. Omenetto and J. D. Winefordner, Prog. Anal. At. Spectrosc., 2 (1/2) (1979) 1.
4 A. Montaser and V. A. Fassel, Anal. Chem., 48 (1976) 1490.
5 B. D. Pollard, M. B. Blackburn, S. Nikdel, A. Massoumi and J. D. Winefordner, Appl. Spectrosc., 33 (1979) 5.
6 S. J. Weeks, H. Haraguchi and J. D. Winefordner, Anal. Chem., 50 (1978) 360.
7 M. S. Epstein, S. Bayer, J. Bradshaw, E. Voigtman and J. D. Winefordner, Spectrochim. Acta, Part B, in press.
8 M. S. Epstein, J. Bradshaw, S. Bayer, J. Bower, E. Voigtman and J. D. Winefordner, Appl. Spectrosc., in press.
9 N. Omenetto, S. Nikdel, R. D. Reeves, J. Bradshaw, J. Bower and J. D. Winefordner, Spectrochim. Acta, Part B, submitted.
10 R. K. Winge, V. J. Peterson and V. A. Fassel, Appl. Spectrosc., 33 (1979) 206.
11 P. W. J. M. Boumans and R. M. Barnes, ICP Info. Newsl., 3 (1978) 445.

Analytica Chimica Acta, 113 (1980) 227—235

INVESTIGATIONS OF REACTIONS INVOLVED IN FLAMELESS ATOMIC ABSORPTION PROCEDURES

Part 7. A Theoretical and Experimental Study of Factors Influencing the Determination of Silicon†

WOLFGANG FRECH and ANDERS CEDERGREN*

Department of Analytical Chemistry, University of Umeå, S-901 87 Umeå (Sweden)

(Received 4th September 1979)

SUMMARY

The ideal conditions for the determination of silicon by graphite-furnace atomic absorption spectrometry have been investigated by using high-temperature equilibrium calculations. All reasonable reaction products resulting from the reaction between Si, C, O, H, S, N, Ar and Na have been considered. The results show that $SiO_2(s)$ is the stable silicon compound for temperatures below 1500 K. For higher temperatures $Si_3N_4(s)$, SiC(s), SiO(g), $SiO_2(s)$, Si(g), SiN(g), $SiCl_2(g)$ and SiS(g) are the main silicon-containing reaction products. SiO(g) is always formed in the interval 1600—2200 K independently of the partial pressure of oxygen. The basic requirement for the quantitative formation of silicon atoms at 2600 K is that the partial pressure of atomic oxygen is less than 10^{-12} atm. The main condition for the formation of silicon carbide is an extremely low partial pressure of oxygen. Losses of silicon by the formation of SiO(g) during heating of the graphite tube were experimentally shown to be reduced by using isothermal atomization. An equilibrium model for the formation of silicon atoms is discussed. This model takes into consideration the decrease in the partial pressure of oxygen during the atomization step. The results obtained show that silicon atoms are formed from SiO(g) at the temperatures pertaining to the beginning of the atomization cycle and from SiC(s) at somewhat higher temperatures.

The trace determination of silicon is of interest in several connections. One example is the determination of silicon in sea water where this element may be present from ultratrace levels to a few mg l^{-1}. Another example concerns the control of silicon in boiler feed water at the 10—20 mg l^{-1} level, since carry-over of silica with steam may cause hard silica deposits on the turbine blades. Interest in silicon has also increased since it became clear that it is an essential element. Carlisle [1], for example, found that silicon-deficient chicks exhibited retarded skeletal development and skull deformations.

The normal method of determining trace concentrations of dissolved inorganic silica involves spectrophotometry, based on the formation of the yellow molybdosilicic acid when an acidic sample is treated with a molyb-

†Part 6. K. Johansson, W. Frech and A. Cedergren, Anal. Chim. Acta, 94 (1977) 245.

date solution. Among several reported interferences are iron, copper, cobalt and nickel. Methods based on atomic absorption in a nitrous oxide—acetylene flame have been reported but their sensitivity is rather poor (0.3—5 ppm).

Several attempts to use graphite furnace a.a.s. have been made [2—7]. Sensitivity was reported to be improved by using graphite tubes impregnated with solutions of Ta, Ti, Hf or Na_2WO_4 [4]; this improvement was thought to result from avoiding the formation of silicon carbide. Lo and Christian [5] discussed possible mechanisms for the formation of silicon atoms. Although their work [5] represents an important contribution and constitutes the most thorough study available, much remains to be done before the processes involved in the determination of silicon are satisfactorily understood.

In this work, high-temperature equilibrium calculations have been used in order to study the conditions associated with the graphite-furnace a.a.s. determination of silicon.

EXPERIMENTAL

Instrumentation, reagents and materials

A Perkin-Elmer HGA 2100 graphite furnace connected to a research spectrometer was used as described earlier [8]. The instrumental parameters are given in Table 1.

Suprapur nitric acid and sodium chloride (Merck) were used. All other chemicals were of analytical-reagent quality. Acid-washed polypropylene vessels were used throughout.

Preparation of silicon standard solution. Sodium hydroxide (10 ml of 7.5 M) was evaporated to dryness in a nickel crucible; 0.5 g of silicon dioxide was added and fused for 5 min. The residue was dissolved in water, acidified with 50 ml of 4 M nitric acid and diluted with water to obtain a solution containing 1000 μg Si g^{-1}.

TABLE 1

Instrumental parameters for the graphite furnace atomic absorption determination

Drying	30s	360K	Wavelength	251.6 nm
Ashing	55s[a]	1600K[a]	Slit width	150 μm
Atomization	10s	3000K[a,b]	Metal lamp current	10 mA
Inert gas flow (l min^{-1})			Hydrogen lamp current	20 mA
internal	50		Sample volume	10 μl
external	1			

[a]Standard settings; in some experiments other parameters were used. [b]Temperature-controlled heating [9], heating rate 1200 K s^{-1}.

Determination of silicon under isothermal conditions

Graphite of quality RWO (Ringsdorff Werk GmbH) was cut into pieces of 3 (± 0.3) mg and cleaned by heating in a graphite tube at maximum temperature for 10 s. Aliquots (1 μl) of 3 μg Si g^{-1} standard solution were pipetted onto these pieces and dried under an electric bulb. The graphite pieces were dropped into the furnace after it had reached the preset temperature of 2900 K. Introduction was facilitated by placing a graphite tube (3.0 mm i.d.) onto the sample port after enlarging the injection hole to 3.0 mm i.d. The lowest part of the light beam was masked in order to prevent its obstruction by the graphite pieces.

High-temperature equilibrium calculations

High-temperature equilibrium calculations were done as described in Part 1 [10]. To obtain a survey of potential interfering elements, the elements selected were H, O, N, Ar, Cl, S, C, Si and Na. The amounts of some of the elements (H, O, Cl and S) used in the calculations and the temperature were both varied over wide ranges so that a general idea of the critical parameters controlling the formation of Si(g) could be obtained. The input amount of carbon was kept rather low in order to simulate its incomplete reaction with oxygen. The input amounts of oxygen were chosen so that its partial pressures at equilibrium varied in the range 10^{-9}—10^{-21} atm (P_O = 3 × 10^{-11}—5 × 10^{-13} atm). The main species considered are given in Table 2.

RESULTS AND DISCUSSION

The silicon—carbon—oxygen system

The basic requirements for the formation of silicon atoms are illustrated in Figs. 1 and 2. Even at a partial pressure of 10^{-21} atm. of oxygen, a temperature of 2600 K is needed for the quantitative formation of Si(g). For clarity, the situation at this temperature is shown in Fig. 2: SiO(g) is formed at an oxygen pressure as low as 10^{-19} atm. (P_O = 10^{-11} atm.). It is interesting to note that SiO(g) is always formed between 1600 and 2000 K independently of the partial pressure of oxygen. It can also be seen that the main prerequisite for the formation of SiC(s) is an extremely low partial pressure of oxygen. The complexity of the system is accentuated by the dramatic changes in the distribution of silicon compounds as a result of relatively small changes in the partial pressure of oxygen. In practice, this means that the structure of carbon must be very important, since it will influence the reaction rate

TABLE 2

Species considered in the equilibrium calculations

Gaseous:	H, H_2, O, O_2, OH, H_2O, N_2, Cl, Cl_2, Ar, S, S_2, SO, HS, H_2S, COS, C, CS, CS_2, CHO, COCl, HCl, CH_4, CO, CO_2, Si, Si_2, $SiCl_2$, $SiCl_3$, SiH, SiN, SiO, SiO_2, SiC, SiC_2, SiS, Na, NaCl
Condensed:	C, Si, SiO_2, SiC, SiS_2, Si_3N_4

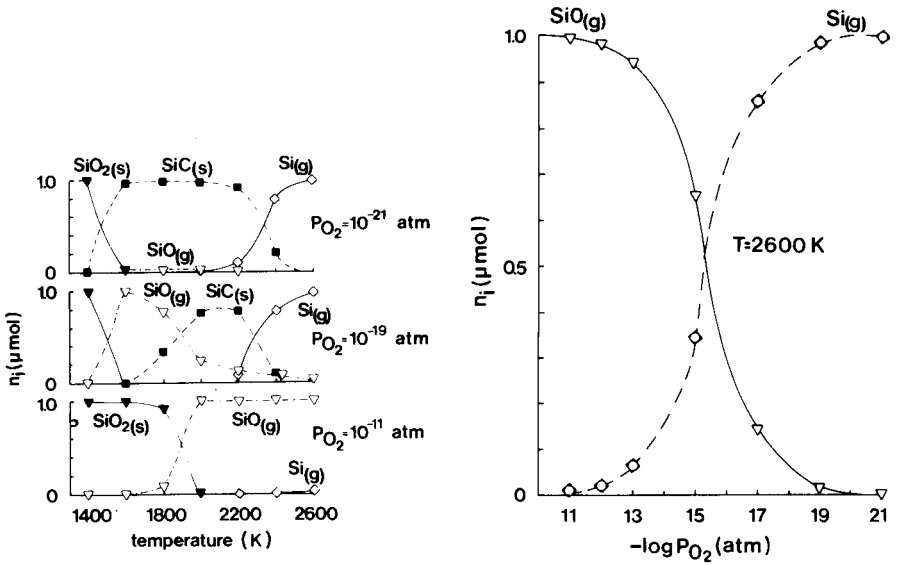

Fig. 1. The distribution of Si(g), SiO(g), SiO_2(s) and SiC(s) as a function of temperature for three different values of the equilibrium partial pressure of oxygen. The input amounts (μmol) used in the calculations were Ar = 2000, Si = 1, C = 15, H = 5 and Na = 10. The input amount of O_2 was varied so that the partial pressure of oxygen (atm.) became 10^{-21}, 10^{-19} and 10^{-11}, respectively, for all temperatures.

Fig. 2. The distribution of SiO(g) and Si(g) at 2600 K as a function of the partial pressure of oxygen. The same input amounts as those given in the legend to Fig. 1 were used for the calculation.

between carbon and oxygen. The extent of this reaction will determine the partial pressure of oxygen, which will decrease during the atomization step as the reaction between carbon and oxygen becomes more complete at higher temperatures. This aspect has been taken into consideration in Fig. 3 by including a rough estimate of the different partial pressures of oxygen in the temperature interval 1400—2600 K. Comparison with the results given in Fig. 1 shows that SiC(s) is stable only at higher temperatures.

The relevance of the basic assumptions made for the calculations which gave the results shown in Fig. 3, was checked by some experiments. Curve A of Fig. 4 shows the relative amounts of silicon atoms in the tube at different final temperatures. The temperature at which absorbance first occurred was found to be between 2100 and 2200 K which is in good agreement with the theoretical calculations given in Fig. 3. Curve B shows the signals obtained at maximum atomization temperatures, after pre-treatment at temperatures in the range 2100—3100 K. In disagreement with the calculations, some silicon was not atomized even at temperatures as high as 2900 K, indicating slow decomposition of SiC(s). It should be noted that temperature-controlled

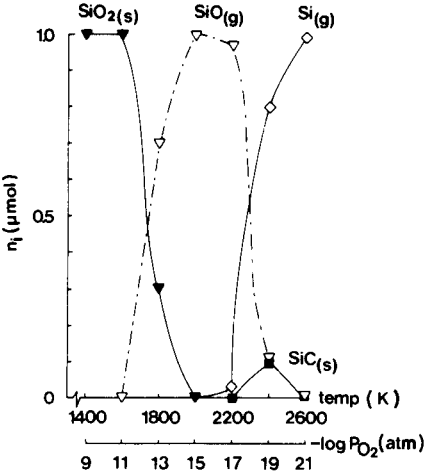

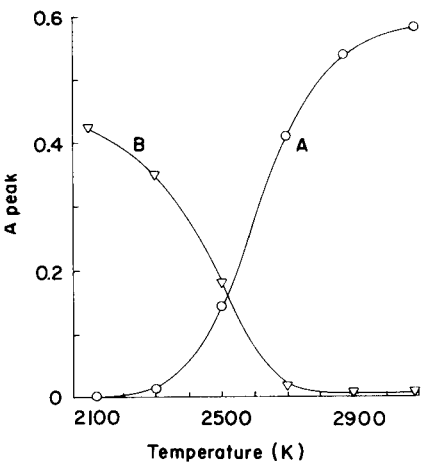

Fig. 3. The distribution of Si(g), SiO(g), SiO_2(s) and SiC(s) as a function of temperature and partial pressure of oxygen. The same input amounts as those given in the legend to Fig. 1 were used for the calculations.

Fig. 4. Curve A shows the peak absorbance values as a function of the atomization temperature used after ashing at 1600 K. Curve B gives the peak absorbance values obtained when atomizing at 2900 K after ashing the samples at the temperatures shown on the abscissa.

heating [9] was used, which means that the heating rate of the tube was the same for the different atomization temperatures used.

The theoretical results in Fig. 3 show that volatile silicon oxide is formed above 1600 K. Experimental results (Fig. 5) showed good agreement with those obtained from the equilibrium calculations. The facts that some silicon is lost from the system even at 1600 K and that a signal for silicon is not obtained below 2150 K (see Fig. 4) prove that a volatile molecule is formed in this temperature interval. Thus during heating of the tube, some of the silicon will be lost as SiO(g), reducing the concentration of silicon atoms. These losses should be minimized by vaporizing the sample isothermally at 2900 K. In order to provide further evidence for the validity of these calculations, the sensitivities obtained under isothermal and non-isothermal atomization conditions were compared at 2900 K. Under isothermal conditions, the sensitivity was improved by a factor of 2.5, which suggests that silicon compounds are removed from the tube during gradual heating. At atomization temperatures above 2900 K, the sensitivity is likely to be decreased because of the formation of SiC_2(g). For example, at 3000 K the percentage fraction of SiC_2(g) at equilibrium is about 10%.

The influence of water

As can be seen in Fig. 5, the peak values for silicon increased by 35% when the ashing temperature was raised from 1300 K to 1500 K. This

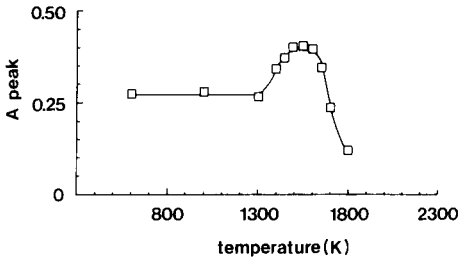

Fig. 5. Peak absorbance values obtained for 0.3 nmol of silicon as a function of the ashing temperature, with atomization at 2900 K.

increase in sensitivity could be due to the reduced amounts of water left in the graphite tube at the higher temperature. That water is tenaciously held by graphite is well known [11] and the role of water in connection with graphite-furnace atomic absorption spectrometry has been discussed in earlier parts of this series [12, 13]. The dependence of the formation of silicon atoms on the amount of water left in the graphite tube was tested as follows. After a silicon sample had been ashed at 1600 K, 10 μl of water was injected alongside the silicon sample and dried. The peak absorbances obtained in the following atomization step were 0.310 ± 0.025. When this extra water was not injected, the peak height absorbance was 0.476 ± 0.017 for the same amount of silicon.

The atomization of silicon in the presence of different amounts of water was simulated by using high-temperature equilibrium calculations. For example, in a situation corresponding to the presence of 0.3 μg of water in the tube during atomization, the calculated decrease in the amount of silicon atoms formed was 8% at a temperature of 2600 K. This happens because the water vapour equilibrium reaction is displaced to the right for increasing input amounts of water. This results in higher equilibrium partial pressures of oxygen as well as hydrogen, compared with a calculation in which only oxygen and carbon are included.

The influence of nitrogen

Higher absorbance values for silicon can be obtained if the tube is flushed with nitrogen instead of argon, in confirmation of the results of Manning and Fernandez [3]. These findings are consistent with the results obtained by theoretical calculations (Fig. 6); the formation of SiO(g) is somewhat depressed because of the formation of $Si_3N_4(s)$.

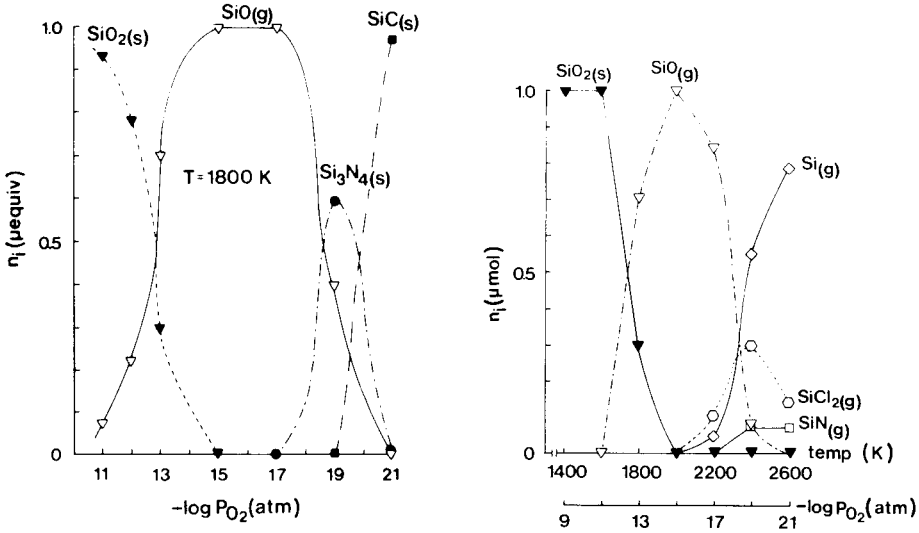

Fig. 6. The distribution of Si(g), SiO(g), SiO_2(s), SiC(s) and Si_3N_4(s) as a function of the partial pressure of oxygen at 1800 K. The input amounts (μmol) used in the calculations were: N_2 = 2000, Si = 1, C = 15,H = 5 and Na = 10.

Fig. 7. The distribution of silicon compounds as a function of temperature and partial pressure of oxygen. The input amounts (μmol) used in the calculations were Si = 1, C = 15, H = 5, N = 4000, Cl = 10 and Na = 10.

Interferences caused by chlorine, sulphur and nitrogen

Figure 7 shows the distribution of silicon compounds calculated for a system containing a 10-fold excess of chlorine over silicon. These results are based on the assumption that the partial pressure of oxygen decreases at higher temperatures (see also Fig. 3). In separate calculations, it was found that the amount of silicon chloride decreased with increased input of sodium, because of the formation of gaseous sodium chloride. Experimental results for the interference of sodium chloride on silicon (Figs. 8 and 9) indicate that even very small amounts of chlorine are of importance. In practice, the amounts of sodium chloride left in the tube after a sample has been ashed, will be only a fraction of the amount injected (0.1 nmol). The decrease in the signal relative to a pure aqueous standard solution should be 15% for stoichiometric formation of $SiCl_2$(g) (Fig. 8). The fact that the experimentally obtained interferences are higher (40%) indicates that sodium chloride affects the formation of silicon atoms differently, e.g. by catalysis. Figure 9 gives further evidence for this hypothesis.

The influence of sodium sulphate on the formation of silicon atoms is illustrated in Figs. 10 and 11. As can be seen, the interference of sodium sulphate can be minimized by extending the ashing time at an optimum temperature. In theoretical calculations which included sodium sulphate,

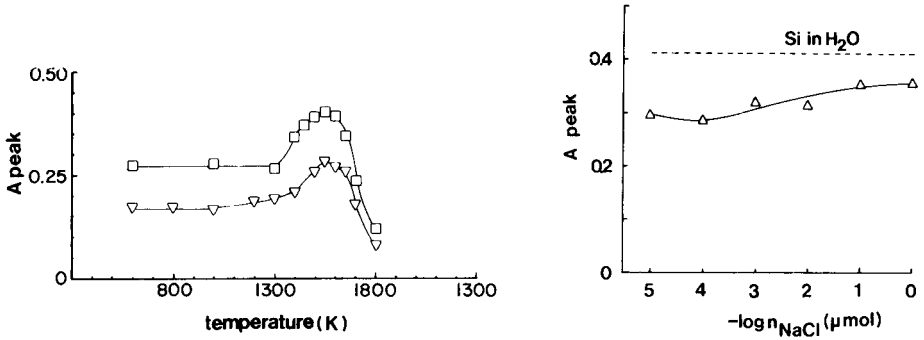

Fig. 8. Peak absorbance values as a function of various ashing temperatures: (□) 0.3 nmol Si; (▽) 0.3 nmol Si + 0.1 nmol NaCl.

Fig. 9. Peak absorbance values obtained for 0.3 nmol of silicon as a function of the amount of NaCl added. The ashing temperature was 1600 K in all cases.

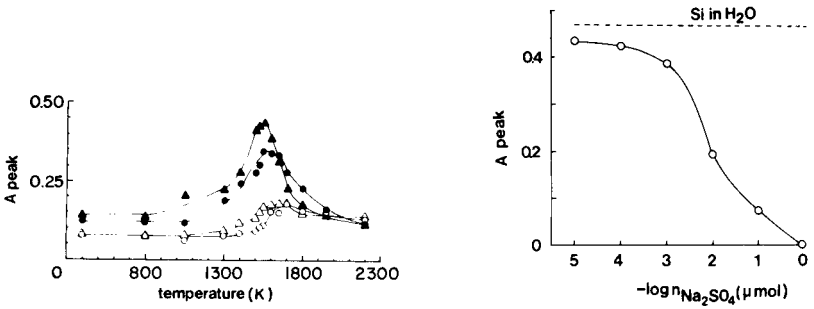

Fig. 10. Peak absorbance values obtained for 0.3 nmol of silicon as a function of ashing time, ashing temperature and amount of Na_2SO_4 added. Na_2SO_4 added: (▲, △) 1 nmol (●, ○) 10 nmol. Ashing time: (▲, ●) 95 s; (△, ○) 55 s.

Fig. 11. Peak absorbance values obtained for 0.3 nmol of silicon as a function of the amount of Na_2SO_4 added. The ashing temperature was 1600 K.

gaseous silicon sulphide was calculated to be formed stoichiometrically at partial pressures of oxygen lower than 10^{-14} atm for temperatures between 1600 and 2600 K. The relatively small interferences found experimentally are probably due to the removal of sulphur at temperatures at which silicon is present in the stable form of SiO_2(s).

Conclusions

In order to minimize chemical interferences during the determination of silicon the following conditions must be fulfilled. The partial pressure of atomic oxygen must be less than 10^{-12} atm during atomization. Losses caused by the formation of volatile silicon compounds are minimized by atomization

under isothermal conditions. Finally, interfering elements like sulphur and chlorine must be removed as completely as possible prior to atomization.

The authors thank Mr. Olof Sundström for valuable technical assistance and Dr. Janice Williams for correcting the manuscript.

REFERENCES

1 E. M. Carlisle, Fed. Proc., 31 (1972) 700.
2 K. C. Thompson, R. G. Godden and D. R. Thomerson, Anal. Chim. Acta, 74 (1975) 289.
3 D. C. Manning and F. Fernandez, At. Abs. Newsl., 9 (1970) 65.
4 H. M. Ortner and E. Kantuscher, Talanta, 22 (1975) 581.
5 D. B. Lo and G. D. Christian, Can. J. Spectrosc., 22 (1977) 45.
6 D. B. Lo and G. D. Christian, Microchem. J., 23 (1978) 481.
7 J. A. Rawa and E. L. Henn, Anal. Chem., 51 (1979) 452.
8 J.-Å. Persson, W. Frech and A. Cedergren, Anal. Chim. Acta, 92 (1977) 95.
9 G. Lundgren, L. Lundmark and G. Johansson, Anal. Chem., 46 (1974) 1028.
10 W. Frech and A. Cedergren, Anal. Chim. Acta, 82 (1976) 83.
11 R. Henning, J. Chim. Phys., 58 (1961) 12.
12 W. Frech and A. Cedergren, Anal. Chim. Acta, 82 (1976) 93.
13 J.-Å. Persson, W. Frech and A. Cedergren, Anal. Chim. Acta, 92 (1977) 85.

Analytica Chimica Acta, 113 (1980) 237—245

PRESERVATION AND STABILITY OF INORGANIC SELENIUM COMPOUNDS AT ppb LEVELS IN WATER SAMPLES

VENGHUOT CHEAM* and HAIG AGEMIAN

Canada Centre for Inland Waters, Special Services Section, Water Quality Branch, P.O. Box 5050, Burlington, Ontario (Canada)

(Received 2nd August 1979)

SUMMARY

The stability of inorganic selenium(IV) and selenium(VI) species at levels of 1 and 10 $\mu g\ l^{-1}$ has been studied under various conditions of pH, type of water and type of container. Polyethylene containers and adjustment to pH 1.5 provide optimum conditions of preservation for both distilled and natural water samples up to 125 days. Algal growth is detrimental to solution stability at natural pH values of 5.4—7.2, but adjustment to pH 1.5 with sulfuric acid successfully avoids this effect. Container size and temperature are also discussed. Storage of samples at 4°C gives satisfactory stability but is less practicable. The essential nature of preservation techniques applicable to interlaboratory quality control studies is emphasized.

Environmental studies are becoming increasingly dependent on analytical service laboratories, which must ensure reliability of results. Reliability, in terms of accuracy, precision and detection limit, is best achieved through intra- and interlaboratory quality control studies, but these in turn must comply with well defined conditions such as types of containers, preservatives and cleaning procedures as well as analytical methods. Sequences of preservation studies followed by interlaboratory quality control studies have been initiated in this laboratory for mercury [1, 2] and for seven herbicidal phenoxy acids [3, 4]. The present study is concerned with inorganic selenium species.

Most trace metals are effectively preserved with 0.2% (v/v) nitric acid [5]. The United States Environmental Protection Agency [6] has recommended nitric acid at pH < 2 for preservation of selenium in natural waters. Shendrikar and West [7] reported a loss of 2% when 1 ppm selenium (mg l^{-1}) was preserved with 0.5% nitric acid in polyethylene bottles for 15 days; an 8% loss was observed at pH 7. However, Pierce and Brown [8, 9] have shown that nitrate interferes seriously with the hydride generation method for selenium. This has been confirmed in this laboratory, and samples have instead been stored at 4°C. However, low-temperature preservation of bulk samples is not practicable for most laboratories and becomes a real problem when interlaboratory quality control samples have to be transported. No documentation for selenium preservation in natural waters other than those

cited seems to be available. The results reported below satisfy the criteria for long-term preservation. The observations made earlier [7] are useful, but are inadequate in assessing the integrity and preservation of environmental samples in round-robin studies for the following reasons: (a) the selenium concentration of 1 ppm used was much higher than that found in most environmental samples where concentrations lie in the ppb ($\mu g\ l^{-1}$) range; (b) only one type of water (probably distilled water) was used, whereas both pure synthetic solutions and contaminated natural waters should preferably be tested; (c) the selenium oxidation state was presumably Se(IV), but both Se(IV) and Se(VI) should be investigated, because both are important in the natural environment; (d) a test period of 15 days [7] is inadequate for a major quality control study, which requires no less than three months from the time of preparation of samples to confirmatory analyses, packaging, shipping and final analyses by participating laboratories.

In the work described here, sulfuric acid was found not to interfere with the hydride generation method and was therefore examined further. The container material and size were also found to be important parameters, particularly for long-term preservation purposes. Since preservation studies are a prerequisite to the success of round-robin analytical studies, the investigation described here took into account the effects of species, water types, concentration levels, pH and temperature.

EXPERIMENTAL

Containers

Two container materials, pyrex and polyethylene, were tested. The polyethylene containers were 25-gallon barrels with spigots (CANBAR Products Ltd.) and 500-ml Nalgene bottles; 500-ml pyrex bottles were also tested.

The stock, intermediate and standard solutions were made in pyrex volumetric flasks. All containers were cleaned with chromic acid, and rinsed with hot tap water and then with deionized distilled water, five times each.

Chemicals

All chemicals were of analytical-reagent grade. Sodium selenite and selenate (Ventron Corp., Alfa Products) were used to prepare 1000 mg l^{-1} stock solutions, which were preserved with 1% (v/v) sulfuric acid. The intermediate and standard solutions were prepared daily. Other chemicals used were: sodium borohydride and sodium hydroxide pellets (Fisher Scientific Co.), concentrated sulfuric acid and concentrated hydrochloric acid (Baker Analyzed Reagent).

Hamilton Harbour water

Table 1 shows some chemical data on Hamilton Harbour water relative to those of the other Great Lakes and to the mean of world river waters.

TABLE 1

Some water quality parameters reported for Hamilton Harbour [12], Lower and Upper Great Lakes [14], and World lake and river water [15][a]

Constituents	Hamilton Harbour	Lake Ontario	Lake Erie	Lake Huron	Lake Superior	Mean of World river waters
Calcium (mg l^{-1})	54	40.1	38	26.0	13.1	15
Magnesium (mg l^{-1})	11.6	8.2	8	7.2	2.8	4.1
Sodium (mg l^{-1})	30	13.1	11.4	3.1	1.2	6.3
Potassium (mg l^{-1})	5.37	1.4	1.2	0.8	0.5	2.3
Chloride (mg l^{-1})	61.2	28.3	24.5	5.6	1.2	7.8
Sulfate (mg l^{-1})	63	28.6	25.0	16.0	2.7	11.2
Hardness, total $CaCO_3$ (mg l^{-1})	183	134	128	95	44	54
Specific conductances (μmho cm^{-1})	511	344	292	207	97	149[b]
Complexing capacity (μg Cu l^{-1})	200[13]	55[13]	—	—	—	—
Total P (μg l^{-1})	73	24	28	5.5	5.0	—
Nitrate (mg N l^{-1})	1.89	0.14	0.337	0.282	0.308	0.23
Ammonia (mg N l^{-1})	1.13	0.01	—	0.003	0.002	—
Iron (mg l^{-1})	0.28	0.018	0.003	0.003	0.0022	0.67
Manganese (mg l^{-1})	0.09	0.0006	0.0005	0.0004	0.0003	—
Copper (mg l^{-1})	0.02	0.0012	0.0025	0.0005	0.001	0.010
Zinc (mg l^{-1})	0.06	0.0022	0.010	0.001	0.0037	0.010

[a]Mean Cu content of ordinary fresh waters is about 0.010 mg l^{-1} [15]. Mean Zn content of ordinary lake and river waters is about 0.010 mg l^{-1} [15]. The values reported for Hamilton Harbour are mean results observed in 1975. [b]Calculated from ref. 13.

The high levels of most contaminants in this water show that this represents the other extreme to distilled water. Furthermore, since the vast majority of water quality samples lies within these two extremes, Hamilton Harbour water becomes a good choice.

Preparation of synthetic and spiked solutions

Four 25-gallon barrels were filled with deionized distilled water and the other four barrels with unfiltered Hamilton Harbour water. The water volume in each barrel was determined by the weight and density of water. The barrels were then spiked with selenium(IV) and selenium(VI) at concentrations near 1 and 10 ppb. Each solution was then homogenized by closed circuit mixing for 3 h with a magnetic drive-pump (Fasco Industry Inc.).

Each spiked barrel was then subsampled into six 500-ml bottles, 3 pyrex and 3 polyethylene. The pH of these samples was adjusted to 1.5 (corresponding to about 0.2% H_2SO_4), 5.4 (the approximate pH of distilled water), and 7.2 (the approximate pH of Hamilton Harbour water). Sulfuric acid was used instead of nitric acid because nitrate interferes with the determination [8, 9] and in fact interferes with the method reported here as well as that routinely used by the Water Quality Branch, Ontario Region [10].

Selenium monitoring

The manifold for the semi-automated method developed in this labora-

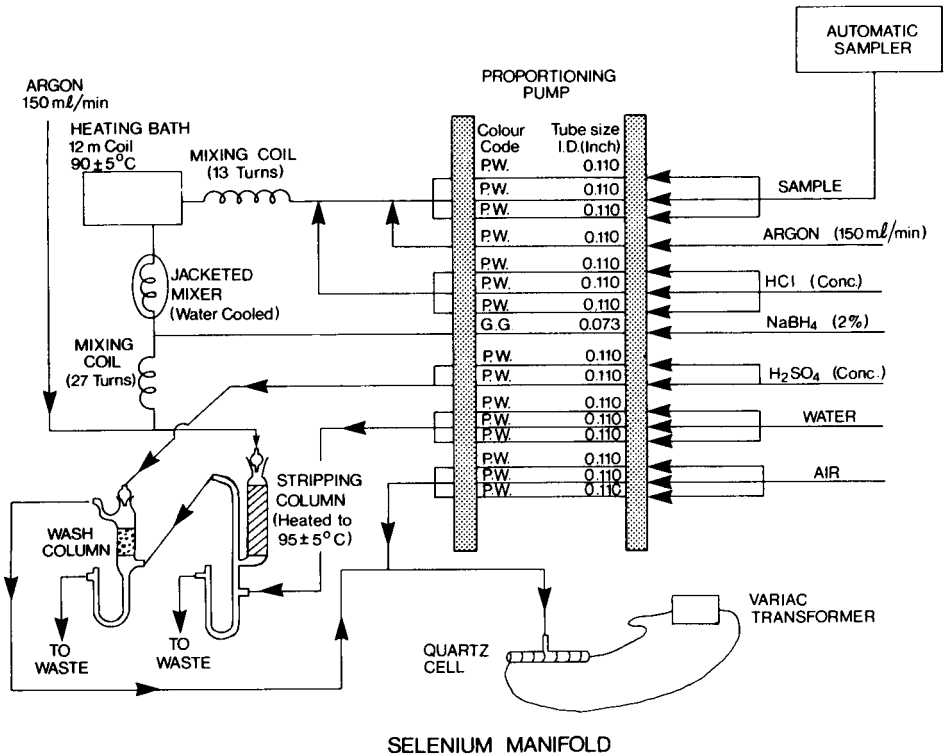

Fig. 1. Selenium manifold.

tory to measure inorganic selenium, i.e. Se(IV) and Se(VI), in water, is shown in Fig. 1. The technique is a modification of the system reported by Agemian and Cheam [11] for the determination of arsenic.

Throughout the study, all containers were kept at room temperature and the samples were monitored for a period of four months, during which many runs were made. The runs were more frequent at the beginning of the study and each consisted of about 60 actual analyses, including those on the barrels and individual bottles. The standards, made from the stocks on the day of each run, were used to produce calibration curves bracketing about every 12 samples.

RESULTS AND DISCUSSION

Before the natural water samples were spiked, the original amount of selenium had to be determined so that recovery data could be calculated. The mean total selenium content of the bulk Hamilton Harbour water was found to be 1.12 $\mu g\ l^{-1}$. The stability data presented in Figs. 2 and 3 are based on the recovery of selenium compared to the sum of original selenium level (zero for distilled water) and the spike level.

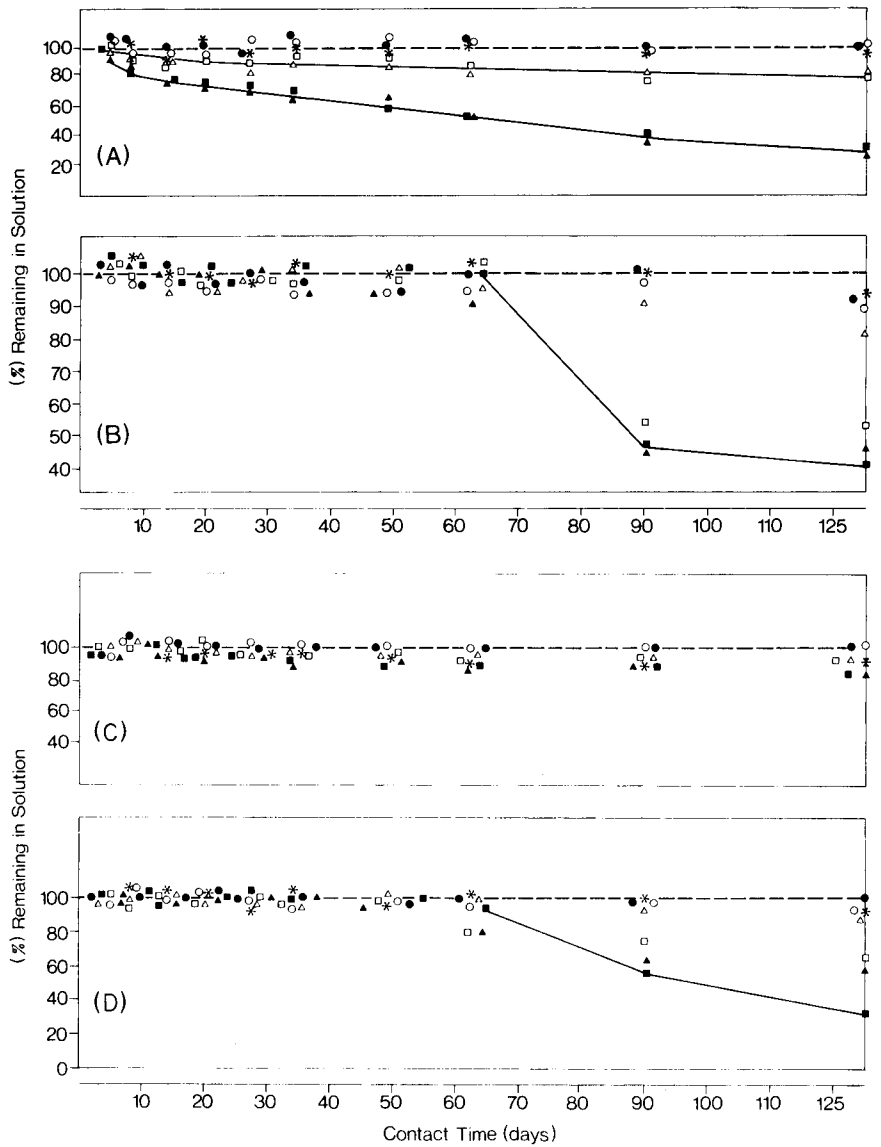

Fig. 2. Time-dependence of species remaining in solution for selenium(IV). (A) 1 ppb in distilled water; (B) 1 ppb in Harbour water; (C) 10 ppb in distilled water; (D) 10 ppb in Harbour water. Polyethylene bottles: (●) pH 1.5, (▲) pH 5.4, (■) pH 7.2. Pyrex bottles: (⊙) pH 1.5, (△) pH 5.4, (⊡) pH 7.2. Polyethylene barrels: (*) pH 5.4 for distilled water or pH 7.2 for Hamilton Harbour water.

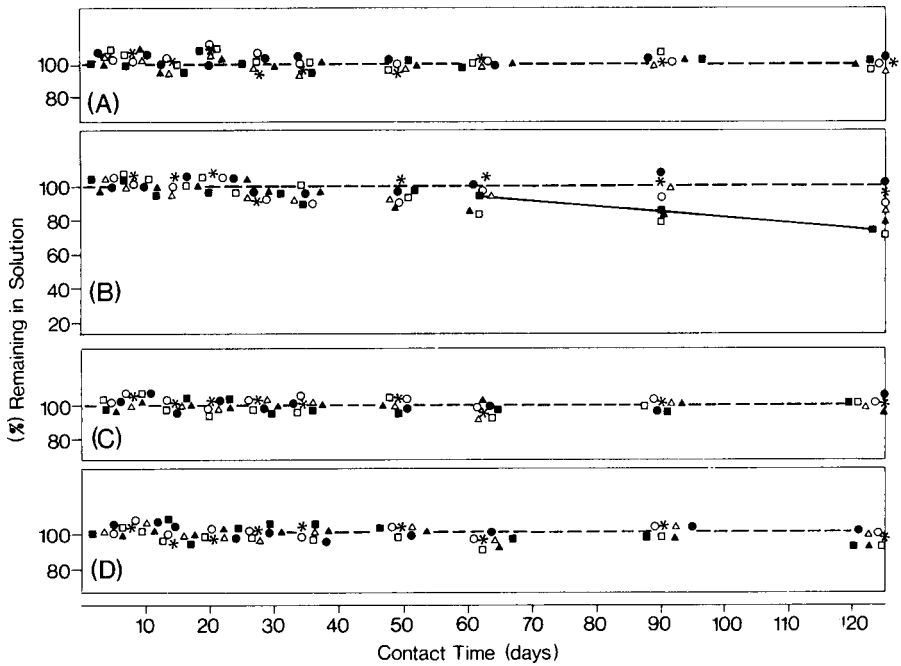

Fig. 3. Time-dependence of species remaining in solution for selenium(VI). (A) 1ppb in distilled water; (B) 1 ppb in Harbour water; (C) 10 ppb in distilled water; (D) 10 ppb in Harbour water. Polyethylene bottles: (•) pH 1.5, (▲) pH 5.4, (■) pH 7.2. Pyrex bottles: (⊙) pH 1.5, (◬) pH 5.4, (⧈) pH 7.2. Polyethylene barrels: (*) pH 5.4 for distilled water or pH 7.2 for Hamilton Harbour water.

Selenium(IV) preservation

As can be seen in Fig. 2, preservation of selenium(IV) at the 1ppb level in 500-ml pyrex or polyethylene bottles at pH 1.5 was satisfactory for both waters tested for the duration of the experiment. The higher pH values proved unsatisfactory in all cases, but pyrex was apparently a better container material than polyethylene, and Hamilton Harbour water a better preservative for selenium(IV) than distilled water. Shendrikar and West [7] have reported that pyrex is a superior material, particularly at pH 7.

An interesting point is that at pH 5.4 selenium(IV) losses occurred in both pyrex and polyethylene bottles, whereas complete recovery was obtained from the 25-gallon barrels for both types of water. This indicates that the size of the container, or rather its surface area per unit volume, directly influences the selenium(IV) stability. The volume of the barrel was 200 times greater and its surface area per unit volume 7 times smaller, than those of the 500-ml bottles, thus the smaller surface area per unit volume minimizes surface interactions. Such interactions are also minimized by increasing acid and ionic content as is shown by the better stability of acidified compared to unacidified samples and Hamilton Harbour water

compared to distilled water. The Hamilton Harbour water was stable under high pH conditions for about 60 days while in distilled water selenium(IV) contents started to deteriorate almost immediately.

Some practical implications can be derived from these results. First, a 25-gallon polyethylene barrel was effective for preserving bulk water samples at natural pH for about 4 months during interlaboratory studies whether distilled or Harbour water was used. This is significant, because full-scale interlaboratory quality control studies require bulk sampling, homogenization, spiking and storage. Secondly, for normal routine monitoring as well as for interlaboratory exchange tests, samples must be acidified to ca. pH 1.5 (with sulfuric acid). Only under such conditions are the effects of container material and water type removed.

Figure 2 also shows preservation curves for selenium(IV) at the 10 ppb level. In general, the results have similar trends as those found at the 1 ppb level, but it is clear that the tenfold increase in selenium(IV) concentration decreases the loss at the higher pH values tested. This effect is especially pronounced for distilled water where surface interaction is more important than for Harbour water.

There was no apparent improvement in the stability of selenium(IV) at the 10 $\mu g\ l^{-1}$ over the 1 $\mu g\ l^{-1}$ level in the Harbour water. However, a very significant observation was made for this type of water in the pH range 5.4—7.2. Traces of algae first appeared after about 6 weeks and became quite substantial after about 2 months. The appearance of algae corresponded quite accurately with the drop in selenium(IV) levels in solution. Evidently selenium(IV) was taken up by the algae. Thus, while an increased concentration of selenium(IV) in solution gave better stability in distilled water, bacterial activity (with resulting algal growth) became a serious source of losses for Harbour water at pH 5.4—7.2; bacterial activity in Hamilton Harbour water is generally high. The addition of 0.2% sulfuric acid effectively removed this bothersome interference from algae formation in all containers. The above data do not indicate differences in stability between 10 and 1 $\mu g\ l^{-1}$ solutions at pH values of 5.4 and 7.2 because any effect is masked by the algal interference.

Meaningful analysis of samples containing algae would require digestion of the whole sample in the original container with all algae destroyed to release the analyte. This is obviously undesirable for routine monitoring or interlaboratory programs, where sample integrity and homogeneity are vital, and blank values should be kept as low as possible. Fortunately, the acidification to pH 1.5 inhibits bacterial activity and provides a clear stable solution which is readily analyzed by the recommended system.

Selenium(VI) preservation

Figure 3 shows the preservation curves for selenium(VI) for different concentration levels, pH values, container materials and water types. Generally, selenium(VI) is more stable than selenium(IV) in aqueous solu-

tions. In the case of distilled water, recoveries are satisfactory for both glass and polyethylene bottles. Changes in pH in the range 1.5—7.2 or in concentration in the range 1—10 μg Se l^{-1} did not affect the stability for the duration of the test. With the harbour water, the selenium(VI) was again more stable than selenium(IV). The interfering effect of algae at pH 5.4 and 7.2 was drastically reduced from about a loss of 60% for selenium(IV) to 10—20% for selenium(VI) at both concentrations tested. Again, glass containers proved better than polyethylene. Acidification to pH 1.5 again provided satisfactory preservation for at least 125 days irrespective of water type, container type or level of the analyte.

These results show clearly that acidification to pH 1.5 (0.2% H_2SO_4) in glass or polyethylene bottles is generally satisfactory for preservation. The stability of selenium(IV) is more dependent on the acidity of solutions and bacterial activity; this is probably the predominant oxidation state in natural waters. Although glass containers give better results than polyethylene bottles at pH 5.4 or 7.2, adjustment to pH 1.5 in plastic vessels is clearly preferable for handling and shipping.

Effect of temperature

At day 125 of the test, 500-ml subsamples were taken from each barrel into eight polyethylene bottles, stored in a 4°C room for about one month, and then analyzed. The results were practically the same as those observed at day 125. Of particular interest is the result on the selenium(IV) sample (1 μg l^{-1}) in distilled water case. Extrapolation of the coresponding line in Fig. 2(A) indicates that the result would have been about 25% lower after storage at room temperature for the same time. Storage of unacidified Harbour water at 4°C would probably also increase the holding time.

Knowledge of the holding time is as important to the management of round-robin studies as that of the best stability conditions. Any samples acidified to pH 1.5 or any sample containing selenium(VI) in distilled water are convenient. However, if the sulfuric acid content interferes with some analytical methods and if natural waters are to be tested, then it may be preferable to use unacidified natural water in polyethylene bottles stored at 4°C.

Interlaboratory quality control study

The preferred conditions of acidification to 0.2% (v/v) sulfuric acid and storage at room temperature in polyethylene bottles were used in a national interlaboratory study [16]. Ten samples with concentrations in the range 0—1000 μg l^{-1} were distributed to 41 laboratories, and preliminary results indicate excellent recoveries throughout the concentration range, thus confirming the effectiveness of the proposed preservation method.

We thank O. ElKei for permission to use unpublished data, and Carm Pacenza for secretarial help.

ɪEFERENCES

1 J. Carron and H. Agemian, Anal. Chim. Acta, 92 (1977) 61.
2 K. I. Aspila and J. M. Carron, Interlaboratory Quality Control Study No. 16, Total Mercury in Natural Waters, Report Series No. 53 (1978), Inland Waters Directorate, Water Quality Branch, Ontario Region.
3 A. S. Y. Chau and K. Thomson, J. Assoc. Off. Anal. Chem., 61 (1978) 1481.
4 H. Agemian and A. S. Y. Chau, Interlaboratory Quality Control Study No. 24, Eight Phenoxy Acid Herbicides in Fresh Natural Water, Report Series, Inland Waters Directorate, Water Quality Branch, Ontario Region, in press.
5 Analytical Methods Manual, Inland Waters Directorate, Water Quality Branch, Ottawa, Canada, 1974.
6 Handbook for Sampling and Sample Preservation of Water and Wastewater, United States Environmental Protection Agency, EPA — 600/4-76-049, September 1976.
7 A. D. Shendrikar and P. W. West, Anal. Chim. Acta, 74 (1975) 189.
8 F. D. Pierce and H. R. Brown, Anal. Chem., 48 (1976) 693.
9 F. D. Pierce and H. R. Brown, Anal. Chem., 49 (1977) 1417.
.0 P. D. Goulden and P. Brooksbank, Anal. Chem., 46 (1974) 1431.
.1 H. Agemian and V. Cheam, Anal. Chim. Acta, 101 (1978) 193.
.2 Hamilton Harbour Study 1975, Ontario Ministry of the Environment, Water Resources Branch, Toronto, Ontario, Canada, August 1977.
.3 V. Cheam, A. Mudroch, P. G. Sly and K. Lum-Shue-Chan, J. Great Lakes Res., 2(2) (1976) 272.
.4 O. ElKei, Great Lakes Water Quality Data (1976), private communication.
5 D. A. Livingstone, Data of Geochemistry, 6th edn., Chemical Composition of Rivers and Lakes, Geol. Surv. Prof. Paper 440-G, Geological Survey, U.S. Department of the Interior, 1963.
.6 V. Cheam and K. I. Aspila, Interlaboratory Quality Control Study No. 26, Arsenic and Selenium in Water Samples. Report Series. Inland Water Directorate, Water Quality Branch, Ontario Region, in preparation.

Analytica Chimica Acta, 113 (1980) 247—252

THE REMOVAL OF CHLORIDE INTERFERENCE IN DETERMINATION OF CHROMATE ION BY ATOMIC ABSORPTION SPECTROMETRY WITH ELECTROTHERMAL ATOMIZATION

KOJI MATSUSAKI*

Department of Industrial Chemistry, Technical College, Yamaguchi University, Tokiwadai, Ube 755 (Japan)

TAKASHI YOSHINO

Department of Industrial Chemistry, Faculty of Engineering, Yamaguchi University, Tokiwadai, Ube 755 (Japan)

YUROKU YAMAMOTO

Department of Chemistry, Faculty of Science, Hiroshima University, Higashisenda-machi, Hiroshima 730 (Japan)

(Received 9th January 1979)

SUMMARY

Two mechanisms of chloride interference in the atomic absorption spectrometry of chromate in a graphite furnace have been established. The first is due to chloride salts remaining at the atomization step; this can be prevented by volatilizing the chlorides or converting them to oxides before atomization. The other arises from formation of chlorochromate ions, which can be removed by addition of an organic acid. The tetra-ammonium salt of EDTA is very suitable for this purpose.

Atomic absorption spectrometry with a graphite furnace is widely used for determination of metals because of its high sensitivity and rapidity. However, interference from cations, anions, acidity, organic substances etc is often encountered. In particular, chloride present in the sample or added during sample preparation may cause severe interference. Several mechanisms such as the formation of a volatile compound [1—3], a vapour-phase process [4—6] and occlusion of analyte in the matrix [7—9] have been proposed for chloride interference. The circumstances of the analyte change many times during the analytical process from the preparation of the sample to the final atomization, and the analyte may be involved in many kinds of interactions.

The process has been divided into three stages for this investigation, namely the dissolution step, the drying and ashing step, and the atomization step. The interference of chloride on the determination of the chromate ion has been measured and methods for its removal have been investigated. Chromium(VI) in solution exists as chromate or dichromate ions depending on the pH. In this paper, if not specified, both ions will be referred to as chromate for simplicity.

EXPERIMENTAL

Apparatus and reagents

A Varian-Techtron carbon-rod atomizer model 63 was used in conjunction with a Varian-Techtron model 1200 atomic absorption spectrometer. A tubular graphite cell was used and the absorption was measured under a nitrogen atmosphere. The signal was recorded with a Hitachi 056 recorder. A Hitachi chromium hollow-cathode lamp was used as the light source and a Varian-Techtron deuterium lamp for background correction. The sample was added with a 5-μl Excalibur Autopet fitted with a disposable tip.

All solutions were prepared from analytical-reagent grade chemicals and demineralized water, and stored in polyethylene bottles. The stock chromate solution (1000 mg Cr l^{-1}) was prepared by dissolving potassium dichromate in 0.1 M nitric acid.

Procedure

A 5-μl sample was deposited in the center of the graphite tube with the micropipette and dried, ashed and atomized with nitrogen flowing over the furnace at 5.5 l min^{-1}. The voltages and times for drying and atomization were always as follows: dry for 30 s at 0.65 V (ca. 110 °C) and atomize for 4 s at 7.0 V. The ashing step was varied as required. The absorption signals at the atomization step at 357.9 nm (0.2-nm bandwidth) were recorded and the peak-height was taken as the analytical signal. A reagent blank was run under the same conditions and a suitable correction applied. The absorption attributed to molecules of a volatile chloride was measured at the same wavelength as chromium by the use of the reagent blank solution under the same conditions. This molecular absorption was confirmed by using a deuterium lamp at the same wavelength. The applied voltage between the atomizer terminals was measured with a digital voltmeter connected in parallel and the temperature of the center of the graphite tube was measured with a platinum/platinum-rhodium thermocouple. The absorbances of chromate solutions containing various concomitants were measured and the ratio of their absorbances to the absorbance in the absence of concomitant (i.e., the relative absorbances) were calculated.

RESULTS AND DISCUSSION

Effect of chloride on atomic absorption of chromium

The effects of chloride concentration, pH of sample solutions, temperature during drying and ashing, and inert-gas flow rate during ashing were investigated. The interferences of the chlorides of H^+, NH_4^+, Na^+, K^+, Mg^{2+}, Ca^{2+}, Sr^{2+}, Ba^{2+}, Cu^{2+}, Fe^{3+} and Al^{3+} were investigated for 10^{-5}—10^{-1} M salt concentrations in hydrochloric acid solutions (pH 3—4) under the same ashing conditions (30 s at 1.6 V, ca. 550°C). As shown in Fig. 1, their effects may be classified as negligible, intermediate and extensive. The compounds

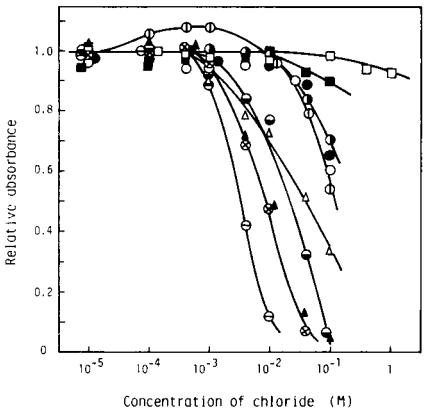

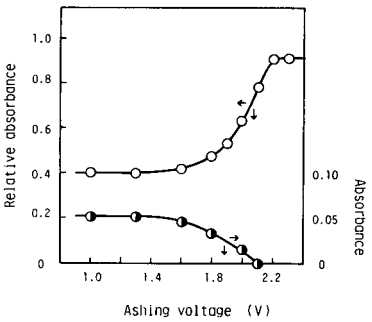

Fig. 1. Effect of some chlorides on the atomic absorption from chromate (0.1 mg Cr l^{-1}). (□) HCl, (■) NH_4Cl, (○) NaCl, (●) KCl, (◑) $MgCl_2$, (◒) $CaCl_2$, (⊙) $SrCl_2$, (▲) $BaCl_2$, (⊖) $CuCl_2$, (△) $FeCl_3$, (⊘) $AlCl_3$. $FeCl_3$ at pH 1; others at pH 4 acidified with HCl.

Fig. 2. Effect of ashing voltage on the atomic absorption from chromate (0.1 mg Cr l^{-1}) in the presence of 0.1 M NaCl. (○) Atomic absorption from chromate ion; (◑) molecular absorption of NaCl.

in the first group are HCl and NH_4Cl, in the second NaCl, KCl, $MgCl_2$ and $AlCl_3$, and in the third $CaCl_2$, $SrCl_2$, $BaCl_2$, $CuCl_2$ and $FeCl_3$ (these will hereafter be referred to as the first, second and third groups).

The effect of varying the ashing voltage for an ashing time of 30 s was examined; the results for 0.1 M sodium chloride are shown in Fig. 2. The absorption of chromium increases above an ashing voltage of 1.6 V (ca. 550°C) and becomes almost constant above 2.2 V (ca. 1000°C). The molecular absorption of NaCl begins to decrease at 1.6 V and has disappeared completely above 2.1 V, suggesting that all the NaCl volatilizes away when the ashing voltage exceeds 2.2 V for 30 s. The dependence of the interference on the ashing temperature for the chlorides in the first and second groups was similar to that for NaCl. These chloride interferences could be removed by controlling the ashing voltage at 0.65, 1.0, 2.2, 1.5 and 2.0 V (30 s) for HCl, NH_4Cl, KCl, $MgCl_2$ and $AlCl_3$, respectively. However, molecular absorption attributed to the third group chlorides was not detected during ashing up to 2.4 V (ca. 1160°C). In the atomization step, however, these molecular absorptions were detected by a deuterium lamp just before the atomization of chromium. Yasuda and Kakiyama [10] reported that the alkaline earth metal chlorides vaporize at 1800°C. The atomization temperature for chromium is 2700°C [11]. The third group chlorides therefore have such high vaporization temperatures that they cannot be removed in the drying and ashing step, and are present during the atomization step.

It is interesting that the interferences of $MgCl_2$ and $AlCl_3$ are not as extensive as those of the third group. After ashing at above 1.5 and 2.0 V for $MgCl_2$ and $AlCl_3$, respectively, their chloride interferences disappeared. Thermal analysis shows that $MgCl_2 \cdot 6H_2O$ decomposes to MgO, with an intermediate, MgClOH, formed at 459°C under a nitrogen atmosphere [12]. Thus magnesium chloride should decompose to magnesium oxide during ashing above 460°C and then behave in the same way as magnesium nitrate. Similar mechanisms apply to aluminium chloride [13].

The effect of pH was examined by testing solutions in the presence of 0.1 M sodium chloride; the pH was adjusted with hydrochloric acid and sodium hydroxide. Ashing was set at 1.3 V (ca. 350°C) for 30 s so that the chloride was retained until the atomization step. As shown in Fig. 3, below pH 6 there was severe suppression of absorption, but this largely disappeared above pH 12. Potassium chloride showed similar behavior. The interference of the other chlorides observed in acidic medium was diminished in alkaline media. However, in alkaline media, the reproducibility of the atomic absorption determination of chromium was invariably poor, presumably because of the precipitation of the hydroxides of these metal ions.

In alkaline medium, chromium(VI) exist as CrO_4^{2-}, but in acidic medium as $HCrO_4^-$ and $Cr_2O_7^{2-}$. In acidic solution, $HCrO_4^-$ reacts with chloride to form chlorochromate ions [14]

$$HCrO_4^- + Cl^- + H^+ = CrO_3Cl^- + H_2O$$

Thermal analysis [15] showed that alkali metal chlorochromates decompose thermally at 275°C as follows

$$8\ MCrO_3Cl \rightarrow M_2Cr_2O_7 + 2\ MCr_3O_8 + 4\ MCl + 2Cl_2 + 0.5\ O_2$$

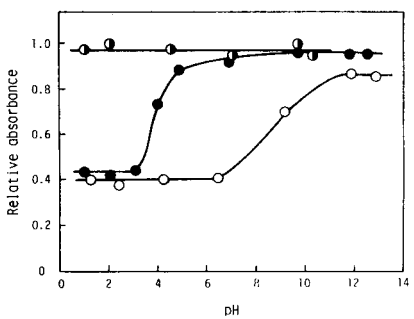

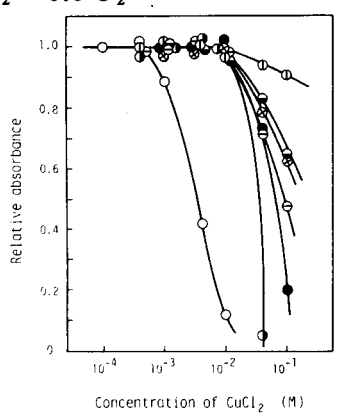

Fig. 3. Effect of pH on the atomic absorption from chromate (0.1 mg Cr l^{-1}) in the presence of 0.1 M NaCl. (○) No addition; (●) 0.01 M acetic acid added; (◑) 0.01 M oxalic acid added.

Fig. 4. Removal of $CuCl_2$ interference (on 0.1 mg Cr l^{-1}) by addition of other reagents. (○) No addition; (◑) 0.2 M HNO_3; (⊖) 0.1 M H_2SO_4; (⊖) 0.1 M glycine (NH_4); (⊛) 0.1 M tartrate $(NH_4)_2$; (●) 0.04 M citrate $(NH_4)_3$; (⊙) 0.05 M EDTA $(NH_4)_4$.

where M indicates an alkali metal; MCr_3O_8 decomposes above 400°C

$$2\ MCr_3O_8 \rightarrow M_2Cr_2O_7 + 2\ Cr_2O_3 + 1.5\ O_2$$

When MCr_3O_8 is mixed with an alkali metal chloride, the rate of decomposition in the absence of oxygen is much slower than that of pure MCr_3O_8, because $MCrO_3Cl$ is regenerated by the reaction

$$2\ MCr_3O_8 + 2\ MCl \rightarrow M_2Cr_2O_7 + 2\ MCrO_3Cl + Cr_2O_3$$

The decomposition of the chlorochromate salt in the furnace should be complete when MCl is volatilized away during the drying and ashing step. When MCl remains until the atomization step, the chlorochromate salt is regenerated as described above. The chlorochromate presumably interferes in the determination of chromate ion.

When acetic acid was added, the chloride interference was diminished above pH 4, and when oxalic acid was added, the interference was diminished even at pH 1, as shown in Fig. 3. It is interesting that acetic acid has a pK_a value of 4.8 and oxalic acid has $pK_{a1} = 1.3$, suggesting that the acetate and oxalate salts of concomitant metal ions prevent the chloride interference. Thermal analysis of mixtures of chromates and oxalates of alkaline earth metals shows that the reduction of Cr(VI) to Cr(V) and Cr(III) occurs at 250—600°C [16]. The acetates and oxalates, therefore, presumably accelerate the decomposition of the chlorochromates and even that of chromate.

The effect of the nitrogen flow-rate during the ashing step for the third group chlorides was measured, with constant nitrogen flow-rate during the atomization step. No effect was observed at low ashing voltage. However, the interference was decreased but not removed completely at flow-rates below 3 l min^{-1} when the ashing voltage was 2.2 V (ca. 1000°C) for 30 s. The same behavior was observed when oxygen was mixed with the nitrogen at high flow-rates. The furnace chamber used was of the open type, and atmospheric oxygen may be mixed into the nitrogen over the furnace at low nitrogen flow-rates. In the presence of air, the reaction with chloride is modified to [15]

$$2\ MCr_3O_8 + 4\ MCl + 2.5\ O_2 \rightarrow 3\ MCr_2O_7 + 2\ Cl_2$$

so that the regeneration of $MCrO_3Cl$ is diminished. Accordingly, chloride interference can also be improved by controlling the ashing temperature and nitrogen flow rate. But the disadvantage of applying this method is that the life of the graphite tube is shortened.

Removal of the interference

Two methods for removal of the chloride interference are indicated in the above discussion. The first is volatilization of the chloride, or conversion of the metal chloride to its oxide, before the atomization step. The other

is the addition of an organic acid to the sample solution. The practicalities of these methods were evaluated.

The third group chlorides ($CaCl_2$, $SrCl_2$, $BaCl_2$, $CuCl_2$ and $FeCl_3$) are difficult to remove completely simply by adjustment of the ashing temperature. Addition of mineral acids and organic salts to the sample solution were therefore tried. Figure 4 shows the relative absorbance of chromium in the presence of various concentrations of $CuCl_2$ and other compounds. The efficiency of these compounds in removing the depressive effect of $CuCl_2$ was in the order: tetraammonium EDTA > H_2SO_4 > diammonium tartrate > ammonium glycinate > triammonium citrate > HNO_3. The same trend was observed with the other metals of the third group, although an alteration of this order was sometimes observed. However, the efficiency of EDTA $(NH_4)_4$ was commonly greatest for all the third group chlorides. These effects may be explained at least partly by the substitution effects of the reagents. Presumably, there is anion substitution resulting in the formation of a readily volatilized chloride such as HCl or NH_4Cl at the ashing step. The resulting residual salts such as those of EDTA, sulfate, tartrate, glycinate, citrate and nitrate will be converted to oxides on heating. The ability of, e.g., EDTA to bind strongly with the cations to form water-soluble complexes also probably assists the substitution effect. The tetra-ammonium salt of EDTA is also a good reagent for removing the chloride interference by the second group of compounds even when lower ashing temperatures are used. The amount of additive needed is at least the quantity equivalent to the total metal ion content, but in practice is best determined for each sample.

REFERENCES

1 D. A. Segar and J. G. Gonzalez, Anal. Chim. Acta, 58 (1972) 7.
2 J. Aggett and A. J. Sprott, Anal. Chim. Acta, 72 (1974) 49.
3 C. W. Fuller, Anal. Chim. Acta, 81 (1976) 199.
4 J.-Å. Persson, W. Frech and A. Cedergren, Anal. Chim. Acta, 92 (1977) 85, 95.
5 W. Frech and A. Cedergren, Anal. Chim. Acta, 82 (1976) 88.
6 E. J. Czobik and J. P. Matousek, Anal. Chem., 50 (1978) 2.
7 R. B. Cruz and J. C. Van Loon, Anal. Chim. Acta, 72 (1974) 231.
8 J. Smeyers-Verbeke, Y. Michotte, P. Van den Winkel and D. L. Massart, Anal. Chem., 48 (1976) 125.
9 D. J. Churella and T. R. Copeland, Anal. Chem., 50 (1978) 309.
10 S. Yasuda and H. Kakiyama, Bunseki Kagaku, 24 (1975) 377.
11 C. W. Fuller, Electrothermal Atomization for Atomic Absorption Spectrometry, The Chemical Society, London, 1977, p. 70.
12 S. Shimada, R. Furuichi and T. Ishii, Kogyo Kagaku Zasshi, 74 (1971) 2006.
13 N. M. Drobot, L. L. Okhapkina and E. I. Kazakova, Izv. Vyssh. Uchebn. Zaved., Khim. Khim. Tekhnol., 14 (1971) 1453.
14 J. Y. Tong and R. L. Johnson, Inorg. Chem., 5 (1966) 1902.
15 J. J. Foster and A. N. Hambly, Aust. J. Chem., 29 (1976) 2137; 30 (1977) 251.
16 E. G. Derouane, Z. Gabelica and R. Hubin, Thermochim. Acta, 14 (1976) 315, 327.

Analytica Chimica Acta, 113 (1980) 253—267

IDENTIFICATION OF BARBITURATES FROM EXTRACTS OF URINE, STOMACH FLUID, LIVER AND KIDNEY BY HIGH-PERFORMANCE LIQUID CHROMATOGRAPHY AND FIELD DESORPTION MASS SPECTROMETRY[a, b]

H.-R. SCHULTEN* and D. KÜMMLER

Institute of Physical Chemistry, University of Bonn, Wegelerstr. 12, 5300 Bonn (Federal Republic of Germany)

(Received 22nd August 1979)

SUMMARY

The characteristic behaviour of a series of important barbiturates in field desorption mass spectrometry (f.d.m.s.) is described. Detection limits are reported for three standard barbiturates by f.d.m.s. and high-performance liquid chromatography (h.p.l.c.). The off-line combination of h.p.l.c. and f.d.m.s. is used in forensic investigations to identify these drugs unequivocally in body fluids such as urine and stomach fluids and in extracts from human liver and kidney tissues. Eighteen barbiturates were tested. The use of f.d.m.s. as an off-line h.p.l.c. detector provides detection limits ($S/N = 3:1$) ranging from 1 ng g^{-1} to 10 ng g^{-1}, depending on the compound and on the preliminary clean-up used.

In clinical and forensic toxicological investigations, urine is the commonly used sample fluid; in cases of acute poisoning, the stomach contents are used. The components of the latter are generally chemically unchanged, whereas in urine taken an hour after ingestion of a substance, metabolism must be considered [1]. In toxicological analysis, the presence of barbiturates can be quite quickly and easily demonstrated by thin-layer chromatography [2]. The identification of individual barbiturates in these body fluids, however, is more difficult and can be done unequivocally only by application of additional analytical techniques such as i.r. spectroscopy [3], n.m.r. spectroscopy [4] and mass spectrometry with electron impact [5] or chemical ionization [6].

High-performance liquid chromatography (h.p.l.c.) can be utilized for separation of polar from non-polar compounds. In contrast to gas chromatography (g.c.), h.p.l.c. separations of most substances are accomplished at room temperature so that thermal lability and involatility of the compounds offer no problems. Derivatization, such as is frequently required for g.c., is usually unnecessary.

[a]High-Resolution Field Desorption Mass Spectrometry Part VIII; for Part VII see: H.-R. Schulten and W. D. Lehmann, Anal. Chim. Acta, 93 (1977) 19.

[b]Presented in part at the European Conference for Biochemical and Instrumental Analysis, Analytica 78, Munich, 1978.

The characteristically high relative abundances of molecular or quasi-molecular ions and the minimal fragmentation of compounds observed in field desorption mass spectrometry (f.d.m.s.) provide good conditions for the application of f.d.m.s. as a substance-specific detector for h.p.l.c. By combining these techniques, analytical problems which are not amenable to solution by g.c.—m.s. can be investigated. The off-line combination of h.p.l.c. and f.d.m.s. has already been applied successfully to the separation and identification of steroids [7], vitamins [8], alkaloids [9], dyes [10], and natural porphyrins and chlorophyll derivatives [11]. The reliable determination and identification of biocides in river water at concentrations of 10—20 ng l^{-1} has also been reported [12].

This paper describes the isolation of barbiturates from human body fluids and structural tissue by h.p.l.c. and their unambiguous identification by low- and high-resolution field desorption mass spectrometry.

EXPERIMENTAL

Isolation of barbiturates from urine

Extraction and purification. Urine and gastric fluids were adjusted to pH 1—2 by addition of dilute hydrochloric acid (pH meter). The barbiturate-containing urine was extracted with methylene chloride with an Extrelut (Merck, Darmstadt) column. All others were liquid—liquid extractions done with chloroform in a separatory funnel.

The raw extract was concentrated under vacuum and the residue was taken up in a mixture of n-hexane and acetonitrile (1 : 1) and thoroughly shaken. The separated acetonitrile phase was used for h.p.l.c.

High-performance liquid chromatography. All separations were made with a Universal h.p.l.c. system (Siemens, S 100) equipped with a fraction collector. A spectrophotometer (Zeiss, PM2 DLC) served as the detector. Eluent and column were thermostatically maintained at 30°C.

For partition chromatography, the silica gel column (LiChrosorb SI 60, 5-μm particle size; Merck) was 250 mm long and 3 mm diameter, and a mixture of methylene chloride, ethanol and water served as eluent [13]. For reverse-phase chromatography, the LiChrosorb RP-18 column (10 μm particle size; Merck) was 250 mm long and 4 mm diameter, and mixtures of methanol/water or acetonitrile/water served as eluents. All the columns used were packed by standard procedures [14] at 400—600 bar.

For mass spectrometric identification, the appropriate h.p.l.c. fractions were concentrated and loaded on field desorption emitters under a microscope (magnification × 100) with microliter syringes [15]. The transfer of the coated emitter into the ion source of the mass spectrometer (including the pumpdown in the vacuum lock), takes approximately 2 min.

Identification by mass spectrometry

A Varian MAT 731 double-focusing mass spectrometer was used with a

combination e.i./f.d. ion source and electric recording. With electric recording, either the f.d. spectra were acquired and plotted with a Varian SS 200 data system or the ion beams of the individual molecular ion groups were integrated with a multichannel analyser (Varian CAT-1024). During the integration, the magnetic scan of the spectrometer externally controlled the multichannel analyser [16]; in this case, the data output was via an X-Y plotter (Hewlett-Packard 7004 B). Figure 1 shows schematically the instrumental setup for the coupling of the multichannel analyser to the magnetic mass spectrometer.

All f.d. spectra were measured after direct heating of the emitter (emitter heating current of 0—35 mA). The accelerating voltage was +8 kV for the field anode and —4 kV for the opposing cathode plate. For all measurements, high-temperature activated carbon emitters were used [17]. All spectra were acquired at a resolution between 1,000 and 2,000 (10% valley definition). High-resolution studies and accurate mass measurements were done as reported previously [18].

The time required for a determination of drugs in body fluids and tissues depends on the compound to be identified and the h.p.l.c. method used for separation. The barbiturate "barbital", for example, was identified in a urine extract (sample II, Fig. 6) in one hour by the procedure described. The time needed for sample preparation and chromatography

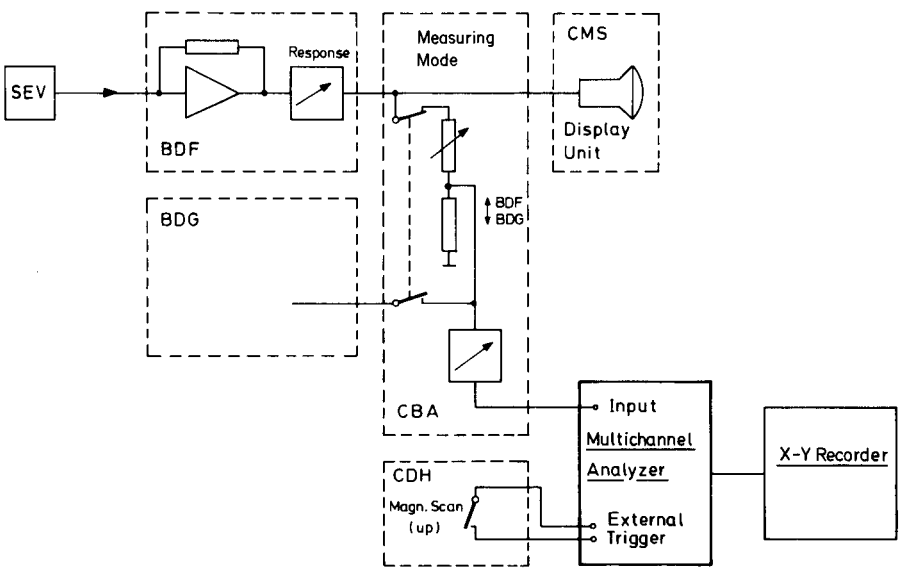

Fig. 1. Block diagram for the coupling of a multichannel analyser to a Varian MAT 731 mass spectrometer. This combination allows the accumulation of e.i., f.i., and f.d. ions generated by repetitive magnetic scans [21].

depends on the type of analytical problem, but the time required for mass spectral identification in routine use can certainly be decreased by the proposed method.

RESULTS AND DISCUSSION

The advantages of using the instrumental combination described above in f.d.m.s. for structural investigations [19, 20] and direct isotope determination [21, 22] of large natural products have been reported recently. The utility of the combination for the determination of endogenous [23] and exogenous [24] compounds from physiological fluids, pesticides in h.p.l.c. extracts [12, 25] and ultratraces of metals in high-purity solvents [26], human body fluids [27], and heart [28] and brain [29] tissues has also been demonstrated. These investigations widened the scope of analytical applications of f.d.m.s. considerably, and suggested the application of this method for forensic and toxicological studies.

F.d.m.s. of barbiturate standards

The barbiturates listed in Table 1 were investigated by f.d.m.s. The f.d. spectra of these drug standards showed the following characteristic properties. First, in every case intense signals were recorded for the molecular ion or for the protonated molecule. Secondly, if the barbiturate carries a cyclic substituent in position 5, the base peak of the f.d. spectrum is from the $[M]^{+\cdot}$ ion. Fragmentation of these barbiturates was observed only for heptabarb (Table 1, No. 17). In the f.d. spectrum of this barbiturate, an intense signal was recorded for a fragment ion of mass 221, which can be explained by loss of the ethyl group at the C-5 position. Thirdly, for barbiturates with only aliphatic substituents, intense signals were obtained in every case for fragment ions. The fragments were produced from cleavage of a side chain or parts of a side chain (e.g. m/z 223 for the $[(M + H) - HBr]^+$ ion in the f.d. spectrum of butallylonal (Table 1, No. 18). All the barbiturates with only aliphatic substituents gave spectra with signals 2—6 times more intense for the $[M + H]^+$ ion than for the molecular ion itself. Fourthly, for homologous compounds which differ only in the number of carbon atoms in the substituent at C-5 (Table 1, Nos. 1—4 and 9), the relative abundance for the $[M + H]^+$ ion increased with increasing carbon number. A hydroxyl group instead of a methyl group in position 2 (Table 1, Nos. 6 and 8) decreased the relative abundance of the $[M + H]^+$ ions. This characteristic behaviour of barbiturates in f.d.m.s. agrees with the results obtained by Games et al. [31].

For phenobarbital, hexobarbital and heptabarb (Table 1, Nos. 11, 13, 17), detection limits were established by the h.p.l.c.—f.d.m.s. method, both for single compounds and in mixtures. With the detection limit defined as a signal-to-noise ratio of 3:1, 50—100 ng of the barbiturate could be detected by the procedure described for application of partition chromatography. By applying reverse-phase chromatography, 10—20 ng of these barbiturates

TABLE 1

Barbiturate standards investigated by f.d.m.s.

No.	Chemical Abstracts Name	Synonyms[a]	M.w.[b]
1	5,5-Diethyl-2,4,6(1H,3H,5H)-pyrimidinetrione	Barbital	184.085
2	5,5-Di-2-propenyl-2,4,6(1H,3H,5H)-pyrimidinetrione	Allobarbital	208.085
3	5-Butyl-5-ethyl-2,4,6(1H,3H,5H)-pyrimidinetrione	Butobarbital	212.116
4	5-Ethyl-5-(1-methylpropyl)-2,4,6(1H,3H,5H)-pyrimidinetrione	Secbutabarbital	212.116
5	5-Methyl-5-phenyl-2,4,6(1H,3H,5H)-pyrimidinetrione	Heptobarbital	218.069
6	5-(2-Methylpropyl)-5-(2-propenyl)-2,4,6(1H,3H,5H)-pyrimidinetrione	Butalbital	224.116
7	5-Ethenyl-5-(1-methylbutyl)-2,4,6(1H,3H,5H)-pyrimidinetrione	Vinylbital	224.116
8	5-(2-Hydroxypropyl)-5-(2-propenyl)-2,4,6(1H,3H,5H)-pyrimidinetrione	Proxibarbal	226.095
9	5-Ethyl-5-(1-methylbutyl)-2,4,6(1H,3H,5H)-pyrimidinetrione	Pentobarbital	226.132
10	5-Ethyl-5-(3-methylbutyl)-2,4,6(1H,3H,5H)-pyrimidinetrione	Amobarbital	226.132
11	5-Ethyl-5-phenyl-2,4,6(1H,3H,5H)-pyrimidinetrione	Phenobarbital	232.085
12	5-(2-Cyclopenten-1-yl)-5-(2-propenyl)-2,4,6(1H,3H,5H)-pyrimidinetrione	Cyclopentobarbital	234.100
13	5-(1-Cyclohexen-1-yl)-1,5-dimethyl-2,4,6(1H,3H,5H)-pyrimidinetrione	Hexobarbital	236.116
14	5-(1-Methylbutyl)-5-(2-propenyl)-2,4,6(1H,3H,5H)-pyrimidinetrione	Secobarbital	238.132
15	5-Ethyl-1-methyl-5-phenyl-2,4,6(1H,3H,5H)-pyrimidinetrione	Methylphenobarbital	246.100
16	5-(2-Furanylmethyl)-5-(methylethyl)-2,4,6(1H,3H,5H)-pyrimidinetrione	Dormovit	250.095
17	5-(1-Cyclohepten-1-yl)-5-ethyl-2,4,6(1H,3H,5H)-pyrimidinetrione	Heptabarb	250.132
18	5-(2-Bromo-2-propenyl)-5-(1-methylpropyl)-2,4,6(1H,3H,5H)-pyrimidinetrione	Butallylonal	302.027

[a]As far as possible the international non-proprietary names (underlined) or common trivial names were used as recommended by the World Health Organization [30]. [b]Exact masses according to the elemental composition.

could be detected, since the smaller self-absorption of the mobile aqueous phase allowed the use of shorter wavelengths. When the detection limits in f.d.m.s. were established by electrically recording the molecular ion region of these barbiturates with repetitive magnetic scans and the multi-channel analyser, the detection limits for the barbiturates listed in Table 1 were found to be 1 ng or less, depending on the substance. For instance

when the molecular ion region of hexobarbital was recorded under optimal f.d. conditions in this manner, a 50-pg amount of material applied to the emitter was clearly detectable (signal-to-noise ratio 3 : 1). In general, these detection limits demonstrate that the sensitivity of the described procedure is sufficient to determine barbiturates in body fluids and tissues not only in cases of acute intoxication but also in therapeutic concentrations of drugs [32].

Identification of barbiturates from body fluids

In order to evaluate the feasibility of the analyses for barbiturates in physiological fluids by h.p.l.c.—f.d.m.s., test mixtures were first investigated. For this purpose, 25-ml samples of urine containing phenobarbital, hexobarbital and heptabarb (100 ml of urine with 1 mg of each barbiturate added) were extracted as described. The extract (25 ml of acetonitrile solution) was used for h.p.l.c. Figure 2 shows the chromatogram obtained from this urine extract with the reverse-phase column. In order to identify the barbiturate in the individual fractions, ten 50-μl aliquots of the urine extract were injected and fractionated. The appropriate fractions were analyzed by f.d.m.s. after evaporation of the solvent. Figure 3 (a—c) shows the molecular ion regions for phenobarbital, hexobarbital and heptabarb from the corresponding h.p.l.c. fractions recorded with f.d.m.s. and repeated

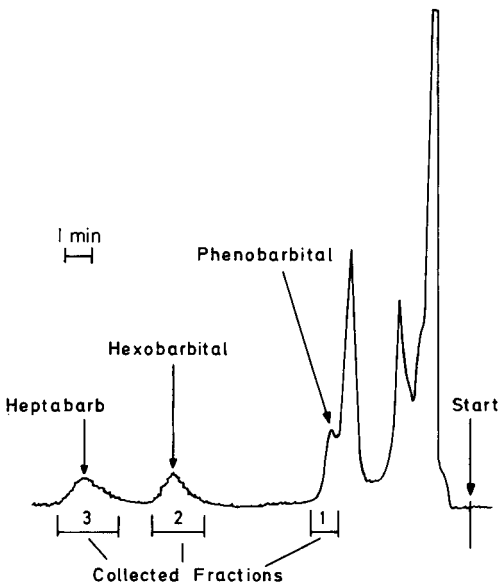

Fig. 2. Reverse-phase chromatography of a simulated urine sample with a barbiturate concentration of ca. 10 μg l^{-1}. Sample volume 50 μl; pressure 150 bar; flow rate 1.5 ml min^{-1}; mobile phase methanol/H_2O, 40 : 60; u.v. detection at 202 nm. The retention times indicate that fractions 1—3 contain phenobarbital, hexobarbital and heptabarb, respectively.

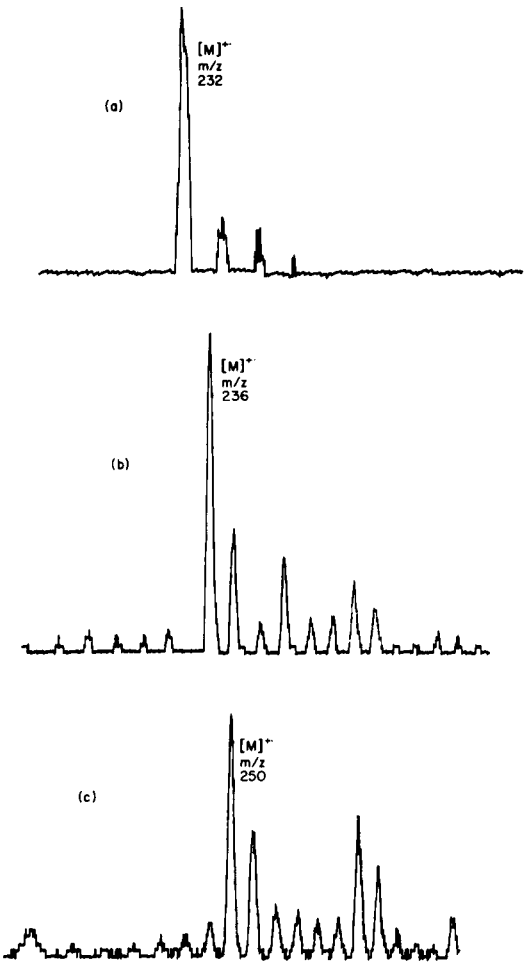

Fig. 3. Molecular ions of the barbiturates identified in the three fractions collected from the effluent of the run shown in Fig. 2. The f.d. mass spectra recorded with the multichannel analyser show the molecular ions of phenobarbital (m/z 232), hexobarbital (m/z 236) and heptabarb (m/z 250) in fractions 1—3, respectively, at the corresponding emitter heating currents; 20 magnetic scans in the range 2^8 (counts) were accumulated.

magnetic scans with the multichannel analyser. The identification of the barbiturates was based on comparison of their chromatographic retention times with the retention times of the corresponding standards (and the corresponding k values respectively) and on the mass spectral detection of their molecular ions in the collected h.p.l.c. fractions.

Identification of barbiturates from forensic samples (urine, gastric fluids, tissues)

After the off-line combination of h.p.l.c. and f.d.m.s. had proved successful

in identifying barbiturates from urines with the compounds added, the procedure was used to investigate two body fluid extracts from the Institute for Forensic Medicine of the University of Bonn. The first sample (I) consisted of a concentrated gastric liquid extract from a case of lethal barbiturate poisoning; the second sample (II) was a concentrated extract from 35 ml of urine obtained from a case of barbiturate intoxication. Both crude extracts were purified as described and dissolved in 25 ml of acetonitrile prior to h.p.l.c. Figure 4 illustrates the chromatogram of the gastric extract obtained under the described conditions; peaks 1—3 were collected with the fraction collector for investigation by f.d.m.s. By comparison of retention times (and k values) these peaks could be ascribed to phenobarbital (peak 1), amobarbital (peak 2) and secobarbital (peak 3). Figure 5 (a—c) shows the corresponding f.d. mass spectra of the collected h.p.l.c. fractions for peaks 1—3; it is apparent that the most intense signals come from the $[M]^{+\cdot}$ or $[M + H]^+$ ion of the barbiturates, indicative of 5,5-substituents. The barbiturates in this gastric liquid extract were identified independently of the methods described here by thin-layer chromatographic separation and i.r. spectroscopy in the Institute for Forensic Medicine; the same result was obtained.

The h.p.l.c. result from the urine extract (sample II; Fig. 6a) shows only one intense peak; this was ascribed to barbital by comparison of retention times. The peak was collected 5 times with the fraction collector and then

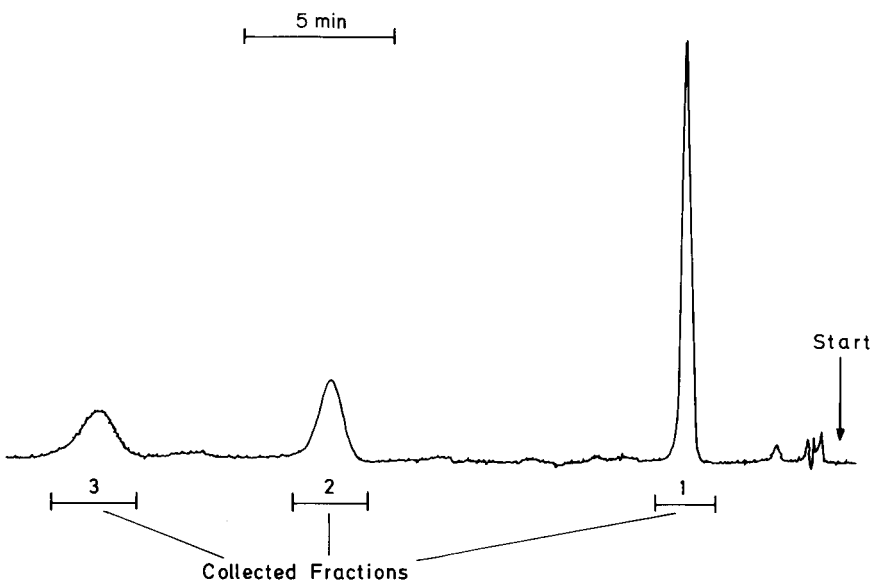

Fig. 4. Reverse-phase chromatography of an extract from stomach fluid (sample I, autopsy case). Sample volume 10 μl; pressure 200 bar; flow rate 2 ml min^{-1}; mobile phase, methanol/H_2O = 30 : 70 + 7% CH_3CN. According to the retention times, fractions 1—3 contain phenobarbital, amobarbital, and secobarbital, respectively.

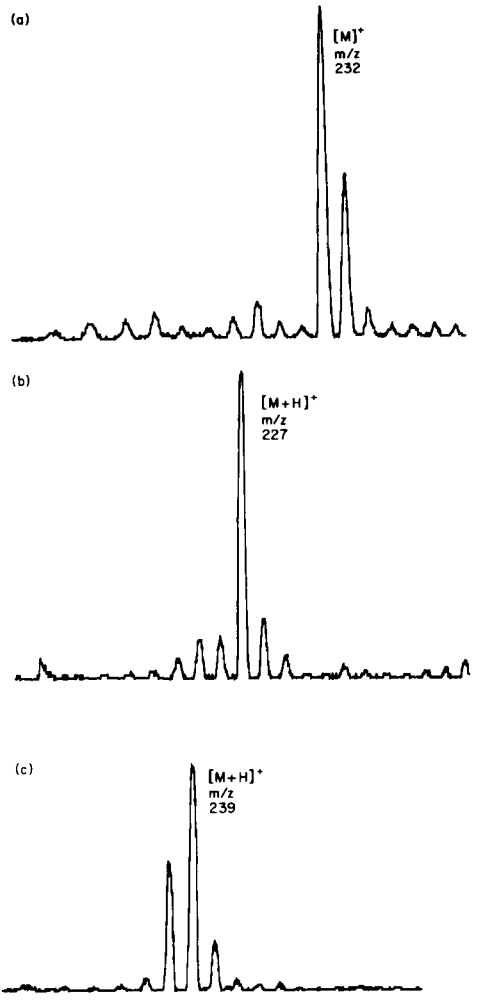

Fig. 5. F.d. mass spectra of the collected fractions as marked in the chromatogram in Fig. 4; 30 magnetic scans were accumulated in the multichannel analyser; the range was 2^9 (counts). The presence of phenobarbital, amobarbital, and secobarbital in fractions 1—3, respectively, was unambiguously confirmed.

investigated mass spectrally. Figure 6(b) shows the spectrum obtained in the range m/z 170—250. The base peak at m/z 185 arises from the $[M + H]^+$ ion of barbital (5,5-diethylbarbituric acid). The relatively high background obvious from this f.d. spectrum was also obtained with other urine extracts after chromatographic separation and is due to contaminating biological material carried over from the urine; the spectra from gastric liquid extracts had only small or no background after the h.p.l.c. separation. This situation, however, does not influence the certainty of the identification of a barbi-

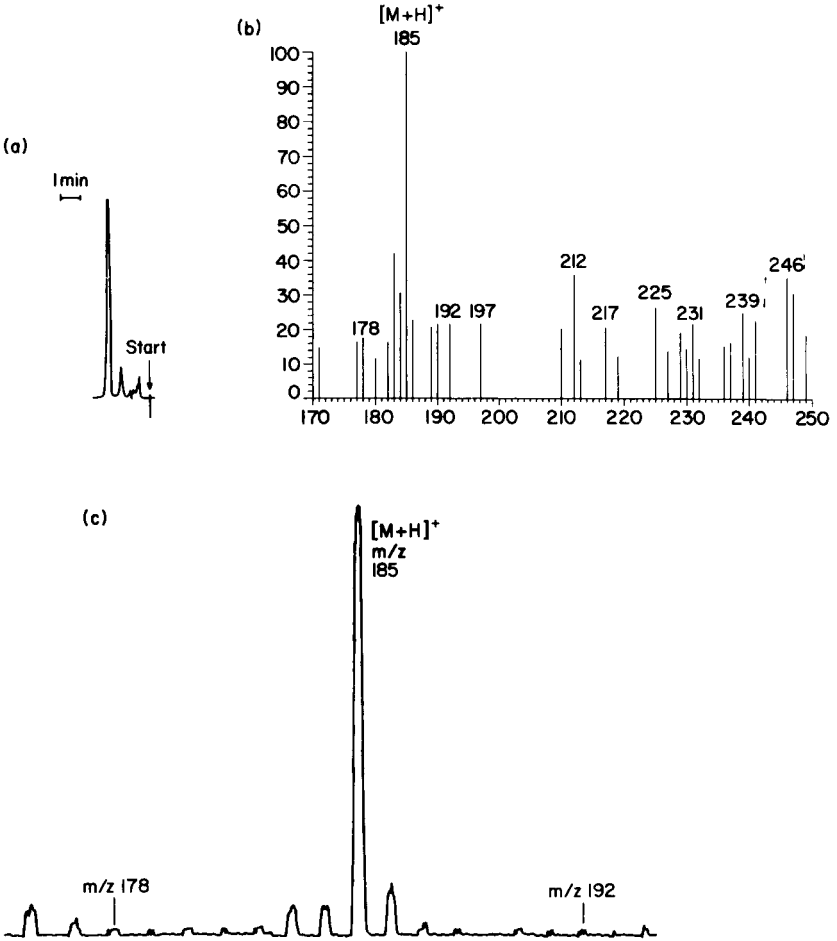

Fig. 6 (a) Reverse-phase chromatography of an extract from 35 ml urine (sample II, case of acute intoxication). Sample volume 10 μl; pressure 200 bar; flow rate 2 ml min^{-1}; mobile phase, methanol/H_2O = 30 : 70 + 7% CH_3CN. The retention time indicated the presence of barbital. (b) The electrically recorded, complete f.d. mass spectrum of the collected h.p.l.c. fraction. Eight consecutive mass spectra in the mass range between m/z 170 and m/z 250 were stored and averaged by the Varian MAT SS 200 data system. The emitter heating current was raised in 1 mA steps beginning from 12 mA. (c) The mass range between m/z 176 and m/z 194 was recorded by using 30 magnetic scans and the multichannel analyser (range 2^9) close to the best anode temperature of barbital.

turate from a urine extract. In general, only about 25% of a h.p.l.c. fraction was used for the qualitative f.d. spectrum of the fraction. In a second run, the f.d. signals of the barbiturate molecular group can, therefore, be investigated over a narrow mass range which allows more accurate analysis. Figure 6(c) shows the $[M+H]^+$ region of barbital recorded by f.d.m.s. with repeated magnetic scanning by a multichannel analyser. The accurate mass

measurement with f.d. and the peak matching procedure gave a value of 185.090 for the $[M + H]^+$ ion. The theoretical value for the elementary composition ($C_8H_{13}N_2O_3$) of this ion is *m/z* 185.093 (reference mass: homovanillic acid *m/z* 182.058). A direct f.d.m.s. analysis for barbital from the urine extract without chromatographic separation did not lead to the desired result. The f.d. mass spectrum in that case showed a multitude of ion signals at practically every mass in the range between *m/z* 18 and m/*z* 400.

When sufficient urine or stomach content is not available, or when the analysis of these body fluids gives negative tests, tissue extracts can be investigated. Barbiturates were identified in specimens from two autopsy cases by the h.p.l.c.—f.d.m.s. combination as follows. The samples were concentrated acidic chloroform extracts of human liver (sample III) and kidney (sample IV) which were prepared in the Institute for Forensic Medicine of the University of Bonn by the Stas—Otto procedure [33]. In both cases urine was not available and the examination of stomach content did not reveal the presence of toxic substances. The crude extracts were prepurified as described under Experimental and dissolved in 25 ml of acetonitrile before h.p.l.c. The chromatograms of both samples showed an intense peak with a retention time of 7.1 min; under the conditions defined for h.p.l.c. this retention time corresponds to the retention time of phenobarbital. By comparing the h.p.l.c. peak heights of the samples with the peak heights of phenobarbital standards, the amount of the barbiturate was estimated for one injection to be 280 ng in the liver extract and 600 ng in the kidney extract. The effluents under these h.p.l.c. peaks were sampled by the fraction collector and separately investigated by f.d.m.s. in order to confirm the identity of the drug. As shown in Fig. 7(b) for the effluent from sample III, the electrically recorded f.d. spectrum in the mass range between *m/z* 150 and *m/z* 350 exhibits the molecular ion of phenobarbital at *m/z* 232 with high relative abundance (base peak). With two exceptions, namely *m/z* 162 and *m/z* 163, all other signals are below 10% relative abundance. In contrast, the f.d. spectrum of 25 μl of the prepurified extract without h.p.l.c. in Fig. 7(a) shows a multitude of abundant ion signals. Owing to the soft ionization mode and judging from the numerous examples of mixture analysis by f.d.m.s., it can be assumed that most of these ions represent molecular ions of impurities. Thus the effectiveness of the clean-up by h.p.l.c. is demonstrated convincingly. In addition, there was still enough sample material available to record a smaller mass range with the multichannel analyser so as to obtain a clear picture of the molecular ion group (Fig. 7c) The isotopic pattern of this group provides further evidence for the correct assignment of the barbiturate, in particular when heteroatoms such as halogens are present, as has been illustrated for the identification of biocides in h.p.l.c fractions of surface water [12]. The final proof, of course, is given by the high-resolution data and it was indeed possible to establish accurate masses of the molecular ions of the barbiturates.

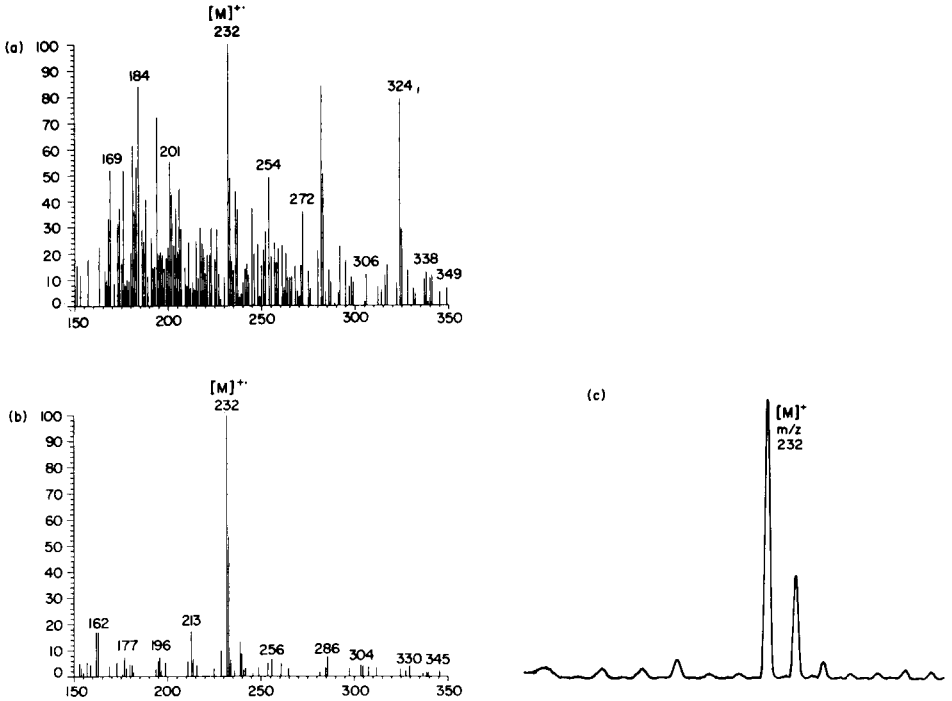

Fig. 7. (a) After prepurification, 25 μl of the crude extract of sample III (chloroform extract from liver tissue) were applied to the f.d. emitter and the mass spectrum recorded electrically (multiplier, data system) in the range between *m/z* 150 and *m/z* 350. (b) After reverse-phase chromatography of the same extract the fraction with the retention time of phenobarbital was collected, transferred to the f.d. emitter and the f.d. spectrum taken under the same conditions as described for (a). (c) Part of the collected h.p.l.c. fraction was used for recording with the multichannel analyser; 38 scans between *m/z* 226 and *m/z* 238 were accumulated (2^{12} range).

Similar results were obtained for the extract from kidney tissue. Figure 8(a) shows the complete f.d. spectrum before h.p.l.c. and Fig. 8(b) after the chromatographic step. Again the comparison proves the effectiveness of h.p.l.c., as the molecular ion at *m/z* 232 is only of 37% relative abundance and becomes virtually hidden in a "forest" of impurity peaks without the prior clean-up. When the multichannel analyser was used (Fig. 8c), almost only the molecular ions of phenobarbital were detected and the impurity at *m/z* 239, which was still prominent in the h.p.l.c. effluent (Fig. 8b), became negligible.

CONCLUSIONS

In summarising these experiences in the analysis of biological material by f.d.m.s., it can be stated that in the $\mu g\ g^{-1}$ range, simple extraction steps are

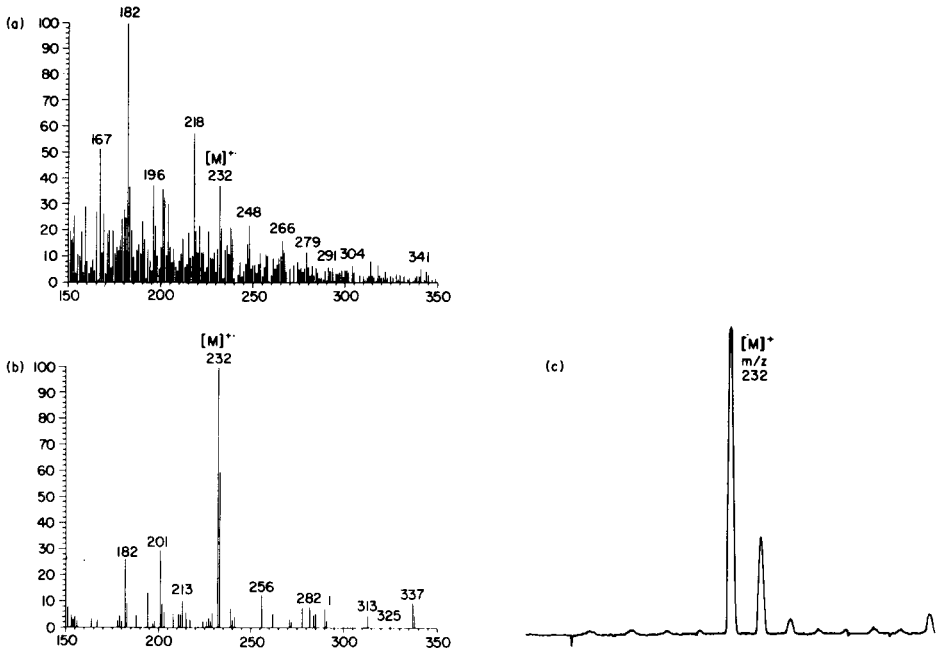

Fig. 8. (a) After prepurification, 25 μl of the crude extract of sample IV (chloroform extract from kidney tissue) were applied to the f.d. emitter. The experimental conditions described in Fig. 7(a) were used to obtain the f.d. mass spectrum. (b) Collection of the fraction "under" the h.p.l.c. peak and f.d.m.s. (c) Part of the collected h.p.l.c. fraction was used for recording with the multichannel analyser; 13 scans were accumulated in the range 2^{10} (see Fig. 7c).

in many cases sufficient for identification and determination. This has been illustrated very clearly for barbiturates in a case of overdose of hypnotics [34] and for an important metabolite of the anticancer drug cyclophosphamide [35]. However, at considerably lower concentrations of the compound in question, e.g. in the ng g^{-1} and pg g^{-1} range, it appears that well-designed h.p.l.c. is a crucial step for the efficient application of f.d.m.s.

The results described have shown, with some commonly used barbiturates as examples, that the combined application of h.p.l.c. and f.d.m.s. provides a reliable, rapid and relatively simple analysis for drugs in extracts of body fluids and tissues. The detection limits for barbiturates (ca. 10 ng g^{-1}) allow definitive identification of these substances, even when only a small amount of biological material is available for extraction. Since the compounds are already in solution in the individual h.p.l.c. fractions, they can be immediately loaded onto an f.d. emitter for mass spectrometry. This simple and direct process of manipulation from the chromatograph to the f.d. mass spectrometer is a special advantage of the technique as has also been demonstrated recently for the characterization of low-molecular-weight polymers

[36]. Thus, the requirement for a special complicated interface for highly polar compounds from the h.p.l.c. is avoided.

We are especially grateful to Prof. Dr. H. D. Beckey, University of Bonn, for his continuous support and interest. We thank Prof. Dr. S. Gonechea and Dr. K. J. Goebel, Institute for Forensic Medicine of the University of Bonn, for the forensic samples and for valuable discussions; R. Müller, Bonn, for technical assistance and cooperation; and the Deutsche Forschungsgemeinschaft, the Ministerium für Wissenschaft und Forschung des Landes Nordrhein-Westfalen, and the Fonds der Deutschen Chemischen Industrie for financial support.

REFERENCES

1 E. Vidic and K. Goebel, Arch. Toxicol., 19 (1961) 85.
2 J. Breiter, Kontakte, 3 (1974) 17.
3 A. Poklis and A. Z. Hameli, Arch. Toxicol., 34 (1975) 77.
4 G. Döring and H. Lackner, Arch. Toxicol., 26 (1970) 237.
5 E. F. Abdel-Bary, G. Bohn and G. Rücker, Fresenius Z. Anal. Chem., 266 (1973) 361.
6 H. M. Fales, G. W. A. Milne and T. Axenrod, Anal. Chem., 42 (1970) 1432.
7 H.-R. Schulten and H. D. Beckey, J. Chromatogr., 83 (1973) 315.
8 K. Habfast and H.-R. Schulten, 21st Annual Conference on Mass Spectrometry and Allied Topics, San Francisco, May 20—25, Paper H-7, 1973.
9 J. F. J. Hughes, N. Evans, D. E. Games, M. J. E. Hewlins, A. H. Jackson, R. Jackson, N. A. Khan, S. A. Matlin, M. Rossiter, R. G. Saxton, H. A. Swaine and K. T. Taylor, in A. Frigerio and N. Castagnoli (Eds.), Advances in Mass Spectrometry in Biochemistry and Medicine, Vol. I, Spectrum Publications, New York, 1976, p. 357.
10 C. N. McEwen, S. F. Layton and S. K. Taylor, Anal. Chem., 49 (1977) 922.
11 N. Evans, D. E. Games, A. H. Jackson and S. A. Matlin, J. Chromatogr., 115 (1975) 325.
12 H.-R. Schulten and I. Stöber, Fresenius Z. Anal. Chem., 293 (1978) 370.
13 C. Hesse and W. Hövermann, Chromatographia, 6 (1973) 345.
14 L. R. Snyder and J. J. Kirkland, Introduction to Modern Liquid Chromatography, J. Wiley, New York, 1974.
15 H. D. Beckey, A. Heindrichs and H. U. Winkler, Int. J. Mass Spectrom. Ion Phys., 3 (1970), App. 9, p. 11.
16 W. D. Lehmann and H.-R. Schulten, Angew. Chem., 89 (1977) 890.
17 H. D. Beckey, E. Hilt and H.-R. Schulten, J. Sci. Instrum., 6 (1973) 1043.
18 H.-R. Schulten and W. D. Lehmann, Anal. Chim. Acta, 93 (1977) 19 and references cited.
19 T. Komori, M. Kawamura, K. Miyahara, T. Kawasaki, O. Tanaka, S. Yahara and H.-R. Schulten, Z. Naturforsch., (1979).
20 R.-P. Hinze, H. M. Schiebel, H. Laas, K.-P. Heise, A. Gossauer, H. H. Inhoffen, L. Ernst and H.-R. Schulten, Liebigs Ann. Chem., (1979) 811.
21 W. D. Lehmann, H.-R. Schulten and H. M. Schiebel, Fresenius Z. Anal. Chem., 289 (1978) 11.
22 H. M. Schiebel and H.-R. Schulten, Tetrahedron, 35 (1979) 1191.
23 W. D. Lehmann, H.-R. Schulten and N. Schröder, Biomed. Mass Spectrom., 5 (1978) 591.
24 W. D. Lehmann and H.-R. Schulten, Fresenius Z. Anal. Chem., 290 (1978) 121.
25 H.-R. Schulten, Fresenius Z. Anal. Chem., 293 (1978) 273.

26 H.-R. Schulten, U. Bahr and W. D. Lehmann, Mikrochim. Acta, (1979) 191.
27 W. D. Lehmann, U. Bahr and H.-R. Schulten, Biomed. Mass Spectrom., 5 (1978) 536.
28 H.-R. Schulten, R. Ziskoven and W. D. Lehmann, Z. Naturforsch., 33c (1978) 178.
29 (a) H.-R. Schulten, W. D. Lehmann and R. Ziskoven, Z. Naturforsch., 33c (1978) 484.
29 (b) C. Achenbach, U. Bahr, F. Köhler, H.-R. Schulten and R. Ziskoven, Angew. Chem., 91 (1979) 944.
30 M. Newger, Organic Chemical Drugs and their Synonyms, Akademie Verlag, Berlin, 1978.
31 D. E. Games, A. H. Jackson, K. T. Taylor and N. J. Haskins, in A. Frigerio and N. Castagnoli (Eds.), Advances in Mass Spectrometry in Biochemistry and Medicine, Vol. I, Spectrum Publications, New York, 1976, p. 383.
32 U. Bahr, H.-R. Schulten, O. R. Hommes and F. Aerts, Clin. Chim. Acta, in press.
33 E. Graf and F. R. Preuß, in Gadamers Lehrbuch der Chemischen Toxikologie und Anleitung zur Ausmittelung der Gifte, Verlag Vandenhoeck Ruprecht, Göttingen, 1969.
34 H. H. Gierlich, H. J. Heinen and H. D. Beckey, Biomed. Mass Spectrom., 2 (1975) 31.
35 W. D. Lehmann and H.-R. Schulten, Fresenius Z. Anal. Chem., 290 (1978) 121.
36 R. P. Lattimer, D. J. Harmon and K. R. Welch, Anal. Chem., 51 (1979) 1293.

Analytica Chimica Acta, 113 (1980) 269—276

THE AMPEROMETRIC DETECTION OF THYROID HORMONES FOLLOWING REVERSE-PHASE HIGH-PERFORMANCE LIQUID CHROMATOGRAPHY†

BRADFORD R. HEPLER, STEPHEN G. WEBER** and WILLIAM C. PURDY*

Department of Chemistry, McGill University, 801 Sherbrooke St. W., Montreal, Quebec, H3A 2K6 (Canada)

(Received 15th August 1979)

SUMMARY

The principle of an assay of the major thyroid hormones by an electrochemical technique is demonstrated. The separation of 3,3′,5-triiodothyronine, 3,3′,5′-triiodothyronine, and thyroxine, by reverse-phase high-performance liquid chromatography is followed by their electrochemical oxidation in a thin-layer electrochemical detection cell with a low-temperature isotropic carbon working electrode. The limits of detection found were in the subnanogram range with linear response in the ranges 0—125 ng for T_3 and 0—500 ng for T_4. The approach makes the simultaneous assay of total serum thyroid hormones feasible.

The assay of the major serum thyroid hormones 3,3′,5-triiodothyronine (T_3), and thyroxine (T_4) in thyrometabolic evaluation can be accomplished in several ways; following the rate of decrease in cerium(IV) ion concentration on the iodine-catalyzed reaction between cerium(IV) and arsenic(III) [1—3], competitive binding assay (c.b.a.) [4], radioimmunoassay (r.i.a.) [5—8], and chemical derivatization followed by gas chromatography with electron capture detection [9, 10]. Recent work by Nachtmann et al. [11] has demonstrated the principle of applying the iodine-catalyzed reaction to a post-column reactor system following separation of the thyroid hormones by reverse-phase high-performance liquid chromatography (h.p.l.c.) in determination of total serum thyroid hormone levels. Additionally, Burman et al. [12] have pointed to determining by r.i.a. levels of 3,3′5′-triiodothyronine (rT_3), a product of an alternative branch of the iodothyronine bio-synthetic pathway, in amniotic fluid and cord blood, as a means of evaluating prenatal and neonatal hypothyroidism. Of the listed methods, only the chromatographic, c.b.a., and r.i.a. techniques offer sufficient selectivity and sensitivity for routine analysis and interpretation in these evaluations of thyrometabolic status.

---

†Presented in part at the Joint Congress on Clinical Chemistry, Montreal, Quebec, Canada, June 25—29, 1979.

**Present address: Department of Chemistry, University of Pittsburgh, Pittsburgh, PA 15260, U.S.A.

Chromatographic techniques have the advantages of simultaneous assay of the major thyroid hormones [10, 11], as well as allowing for the assay of other iodinated thyronines and precursors [10, 11, 13—15]. This makes the chromatographic approach analytically attractive as more information is obtained per analysis in potentially less time. Electron-capture g.c. techniques, however, are in practice difficult to apply in routine analysis because of the necessity of derivative preparation [9, 10]. The ingenious post-column catalytic reaction—h.p.l.c. system suffers from band broadening and limitations on chromatographic conditions as sensitivity is lost with increasing organic content of the mobile phase [11]. Therefore, it would seem that a simple and flexible chromatographic determination of the iodinated thyronines still remains to be demonstrated.

Electrochemical detection of h.p.l.c. effluents, which has an acknowledged sensitivity and selectivity when applied to biochemical, clinical, and pharmaceutical analysis [16—18], offers a solution to this dilemma. In this work, the principle of thin-layer electrochemical detection (TLED) cell oxidation is demonstrated for the iodinated thyronines T_3, rT_3 and T_4, following their separation by reverse-phase h.p.l.c. Subnanogram detection limits were obtained.

EXPERIMENTAL

Apparatus

The liquid chromatographic system utilized consisted of a Waters 6000A solvent delivery unit used isocratically at a flow rate of 1.0 ml min^{-1}. The mobile phase was continually degassed by a laboratory-designed helium purge system. A Waters U6K injection valve was used to introduce samples to the chromatographic stream, either by a liquid syringe (Precision Sampling Corporation, pressure-Lok B-110 series) or a Hamilton gas-tight syringe (1725-SN). The column was a Waters μBondapak C_{18} column (0.39 × 30 cm), thermostated by a laboratory-designed water jacket at 60°C. Detection was done with a Waters model 440 absorbance detector at 254 nm connected in series with the laboratory-designed TLED cell seen in Fig. 1.

The cell was designed in the conventional configuration [19] machined from Kel-F, with an entry at C, and an exit at L, directly into a Kel-F conventionally designed external reference electrode chamber [16] which contained an Ag/AgCl reference electrode. A stainless steel capillary formed the exit conduit from this chamber and also served as the auxiliary electrode. This TLED cell design allowed for a low-temperature isotropic carbon (LTIC) [20] plate electrode E (a gift from the General Atomic Co., San Diego, CA 92138) to form one wall of the cell and function as a working electrode. A polytetrafluoroethylene (PTFE) template D (0.0025 cm thick; Johnson Plastics, Montreal, P.Q.) formed the inner chamber of the cell producing a total cell volume of 1.5 μl, while providing

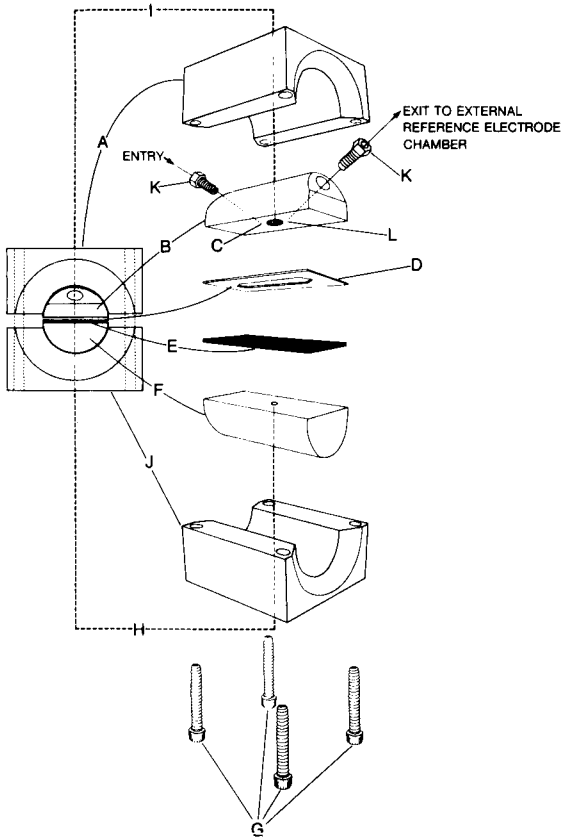

Fig. 1. Hemicylindrical TLED cell end view at left, exploded view at right. (A) and (J) are the upper and lower yokes machined from polyvinyl chloride for holding the hemicylindrical cell together; (B) and (F) are the upper and lower cell halves machined from Kel-F. (C) Entry port into inner chamber of cell; (D) PTFE spacer; (E) LTIC plate electrode; (G) stainless steel screws for holding yokes together; (H) electrical contact to LTIC plate; (I) Pt wire contact to implanted Pt disk electrode; (K) Altex 1/16-in. fittings; (L) exit port from inner chamber to external reference electrode chamber.

a working electrode area of 0.60 cm^2. Besides the novelty of the LTIC plate as a working electrode, a 0.78-cm^2 platinum disk, I, implanted on the opposite wall to the working electrode within the cell was "short-circuited" to the Ag/AgCl external reference electrode. This had the effect (Fig. 2a, c) of increasing the sensitivity by an order of magnitude, while qualitatively improving control of the potential across the working electrode. This latter fact became clear when similar relative peak height patterns were obtained for the short-circuited geometry at lower potentials compared to the standard external reference—auxiliary electrode geometry (Fig. 2b, c). Figure 2d is an example of a typical u.v. tracing observed regardless of the TLED cell geometry or potential applied. The elution order in all cases

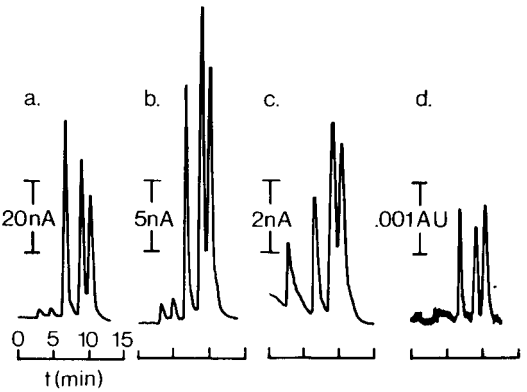

Fig. 2. Chromatograms of thyroid hormone separation at 1.0 ml min^{-1} flow rate, using a 50:50 0.1% H_3PO_4/methanol mobile phase, at a column temperature of 60°C, for 20-μl injections of a mixture of 100 ng each. Retention order is T_3, rT_3 followed by T_4. (a) Tracing for TLED cell at an applied potential of 1.000 V vs. the Pt disk short-circuited to the external Ag/AgCl reference electrode. (b) TLED cell at an applied potential of 0.800 V vs. the short-circuited reference electrode geometry. (c) TLED cell at an applied potential of 1.000 V vs. conventional external Ag/AgCl reference electrode configuration. (d) Representative u.v. detector tracing.

was T_3, rT_3 followed by T_4 for a 20-μl injection containing 100 ng of each hormone. Since the u.v. detector preceded the TLED cell, effects of extra-columnar band broadening and mixing were less so that band resolution was better. Even at this level the baseline noise in the absorbance detector chromatogram is quite evident.

The potentiostat utilized was a PAR-174A Polarographic Analyzer. Two Heath-Schlumberger, model SR-204 strip-chart recorders were used to record results at chart speeds of 0.1 in min^{-1}.

Reagents

The sodium salts (Sigma Chemical Company) were used to prepare stock 1.00 mg ml^{-1} standards of T_3 and T_4 in spectrograde methanol (American Chemicals Ltd.); these were stored at −20°C. The stock rT_3 standard (1.00 mg ml^{-1}) was prepared from rT_3 (Nuclear Medical Laboratories) in 0.1 M phosphate buffer pH 11 and stored at 4°C. Working standards were prepared as needed and diluted in the appropriate mobile phase. Chlorotrimethylsilane was obtained from Aldrich Chemical Company. All other reagents were of analytical-reagent grade.

Procedures

All glassware used was silylated with 10% (v/v) chlorotrimethylsilane—20% (v/v) pyridine in benzene solution. Chromatographic conditions were chosen on the basis of an in-depth chromatographic study presented elsewhere [14]. For this work, a 50:50 0.1% phosphoric acid/methanol mobile

phase was utilized at the conditions indicated. The u.v. detector and TLED cell followed the column in that order.

Hydrodynamic voltammograms were obtained by determination of peak heights (in duplicate) from chromatograms of 20-μl injections containing 100 ng each of T_3, rT_3 and T_4. Potential was varied from a region where no oxidation occurred to one in which a hydrodynamic plateau (potential-invariant peak heights) was observed.

To obtain precision data, 10 injections of the above-mentioned mixture were made at an applied potential of 1.000 V. Independently, calibration curves for T_3 and T_4 were obtained with only the TLED cell on line after the h.p.l.c. column. Duplicate injections (ranging from 1.0 to 100 μl) were made for a range of 0.625—100 ng for T_3, or 0.625—425 ng for T_4. These data were analyzed by the McGill Computing Cell using Calcomp. Detection limits were obtained by calculation of the size that the analytical signal would have at a signal-to-noise peak to peak ratio of 2:1.

RESULTS

In order to demonstrate the feasibility of the integrated electrochemical—h.p.l.c. technique, several points had to be studied. The iodothyronines had to have demonstratable electroactivity in the system studied, with good precision characteristics (no evidence of electrode fouling). Most important, adequate sensitivity was required for analysis in the clinically useful range.

The combined 4-e oxidation and hydrolysis of T_4 and several other iodinated precursors at a carbon paste (CP) electrode in a stationary system has been previously reported [21]. Because of the similar electrochemical behavior of the LTIC and CP electrode materials [20], it was considered that the iodinated thyronines would be amenable to oxidation in a TLED cell at an LTIC working electrode. Indeed, this was found to be the case, as can be noted from the chromatographic hydrodynamic voltammograms seen in Fig. 3.

With the absorbance and TLED detectors in series, the response of the electrochemical detector can be referred to that of the u.v. detector for each analyte tested. These ratios are functions of the chromatographic process, analyte concentration, detector geometries and the absorptive as well as the electrochemical characteristics of the specific analyte tested under the given experimental conditions. The plots of these ratios for 10 injections (in sequence) of a mixture of T_3, rT_3 and T_4 (100 ng each in 20 μl of mobile phase) are presented in Fig. 4. If loss of electrode area by polymerization, adsorption or filming effects was a problem, one would expect to see downward slopes in these plots as a function of number of injections. This is not observed; there is a random fluctuation about a central value. The precision (relative standard deviation) in these measurements was 0.0140, 0.0207 and 0.0161, respectively, for T_3, rT_3 and T_4. Similar electrochemical behavior was observed throughout a range of 45—65% (v/v) methanol

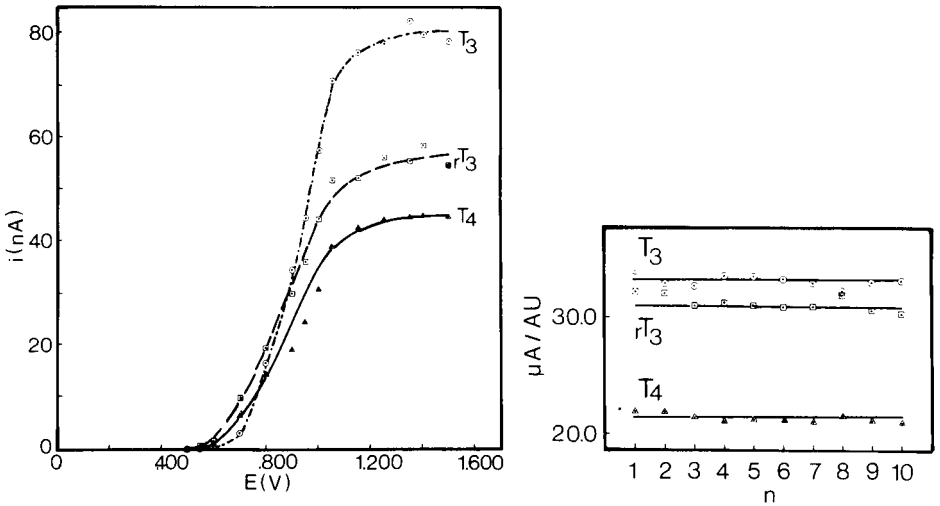

Fig. 3. Hydrodynamic voltammograms for (○)T_3, (□)rT_3 and (△)T_4. Peak heights vs. current are plotted as a function of applied potential utilizing the short-circuited reference electrode geometry. Values plotted are the average of two determinations. Chromatographic conditions are the same as in Fig. 2.

Fig. 4. Plot of the ratio of the TLED cell response to the absorbance detector response as a function of 10 sequential injections. Applied potential is 1.000 V vs. the short-circuited reference electrode geometry. Chromatographic conditions are the same as in Fig. 2.

content in the mobile phase, within which the area of practical chromatographic utility lies [14].

The calibration curves obtained for T_3 and T_4 were rectilinear in the ranges 0—125 ng T_3 ($Z = X - 29.740$; $Y = + 0.8969\ Z + 26.786$) and 0—500 ng T_4 ($Z = X - 66.450$; $Y = + 0.5928\ Z + 39.695$). The sensitivities (from the slopes) were 0.892 and 0.593 nA ng^{-1}, respectively, with intercepts of 0.108 and 0.306 nA. The detection limits were 0.120 ng for T_3 and 0.180 ng for T_4. Similar results would be expected for rT_3. For comparison, detection limits for the u.v. system were on the order of 10 ng for each hormone [14]. This agrees with values in the literature [13].

DISCUSSION

If one considers the normal serum ranges of total T_3 (TT_3) and total T_4 (TT_4) to be 1.2—3.1 $\mu g\ l^{-1}$ and 50—130 $\mu g\ l^{-1}$, respectively [22], it is easy to calculate that the total amount of T_3 or T_4 present in a 1.0-ml sample would be all that is necessary in principle for analysis by the combined h.p.l.c.-TLED technique over the ranges studied. Similar sample sizes would be predicted for total rT_3 (TrT_3) and TT_4 from amniotic fluid and cord

blood specimens [12]. The ability to run simultaneous assays for the major serum thyroid hormones is attractive in the context of potential savings in both time and cost.

Although the ultimate avenue for thyroid evaluation by laboratory methods may rest with the analysis of free circulating hormone (i.e. FT_3, FT_4 and FrT_3) levels [7, 8, 23], current work by Homburger and Hewan-Lowe [22] demonstrates the real usefulness of TT_3 and TT_4 serum levels in combination with the total serum thyrotropin level for predicting thyrometabolic status. Additionally, the elegant polyacrylamide gel filtration techniques [7, 8] with r.i.a. for quantification, which have been developed for FT_3 and FT_4 assay, still utilize a TT_4 as a screening device [8].

Work is currently underway to demonstrate clinical application of this technique, as well as to extend the principle of the h.p.l.c.-TLED approach to the lower limits of detection necessary for assay of free hormone. Since it is possible to obtain hydrodynamic plateaux in this analysis (Fig. 3) theory [24] predicts that greater sensitivities can be achieved with thinner cell thicknesses, larger working electrode areas, slower flow rates and/or changes to four-electrode geometry [25, 26], making this goal possible with existing techniques.

We thank Bruce Jon Compton for his interest and helpful discussions, and Dr. Russell Saunders for the gift of rT_3. We are very grateful to William Bastian for construction of the TLED cell utilized and to the Medical Research Council of Canada for their support.

REFERENCES

1 S. B. Barker, M. J. Humphrey and M. H. Soley, J. Clin. Invest., 30 (1951) 55.
2 E. B. Man, D. M. Kydd and J. P. Peters, J. Clin. Invest., 30 (1951) 531.
3 V. J. Pileggi, N. D. Lee, O. J. Golub and R. J. Henry, J. Clin. Endocrinol., 21 (1961) 1272.
4 B. E. P. Murphy and C. J. Pattee, J. Clin Endocrinol., 24 (1964) 187.
5 I. J. Chopra, D. H. Solomon and R. S. Ho, J. Clin. Endocrinol. Metab., 33 (1971) 865.
6 H. Gharib, R. J. Ryan and W. E. Mayberry, Mayo Clin. Proc., 47 (1972) 934.
7 L. J. McDonald, N. I. Robin and L. Siegel, Clin. Chem., 24 (1978) 652.
8 L. Siegel, L. J. McDonald and N. I. Robin, Clin. Chem., 24 (1978) 1891.
9 C. S. Hollander, Trans. Assoc. Am. Physicians, 81 (1968) 76.
10 B. A. Petersen, R. N. Hanson, R. W. Giese and B. L. Karger, J. Chromatogr., 126 (1976) 503.
11 F. Nachtmann, G. Knapp and H. Spitzy, J. Chromatogr., 149 (1978) 693.
12 K. D. Burman, J. Read, R. C. Dimond, D. Strum, F. D. Wright, W. Patow, J. M. Earll and L. Wartofsky, J. Clin. Endocrinol. Metab., 43 (1976) 1351.
13 M. T. W. Hearn, W. S. Hancock and C. A. Bishop, J. Chromatogr., 157 (1978) 337.
14 B. R. Hepler and W. C. Purdy, presented at the Joint Congress on Clinical Chemistry, Montreal, Quebec, June 25—29, 1979.
15 N. M. Alexander and M. Nishimoto, Clin Chem., 25 (1979) 1063 A.
16 P. T. Kissinger, Anal. Chem., 49 (1977) 447A.
17 P. T. Kissinger, C. S. Bruntlett, G. C. Davies, L. J. Felice, R. H. Riggin and R. E. Shoup, Clin. Chem., 23 (1977) 1449.

18 C. Bollet, P. Oliva and M. Caude, J. Chromatogr., 149 (1978) 625.
19 P. T. Kissinger, C. Refshauge, R. Dreiling and R. N. Adams, Anal. Lett., 6 (1973) 465.
20 B. R. Hepler, S. G. Weber and W. C. Purdy, Anal. Chim. Acta, 102 (1978) 41.
21 S. V. Tatwawadi, S. Piekarski, M. D. Hawley and R. N. Adams, Chem. Listy, 61 (1967) 624.
22 H. A. Homburger and K. Hewan-Lowe, Clin. Chem., 25 (1979) 669.
23 S. Berger and J. L. Quinn, Thyroid Function, in N. Tietz (Ed.), Fundamentals of Clinical Chemistry, W. B. Saunders, Philadelphia, 1976.
24 S. G. Weber and W. C. Purdy, Anal. Chim. Acta, 100 (1978) 531.
25 R. J. Fenn, S. Siggia and D. J. Curran, Anal. Chem., 50 (1978) 1067.
26 S. G. Weber and W. C. Purdy, Presented at the ACS/CSJ Chemical Congress, Honolulu, Hawaii, April, 1979.

Analytica Chimica Acta, 113 (1980) 277—285

THE THIRD ELEMENT EFFECT IN ANODIC STRIPPING VOLTAMMETRY

E. YA. NEIMAN, L. G. PETROVA, V. I. IGNATOV* and G. M. DOLGOPOLOVA

I.P. Bardin Central Scientific Research Institute of Ferrous Metallurgy, Moscow (U.S.S.R.)

(Received 5th July 1979)

SUMMARY

In anodic stripping voltammetry (a.s.v.) at graphite or mercury-film graphite electrodes, systematic errors caused by intermetallic compound formation can often be reduced or eliminated by addition of a "third" element. A theoretical background is discussed. Suitable "third" elements for a particular binary system can be chosen on the basis of the positions of the system components in the Periodic System. Experimental results for a.s.v. of zinc and of the copper—cadmium system are described in detail.

One of the main reasons for incorrect results in anodic stripping voltammetry (a.s.v.) at graphite electrodes is the interaction of deposited components on the electrode [1—4]. This interaction between the elements during electrolysis results in the formation of solid solutions, intermetallic or chemical compounds [1, 3, 5, 6]. In modern a.s.v. the simplest binary systems produced electrochemically may be subdivided [4] into the following main types. First, there are systems where components do not interact on the electrode surface at all; elements forming binary and more complex systems of this type comprise *d*-elements of Group II of the Periodic System (Zn, Cd, Hg), *p*-elements of Group III and IV (In, Tl, Sn, Pb) and bismuth electrodeposited in various combinations on graphite electrodes. Secondly, there are systems where components interact to form solid solutions during the electrolysis; among the elements forming deposits of this type, there are the *d*-elements of Group I of the Periodic System (Cu, Ag, Au) deposited with each other and also with Pb, Tl or Hg (metals of period 6). Thirdly, there are systems where components form intermetallic or chemical compounds during the electrolysis stage so that the stripping currents cannot serve as analytical signals in a.s.v. Systems of this group can be formed by simultaneous electrodeposition of *d*-elements of Group I with *p*-elements of Group II (Zn, Cd), *p*-elements of Groups III (Ga, In) and IV (Ge, Sn) and also with metals of the iron subgroup. In the fourth type, components forming binary systems interact during electrolysis to produce electrochemically active compounds, the stripping currents of which in the working potential range of the electrode can serve as analytical signals in a.s.v. Binary systems of this group are produced by simultaneous electrodeposition of As, Se, Te and metals of the

platinum subgroup with metals such as Pb, Sn, Hg, Cd, Au, Ag and Cu.

During the formation of systems of the second and third types at the electrode, accounting for, or eliminating, the mutual influences of the components becomes a necessary condition for obtaining accurate results in a.s.v. For this purpose, a mercury-film electrode has been recommended [7—12]; in many instances, this allows a considerable decrease of the interaction between the metals and improves the accuracy and precision of the method. However, it has been shown [13] that the use of the mercury-film electrode does not lead to suppression of the interaction processes in all the cases that can affect the accuracy of the analytical results. This is the reason for discussing [14, 15] the possibility of eliminating the mutual influences of the components determined by a.s.v., by introducing "third" elements [14] along with the mercury-film electrode into the test solution. This paper is devoted to applications of this effect in a.s.v. practice.

THEORY

In a.s.v., simultaneous electrodeposition of two elements Me_1 and Me_2 on a graphite electrode with formation of systems of the second or third type is characterized by the formation energy of the products of interaction, the change of Gibbs free energy ($\Delta G_{1\text{-}2}$) being the measure. In this case the analytical signal from the component Me_1 to be determined (maximum stripping current of Me_1 = $I_{max,1}$) is usually [15] described by the relation $I_{max,1} = K_{d,1}C_1$, where $K_{d,1}$ is a proportionality factor which depends on typical features of the particular electrode process and polarization conditions, and C_1 is the concentration of component Me_1. In the presence of component Me_2 in the solution and deposit, $I_{max,1}$ is expressed by the function $I_{max,1} = f(C_1, C_2)$, or for constant C_1, $I_{max,1} = f(C_2/C_1)$.

If the text solution contains a third component Me_3, which can deposit on the electrode during the deposition of Me_1 and Me_2 and interact with component Me_2 to form a more stable compound than the Me_1—Me_2 compound ($\Delta G_{2\text{-}3} \gg \Delta G_{1\text{-}2}$), then a new electrode process starts on the electrode and $I_{max,1} = f(C_1, C_2$ and $C_3)$. If C_2/C_1 is kept at a constant value (A), then $I_{max,1} = f(C_3/A)$. Thus, component Me_3 will influence the value $I_{max,1}$ depending on the ratio C_2/C_1 in the test solution.

There are several interesting cases from the analytical point of view. When the ratio C_2/C_1 exceeds the stoichiometric ratio C_2/C_1 for the Me_1—Me_2 compound, compounds between components Me_1 and Me_2 and also between Me_3 and the excess of Me_2 should be formed on the electrode. Under these conditions the influence of Me_2 on the analytical signal of Me_1 remains the same as in the absence of Me_3, and the effect of the "third" element is not observed.

With increase of C_3 in the test solution and of the content of Me_3 in the deposit on the electrode, the amount of component Me_2 interacting with Me_3 will increase and finally free atoms of component Me_2 will not be present on the electrode surface. Subsequent increase of C_3 will cause an increase in

the quantity of the Me_2—Me_3 compound in accordance with the relation $\Delta G_{2\text{-}3} \gg \Delta G_{1\text{-}2}$, and consequently the amount of the Me_1—Me_2 compound should be reduced. Thus some of component Me_1 does not participate in the formation of the Me_1—Me_2 compound, and can deposit on the electrode together with the Me_1—Me_2 and Me_2—Me_3 compounds, giving rise to the signal $I_{max,1}$.

When all the atoms of component Me_2 deposited on the electrode are involved in the Me_2—Me_3 compound, the analytical signal $I_{max,1}$ will no longer depend on C_2, and $I_{max,1} = f(C_1, C_3)$. If component Me_3 does not interact with component Me_1, then $I_{max,1} = f(C_1)$ and the effect of the "third" element eliminates the systematic error in the determination of component Me_1 in the presence of Me_2.

From these considerations, the main requirements for the "third" element in a.s.v. can be formulated as follows. First, the "third" element should not form solid solutions, intermetallic compounds or chemical compounds with the component to be determined. Secondly, the stripping potential of the "third" element from the electrode surface should be sufficiently different from the stripping potential for the test component to avoid superimposition of the anodic currents of the two components. Thirdly, the content of the "third" element in the test solution should be such that the analytical signal of the element determined does not depend on the ratio C_3/C_2, i.e., a sufficient excess of the "third" element should be added.

EXPERIMENTAL

The d.c. polarographs used were the 7-77-4/b (Hungary) and PO-5122 (U.S.S.R.) models. The electrodes were microdisc (surface area 0.04 cm^2) graphite working electrodes [16, 17] and a saturated calomel reference electrode.

Electrochemical deposition of components of the test systems was done at a potential corresponding to the limiting cathodic current of the most negative component of the system. In the case of mercury-film graphite electrodes produced in situ [8, 10, 12], electrochemical cleaning of the electrode was done for 2 min in a stirred solution at a potential 0.2 V more positive than the potential of the anodic mercury current maximum. In the case of graphite electrodes, the electrode surface was cleaned mechanically after each measurement.

Solutions were deaerated with argon of high purity. All the supporting electrolytes were prepared from high-purity reagents with triply-distilled water. The standard metal solutions were obtained by dissolving the appropriate metals (99.999% pure) in high-purity acids.

RESULTS AND DISCUSSION

Some examples of the application of "third" element effects in a.s.v. and general recommendations for the choice of "third" elements depending on the particular binary system are discussed below.

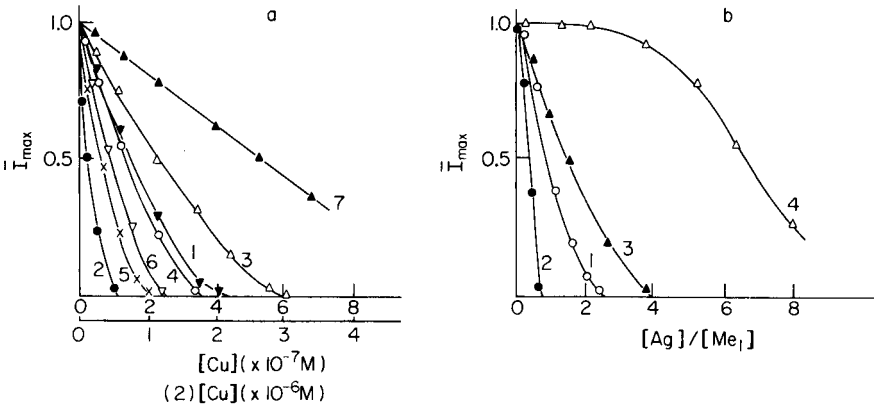

Fig. 1. Analytical signals of some metals vs. copper (a) and silver (b) concentrations in the test solutions. Electrodeposition time 2 min; scan rate 0.034 V s^{-1}. The lines in (a) correspond to: (1) Zn; (2) Ga; (3) Cd; (4) In; (5) Fe; (6) Sn; (7) Pb. Supporting electrolytes are: (1—4) 1 M KCl; (5) 1 M KOH + 2% potassium tartrate; (6) 1 M HCl; (7) 1 M sodium acetate. Molarities of Zn, Cd, In, Sn and Pb are 5×10^{-7} M; [Ga] = 1×10^{-5} M; [Fe] = 4×10^{-6} M. Electrodeposition potentials (V): (1) —1.3; (2) —1.5; (3) —1.0; (4) —1.1; (5) —1.7; (6, 7) —1.0.

The lines in (b) correspond to (1) Zn; (2) Ga; (3) Cd; (4) Cu. Supporting electrolyte is 1 M KNO_3 in all cases. Molarities of Zn, Cd and Cu are 5×10^{-7} M; [Ga] = 5×10^{-6} M. Electrodeposition potentials (V): (1) —1.2; (2) —1.5; (3) —1.0; (4) —0.6.

Figure 1 shows the dependence of the peak stripping currents for Zn, Ga, Cd, In, Fe, Sn and Pb on the copper(II) concentration and of those for Zn, Cd, Ga and Cu on the silver(I) concentration in the test solutions. These investigations were done with constant concentrations of the metals determined, i.e. the relation $I_{max,1} = f(C_2/C_1)$ was recorded.

Figure 1 shows the relative values of the analytical signals of the determined component $\bar{I}_{max,1} = I'_{max,1}/I_{max,1}$, where $I_{max,1}$ is the peak stripping current of Me_1 at $C_2 = 0$ and $I'_{max,1}$ is the same current at $C_2 \neq 0$. In almost all the systems investigated, C_2 has a pronounced influence on $I_{max,1}$, which leads to complete suppression of the analyte signals; under these conditions, quantitative analysis is impossible or nearly so. Figure 1 shows that the degree of influence of the second component on $I_{max,1}$ for the various metals differs considerably. The parameter $R = [\delta I_{max,1}/\delta C_2]$ at $C_2 \to 0$ and constant C_1 can be used to provide a quantitative estimate of these effects. The R values for some of the binary systems containing copper are listed in Table 1. These data show that the effect of copper on the analyte signals decreases in the order Ga > Fe > Sn > Zn ≅ In > Cd > Pb. In the case of binary systems containing silver the sequence is Ga > Zn > Cd > Cu. It should be noted that these sequences correlate with the $\Delta G_{1\text{-}2}$ values for the appropriate binary alloys [18].

Figure 2 shows the influence of mercury(II) concentrations on the signals for Zn, Cd or Pb when the test solution also contains copper(II). In the

TABLE 1

Parameter $R = (\delta I_{max,1}/\delta C_2)$ at $C_2 \rightarrow 0$ for binary systems with copper (for conditions, see legend to Fig. 1)

Me_1	Zn[a]	Cd[a]	Sn[a]	In[a]	Fe[b]	Ga[a]
R ($\mu A\ M^{-1}$)	0.104	0.083	0.132	0.107	0.144	0.148

[a]Intermetallic compound formation is known [18]. [b]No data are available.

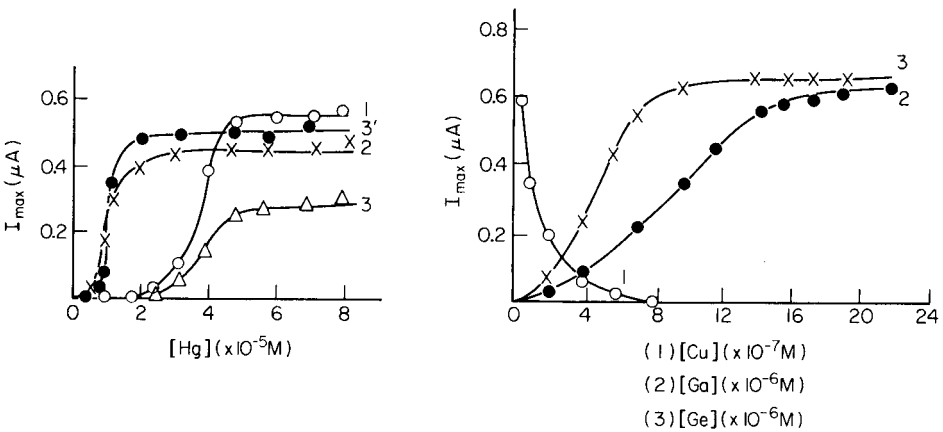

Fig. 2. Peak stripping currents for: (1) Cd, (2) Pb and (3) Zn in the presence of copper(II) vs. mercury(II) concentration in 1 M KBr. Electrodeposition potential, −1.5 V; deposition time, 3 min; scan rate 0.1 V s^{-1}; [Zn] = [Cd] = [Pb] = 2×10^{-7} M. Copper concentrations: (1, 2) 6×10^{-7} M; (3) 1×10^{-7} M; (3′) 0.

Fig. 3. Peak stripping current for zinc vs. copper(II) concentration (curve 1), gallium(III) concentration (curve 2) and germanium(IV) concentration (curve 3) for a mercury film electrode. [Zn] = 5×10^{-7} M; [Hg] = 4×10^{-5} M. Deposition potential, −1.5 V; scan rate, 0.017 V s^{-1}; deposition time, 4 min. For further details see text.

Cd—Cu and Pb—Cu systems, mercury present as the "third" element has a positive effect and practically eliminates the influence of copper on the determination of cadmium and lead (Fig. 2, curves 1 and 2). Simultaneous electrodeposition of the metals with mercury and the use of the mercury-film electrode in the case of the Zn—Cu system, however, do not completely suppress the influence of copper (curves 3 and 3′): the systematic error remains.

Effects on the determination of zinc

With the mercury-film electrode in 1 M KCl or potassium thiocyanate solutions, the zinc signal decreases with increase of copper(II) concentration and vanishes at molar ratios of Cu : Zn $\geqslant$ 1 : 3 (Fig. 3, curve 1). When

gallium(III) is introduced into 1 M KCl solution containing equimolar amounts of zinc(II) and copper(II) with at least an 80-fold molar ratio of mercury(II) with respect to copper(II), then the zinc stripping current starts to appear at Ga : Cu ratios exceeding 2. This current increases with increase in the gallium-(III) concentration (Fig. 3, curve 2). The zinc signal reaches its maximum value at ratios of Ga : Cu $\geqslant$ 15 : 1 and then remains practically constant. Under these conditions, the value of $I_{max,Zn}$ exceeds the corresponding value obtained in pure KCl solution when the mercury-film electrode is used. A similar effect is observed when germanium(IV) is added as the "third" element. Curve 3 in Fig. 3 shows the relationship between the zinc peak current and the germanium concentration for the Zn—Cu—Ge—Hg system at the graphite electrode in 0.5 M potassium carbonate containing 0.25 M EDTA with equimolar amounts of copper and zinc. The curve shows that the effect of germanium as the "third" element on the Zn—Cu system is stronger than that of gallium and that a constant zinc signal is reached at Ge : Cu $\geqslant$ 8.

The increase in the zinc peak current with increased concentrations of gallium(III) or germanium(IV) can be explained by the formation of Ga—Cu or Ge—Cu intermetallic compounds which are more stable than the Zn—Cu intermetallic compounds. With increase in the gallium (or germanium) concentration in the solution and in the deposit on the electrode, the quantity of copper interacting with zinc decreases. With a sufficient excess of gallium (germanium), all the electrodeposited copper is present as a compound with the "third" element, so that the effect of copper on the zinc signal becomes insignificant. As gallium and germanium do not interact with zinc under the conditions used, a plateau appears in the curves shown in Fig. 3 and the zinc signal becomes independent of the composition of the test solution. Thus the "third" element effect allows a considerable reduction in the systematic errors.

Effects on the cadmium—copper system

The "third" element can have a negative effect on the accuracy of a.s.v. determinations if it interacts with both components of the binary system. To illustrate this effect, the Cd—Cu—Te system is considered. In 0.02 M HCl solutions containing constant cadmium and copper contents, increase in the tellurium(IV) concentration leads to changes (Fig. 4) in the analytical signals of both elements. Initially there is a sharp decrease in the peak current for copper (Fig. 5, curve 1) and this signal is almost completely suppressed at Te : Cu ratios of ca. 1 : 4. In contrast, the peak currents for cadmium reach a maximum as the tellurium(IV) concentration increases and there is then a rapid decrease with a simultaneous rapid increase in the peak current at +0.37 V. At a Cd : Te molar ratio of about 1 : 1 (reading from the moment that the copper peak disappears) the cadmium stripping current also vanishes. At higher tellurium(IV) concentrations, only the stripping peak at +0.37 V increases.

Interpretation of curves 1 and 2 of Fig. 5 up to the complete suppression

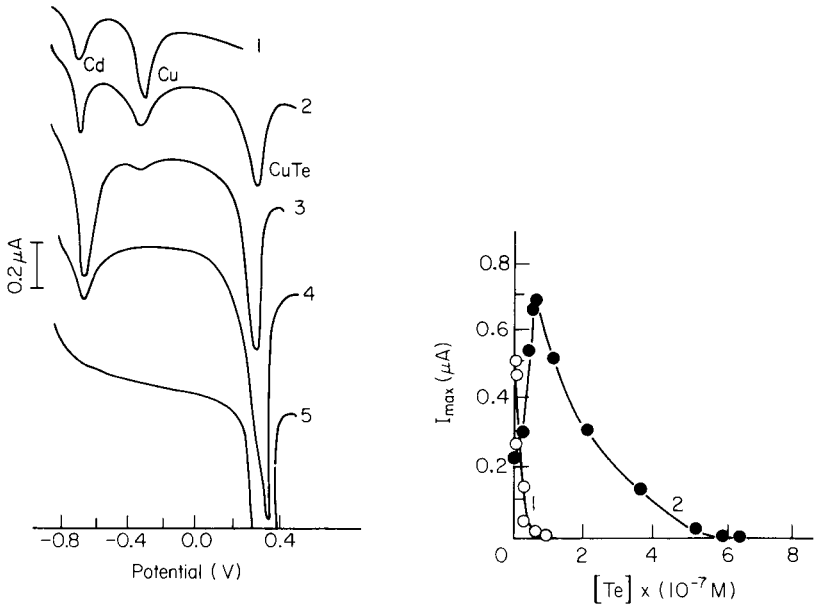

Fig. 4. Anodic stripping curves for the deposits formed by electrolysis of 0.02 M HCl containing 2×10^{-7} M copper(II), 6×10^{-7} M cadmium(II) and variable quantities of tellurium(IV). Deposition potential, −0.8 V; deposition time, 5 min; scan rate, 0.1 V s^{-1}. Tellurium concentration: (1) 0; (2) 2×10^{-8} M; (3) 5×10^{-8} M; (4) 2×10^{-7} M; (5) 7×10^{-7} M.

Fig. 5. Peak stripping current for copper (curve 1) and cadmium (curve 2) vs. tellurium(IV) concentration in 0.02 M HCl. Experimental conditions as in Fig. 4.

of the current peak for copper is the same as that outlined above for the behaviour of the Zn—Cu—Ga and Zn—Cu—Ge systems. In the absence of tellurium(IV) on the electrode, cadmium and copper are discharged simultaneously with the formation of an intermetallic compound of these two metals. During simultaneous electrodeposition of cadmium, copper and tellurium on the electrode with the formation of a Cd—Cu compound, a reaction between free copper and tellurium begins. If all the free copper is bound with tellurium, formation of the Cu—Cd compound is hindered because of the formation of a copper—tellurium compound and the peak current for cadmium is increased. Near the maximum of curve 2 (Fig. 4), copper has no effect on the cadmium signal. In the range of tellurium(IV) concentrations tested its effect as the "third" element does not differ from those of germanium and gallium in the Zn—Cu system. However, with subsequent increase in the tellurium(IV) concentration, simultaneous formation of cadmium and copper tellurides begins on the electrode and the cadmium signal begins to decrease. When all the cadmium deposited on the electrode forms the telluride, the cadmium stripping current disappears. Further increase in the tellurium(IV) concentration produces three simultaneous

processes on the electrode: formation of the cadmium and copper tellurides and deposition of elemental tellurium.

On the basis of the numerous experimental data obtained here and elsewhere, it can be concluded that the choice of a "third" element for the majority of binary systems in a.s.v. can be guided by the position of the component in the Periodic System. There appear to be two main rules.

(1) The stability of the binary compounds formed by simultaneous electrodeposition of two metals on the graphite electrode surface increases with the distance between the metals in the same period. For example, for binary deposits of copper with elements of the fourth and fifth periods, the relative stabilities lie in the sequences Zn—Cu < Ga—Cu < Ge—Cu and Cd—Cu < In—Cu < Sn—Cu.

(2) The stability of binary compounds formed in a.s.v. decreases with the increase in atomic mass of one of the components within the same group of the Periodic System. For example, the relative stabilities of deposited binary copper compounds with metals of groups II—IV lie in the sequences Zn—Cu > Cd—Cu > Hg—Cu, Ga—Cu > In—Cu > Tl—Cu, and Ge—Cu > Sn—Cu > Pb—Cu.

Some of the binary systems investigated and the "third" elements recommended for them are listed in Table 2.

The choice of the "third" element most suitable for the determination of a particular element by a.s.v. can be made on the basis of the requirements for the "third" element defined at the start of this paper and of the sequences listed above.

TABLE 2

"Third" elements recommended for some binary systems in a.s.v.

Element determined	Binary system	"Third" element	Element determined	Binary system	"Third" element
Zn[a]	Zn—Cu	Ga, Ge	Sb[a]	Sb—Se	Hg
Zn[a]	Zn—Ag	Ga	Sb[b]	Sb—Te	Hg
Cd[b]	Cd—Cu	Sn, Hg	Se[b]	Se—Sb	Cu
Cd[a]	Cd—Sb	Cu	Pb[a]	Pb—Cu	Hg
In[a]	In—Cu	Te	Tl[a]	Tl—Cu	Hg

[a]Mercury-film graphite electrode. [b]Graphite electrode.

REFERENCES

1 E. M. Roizenblat and Kh. Z. Brainina, Elektrokhimiya, 5 (1969) 396.
2 L. N. Vasil'eva and T. A. Koroleva, Zh. Anal. Khim., 26 (1971) 1682.
3 E. Ya. Neiman, G. M. Dolgopolova, Yu. A. Figelson and V. G. Yakovleva, Modern Problems of Anodic Stripping Voltammetry, Tomsk. Politekhnich. Inst. 1975, p.178.
4 E. Ya. Neiman, Zh. Anal. Khim., 30 (1975) 2293.
5 E. Ya. Neiman and I. N. Nikulina, Zh. Anal. Khim., 29 (1974) 1177.
6 E. M. Mal'kov, Zavod. Lab., 34 (1968) 504.

7 W. R. Matson, D. K. Roe and D. E. Carriet, Anal. Chem., 37 (1965) 1594.
8 T. M. Florence, J. Electroanal. Chem., 27 (1970) 273.
9 D. N. Hume and J. N. Carter, Chem. Anal. (PRL), 61 (1975) 205.
10 E. Ya. Neiman, Kh. Z. Brainina and A. A. Nemodruk, Zh. Anal. Khim., 30 (1975) 1668.
11 Z. Stojek, B. Stepnik and Z. Kublik, J. Electroanal. Chem., 74 (1976) 277.
12 W. Lund and M. Salberg, Anal. Chim. Acta, 76 (1975) 131.
13 E. Ya. Neiman, L. G. Petrova, G. M. Dolgopolova and V. I. Ignatov, Zh. Anal. Khim., 32 (1977) 1333.
14 E. Ya. Neiman, Zh. Anal. Khim., 29 (1974) 438.
15 T. R. Copeland, R. A. Osteryoung and R. K. Skogerboe, Anal. Chem., 46 (1974) 2093.
16 Kh. Z. Brainina, Talanta, 18 (1971) 513.
17 E. M. Roizenblat, L. V. Levchenko and G. N. Veretina, Zh. Anal. Khim., 28 (1973) 33.
18 K. Hultgren, R. L. Orr, P. D. Anderson and K. K. Kelley, Selected Values of Thermodynamic Properties of Metals and Alloys, Wiley, New York, 1963, p. 247.

Analytica Chimica Acta, 113 (1980) 287—294

COMPARATIVE STUDY ON THE PRECISION OF POTENTIOMETRIC TECHNIQUES APPLIED WITH ION-SELECTIVE ELECTRODES

Part 1. Direct Techniques

G. HORVAI and E. PUNGOR*

Institute for General and Analytical Chemistry, Technical University, Budapest (Hungary)

(Received 18th July 1979)

SUMMARY

The measurement techniques used with ion-selective electrodes, e.g. standard edition, double known addition, known subtraction, etc., are summarized. In each case, the error in the unknown concentration measured (c_x) can be characterized by the term $[\sigma(c_x)/c_x]/\sigma(E)$ where $\sigma(E)$ is the standard deviation of the potential measurement. The formulae developed make it possible to calculate the expected error for any strategy of standard addition or subtraction and to optimize precision by proper selection of the concentration and volumes of standard solutions.

Potentiometric techniques have been discussed in several books [1—6] devoted to ion-selective electrodes and their applications, and also in various reviews [7—10]. Numerous studies have been concerned with the evaluation, precision and accuracy of one or other potentiometric method [11—64]. It seems, however, that no generalized comparative treatment has so far been attempted. The present paper may be considered as a step in this direction.

Many sources of error may be encountered in a potentiometric determination: the error in the potential measurement, the error in the determination of the volume and/or concentration of the standard solutions, errors resulting from equilibrium dissociation, effects of interfering ions, etc. In many cases, however, the error in the measurement of the potential (E) is the most important, and this source of error is therefore discussed in detail here.

In this study, it is assumed that the standard deviation of the measured potential, $\sigma(E)$, is constant, and that there is no bias in E. It is also assumed that the electrodes show Nernstian response, i.e. $E = E' + S \log a + E_{err}$, where a is the activity of the measured species, and E' and S are constants; E_{err} is the error of the potential measurement which is expected to be zero, the standard deviation being $\sigma(E)$. These assumptions are valid for numerous electrodes and instruments, and have been used frequently [13, 14, 18, 20, 21, 36, 40, 46], but they are not valid in some cases, e.g. if the potential is drifting. Thus the present conclusions will be quantitative only if these assumptions hold; otherwise they will be only approximate. The error in the determination

of the sample concentration, c_x, caused by the error of the potential measurement must be characterized. It will be seen that in all cases where an explicit expression can be given for the relative standard deviation of c_x (i.e. $\sigma(c_x)/c_x$), the ratio of $\sigma(c_x)/c_x$ to $\sigma(E)$ is independent of $\sigma(E)$ itself. Hence $[\sigma(c_x)/c_x]/\sigma(E)$ is an appropriate quantity for characterizing the error in c_x caused by the error in E.

Different types of potentiometric technique

The potentiometric techniques considered here are listed in Table 1 together with the symbols used in each case. For clarity, each technique is briefly described below; further details are readily available [1—10]. To simplify the treatment, the difference between concentration and activity will be disregarded.

(1) Direct measurement after multipoint calibration. Several (n) standard solutions of concentration c_i (i = 1,2,...n), dispersed over the expected sample concentration range, are used for calibration of the electrode. The sample concentration c_x is determined from the potential of the electrode measured in the sample, by using the least-squares calibration line.

(2) Direct measurement after two-point calibration. This is a subcase of (1) with n = 2. It is treated separately because of its importance: many automated potentiometric analysers are based on this technique.

(3) Two-point calibration followed by sample addition. The potential is measured first for a standard of concentration c_1 and volume V_1; then a standard of concentration $c_2 > c_1$ and volume V_2 is added and the potential measured again; finally the sample is also added (c_x, V_x) and a third potential reading is made. With this method the electrodes need not be transferred between different solutions for calibration and sample determination, respectively.

(4) Standard or known addition. The potential is measured first in the sample (c_x, V_x); this is followed by addition of a standard solution (c_{st}, V_{st}) and a second potential measurement.

(5) Double known addition. As (4) but followed by a second standard addition (thus c_1, V_1 and c_2, V_2).

(6) Multiple standard addition. As (5) but with more than two standard additions; the concentration of the k-th charge of standard solution is c_k, and its volume is V_k, k = 1,2,...n.

(7) Standard addition, slope by dilution [22]. Standard addition (i.e. method 4; $c_{st} = c_1$, $V_{st} = V_1$) is followed by addition of diluent (volume V_2) and potential measurement.

(8) Analyte addition [36]. This is the reverse of standard addition, i.e. the potential is measured first in the standard (c_{st}, V_{st}) and then the sample (c_x, V_x) is added and the potential read again.

(9) Known subtraction. After the measurement of the potential in the sample (c_x, V_x), an analytical reagent which reacts quantitatively with the analyte (c_r, V_r) is added and the potential is read again. The concentrations are expressed in equivalents per volume ($c_x V_x > c_r V_r$).

TABLE 1

Potentiometric techniques and symbols used

(1) Direct measurement after multipoint calibration	c_i (i = 1,2,...n)	c_x
(2) Direct measurement after two-point calibration	c_1, c_2	c_x
(3) Two-point calibration followed by sample addition	c_1V_1, c_2V_2	c_xV_x
(4) Standard (known) addition	c_xV_x	$c_{st}V_{st}$
(5) Double known addition	c_xV_x	c_1V_1, c_2V_2
(6) Multiple standard addition	c_xV_x	c_kV_k (k = 1,2,...n)
(7) Standard addition, slope by dilution	c_xV_x	c_1V_1, V_2
(8) Analyte addition	$c_{st}V_{st}$	c_xV_x
(9) Known subtraction	c_xV_x	c_rV_r
(10) Sample subtraction	c_rV_r	c_xV_x
(11) Potentiometric titration	c_xV_x	c_rV_i

(10) Sample subtraction. This is the reverse of known subtraction, i.e. the potential is measured first in the reagent (c_r, V_r) and then again after reaction with the sample (c_x, V_x); the concentrations are expressed in equivalents per volume ($c_rV_r > c_xV_x$).

(11) Potentiometric titration. The reagent (c_r) is added in increments (ΔV_i) to the sample (c_x, V_x) and the equilibrium potential after each addition is measured. Thus $V_i = \Sigma_{k=1}^{i} \Delta V_k$. The concentrations are expressed in equivalents per volume.

It is obvious that the single addition or subtraction methods require prior knowledge of S, the slope of the calibration line, whereas this is not needed with methods 5, 6, 7 and 11.

CALCULATION OF ERRORS

As mentioned earlier, it is assumed that the measured potential values have the standard deviation $\sigma(E)$. From this assumption, it is possible to calculate, for most of the methods listed, the relative standard deviation of the sample concentration, i.e. $\sigma(c_x)/c_x$. Since the factor $\sigma(E)\ 2^{1/2}/|S^*|$ (where $S^* = S/\ln 10$) is common to all expressions, the ratios of $\sigma(c_x)/c_x$ to this factor were calculated. The results are shown in Table 2. The calculations were made using

$$\sigma^2(c_x) = \sum_{i=1}^{n} (\delta c_x/\delta E_i)^2\ \sigma^2(E) \tag{1}$$

where E_i is the i-th measured potential value. For example, in the case of standard (known) addition method the derivation was made as follows.

$$E_1 = S^* \ln c_x \tag{2}$$

$$E_2 = S^* \ln (c_xV_x + c_{st}V_{st})/(V_x + V_{st}) \tag{3}$$

TABLE 2

Values of the ratio $[\sigma(c_x)/c_x]/[2^{1/2}\,\sigma(E)/|S^*|]$ for the different methods 1—11

(1) $2^{-1/2}$, if the calibration line is exactly known (see text)

(2) $2^{-1/2}[(\ln c_x/c_2)^2 + (\ln c_x/c_1)^2 + (\ln c_2/c_1)^2]^{1/2}/\ln(c_2/c_1)$

(3) $$\left[\frac{(c_xV_x + c_1V_1 + c_2V_2}{c_xV_x}\right]\left[\left(\ln\frac{c_xV_x + c_1V_1 + c_2V_2}{c_1(V_x + V_1 + V_2)}\right)^2 + \left(\ln\frac{c_1V_1 + c_2V_2}{c_1(V_1 + V_2)}\right)^2 - \ln\frac{c_xV_x + c_1V_1 + c_2V_2}{c_1(V_x + V_1 + V_2)}\cdot\ln\frac{c_1V_1 + c_2V_2}{c_1(V_1 + V_2)}\right]^{1/2}\Big/\left[\ln\frac{c_1V_1 + c_2V_2}{c_1(V_1 + V_2)}\right]$$

(4) $1 + (c_xV_x/c_{st}V_{st})$

(5) $$\left[\left(\ln\frac{c_xV_x + c_1V_1}{c_x(V_x + V_1)}\right)^2 + \left(\ln\frac{c_xV_x + c_1V_1 + c_2V_2}{c_x(V_x + V_1 + V_2)}\right)^2 - \ln\frac{c_xV_x + c_1V_1}{c_x(V_x + V_1)}\cdot\ln\frac{c_xV_x + c_1V_1 + c_2V_2}{c_x(V_x + V_1 + V_2)}\right]\Big/\left|\frac{c_1V_1}{c_xV_x + c_1V_1}\ln\frac{c_xV_x + c_1V_1 + c_2V_2}{c_x(V_x + V_1 + V_2)} - \frac{c_1V_1 + c_2V_2}{c_xV_x + c_1V_1 + c_2V_2}\ln\frac{c_xV_x + c_1V_1}{c_x(V_x + V_1)}\right|$$

(6) See Part 2 [65]

(7) $$\left[\frac{c_xV_x + c_1V_1}{c_1V_1}\right]\left[\left(\ln\frac{V_x + V_1 + V_2}{V_x + V_1}\right)^2 + \left(\ln\frac{c_xV_x + c_1V_1}{c_x(V_x + V_1)}\right)^2 - \ln\frac{V_x + V_1 + V_2}{V_x + V_1}\cdot\ln\frac{c_xV_x + c_1V_1}{c_x(V_x + V_1)}\right]^{1/2}\Big/\left[\ln\frac{V_x + V_1 + V_2}{V_x + V_1}\right]$$

(8) $1 + (c_{st}V_{st}/c_xV_x)$

(9) $(c_xV_x/c_rV_r) - 1$

(10) $(c_rV_r/c_xV_x) - 1$

(11) See Part 3 [65]

c_x can be expressed explicitly from these two equations:

$$c_x = c_{st}V_{st}/\{(V_x + V_{st}) \exp [(E_2 - E_1/S^*) - V_x]\} \quad (4)$$

By derivation with respect to E_i ($i = 1,2$):

$$(\delta c_x/\delta E_i)^2 = [(c_x/S^*)(1 + c_x V_x/c_{st}V_{st})]^2 \quad (5)$$

and thus

$$\sigma(c_x)/c_x = (2^{1/2}/|S^*|)(1 + c_x V_x/c_{st}V_{st})\,\sigma(E) \quad (6)$$

which is in accordance with the result shown in Table 2. In some cases such as the double known addition method, c_x could not be expressed explicitly and implicit derivation had to be used.

The precision of direct measurement after multipoint calibration (method 1) depends on the choice of the number and distribution of the calibration points: however here only the limiting case is considered, i.e. when an infinite number of calibration points is taken, distributed over a large enough interval to include all sample concentrations. In this case there will be no error in the determination of the calibration line, and thus the only source of error is the error in the potential measurement in the sample. Therefore

$$\sigma(c_x)/c_x = \sigma(E)/|S^*| = (1/2^{1/2})\,2^{1/2}\,\sigma(E)/|S^*| \quad (7)$$

i.e., if the calibration line is absolutely correct, the factor for the direct measurement in Table 2 will be $2^{-1/2}$. Multipoint calibration has been discussed in an analogous manner by Ebel et al. [18].

DISCUSSION

The formulae given in Table 2 make it possible to calculate the expected error for any addition strategy, i.e. for any choice of c_i and V_i values and for a given or approximately known c_x. It can be seen from Table 2 that most of the ratios exceed $2^{-1/2}$ or even 1. This means that for univalent measured species, the relative standard deviation in c_x for a 1-mV standard deviation in E is more than 4%. The only notable exceptions are the subtraction methods, where the proportionality factor may approach zero, i.e. the error in c_x caused by the error in E can practically vanish. This result has led to the development of a single-point titration method, discussed elsewhere [57]. It should be noted that case 10 has been already discussed, with the same result, by Matsushita and Ishikawa [21].

The proportionality factors in Table 2 allow some interesting conclusions to be drawn regarding the merits of different techniques. For example, it has been stated [22] that double known addition gave astonishingly bad results, while the method based on standard addition and slope determination by dilution was quite satisfactory. By insertion of the relevant numerical values into the respective formulae in Table 2 one can easily confirm the results mentioned. However, numerical trials have shown here that by a strategy different

from that used in the above-mentioned work [22], the double known addition method can also be made more precise. If, for example, $c_x = 10^{-5}$ M and $V_x = 10$ ml, the choice of $c_1 = 2 \times 10^{-5}$ M, $V_1 = 30$ ml and $c_2 = 2 \times 10^{-3}$ M, $V_2 = 1$ ml gives a proportionality factor of 1.6 which can be regarded as quite good. It is clear, of course, that in this case great care must be exercised, because the sample matrix may be changed by the large volume (30 ml) of standard solution added.

In contrast, it is possible to show that if V_1 and V_2 are both much smaller than V_x in the double known addition method then the proportionality factor will remain very high for all practical cases. The proportionality factor was calculated as a function of $v = (c_x V_x + c_1 V_1 + c_2 V_2)/c_x V_x$ for different values of $u = (c_x V_x + c_1 V_1)/c_x V_x$, assuming that $V_1 \ll V_x$ and $V_2 \ll V_x$. The semi-logarithmic representation of these curves in Fig. 1 proves the correctness of the foregoing statement, because for any practical value of u, v must be made impractically high in order to obtain comparatively low errors.

The errors of methods 6 and 11, i.e. multiple standard addition and potentiometric titration, were not calculated in the same way as those of the other methods, because the data are too abundant for the deterministic calculation of c_x, which must therefore be obtained by regression analysis. These two methods will be dealt with in Parts 2 and 3.

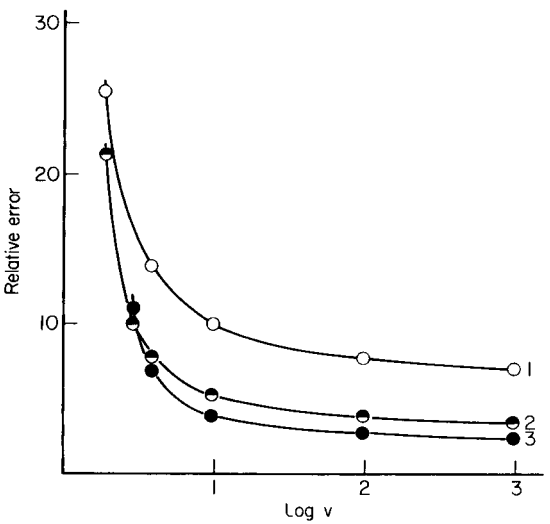

Fig. 1. Relative error of double known addition with V_1, $V_2 \ll V_x$. The relative error is expressed as $[\sigma(c_x)/c_x]/[2^{1/2}\,\sigma(E)/|S^*|]$. For the definitions of u and v, see text. (1) $u = 1.2$; (2) $u = 1.5$; (3) $u = 2.0$.

REFERENCES

1 R. A. Durst (Ed.), Ion-selective Electrodes, National Bureau of Standards Spec. Publ. No. 314, 1969.
2 G. J. Moody and J. D. R. Thomas, Selective Ion-sensitive Electrodes, Merrow, Watford, 1971.
3 P. L. Bailey, Analysis with Ion-selective Electrodes, Heyden, London, 1976.
4 K. Camman, Das Arbeiten mit ionenselektiven Elektroden, 2nd edn., Springer, Berlin, 1977.
5 S. Ebel and W. Parzefall, Experimentelle Einführung in die Potentiometrie, Verlag Chemie, Weinheim, 1975.
6 N. Lakshminarayanaiah, Membrane electrodes, Academic Press, New York, 1976.
7 R. P. Buck, Anal. Chem., 46 (1974) 28R; 48 (1976) 23R; 50 (1978) 17R.
8 J. Koryta, Anal. Chim. Acta, 61 (1972) 329; 91 (1977) 1.
9 S. Ebel and A. Seuring, Angew. Chem., 89 (1977) 129.
10 G. Svehla, Automatic Potentiometric Titrations, Pergamon, Oxford, 1978, pp. 187—204.
11 J. Buffle, N. Parthasarathy and D. Monnier, Anal. Chim. Acta, 59 (1972) 427.
12 J. Buffle, Anal. Chim. Acta, 59 (1972) 439.
13 N. Parthasarathy, J. Buffle and D. Monnier, Anal. Chim. Acta, 59 (1972) 447.
14 S. L. Burden and D. E. Euler, Proc. Indiana Acad. Sci., 82 (1973) 167; Anal. Chem., 47 (1975) 793.
15 T. Eriksson, Anal. Chim. Acta, 58 (1972) 437.
16 F. Ingman and E. Still, in E. Wänninen (Ed.), Analytical Chemistry, Pergamon, Oxford, 1977, pp. 183—188.
17 L. Pehrsson, F. Ingman and A. Johansson, Talanta, 23 (1976) 769.
18 S. Ebel, E. Glaser and H. Mohr, Fresenius Z. Anal. Chem., 293 (1978) 33.
19 S. Ebel, E. Glaser and A. Seuring, Fresenius Z. Anal. Chem., 291 (1978) 108.
20 K. Waldmeier and W. Rellstab, Fresenius Z. Anal. Chem., 264 (1973) 337.
21 H. Matsushita and N. Ishikawa, Nippon Kagaku Kaishi, (1975) 2028.
22 Orion Newsl., 2 (1970) 33, 49.
23 M. J. D. Brand and G. A. Rechnitz, Anal. Chem., 42 (1970) 1172.
24 H. Matsushita and S. Furuta, Bunseki Kagaku, 21 (1972) 1639.
25 C. McCallum and D. Midgley, Anal. Chim. Acta, 65 (1973) 155.
26 S. Ebel and J. Hocke, Fresenius Z. Anal. Chem., 294 (1979) 16.
27 P. Gilgen and H. Kobler, Chimia, 32 (1978) 302.
28 T. Anfält and D. Jagner, Anal. Chim. Acta, 57 (1971) 165; 66 (1973) 152.
29 A. Ivaska, Academic dissertation, Åbo Akademi, Åbo, 1975.
30 L. M. Schwartz and R. I. Gelb, Anal. Chem., 50 (1978) 1571.
31 P. W. Carr, Anal. Chem., 44 (1972) 452.
32 N. G. Sellers and J. A. Caruso, J. Chem. Educ., 50 (1973) 547.
33 S. Ebel and R. Krömmelbein, Fresenius Z. Anal. Chem., 264 (1973) 342.
34 D. Jagner and K. Åren, Anal. Chim. Acta, 52 (1970) 491.
35 T. Eriksson and G. Johansson, Anal. Chim. Acta, 52 (1970) 465.
36 R. A. Durst, Mikrochimica Acta, (1969) 611.
37 F. J. C. Rosotti and H. Rosotti, J. Chem. Educ., 42 (1965) 375.
38 A. Liberti and M. Mascini, Anal. Chem., 41 (1969) 676.
39 W. Selig, Mikrochimica Acta, (1973) 87.
40 A. F. Isbell, R. L. Pecsok, R. H. Davies and J. H. Purnell, Anal. Chem., 45 (1973) 2363.
41 P. Kivalo, R. Virtanen, K. Wickström, M. Wilson, E. Pungor, K. Tóth and G. Sundholm, Anal. Chim. Acta, 87 (1976) 387.
42 P. Kivalo, R. Virtanen, K. Wickström, M. Wilson, E. Pungor, G. Horvai and K. Tóth, Anal. Chim. Acta, 87 (1976) 401.
43 H. F. Osswald, R. E. Dohner, T. Meier, P. C. Meier and W. Simon, Chimia, 31 (1977) 50.

44 J. M. Ariano and W. F. Gutknecht, Anal. Chem., 48 (1976) 281.
45 J. W. Frazer, A. M. Kray, W. Selig and R. Lim, Anal. Chem., 47 (1975) 869.
46 J. J. Zipper, B. Fleet and S. P. Perone, Anal. Chem., 46 (1974) 2111.
47 B. Fleet and A. Y. W. Ho, Talanta, 20 (1973) 793.
48 G. Horvai, L. Domokos and E. Pungor, Fresenius Z. Anal. Chem., 292 (1978) 132; Magy. Kém. Foly., 84 (1978) 481.
49 G. Horvai, K. Tóth and E. Pungor, Magy. Kém. Foly., 84 (1978) 483.
50 B. M. Gulin and A. A. Resetilo, Zh. Anal. Khim., 31 (1976) 2097.
51 T. Mussini, Chim. Ind. (Milan), 58 (1976) 179.
52 J. G. Frost, Anal. Chim. Acta, 48 (1969) 321.
53 M. J. D. Brand, Proc. Soc. Anal. Chem., 10 (1973) 118.
54 A. B. Gyllenspetz, D. Kitchen and T. D. Rees, Chem. Ind. (London), (1973) 640.
55 Å. Olin and B. Wallén, Talanta, 24 (1977) 303.
56 T. Meites and L. Meites, Talanta, 19 (1972) 1131.
57 G. Horvai, K. Tóth and E. Pungor, Anal. Chim. Acta, 107 (1979) 101.
58 H. J. Keller and W. Richter, Metrohm Bull., 2 (1971) 173.
59 F. L. Hahn, M. Frommer and R. Schulze, Z. Phys. Chem., 133 (1928) 390.
60 J. M. H. Fortuin, Anal. Chim. Acta, 24 (1961) 175.
61 R. Kohn and V. Zitko, Chem. Zvesti, 12 (1958) 261.
62 D. C. Cörmös and I. Marusciac, Stud. Univ. Babes-Bolyai, Ser. Chem., 16 (1971) 27.
63 G. Gran, Analyst, 77 (1952) 661.
64 L. Meites, Crit. Rev. Anal. Chem., 8 (1979) 1.
65 G. Horvai and E. Pungor, Anal. Chim. Acta, 113 (1980) 295.

Analytica Chimica Acta, 113 (1980) 295—299

COMPARATIVE STUDY ON THE PRECISION OF POTENTIOMETRIC TECHNIQUES APPLIED WITH ION-SELECTIVE ELECTRODES
Part 2. Multiple Standard Addition

G. HORVAI and E. PUNGOR*

Institute for General and Analytical Chemistry, Technical University, Budapest (Hungary)

(Received 18th July 1979)

SUMMARY

The errors in multiple standard addition techniques depend on whether or not the slope of the calibration graph is known. The precision obtainable by regression techniques with and without Gran transformation of the experimental data are compared. Monte Carlo simulation is used to estimate the precision of the result obtained by non-linear regression.

The error in potentiometric determinations of sample concentrations depends to a great extent on the error in the potential measurement. The interdependence of these errors was discussed for a number of frequently used potentiometric techniques in Part 1 [1] of this series. Multiple standard addition and potentiometric titrations require separate treatment if the complications of applying error propagation calculations to non-linear regression are to be avoided.

Two different versions of the multiple standard addition technique are generally used. In one case, the slope, S, of the calibration line of the electrode is already known from separate measurements while in the other case S is not known in advance. If S is known, then even two additions of standard solution can be regarded as multiple addition in the sense that the number of potential measurements is more than the minimum number required for the calculation of the sample concentration c_x. This is so because if S is known then a single standard addition suffices to determine c_x (cf. Part 1). Thus, if two or more additions of standard solution are made, the data obtained are sufficiently abundant for regression analysis to be applied to the data to increase the precision of the calculation of c_x compared to single known addition. If S is not known in advance, then multiple standard addition means at least three additions, because the calculation of c_x requires at least two standard additions (cf. the discussion of the double known addition technique in Part 1). If more than two additions are made, the additional data may be used in a regression to increase the precision compared to double known addition. It is important to note that the precision is increased compared to the double and not the single known addition technique in this case.

CALCULATION OF c_x

The calculation of c_x in a multiple standard addition with n additions is started by setting up the Nernst equation in an appropriate form for the $(n + 1)$ potentials measured:

$$E_i = E' + S \log \left[\left(c_x V_x + \sum_{k=1}^{i} c_k V_k \right) \Big/ \left(V_x + \sum_{k=1}^{i} V_k \right) \right] \quad (1)$$

where E_i is the potential measured after the i-th addition ($i = 0,1,2,\ldots n$); the other notations are as defined in Part 1. The aim of the regression calculation is to determine the best set (E', c_x) if S is known, or the best set (E', S, c_x) if S is not known in advance, which minimizes the sum of the squared differences between the right-hand sides and the respective left-hand sides of the $(n + 1)$ equations above. This approach implies the assumption that the variance of E_i is independent of i, because otherwise weighted least squares should be used. As to the technical details of this regression calculation, different approaches have been reported [2—4] in the literature.

Alternatively, the regression calculation may be started by the Gran transformation of eqn. (1):

$$\left(V_x + \sum_{k=1}^{i} V_k \right) 10^{E_i/S} = 10^{E'/S} c_x V_x + 10^{E'/S} \sum_{k=1}^{i} c_k V_k \quad (2)$$

The left-hand side of eqn. (2) is a Gran-type function. The Gran transformation is used quite often if S is known in advance, because the right-hand side of eqn. (2) is a linear function of the independent variable $\Sigma_{k=1}^{i} c_k V_k$, and thus, the familiar method of linear regression may be used. It should be noted, however, that it is only seldom realised [5—7] that the use of weighted linear regression is essential in this case because the variance of the Gran-type function on the left-hand side of eqn. (2) is not independent of i. Thus, the usual graphical evaluation is also incorrect from the statistical point of view. It must also be noted that the results obtained from eqns. (1) and (2) are the same if correct weighting is applied in the least-squares procedure.

Estimation of the error of c_x

If S is known and c_x is calculated by linear regression on the Gran-type function, the error in c_x may be calculated as described by Buffle et al. [5]. If the known value of S is itself also in error, this may greatly increase the error in c_x [6, 7].

If S is not known in advance, i.e. if nonlinear three-parametric regression has to be applied, the analytical calculation of the error in c_x becomes more complicated but the error can be easily determined by a mathematical simulation technique [8], the Monte Carlo method. This method allows for the estimation of the variance $\sigma(c_x)$ at a given set (E', S, c_x) and a given variance in the potential, $\sigma(E)$, for a certain addition strategy, i.e. a certain choice of the c_k and V_k values and of V_x. This means that the method is

applied normally for the investigation of specific examples. Such an example will be discussed below. The simulation of a multiple standard addition measurement consists of calculating the E_i values from the given (E', S, c_x) set and superimposing normally distributed random errors on these with a variance $\sigma(E)$. The thus distorted E_i values are used to calculate c_x by non-linear regression. The value obtained will, in general, differ from the true c_x. The whole procedure may be repeated many times with new sets of generated random errors. This procedure is essentially equivalent to carrying out numerous parallel measurements. The results are then evaluated for the variance of the c_x values obtained and for the difference between the average of the calculated c_x values and the originally given c_x value, i.e. for the systematic error in c_x.

The following example will demonstrate the usefulness of the simulation method. Brand and Rechnitz [2] used a lead-selective electrode in a five-fold standard addition measurement. Their result for the lead concentration of a standard solution was about −25% in error and this was attributed to an erratic electrode response. This seems to be wrong, because the same data yield a good calibration line when the true concentration of their sample is used. Their measurement has been simulated 100 times (Table 1, third column). The relative standard deviation of c_x was 15.2% and this may explain the large error obtained in a single measurement. It should also be noted that dividing $\sigma(c_x)/c_x$ = 15.8% by $\sigma(E)/S^*$ = 4.8% gives a quotient of about 3, whereas the same quotient for a well-designed single known addition is something between 2 and 3. This means that a properly done single known addition is about as precise as a five-fold standard addition. This seemingly contradictory statement can be explained by recognising that in the single known addition S is assumed to be known exactly, whereas in multiple addition S is also calculated from the data measured.

In the above example, it could be shown by the simulation method that the relative standard deviation of c_x is large compared with $\sigma(E)/S^*$. The situation is the same if $\sigma(E)$ is smaller, e.g. 0.1 mV instead of 0.6 mV (cf. Table 1, second column). One might suggest, however, that a better addition

TABLE 1

Results of simulated multiple standard addition experiments[a]

Standard deviation of e.m.f. (mV) taken for the simulation	0.1	0.6[b]
True c_x(M)	2×10^{-6}	2×10^{-6}
Average of calculated c_x (M)	2.008×10^{-6}	2.072×10^{-6}
Relative standard deviation of calculated c_x (%)	2.6	15.2
$\sigma(E)/S^*$ (%)	0.8	4.8

[a]Based on the data of Table IV in ref [2].
[b]Approximate value of the standard deviation of the e.m.f. calculated from Table IV in ref. [2].

strategy be used, i.e. that the concentration and the volumes of standard solution added be changed in such a manner that the precision of the method increases. It is considered that such a strategy cannot be found if S is not established previously and if the total volume of standard solution added is kept small. The reason is that such a measurement can be regarded as being derived from double known addition with V_1, $V_2 \ll V_x$ by interspersing some further points to increase precision. It has been shown [1] that such a double known addition is quite imprecise, so that the increase in precision mentioned is relative to a rather low level. A quite different situation is encountered if S is known in advance because here the precision is increased relative to single known addition which may give satisfactory precision even if $V_{st} \ll V_x$, as can be seen from eqn. (2) in Table 1 of Part 1. Figure 1 shows that if S is not known in advance, it may be impossible in practice to distinguish between two widely differing sets of parameters even by twenty-fold standard additions.

Multiparametric curve-fitting

Multiparametric curve-fitting is extensively used in the evaluation of experimental results. The above discussion indicates that it is not enough simply to calculate the sought parameters by this method; the dispersion and bias of these parameters should also be estimated. Monte Carlo simulation is a useful method for this purpose. Its application is, however, restricted to particular cases and generalizations are difficult to make. If it is necessary to draw general conclusions, it may be useful to investigate the statistical behaviour of the appropriate deterministic model, i.e. the case where the number of measured data is just enough to calculate the parameters. This method has been used above in the discussion of the precision of multiple standard addition when precision is derived from single or multiple additions.

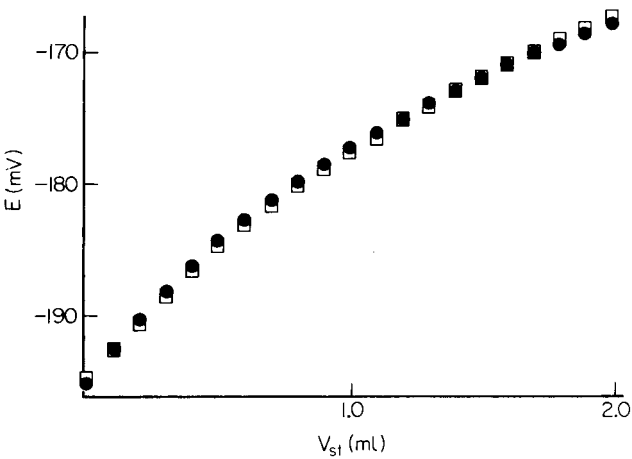

Fig. 1. Comparison of two multiple standard addition measurements with widely differing parameter sets. No error is included in the calculated potentials. V_x = 100.0 ml and c_{st} = 10^{-3} M in both cases. (□) E' = 100.00 mV; S = 59.00 mV/decade; c_x = 1.000 × 10^{-5} M. (●) E' = 71.01 mV; S = 52.33 mV/decade; c_x = 0.819 × 10^{-5} M.

REFERENCES

1 G. Horvai and E. Pungor, Anal. Chim. Acta, 113 (1980) 287.
2 M. J. D. Brand and G. A. Rechnitz, Anal. Chem., 42 (1970) 1172.
3 T. Meites and L. Meites, Talanta, 19 (1972) 1131.
4 G. Horvai, L. Domokos and E. Pungor, Fresenius Z. Anal. Chem., 292 (1978) 132.
5 J. Buffle, N. Parthasarathy and D. Monnier, Anal. Chim. Acta, 59 (1972) 427.
6 J. Buffle, Anal. Chim. Acta, 59 (1972) 439.
7 N. Parthasarathy, J. Buffle and D. Monnier, Anal. Chim. Acta, 59 (1972) 447.
8 Y. Bard, Nonlinear Parameter Estimation, Academic Press, New York, 1974.

Analytica Chimica Acta, 113 (1980) 301—306

DETERMINATION OF SODIUM IN ALUMINOUS MATERIALS WITH A SODIUM-SELECTIVE ELECTRODE

THOMAS A. PALMER* and JOHN M. WINKLER

Analytical Research Department, Kaiser Aluminum & Chemical Corporation, Center for Technology, Pleasanton, California 94566 (U.S.A.)

(Received 13th August 1979)

SUMMARY

A simple, reliable method is described for determining sodium in aluminous materials such as reduction-grade alumina, specialty aluminas, reacted alumina, and dried red mud. Samples were dissolved in concentrated phosphoric acid, monoethanolamine was added to adjust the solution to pH 9.5 and prevent the precipitation of aluminum hydroxide, and the sodium ion activity was measured with a sodium-selective glass electrode. Hydrogen and cesium ions did not interfere. The samples contained 0.02—1.5% sodium. The median relative standard deviation was 2%. Accuracy was established by comparison with standard methods; the median relative difference was 3%.

The sodium content of the alumina used in the aluminum reduction process must be known to maintain the proper cell bath ratio. An accurate method for determining sodium in calcined specialty aluminas is also needed, as material specifications may require a sodium content range or a maximum sodium value. Neither optical emission nor x-ray spectrometry (x.r.s.) is satisfactory for the determination of sodium in alumina. Optical emission spectroscopy gives poor precision and x.r.s. lacks sensitivity for determining $\leqslant 0.2\%$ sodium [1]. Flame emission (f.e.s.) and atomic absorption spectrometry (a.a.s.) are commonly used in determining sodium [2, 3]. In analyzing calcined alumina by these methods, a fusion with lithium metaborate or lithium carbonate plus boric acid is required. A blank determination of the sodium contamination in the flux material(s) is necessary, and aluminum(III) must be added to the standard solutions in equivalent concentration to the samples. The f.e.s. and a.a.s. techniques have a limited analytical range and often require dilutions to assure uniformity of aluminum and flux concentrations in standard and sample solutions.

The sodium-selective electrode has been used in analyzing aluminous materials. Strauss and Rutkowski [4] determined sodium in precipitated silicic acid and in sodium aluminum silicates with a sodium content of 0.9—4.3%. Thompson and Danchik [5] determined sodium in the range of 0.02—1.6% in unspecified types of alumina after a boric acid sinter, but presented no precision data for samples containing less than 0.4% sodium.

The present paper reports a procedure for determining sodium in aluminous

materials with an ion-selective electrode after dissolution of the sample in phosphoric acid.

EXPERIMENTAL

Apparatus and reagents

An Orion 401 Specific Ion Meter was used with a Beckman 39278 sodium ion electrode (stored in 0.1 M NaCl) and a Beckman 39402 ceramic junction calomel reference electrode filled with saturated KCl solution.

Standard NaCl solution (0.200 mg Na^+ ml^{-1}). Dissolve exactly 0.5084 g of reagent-grade NaCl (dried at 110°C) in distilled water and dilute to 1000.0 ml in a volumetric flask. Store in a polyethylene bottle.

Phosphoric acid (85%, reagent grade). Select a lot of acid which contains <0.0004% Na. Store in a polyethylene bottle.

Monoethanolamine (MEA), 60% solution. Select a lot of reagent-grade material containing <0.0001% Na. Add 600 ml of reagent to 400 ml of distilled water. Mix well, cool, and store in a polyethylene bottle.

Procedure

Weigh accurately 0.10 g of well-blended sample (<150 μm) into a 30-ml platinum crucible. Add 3.0 ml of phosphoric acid. Initially, warm gently over a Meker burner to dehydrate the acid partially. Carefully increase the temperature, continually swirling to aid the dissolution. If necessary, for refractory samples, heat to white fumes. After dissolution is complete, cool and add 20 ml of water, warm, and mix with a platinum rod or wire. Transfer the solution quantitatively to a 100-ml volumetric flask. Add 10.0 ml of MEA solution. Cool, dilute to volume with distilled water and mix. Into three 100-ml volumetric flasks, pipet 3 aliquots of standard NaCl solution which cover the range of sodium expected in the test sample. To each flask, pipet 3.0 ml of phosphoric acid and 10.0 ml of MEA solution. Cool, dilute to volume with distilled water, and mix. Transfer the test and standard solutions to 150-ml polypropylene beakers. Place the electrodes into the low Na^+ standard solution, stir using a magnetic stirrer and note the millivolt reading (to the nearest 0.1 mV) after 3.0 min. Measure the Na^+ potentials of the higher standard solutions in the same manner. On semi-log paper, plot log Na^+ concentration versus linear mV and draw a smooth curve through the three calibration points. Alternately, measure the mV reading of the sample and standard (close concentration to sample) solutions. Correct for any drift in the potential of the standard potential. From the calibration curve, read the Na^+ concentration corresponding to the corrected mV reading.

RESULTS AND DISCUSSION

Choice of analytical technique and dissolution method

The use of the sodium-selective electrode in determining sodium has several advantages. The electrodes are simple to use and are adaptable for control purposes. Only monovalent cations such as hydrogen, lithium, and silver may interfere with the electrode technique [6]. The procedure has a wide analytical range which simplifies the selection of proper sample weights and calibration solutions.

Fusion procedures were not feasible because of potential interference from high concentrations of alkali metals. Since many of the samples were refractory materials, mere acid treatment was not effective in dissolving them. Thompson and Danchik [5] extracted sodium ion from alumina using a boric acid sintering process. This technique may be efficient, but since the sample is not completely dissolved, visual inspection gives no assurance of quantitative sodium extraction.

Phosphoric acid has been proposed as a dissolving acid in analyzing alumina [7], chrome ores and refractories [8], firebrick [9], and β-alumina [3]. Initially, 4 ml of (1 + 1) phosphoric acid was used to dissolve 100 mg of reduction-grade alumina. This procedure was discontinued because of excessive splattering during the acid dehydration step and because of incomplete dissolution of the samples. It was established that 3 ml of concentrated (85%) phosphoric acid was sufficient to dissolve 100 mg of alumina.

A Meker burner proved best for use in dissolving calcined alumina. The phosphoric acid dehydrates at ca. 200°C and the sample dissolves at ca. 310°C. The sample—acid mixture must be swirled continually to effect dissolution. The use of a hot plate was abandoned because it was difficult to control the heating rate and it was time-consuming. The lowest temperature possible should be used in the dissolution process. Too high a temperature causes formation of a white refractory material (presumably $AlPO_4$) which could occlude Na^+ and negate the analysis.

The American Chemical Society specification for sodium in reagent-grade 85% phosphoric acid is $\leq 0.025\%$. Five lots of acid were analyzed for sodium by atomic absorption spectrometry. The results indicated that all lots contained $<0.003\%$ sodium. An acid lot containing 0.0003% sodium was used in subsequent analyses. This acid contributed 0.02 mg of sodium background per determination.

Choice of pH buffer and aluminum(III) complexant

Hydrogen ion can interfere in determining sodium by the electrode. According to the manufacturer's instructions, the pH must be at least 4 units greater than the highest pNa measured. In this work sodium concentration was measured as low as 7×10^{-6} M (pNa ≈ 5.2). Therefore, it would be desirable to have a reagent which retains aluminum(III) in solution and provides buffering action at pH >9.2. Strauss and Rutkowski [4] used

triethanolamine (at pH 8.0) in analyzing aluminous materials with the sodium-selective electrode. They were determining sodium levels at least a hundred times more concentrated than those in the present studies. Thompson and Danchik [5] used ammonium citrate (pH 8.7) to prevent aluminum(III) precipitation; however, negligible aluminum was dissolved by their boric acid sintering technique. Large amounts of ammonium ion cause high values for sodium in this analysis [10]. Wilson et al. [11] proposed monoethanolamine (MEA) as the pH buffer in determining sodium ion with the electrode. The pK_a of the monoethanolammonium ion is 9.5 [12], which provides excellent buffer capacity at the pH required for analysis.

When the amount of MEA specified in the recommended procedure was used, it was established that as much as 0.1 g of aluminum(III) could be complexed and retained in solution at pH 9.6. This aluminum level is twice the level which is detailed in the procedure. Two lots of reagent-grade MEA were analyzed for sodium. The a.a.s. results indicated <0.0002% Na for each lot. The MEA contributed a background of <0.01 mg Na^+ for each determination.

Interferences

An extensive interference study was not conducted. Potential hydrogen ion interference was eliminated by pH control. No significant amounts of lithium or silver ions were present in the samples analyzed. The iron in the samples was completely dissolved in the phosphoric acid, and the MEA effectively prevented precipitation of hydrated iron(III) oxide. Small amounts of silica did not interfere. In analyzing a gel alumina containing 5% SiO_2, the recommended procedure gave results similar to those obtained with an established method. A cesium-containing catalyst support was analyzed for sodium by using the electrode procedure. The effect of cesium ion on the sodium electrode response was determined; the results in Table 1 indicate no detrimental effect of <10% cesium(I).

Sensitivity, accuracy and precision

In the range 0.2—0.8 mg of sodium, the calibration graph is a straight line with a slope of 55 mV/decade change in concentration. The calibration graph for the low sodium range of 0.005—0.05 mg shows slight curvature, the change in mV reading over this range being 20 mV. The slope at 0.02 mg is only 23 mV/decade. The curvature is ascribed, in part, to the significant contribution of the sodium present in the phosphoric acid and MEA reagents.

TABLE 1

Effect of cesium on the determination of 0.400 mg of sodium by the recommended procedure

Cs^+ added (mg)	1	12	100
Na^+ found (mg)	0.402	0.403	0.412
Recovery (%)	100.5	101	103

TABLE 2

Statistical data[a] for the analyses of Kaiser standard reference aluminas and various other materials

Material	N	$\bar{X}$ (%)	s	s_r(%)
Standard 384-9-1	3	0.495	0.0083	1.7
384-9-3	4	0.395	0.0078	2.0
384-9-4	3	0.395	0.0043	1.1
384-9-5	5	0.432	0.0086	2.0
Inter-plant check alumina 1075	4	0.317	0.013	4.2
Reacted alumina 1075	4	1.53	0.034	2.2
Dried red mud	2	1.41	0.018	1.3
Exptl. silica-stabilized gel alumina	5	0.016	0.0047	30
Alumina catalyst support	4	0.084	0.0069	8.2
Kaiser crushed A-201 desiccant	2	0.268	0.0071	2.7
Kaiser C-5R calcined alumina	3	0.287	0.0065	2.3
Kaiser KT-1061-6 tabular alumina	4	0.061	0.0020	3.2
Exptl. Fe-doped thermally stable alumina support (TSS)	2	0.050	0.0071	14
Exptl. Cs-doped TSS	2	0.283	0.0045	1.6
Exptl. Zn-doped TSS	2	0.056	0.00089	1.6
Kaiser KH-31 hydrated alumina	4	0.144	0.0005	0.3

[a]Number of determinations, mean result, standard deviation and relative standard deviation.

If the calibration curve is redrawn to include the sodium present in the reagents, a straight line is obtained.

As shown in Table 2, the precision as measured by the relative standard deviation (s_r) ranged from 0 to 30%. The median s_r value was 2%. Generally, the worst precision was observed for those samples which contained the least sodium and is attributable, in part, to instrumental error. At the 0.4-mg sodium level with the calibration curve which had a slope of 55 mV/decade of concentration, an error of ±0.5 mV in the potential measurement is equivalent to a relative error of 2%. At the 0.02-mg sodium level in the calibration curve with a slope of 23 mV/decade the same reading error is equivalent to 5% relative error.

Accuracy was estimated by comparing the results obtained by the proposed method with the results of independent methods. Table 3 shows the comparison with Li_2CO_3/H_3BO_3 fusion and a.a.s. and f.e.s. measurements [13]. The mean relative difference was 0.8%. All other samples were compared with a lithium borate fusion/a.a.s. method. The results in Table 4 indicate a 3% median relative difference between this and the electrode method.

TABLE 3

Comparative results in the analyses of Kaiser standard reference aluminas

Standard	Average sodium found (%)		
	Proposed method	Li_2CO_3/H_3BO_3 + a.a.s.	Li_2CO_3/H_3BO_3 + f.e.s.
384-9-1	0.495	0.483	0.502
384-9-3	0.395	0.395	0.390
384-9-4	0.395	0.390	0.391
384-9-5	0.432	0.434	0.434

TABLE 4

Comparative results in the analyses of various materials

Material	Na found (%)		Material	Na found (%)	
	Proposed method	$LiBO_2$/ a.a.s. method		Proposed method	$LiBO_2$/ a.a.s. method
KACC standard 384-9-3, 0.39% Na	0.39	0.40	Alumina catalyst support	0.084	0.075
Inter-plant check alumina 1075	0.32	0.33	Kaiser crushed A-201 desiccant	0.27	0.27
Reacted alumina 1075	1.53	1.56	Kaiser C-5R calcined alumina	0.26	0.24
Dried red mud	1.41	1.31	Kaiser KT-1061-6 tabular alumina	0.061	0.059
Exptl. silica-stabilized gel alumina	0.016	0.016	Kaiser KH-31 hydrated alumina	0.14	0.13

REFERENCES

1 H. Bennett, G. J. Oliver and M. Holmes, Trans. J. Br. Ceram. Soc., 76 (1977) 11.
2 British Standards Institution BS4140:1967. Addendum No. 2 (1974).
3 B. K. Tamnev, I. Khavezov and L. K. Iotova, Fresenius Z. Anal. Chem., 271 (1974) 349.
4 H. Strauss and R. Rutkowski, Chem. Tech. (Leipzig), 26 (1974) 718.
5 D. E. Thompson and R. S. Danchik, Anal. Lett., 8 (1975) 699.
6 Beckman Instruments, Inc., Fullerton, CA, Bulletin 7145-A (1973).
7 United Kingdom Atomic Energy Authority Report PG628(S) (1965).
8 R. P. Lucas and B. C. Ruprecht, Anal. Chem., 43 (1971) 1013.
9 M. E. Hofton and S. Baines, U. S. NTIS PB Rep. No. 240596 (1975).
10 E. L. Eckfeldt and W. E. Proctor, Anal. Chem., 43 (1971) 332.
11 M. F. Wilson, E. Haikala and P. Kwalvo, Anal. Chim. Acta, 74 (1975) 395.
12 L. G. Sillén and A. E. Martell, Stability Constants of Metal Ion Complexes, Spec. Publ. No. 17, The Chemical Society, London, 1964.
13 International Standard Organization, Technical Committee ISO/TC 47, Chemistry Working Group 8, Document 421 (1965).

Analytica Chimica Acta, 113 (1980) 307—314

EXTRACTION OF WATER-SOLUBLE ACID DYES BY ION-PAIR FORMATION WITH TRI-n-OCTYLAMINE

M. PUTTEMANS, L. DRYON and D. L. MASSART*

Farmaceutisch Instituut V.U.B., Laarbeeklaan 103, B-1090 Brussels (Belgium)

(Received 30th July, 1979)

SUMMARY

Water-soluble acid dyes can be quantitatively extracted from aqueous solutions as ion pairs with tri-n-octylamine in chloroform or n-heptane. The parameters influencing the extraction are discussed. Back-extraction of the dye to an aqueous phase is possible with perchlorate ions.

The classical method for the extraction of organic acids from an aqueous to an organic phase is based on the higher solubility of the undissociated molecules in organic solvents. However, given the very hydrophilic character of acid dyes, it is difficult to obtain an analytical extraction of these molecules from water to a less polar phase, and other methods must be sought.

The ion-pair extraction method introduced mainly by Schill and coworkers [1] consists in forming a complex between an ionized, more or less hydrophilic substance, and an ion of opposite charge. The complex is more hydrophobic than the ionized molecule and is therefore extracted to a greater extent into organic solvents. To achieve extraction of anions through ion pair formation the extractant has to be cationic, the conventional choices being quaternary ammonium derivatives or amines. The former are cationic over the whole pH range, while the latter are protonated only below a certain pH value. The extraction of dyes with quaternary ammonium derivatives has been described by several authors [2—4], but amines have rarely been studied.

In the work described here a tertiary amine, tri-n-octylamine (TOA), was chosen as counter-ion. The acid-and anion-binding properties of TOA have frequently been used for the extraction of mineral acids and metal complexes [5—7]. There are, however, few examples of extractions of organic anions with TOA. Lactic acid has been extracted into chloroform with TOA [5] and it has also been used as a stationary phase in a reversed-phase h.p.l.c. system for the separation of several anionic compounds [8] such as aromatic sulphonic acids, phenols, etc. Several parameters that can influence the extraction of the dyes, e.g., counter-ion concentration, pH of the aqueous phase and nature of the solvent, are discussed below. The back-extraction of the dye to an aqueous phase is also described.

EXPERIMENTAL

Apparatus and chemicals

All u.v. and visible photometric measurements were done with a Perkin-Elmer Hitachi 200 spectrophotometer. The pH values were measured with an Orion Ionalyser model 801 and a combined glass electrode.

The dyes listed in Table 1 (P. Entrop, Machelen, Belgium) were used as received. Tri-n-octylamine (Aldrich) was also used as received. All other reagents and solvents were of analytical grade (Merck). Chloroform was freed from ethanol by repeated shaking with water. Buffers of constant ionic strength (0.1) were prepared from sodium hydrogen phosphates except at pH 4 where acetate buffer was used.

Procedure

For batch extraction, equal volumes (10 ml) of the aqueous and organic phases were shaken in centrifuge tubes. The aqueous phase consisting of a dye solution at a given concentration in a buffer of ionic strength 0.1 was shaken for 30 min in a thermostatted bath at 25°C with a suitable TOA solution. The phases were separated after centrifugation. The concentration of dye in the aqueous layer was determined by u.v. or visible photometry. Each partition experiment was carried out in triplicate; the results are the average of these values.

RESULTS AND DISCUSSION

Theory

The following equilibria compete in the distribution of an acid HX between an aqueous (subscript w) and an organic phase (subscript o) containing a long-chain amine A [8]: (1) liquid—liquid distribution of the undissociated acid HX, $[HX]_w \rightleftharpoons [HX]_o$; (2) dissociation of the acid HX in the aqueous phase, $[HX]_w \rightleftharpoons [H^+]_w + [X^-]_w$; (3) extraction of the anion X^- by ion-pair formation, $[A]_o + [H^+]_w + [X^-]_w \rightleftharpoons [AHX]_o$. In the back-extraction of X^- to an aqueous phase containing Y^-, the ion-exchange reaction is [5—8]: $[AHX]_o + [Y^-]_w \rightleftharpoons [AHY]_o + [X^-]_w$.

In the present study, chloride and perchlorate ions were used to obtain back-extraction of X^-. The results of these experiments are conventionally expressed by percentage extraction or the distribution ratio D: D = (total concentration of HX in the organic phase)/(total concentration of HX in the aqueous phase) = $[HX]_o/[HX]_w$.

Preliminary experiments

Initially, extractions were tested with tri-n-octylamine (TOA) and tri-iso-octylamine. Chrysoine S was used as the test dye and was extracted with a 0.1 M solution of the amine in chloroform and in n-heptane. The results (Table 2) showed that the normal isomer is a much better extractant than

TABLE 1

Structures of dyes studied [9]

Trivial name	Systematic name	Formula	C.I. no.
Chrysoine S	Food Yellow 8	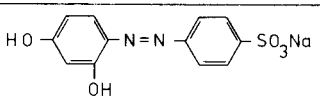	14270
Cochineal red A	Food Red 7	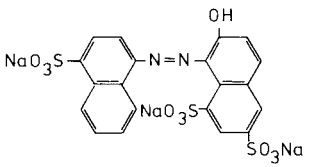	16255
Tartrazine	Food Yellow 4	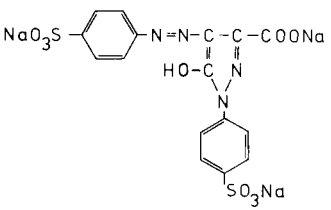	19140
Brilliant Green BS	Food Green 4	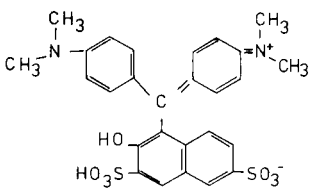	44090
Indigotin I	Food Blue 1	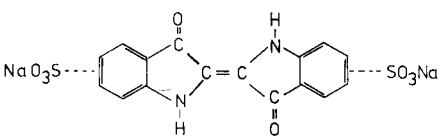	73015
Erythrosine	Food Red 14	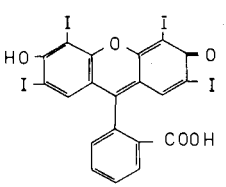	45430
Ponceau 6R	Food Red 8	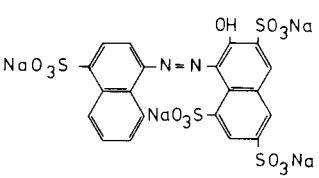	16290

TABLE 1 (cont.)

Trivial name	Systematic name	Formula	C.I. no.
Brilliant Black BN	Food Black 1	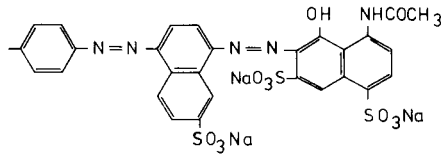	28440

TABLE 2

Percentage extraction of 10^{-5} M chrysoine S with 0.1 M trioctylamine isomers in chloroform and n-heptane from an aqueous buffer solution (pH 3.6; ionic strength 0.1)

	Pure solvent	Tri-n-octylamine	Tri-iso-octylamine
Chloroform	9.4	100	98
n-Heptane	4.0	73.5	6.0

tri-iso-octylamine. The more compact structure of the latter isomer makes the nitrogen atom less accessible, so that the extracting power decreases [6]. All further experiments were done with tri-n-octylamine.

Influence of the solvent and of TOA concentration

Extractions were tested with n-heptane and chloroform solutions. Examination of the results listed in Tables 2 and 3 shows that n-heptane is a poorer solvent than chloroform. These data suggest that the ion-pair is better solvated in chloroform than in the less-polar solvent, probably because of hydrogen bond formation.

To investigate the influence of counter-ion concentration on the extraction yield, partition experiments were done near the pH of maximal extraction. The results (Table 3) prove that in the TOA concentration range studied extraction into chloroform is very efficient. To investigate the extraction mechanism, some similar experiments were also carried out in the poorer solvent, n-heptane (Table 3). In this case, several side-reactions such as ion-pair formation in the aqueous phase, dimerization of the ion-pair, dissociation of the ion-pair in the organic phase or adduct-formation may occur [1]. In the last case, the dye would be extracted as the adduct AHX. A together with the normal ion-pair AHX. If this is the only side-reaction, the slope of a logarithmic plot of the distribution ratio versus the TOA concentration, should yield the number of molecules of TOA in the complex. Figure 1 shows the graphs obtained for chrysoine S and cochineal red A. The slopes are 1.39 and 1.03, respectively, which indicate the presence of

TABLE 3

Percentage extraction of dyes with different concentrations of TOA in chloroform or n-heptane from aqueous buffer solutions with pH 5.0 (ionic strength 0.1)

	Dye concn. (M)	TOA concentration (M)				
		10^{-1}	5×10^{-2}	10^{-2}	5×10^{-3}	0
Extraction into chloroform						
Chrysoine S	5×10^{-5}	100	99.5	99	—	4
Cochineal red A	5×10^{-5}	100	100	99	—	1
Tartrazine	6×10^{-5}	100	100	100	—	2
Brilliant Green BS	10^{-5}	100	100	99.5	—	2
Indigotin	10^{-5}	96	90	79	—	3
Erythrosine	10^{-5}	98	97	96.4	—	4
Ponceau 6 R	5×10^{-5}	100	99.4	99		3
Brilliant Black BN	10^{-5}	100	100	99.5	—	2
Extraction into n-heptane						
Chrysoine S	5×10^{-5}	98	94	67	39	—
Cochineal red A[a]	5×10^{-5}	99	98	92	84	—

[a]At pH 7.

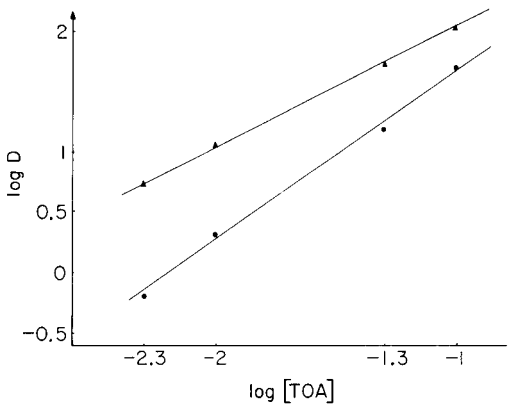

Fig. 1. Logarithmic plot of the distribution ratio as a function of the logarithm of the TOA concentration in n-heptane. (•) Chrysoine S (5×10^{-5} M). (▲) Cochineal red (5×10^{-5} M).

both AHX and AHX.A for chrysoine S and AHX for cochineal red A. These conclusions are valid for n-heptane, but not necessarily for other solvents, because the extraction mechanism may be solvent-dependent.

Influence of pH

The pH is an important factor in the extraction for two reasons: the dye can be extracted only as the ion and the amine has to be protonated. The

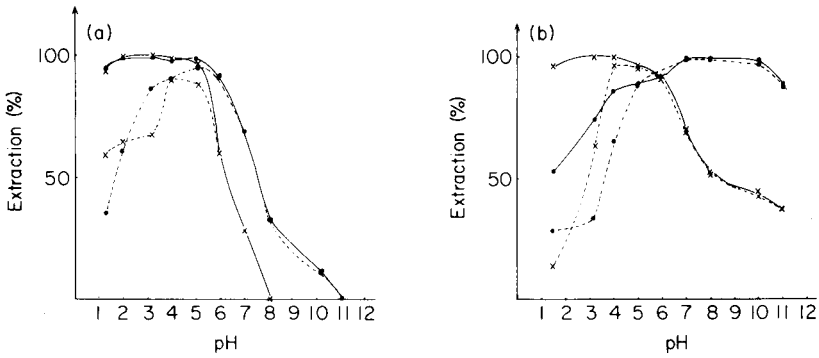

Fig. 2. Percentage extraction of (a) 5×10^{-5} M chrysoine S and (b) 5×10^{-5} M cochineal red A as a function of pH. (×) with 10^{-2} M TOA in chloroform; (•) with 10^{-1} M TOA in n-heptane. The full lines show the original results; the dashed lines indicate the results obtained after subtraction of the extraction caused by the solvent alone.

presence of a maximum in the graph of percentage extraction versus pH would therefore be expected. In order to demonstrate the effect of the pH on the degree of extraction by ion-pair formation, extraction of the dye by the pure organic solvent must also be considered, for at low pH values the undissociated dye is extracted slightly by the solvent alone. Cochineal red A and chrysoine S were extracted with 10^{-2} M TOA in chloroform, 10^{-1} M TOA in n-heptane and with the pure solvents from aqueous buffers at ionic strength 0.1. Figure 2 shows that maxima are obtained over broad pH intervals. After subtraction of the amount of dye extracted by the pure solvent from the total extraction, the pH effect on the ion-pair process is clarified (Fig. 2). The extractions into chloroform show narrower maxima than into n-heptane. The pH values at the maxima differ for the two solvents, because the basic strength of TOA depends on the solvent [5]. It is interesting to note that chrysoine S is not extracted at pH > 8 in chloroform and at pH > 11 in n-heptane, while cochineal red A is. This probably happens because chrysoine S (a diphenol) forms a water-soluble phenolate above a given pH value, which suggests that TOA is a poor counter-ion for extraction of phenols.

Extraction of water-soluble acid dyes

The above results indicate that the best conditions for extraction are: 0.1 M TOA in chloroform as the organic phase and a buffer solution of pH 5 as the aqueous phase. Under such conditions, extraction is essentially quantitative in all cases (Table 3). The dye concentrations were chosen mainly so that direct u.v. or visible photometry could serve to measure concentrations. Lower concentrations of dyes could also be extracted completely with TOA concentrations less than 0.1 M. Only indigotin was not extracted

TABLE 4

Back-extraction from 0.1 M TOA in chloroform by an aqueous 0.1 M sodium hydroxide solution

	Phenol functions	Dye concn. (M)	Back-extraction (%)
Chrysoine S	2	5×10^{-5}	97
Cochineal red A	1	5×10^{-5}	75
Tartrazine	—	5×10^{-5}	9
Brilliant green BS	1	10^{-5}	84
Indigotin	—	10^{-5}	64

quantitatively, probably because its structure is quite different from those of the other dyes studied.

Back-extraction

Different methods were investigated for the back-extraction of the dyes from chloroform to an aqueous phase. A 0.1 M sodium hydroxide solution was excellent for back-extraction of chrysoine S, which contains two phenol groups. An examination of other dyes with and without phenol groups (Table 4) proved the existence of a phenolate effect. Consequently, satisfactory back-extractions by sodium hydroxide solutions are caused mainly by the high solubility of phenolates in water. The relatively high back-extraction of indigotin is probably due to the fact that it is not well extracted initially.

Vollaire-Salva [2] back-extracted dyes from their extracted ion-pairs with quaternary ammonium compounds, by repeatedly shaking with small portions of concentrated hydrochloric acid. In the case of TOA extracts, however, this mode of back-extraction was unsatisfactory: only 70—80% of the dyes present in the chloroform layer were back-extracted.

Schill [1] extracted tetrabutylammonium with perchlorate ions and Kraak and Huber [8] employed perchlorate in their h.p.l.c. procedure with TOA as the stationary phase. Back-extraction with aqueous perchlorate solutions was therefore tested. Table 5 indicates that perchlorate solutions gave good back-extractions with both acidic and neutral media.

In summary, TOA is shown to be a good reagent for extraction of synthetic water-soluble food dyes into chloroform. When n-heptane is used, the pH is more critical. Satisfactory back extractions are obtained with perchloric acid.

The authors acknowledge the financial help of F.G.W.O.

TABLE 5

Back-extractions from 0.1 M TOA in chloroform by perchloric acid and perchlorate solutions

	Dye conc. (M)	$HClO_4$		$NaClO_4$ 0.1 M
		1 M	0.1 M	
Chrysoine S	5×10^{-5}	100	100	99
Cochineal red A	5×10^{-5}	100	99	99
Tartrazine	5×10^{-5}	100	99	98
Brilliant green BS	10^{-5}	100	30	28

REFERENCES

1 G. Schill, Separation Methods for Drugs and Related Organic compounds, Apotekarsocieteten, Stockholm, 1978.
2 J. Vollaire-Salva, Ann. Fals. Exp. Chim., (1961) 17.
3 B. Drevon and J. Laur, Ann. Fals. Fraud., (1959) 155.
4 J. Sohár, Z. Lebensm. Unters. Forsch., 132 (1967) 359.
5 Y. Marcus and A. S. Kertes, Ion Exchange and Solvent Extraction of Metal Complexes, Wiley-Interscience, New York, 1969.
6 V. S. Shmidt, Amine Extraction, Israel Program for Scientific Translations Ltd., Jerusalem, 1971.
7 T. Braun and G. Ghersini, Extraction Chromatography, Elsevier, Amsterdam, 1975.
8 J. C. Kraak and J. F. K. Huber, J. Chromatogr., 102 (1974) 333.
9 Färbemittel für Kosmetika, 3. Auflage 1968, 1. Nachtrag 1971, Franz Steiner Verlag, Wiesbaden.

Analytica Chimica Acta, 113 (1980) 315—321

THE SOLVENT EXTRACTION OF EUROPIUM AND BARIUM WITH 1-ARYL-3-METHYL-4-AROYL-5-PYRAZOLONES

SHIGEO UMETANI, MASAKAZU MATSUI, JUN'ICHI TÔEI and TSUNENOBU SHIGEMATSU*

Institute for Chemical Research, Kyoto University, Uji, Kyoto 611 (Japan)

(Received 5th July 1979)

SUMMARY

Eleven 1-aryl-3-methyl-4-aroyl-5-pyrazolone derivatives were synthesized. Their acid dissociation constants were determined spectrophotometrically; there was a linear relationship between them and Hammett's σ values. Europium and barium ions were readily extracted into benzene and n-octyl alcohol, respectively, at very low pH.

1-Phenyl-3-methyl-4-benzoyl-5-pyrazolone (HPMBP) has proved to be a very versatile reagent for the solvent extraction of metal ions, especially lanthanide and alkaline earth ions [1—9]. It is a β-diketone, but it is able to extract most metal ions at a lower pH (10—14) than even trifluoromethyl-substituted β-diketones such as thenoyltrifluoroacetone, because it has a very small acid dissociation constant. Therefore, it would be expected that the introduction of electron-withdrawing substituents and bulky groups into the 4-aroyl group of the pyrazolone would enhance the acidity of the compounds and increase their solubilities in an organic solvent, and that metal ions might still be extracted at a low pH, with a larger distribution ratio. The present paper examines the possible uses of 4-aroyl derivatives of 5-pyrazolones (I) as reagents for the solvent extraction of metal ions.

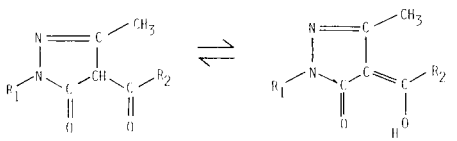

(I)

EXPERIMENTAL

Apparatus

Radioactivity was counted with a Metro Electronics NaI(Tl) (44.5 mm diam. × 50.8 mm) well-type scintillation counter, Model PbW-6, connected to a Metro automatic scaler, Model SS-1060H. Other instrumentation included a Hitachi-Horiba pH meter (model F-7ss), a Hitachi 323 recording

spectrophotometer (for spectra) and a Hitachi 139 spectrophotometer (for absorbance measurements) with 1-cm cells.

Reagents

1-Aryl-3-methyl-4-aroyl-5-pyrazolone derivatives were synthesized from 1-aryl-3-methyl-5-pyrazolones and the appropriate acid chlorides, as described by Jensen [15]. The crude products were purified by recrystallizing twice from aqueous dioxane and dried under reduced pressure. The elemental analyses of the compounds obtained are shown in Table 1.

The $^{152, 154}$Eu and ^{133}Ba isotopes, as their chloride salts, were supplied by New England Nuclear, Boston, Mass. The solutions were diluted with 2 M hydrochloric acid to 1 μCi ml^{-1}. Carrier solutions of europium and barium were prepared by dissolving europium oxide and barium carbonate in hydrochloric acid.

All other solvents and reagents were reagent-grade materials and were used without further purification.

TABLE 1

Elemental analyses of the compounds studied

Reagent No.	R_1	R_2	Analysis (%)			M.p. (°C)
			Calc. C found	H	N	
1	Phenyl	Phenyl	73.37	5.07	10.07	92—92.5
			73.50	4.99	10.22	(lit. 92)[a]
2	Phenyl	4-Nitrophenyl	63.16	4.05	13.00	202
			63.10	3.92	13.11	(lit. 200)[a]
3	Phenyl	2-Chlorophenyl	65.29	4.19	8.96	150—151
			65.21	4.09	8.98	
4	Phenyl	2, 4-Dichlorophenyl	58.81	3.48	8.07	157—158
			58.66	3.44	8.05	
5	Phenyl	2-Chloro-4-nitrophenyl	57.08	3.38	11.75	194—195
			57.08	3.35	11.93	
6	4-Nitrophenyl	Phenyl	63.16	4.05	13.00	224—225
			62.83	4.04	13.21	(lit. 224)[a]
7	4-Methylphenyl	Phenyl	73-96	5.52	9.58	111—112
			73.99	5.55	9.77	
8	Phenyl	4-Methylphenyl	73.96	5.52	9.58	100
			74.01	5.46	9.66	
9	Phenyl	3-Methylphenyl	73.96	5.52	9.58	94—95
			73.72	5.39	9.38	
10	Phenyl	2-Methylphenyl	73.96	5.52	9.58	111—112
			73.64	5.52	9.33	
11	Phenyl	2-Naphthyl	76.81	4.91	8.53	101
			76.93	4.96	8.55	

[a]See ref 15.

Extraction procedure

Extractions were done by shaking 10 ml of the aqueous sample solution with 10 ml of the organic solvent containing one of the pyrazolones for 1 h at 25 ± 1°C. The aqueous sample solution, adjusted to the desired pH, contained a few ppm of metal ion ($2-3 \times 10^4$ cpm), sodium perchlorate (0.1 M), and acetic acid—sodium acetate (0.02 M) buffer. The organic solvent phase was 0.02 or 0.01 M pyrazolone derivative in benzene, isoamyl alcohol or n-octyl alcohol. After the layers had been separated centrifugally, 2 ml of each phase was pipetted into test tubes and the radioactivities were counted. After the extraction the pH value of the aqueous phase was again measured.

RESULTS AND DISCUSSION

Acid dissociation constants of the pyrazolones

The 4-aroyl-5-pyrazolone derivatives are soluble in various organic solvents including chloroform, benzene and alcohols, as well as in alkaline aqueous solutions, but are sparingly soluble in water. Therefore absorbances were measured in 10% (v/v) dioxane—water at 25°C. Sodium perchlorate was added to adjust the ionic strength to 0.1, and 0.01 M acetic acid—sodium acetate was used to buffer the solution.

The acid dissociation constant of the 5-pyrazolone derivative is defined by $K_a = [H^+][A^-]/[HA]$, where [HA] and $[A^-]$ are the concentrations of the neutral and anionic species of the derivative, respectively. This equation can be rewritten: $pK_a = pH - \log([A^-]/[HA]) = pH - \log(\epsilon - \epsilon_{A^-})/(\epsilon_{HA} - \epsilon)$ where ϵ_{HA} and ϵ_{A^-} are the molar absorptivities of [HA] and [A] and ϵ is the total molar absorptivity of [HA] and $[A^-]$ at any given pH and at the same wavelength.

Figure 1 shows some typical examples of the linear plots of $\log(\epsilon - \epsilon_{A^-})/(\epsilon_{HA} - \epsilon)$ vs. pH obtained. The pK_a values obtained from these plots are listed in Table 2. As can be seen each derivative has a very low pK_a value, even compared with trifluoromethyl-substituted β-diketones; for example, thenoyltrifluoroacetone has a pK_a value of 6.23 [16].

Further, there is a linear relationship between these acidity constants and the Hammett σ values for R_1 and R_2 substitution (Fig. 2). It is very interesting that the influence of R_1 substitution on the acid dissociation of 5-pyrazolone derivatives is larger than that of R_2 substitution.

Extraction of europium

In the extraction of triply-charged metal ions such as europium with HPMBP derivatives (HR) the extraction equilibrium and the extraction constant, K_{ex}, can be expressed by

$$M^{3+}_{aq} + 3HR_{org} \rightleftharpoons MR_{3org} + 3H^+_{aq}$$

$$K_{ex} = ([MR_3]_{org}[H^+]^3_{aq})/([M^{3+}]_{aq}[HR]^3_{org})$$

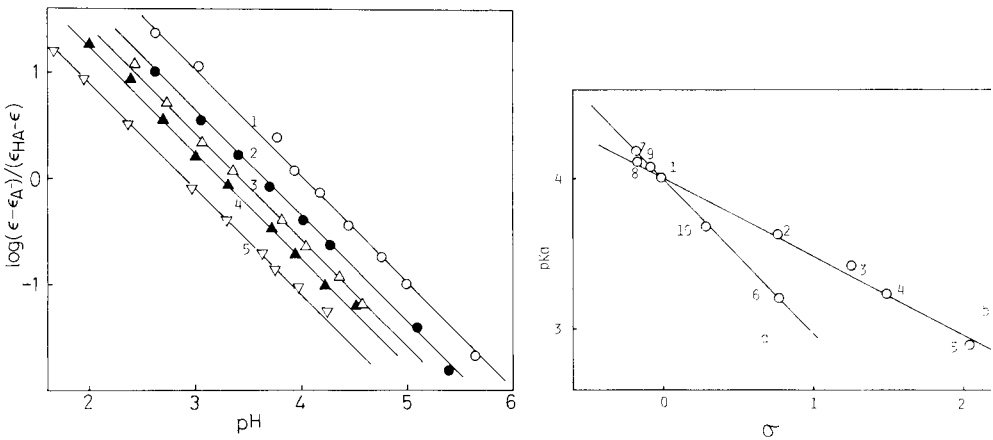

Fig. 1. Plots for measuring the dissociation constants of the 4-aroyl derivatives. The numerals show the reagent number in Table 1.

Fig. 2. Plot of pK_a value vs. Hammett's σ values for the various pyrazolones: (a) 1-aryl derivatives of 3-methyl-4-benzoyl-5-pyrazolone; (b) 4-aroyl derivatives of 1-phenyl-3-methyl-5-pyrazolone.

If the concentrations of intermediate complexes such as MR^{2+} and MR_2^+ are negligible, the distribution constant is given by $D = [MR_3]_{org}/[M^{3+}]_{aq} = K_{ex}[HR]^3_{org}/[H^+]^3_{aq}$. Thus $-\log K_{ex} = pH_{1/2} + 3\log[HR]_{org}$.

The extraction curves for the europium chelates, using benzene as the organic solvent, are shown in Fig. 3. In each case, the logarithm of the distribution ratio is linearly dependent upon pH, when the concentration of extractant is constant. The slope of all the plots is almost three, indicating that three hydrogen ions are released in the formation of each europium chelate in each case. The pH values at half-extraction, $pH_{1/2}$, and the extraction constants calculated therefrom, are summarized in Table 2. As is shown in the Table, the value of $pH_{1/2}$ decreases as that of pK_a decreases. When benzene was used for the organic phase in the extraction of other europium β-diketone chelates, the value of $\log K_{ex}$ was -18.9 for dibenzoylmethane [17] and -7.66 for thenoyltrifluoroacetone [18]. The value of $\log K_{ex}$ for 4-aroyl-5-pyrazolone derivatives is -4.92 to -1.56. Thus, these 5-pyrazolone derivatives have a larger extraction constant for europium than other β-diketones. Further, there is a linear relationship between $\log K_{ex}$ and pK_a, as is shown in Fig. 4. This suggests that the effect of the proton dissociation on the resonance of the ligand plays a more important role in the extraction behaviour than the π-electron distribution of the europium chelate rings. Figure 4 also suggests that the steric effect of a terminal group of the 1-aryl-4-aroyl-5-pyrazolones such as β-naphthyl, 2, 4-dichlorophenyl or 2-methylphenyl groups did not have an important influence on the chelate formation with europium.

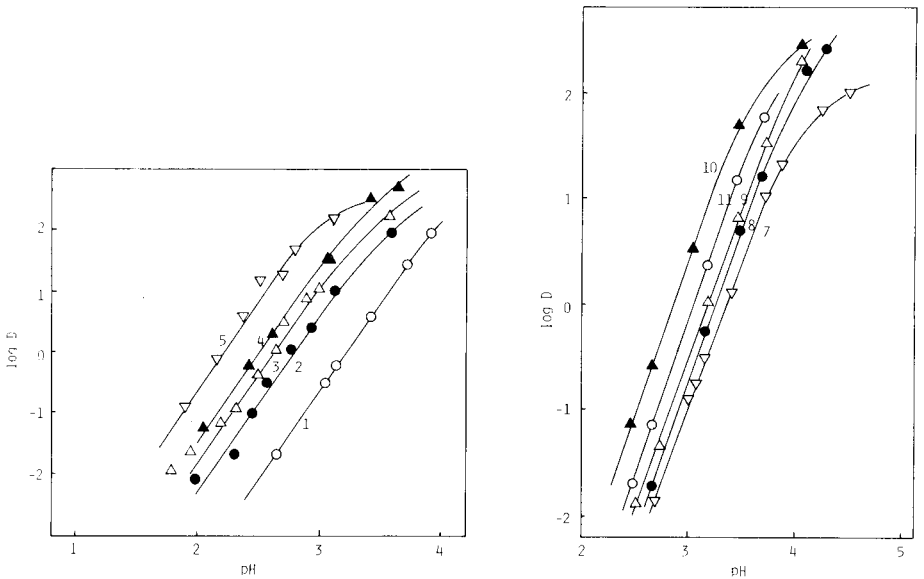

Fig. 3. Logarithm of the distribution ratio of europium(III) as a function of pH. Reagent: 2×10^{-2} M in benzene.

TABLE 2

pK_a values for the pyrazolone derivatives, and extraction parameters for the europium and barium complexes

Reagent No.[a]	pK_a in 10% (v/v) dioxane	Europium		Barium	
		$pH_{1/2}$	log K_{ex}	$pH_{1/2}$	log D_{max}
1	4.02	3.22	−4.56	5.95	0.76
				(5.90)[d]	(1.30)[d]
2	3.64	2.79	−3.27	—	−0.86[c]
3	3.43	2.62	−2.76	5.28	0.96
4	3.24	2.51	−2.43	5.12	1.05
				(5.08)[d]	(1.50)[d]
5	2.90	2.22	−1.56	—	−0.58[c]
6[b]	3.21	3.26[a]	−2.88	—	—
7	4.19	3.34	−4.92	6.00	1.12
8	4.13	3.25	−4.65	5.98	1.14
9	4.08	3.18	−4.44	5.82	1.26
10	3.70	2.84	−3.42	5.52	1.20
11	4.00	3.05	−4.05	5.74	1.38
				(5.78)[d]	(1.88)[d]

[a]See Table 1. [b]Not soluble in alcohol. [c]5×10^{-3} M reagent. [d]Reagent in n-octyl alcohol.

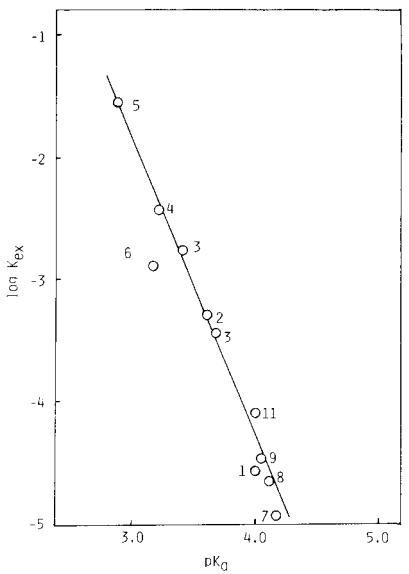

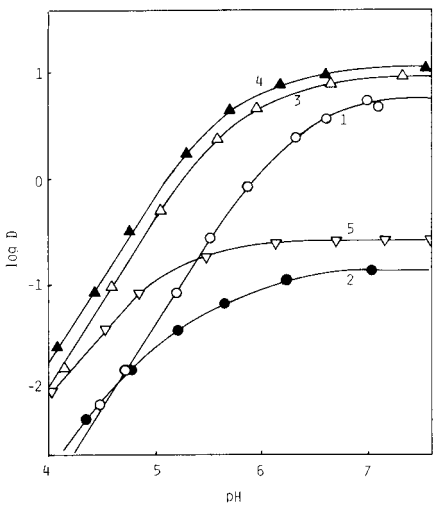

Fig. 4. Plot of log K_{ex} vs. pK_a plot for the europium(III) chelates.

Fig. 5. Logarithm of the distribution ratio of barium(II) as a function of pH. Organic phase, 1×10^{-2} M of reagent 1, 3 or 4 or 5×10^{-3} M of reagent 2 or 5 in isoamyl alcohol.

Extraction of barium

Barium ions are one of the most poorly extractable metal ions. Hence, the extraction of barium ions was investigated with the various 5-pyrazolone derivatives as the extractant. When benzene was utilized for the organic phase, barium ions were scarcely extracted at pH 6—10. This may be because the co-ordination number of barium (six) is not satisfied by the oxygen atoms of the chelating agent. At least two water molecules might be retained by the barium ion and thus decrease the distribution ratio. In the present work, isoamyl alcohol and n-octyl alcohol were used as oxygen-containing solvents which might replace the water molecules. Figure 5 shows typical examples of the log D vs. pH plot for the extraction of barium chelates with isoamyl alcohol. 5-Pyrazolone derivatives containing a nitro group are somewhat sparingly soluble in the higher alcohols, so that concentrations of 5×10^{-3} M were used for the nitro-derivatives, as compared to 1×10^{-2} M for the other derivatives. The slopes of the straight lines are less than 2, the theoretical value. The deviation from the theoretical value may principally be due to the incomplete partition of the uncharged chelate. As is shown in Fig. 5, the nitro group decreased the distribution ratio, but the chloro group increased it. Further, an increase of the distribution ratio for barium can be expected if an alcohol with more carbon atoms is used for the solvent. As is shown in Fig. 6, n-octyl alcohol increased the distribution ratio of the barium chelate compared with isoamyl alcohol. The

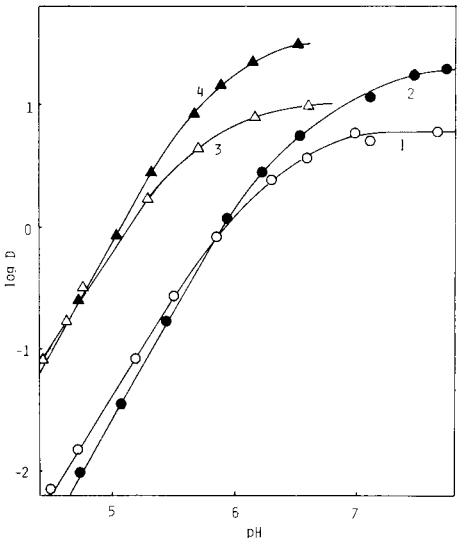

Fig. 6. Logarithm of the distribution ratio of barium(II) as a function of pH. (1) HPMBP in isoamyl alcohol; (2) HPMBP in n-octyl alcohol; (3) reagent 4 in isoamyl alcohol; (4) reagent 4 in n-octyl alcohol. Reagent: 1×10^{-2} M in all instances.

pH value at half extraction, $pH_{1/2}$ and maximum distribution ratio of barium, $\log D_{max}$, are summarized in Table 2; 99% of the barium could be extracted into n-octyl alcohol by using a 0.01 M solution of the 2-naphthyl substituent.

REFERENCES

1 Yu. A. Zolotov and V. G. Lambrev, Zh. Anal. Khim., 20 (1965) 659.
2 Yu. A. Zolotov, M. K. Chmutova and P. N. Palei, Zh. Anal. Khim., 21 (1966) 1217.
3 M. K. Chmutova, P. N. Palei and Yu. A. Zolotov, Zh. Anal. Khim., 23 (1968) 1476.
4 M. K. Chmutova and N. E. Kochetkova, Zh. Anal. Khim., 24 (1969) 216.
5 B. F. Myasoedov and N. P. Molochnikova, Zh. Anal. Khim., 24 (1969) 702.
6 M. K. Chmutova, N. E. Kochetkova and Yu. A. Zolotov, Zh. Anal. Khim., 24 (1969) 711.
7 Yu. A. Zolotov, N. T. Sizonenko, N. T. Zolotovitskaya and E. I. Yakovenko, Zh. Anal. Khim., 24 (1969) 20.
8 Yu. A. Zolotov and L. G. Gavrilova, J. Inorg. Nucl. Chem., 31 (1969) 3613.
9 Yu. A. Zolotov, O. M. Petrukhin and L. G. Gavrilova, J. Inorg. Nucl. Chem., 32 (1970) 1679.
10 Y. Akama, T. Nakai and F. Kawamura, Jpn. Anal., 25 (1976) 496.
11 Y. Akama, H. Naka, T. Nakai and F. Kawamura, Jpn. Anal., 27 (1978) 680.
12 G. N. Rao and H. C. Arora, J. Inorg. Nucl. Chem., 19 (1977) 2057.
13 A. Roy and K. Nag, J. Inorg. Nucl. Chem., 40 (1978) 331.
14 B. Jensen, Acta. Chem. Scand., 13 (1959) 1890.
15 B. Jensen, Acta. Chem. Scand., 13 (1959) 1668.
16 J. C. Reid and M. Calvin, J. Am. Chem. Soc., 72 (1950) 2948.
17 J. Stary and E. Hladky, Anal. Chim. Acta, 28 (1963) 227.
18 H. Irving and D. N. Edgington, J. Inorg. Nucl. Chem., 21 (1961) 169.

Analytica Chimica Acta, 113 (1980) 323—329

QUANTITATIVE SEPARATION OF GALLIUM FROM URANIUM, COBALT, ALUMINIUM AND MANY OTHER ELEMENTS BY CATION-EXCHANGE CHROMATOGRAPHY IN MIXTURES OF HYDROCHLORIC OR HYDROBROMIC ACID WITH ACETONE

F.W.E. STRELOW

National Chemical Research Laboratory, P.O. Box 395, Pretoria 0001 (South Africa)

(Received 29th May 1979)

SUMMARY

Gallium can be separated from U(VI), Co(II), Al, Li, Na, Be, Mg, Ca, Ba, La, Ti(IV), Th, Mn(II) and Ni(II) by elution with 0.20 M hydrochloric acid in 84% acetone or with 0.50 M hydrobromic acid in 86% acetone from a column of AG50W-X4 cation-exchange resin (200—400 mesh), while all these elements are retained. Separations are sharp, quantitative and applicable to microgram and millimolar amounts of gallium. When elements forming bromide complexes, e.g. zinc and cadmium, are eluted with 0.50 M hydrobromic acid in 80% acetone prior to elution of gallium, the method separates gallium from almost all other elements. Relevant elution curves and results of the analysis of synthetic mixtures are presented.

It has been shown recently that elements such as Zn, Cu(II), In, Cd, Pb(II), Bi(III), Au(III), Pt(IV), Pd(II), Tl(III), Sn(IV) and Fe(III) which have a relatively strong tendency to bromide complex formation can be eluted with 0.50 M hydrobromic acid in 80% acetone from AG50W-X4 cation-exchange resin while gallium is retained quantitatively [1]. Elements such as Al, Ti(IV), Zr, Hf, alkaline earths, alkali metals, rare earths, Mn(II), Ni(II), Co(II), U(VI) and others, which have weaker tendencies to bromide complex formation, are retained together with gallium. In order to separate gallium from all these elements, an eluting agent is required which selectively elutes gallium. An inspection of available distribution coefficients [2, 3] reveals that either 0.20 M hydrochloric acid containing 84% acetone or 0.50 M hydrobromic acid containing 86% acetone should effectively elute gallium without eluting the other elements. The separation of gallium from these other elements therefore has been investigated in more detail using a resin of 4% cross-linkage in order to minimize the known tailing effects for gallium [3, 4].

EXPERIMENTAL

Reagents and apparatus

Gallium chloride prepared from 99.99% gallium (Fluka) was used. All

other reagents were of analytical-reagent grade. Water was distilled and then deionized. The columns were of borosilicate glass with glass sinters (No. 2 porosity) and a buret tap at the bottom.

The reagent concentrations are rather critical for the separations described. Thus the reservoir for the eluting agent must be protected against acetone evaporation by a stopper through which passes a thick-walled capillary, and reagents must be measured accurately. For example, 0.35 M hydrobromic acid in 83% acetone means 140.0 ml of 2.50 M hydrobromic acid, plus 30 ml of deionized water, plus 830 ml of acetone, disregarding volume changes on mixing. Volumes should be measured to better than ± 0.5%.

Elution curves

An ion-exchange column containing 65 ml (15 g dry weight) of AG50W-X4 resin (200—400 mesh; Bio-Rad Laboratories, Richmond, California) was equilibrated by passing 100 ml of 0.2 M nitric acid containing about 70% acetone. The resin column was 18 cm long and 2.15 cm in diameter before equilibration. A solution containing about 1 mmol each of gallium and uranium(VI) in about 25 ml of 0.2 M nitric acid containing 70% acetone was passed through the column and washed onto the resin with the same reagent. The gallium was then eluted with 0.20 M hydrochloric acid in 84% acetone at a flow rate of 3.0 ± 0.5 ml min^{-1} until the uranium(VI) also appeared in the eluate; 25-ml fractions were taken with an automatic fractionator from the beginning of the gallium elution step. After the fractions had been evaporated to dryness, the residues were dissolved in 10 ml of 0.1 M hydrochloric acid. Gallium was determined by atomic absorption spectrometry after appropriate dilution if required, and uranium(VI) was determined spectrophotometrically (see Table 1). The experimental elution curve is presented in Fig. 1.

When the experiment was repeated but with 0.50 M hydrobromic acid in 86% acetone for elution of gallium, no uranium(VI) was found in the

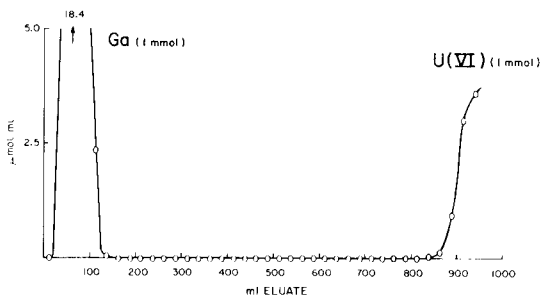

Fig. 1. Elution curve for gallium and uranium(VI) with 0.20 M HCl in 84% acetone.

TABLE 1

Analytical methods used

Element	Method
Ga, Al	Complexometric with DCTA; back-titration with $ZnSO_4$ at pH 5.5 (xylenol orange). Small amounts and elution curves of Ga by atomic absorption spectrometry (294.4-nm line; air—acetylene flame)[a]
U(VI)	Gravimetric as U_3O_8. Small amounts by spectrophotometry of the arsenazo-III complex at 655 nm in presence of DTPA at pH 2.
Co(II)	Titrimetric with EDTA at pH 6 (pyridine buffer; naphthyl azoxine S). Small amounts by atomic absorption spectrometry.[a]
Li, Na	Atomic absorption spectrometry.
Be	Gravimetric with cupferron at 10°C and pH 5.7.
Mg	Titration with EDTA at pH 10 (eriochrome blueblack B).
Ca, Mn(II)	Titration with EDTA (methylthymol blue); hydroxylammonium chloride present for Mn(II).
Ba	Gravimetric as $BaSO_4$.
La	Titration with DCTA at pH 5.5 (xylenol orange).
Ti(IV)	Spectrophotometrically as complex with H_2O_2.
Th	Gravimetrically as ThO_2 after precipitation as oxalate.
Ni(II)	Titration with EDTA (murexide).

[a]With a Perkin-Elmer 303 or a Varian-Techtron AA5 spectrometer.

first 1000 ml and the gallium peak was slightly wider. When cobalt(II) (the element with the next strongest tendency to chloride and bromide complex formation of the multivalent elements retained together with gallium) was tested, no cobalt was detected in the first 1000 ml of eluate with either eluting agent.

Since gallium can be selectively eluted after Zn, Cu(II), In and other elements forming relatively stable bromide complexes have been eluted with 0.5 M hydrobromic acid in 80% acetone and because some of the retained elements can move on the column quite appreciably during this elution, some elution curves were prepared which included this preceding elution step. Figure 2 shows an elution curve obtained for a mixture of

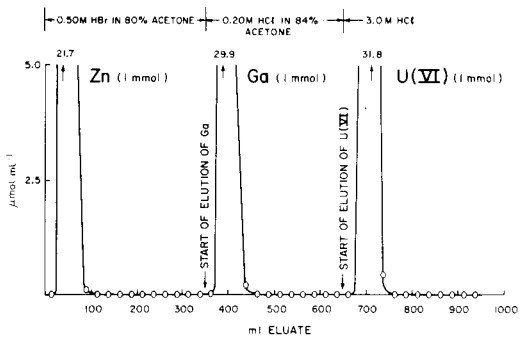

Fig. 2. Elution curve for zinc, gallium and uranium(VI). Elution of gallium is with 0.20 M HCl in 84% acetone.

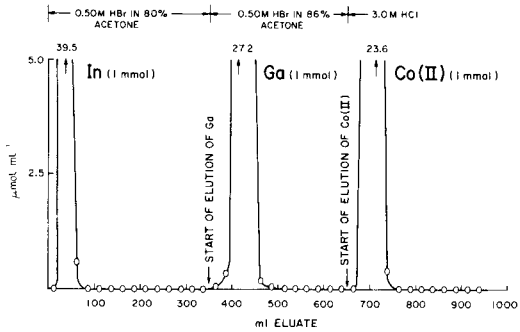

Fig. 3. Elution curve for indium, gallium and cobalt(II). Elution of gallium is with 0.50 M HBr in 86% acetone.

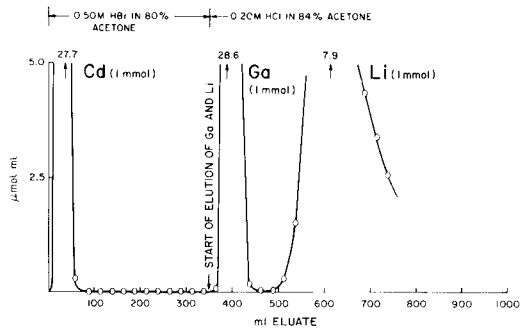

Fig. 4. Elution curve for cadmium, gallium and lithium (see text).

zinc, gallium and uranium(VI), while Fig. 3 shows an elution curve for a mixture of indium, gallium and cobalt(II). The flow rate was 3.0 ± 0.5 ml min^{-1} throughout. Figure 4 shows the elution of cadmium with 0.50 M hydrobromic acid in 80% acetone followed by elution of gallium and lithium with 0.20 M hydrochloric acid in 84% acetone. Figure 5 shows the elution of copper(II) with 0.35 M hydrobromic acid in 83% acetone followed by elution of gallium with 0.20 M hydrochloric acid in 84% acetone and of lithium by aqueous 1.0 M hydrochloric acid.

Quantitative separations of synthetic mixtures

Standard solutions of gallium and one other element in dilute nitric acid were measured (in triplicate), mixed and evaporated to a small volume. Enough water, nitric acid and acetone were added to make the final concentration about 0.3 M nitric acid in 70% acetone. Three standards each of gallium and of the other element were measured out and kept separate for comparison. The synthetic mixtures were passed through columns of the

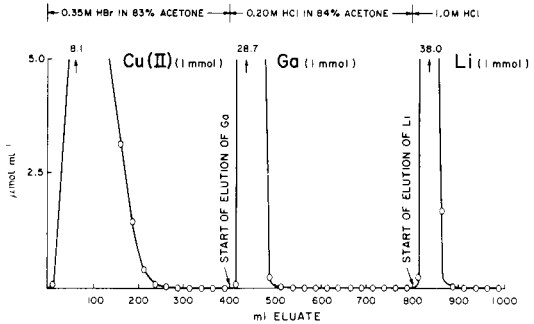

Fig. 5. Elution curve for copper(II), gallium and lithium (see text).

AG50W-X4 resin prepared and equilibrated as described under *Elution curves*. Gallium was then eluted with 200 ml of 0.20 M hydrochloric acid in 84% acetone. Flow rates of 3.0 ± 0.5 ml min^{-1} were used in this and subsequent steps. Acetone was washed from the column by passing through 100 ml of 0.1 M hydrochloric acid. The other element was then normally eluted with 200 ml of 3.0 M hydrochloric acid, but 200 ml of 1.0 M hydrochloric acid was used for lithium, 350 ml of 4.0 M hydrochloric acid for lanthanum and zirconium, 250 ml of 3.0 M nitric acid for barium, and 500 ml of 5.0 M nitric acid for thorium. About 50 ml of deionized water was added to the gallium-containing eluates, which were then passed through columns (7.0 cm long, 2.0 cm i.d.) containing 22 ml (5 g) of AG50W-X4 resin. Acetone was washed from the columns with 50 ml of 0.1 M hydrochloric acid and gallium was then eluted with 150 ml of 3.0 M hydrochloric acid. This separation of gallium from acetone is necessary for accurate work because gallium is lost in small amounts (0.5—2%) when acetone-containing solutions of hydrochloric and hydrobromic acid are evaporated, even on a water bath.

The aqueous hydrochloric acid solutions containing gallium, and the eluates containing the other elements, were then evaporated to dryness on the water bath and the elements were determined after suitable dilution or aliquotting (Table 1). Duplicate blank runs on all the reagents used were carried out simultaneously and the results were corrected accordingly. In a few cases, 1 mmol of zinc as an element with strong tendencies to halide complex formation was also added to the mixtures; the zinc was eluted with 350 ml of 0.35 M hydrobromic acid in 83% acetone before the elution of gallium with 0.20 M hydrochloric acid in 84% acetone was started, but was not determined. Atomic absorption tests indicated that the amount of zinc in the gallium fraction was less than 1 μg. The analytical results for the separations are presented in Table 2.

TABLE 2

Quantitative separations of synthetic mixtures[a]

Taken			Found	
Ga(mg)	Other element	mg	Ga(mg)	Other element (mg)
71.91	U(VI)	237.2	71.90 ±0.05	237.1 ± 0.2
0.360	U(VI)	474.4	0.360 ± 0.003	474.4 ± 0.3
143.8	U(VI)	0.0949	143.8 ± 0.1	0.0948 ± 0.0006
71.91	Co(II)	58.71	71.91 ± 0.03	58.72 ± 0.04
0.360	Co(II)	117.4	0.359 ± 0.004	117.4 ± 0.1
143.8	Co(II)	0.117	143.7 ± 0.1	0.117 ± 0.001
71.91	Al	27.12	71.91 ± 0.4	27.12 ± 0.02
71.91	Li	6.89	71.92 ± 0.04	6.88 ± 0.03
71.91	Na	23.12	71.91 ± 0.05	23.11 ± 0.09
71.91	Be	9.04	71.90 ± 0.04	9.03 ± 0.03
71.91	Mg	24.18	71.91 ± 0.03	24.17 ± 0.02
71.91	Ca	40.27	71.91 ± 0.05	40.28 ± 0.03
71.91	Ba	138.1	71.90 ± 0.03	138.0 ± 0.1
71.91	La	138.3	71.91 ± 0.04	138.3 ± 0.1
71.91	Ti(IV)	47.82	71.92 ± 0.04	47.81 ± 0.09
71.91	Th	231.6	71.91 ± 0.05	231.6 ± 0.2
71.91	Mn(II)	54.78	71.91 ± 0.03	54.79 ± 0.04
71.91	Ni(II)	58.90	71.91 ± 0.04	58.88 ± 0.05
71.91[b]	U(VI)	237.2	71.91 ± 0.04	237.2 ± 0.1
71.91[b]	Co(II)	58.71	71.90 ± 0.03	58.69 ± 0.04
71.91[b]	Li	6.89	71.91 ± 0.05	6.89 ± 0.03

[a] Averages of 3 determinations.
[b] Zinc present and eluted with 350 ml of 0.35 M HBr in 83% acetone before elution of gallium.

DISCUSSION

The described method provides an excellent means for the quantitative separation of gallium from elements which have low tendencies to halide complex formation such as U(VI), Co(II), Al, Li, Na, Be, Mg, Ca, Ba, La, Ti(IV), Th, Mn(II), and Ni(II). All these elements are retained when gallium is eluted with either 0.20 M hydrochloric acid in 84% acetone or with 0.50 M hydrobromic acid in 86% acetone from AG50W-X4 resin. In general, 0.20 M hydrochloric acid in 84% acetone was preferred because the gallium peak is slightly sharper and the light alkali metals are more strongly retained. The tailing effects sometimes observed for gallium on 8% cross-linked resins on elution with dilute hydrochloric acid containing acetone [2] disappear completely.

It proved possible to separate 360 μg of gallium from almost 500 mg of uranium and from more than 100 mg of cobalt. These are the most critical of the multivalent elements because of their relatively high tendency to halide complex formation. Figure 1 indicates that even larger amounts of

uranium(VI), the most critical multivalent element, should be retained from 0.2 M hydrochloric acid in 84% acetone. Furthermore, about 100 μg of uranium and cobalt could be separated from more than 100 mg of gallium, and there do not seem to be problems in separating considerably smaller amounts of these elements from considerably larger amounts of gallium. Some other elements with low tendencies to halide complex formation such as K, Rb, Cs, Sr, Hf, Sc, Y and other lanthanides were not investigated in detail, but according to their known distribution coefficients [2] these elements should also be easily separated.

Separations are sharp and recoveries quantitative (>99.9%). Considerably smaller columns can be used in many cases as is evident from Fig 1. When large amounts of gallium have to be separated from small or trace amounts of the elements, adsorption should be done from 0.50 M hydrobromic acid in 86% acetone; quite small columns can then be used.

When combined with a preceding elution step involving 0.50 M hydrobromic acid in 80% acetone for elements such as zinc, cadmium etc. forming stable bromide complexes [1], the method described seems to be one of the most selective available for the separation of gallium from other elements (Figs. 2 and 3). Iron(III), uranium(VI) and antimony(V), which accompany gallium in its well known anion-exchange separation in hydrochloric acid [4], are separated. The separation of iron(III) is not complete [1]; a little iron(III) (0.5—2.0%) accompanies gallium together with some lithium which is not satisfactorily separated (Fig. 4). The latter effect occurs because lithium moves fairly rapidly on the column with 0.5 M hydrobromic acid in 80% acetone, the distribution coefficient with an 8% cross-linked resin being about 44 [3]. By decreasing the hydrobromic acid concentration to 0.35 M and increasing the acetone concentration to 83%, this value for a 4% cross-linked resin can be increased to 60—70 while the distribution coefficients of copper(II) and iron(III), the most critical elements of the zinc group [1], remain almost unchanged. Thus the separation of lithium also becomes quite satisfactory as shown in Fig. 5, though the copper(II) peak is slightly wider; the tailing of iron(III) also shows an analogous slight increase.

The acetone concentration especially in this last version of the separation described is rather critical and reagents must be measured out accurately.

REFERENCES

1 F. W. E. Strelow, Talanta, submitted.
2 F. W. E. Strelow, A. H. Victor, C. R. van Zyl and C. Eloff, Anal. Chem., 43 (1971) 870.
3 F. W. E. Strelow, M. D. Hanekom, A. H. Victor and C. Eloff, Anal. Chim. Acta, 76 (1975) 377.
4 K. A. Kraus, F. Nelson and G. W. Smith, J. Phys. Chem., 58 (1954) 11.

Analytica Chimica Acta, 113 (1980) 331—342

A COMPUTER-CONTROLLED MULTICHANNEL CONTINUOUS FLOW ANALYSIS SYSTEM APPLIED TO THE MEASUREMENT OF NITRATE, CHLORIDE AND AMMONIUM IONS IN SMALL SAMPLES OF RAIN WATER

J. SLANINA*, F. BAKKER, A. BRUYN-HES and J. J. MÖLS

Netherlands Energy Research Foundation (ECN) Petten, N.H. (The Netherlands)

(Received 12th June, 1979)

SUMMARY

A multichannel continuous flow system based on spectrophotometric determinations is described. Samples are injected into a water stream which is then mixed with appropriate reagents by merging flows; this mode improves the background signals. The system is controlled by a PDP 11 computer. Calibration, analysis of samples and quality control are done automatically. The system is applied to the determination of nitrate, chloride and ammonium ions in small ($\leq$ 0.5 ml) samples of rain water in the range 0.2—20 ppm. The accuracy is typically better than 3%. The sampling rate is 18—35 per hour.

Determinations of fluoride, chloride, ammonium and hydrogen ions in rain-water samples by means of computer-controlled ion-selective electrode methods have been described recently [1]. These methods have been employed for several years in the precipitation chemistry program of ECN. The results were very good, but the starting-up of some i.s.e. methods was very time-consuming; the gas-sensing ammonia electrodes and the silver chloride or calomel electrodes sometimes needed as much as 2 days before functioning properly. It was decided, therefore, to investigate the possibilities of continuous flow methods as alternatives.

Flow injection analysis with spectrophotometric detection as described by Stewart and Růžička [2] seemed a suitable technique, as only a small volume of sample is needed to obtain fairly accurate results, but various difficulties were encountered in these methods when samples of low concentration were analysed. Betteridge [3] has outlined one explanation for this phenomenon: the partial mixing of sample and reagents with different optical refractive indexes results in distortion of the light beam in the photometric cell and hence of the background signal. As the concentrations of most species in rain water are rather low, these background fluctuations can affect the results seriously. Accordingly, a variant of flow injection analysis was investigated: the samples were injected into a water stream which was then fully mixed with all the necessary reagents. Very low detection limits and high accuracy for the spectrophotometric determination of nitrate were obtained in this way [4].

The system described here is computer-controlled in the same way as was done for i.s.e. methods [1], i.e. each determination is calibrated automatically, the calibration is checked, quality control is done by frequent measurement of standards followed by recalibration if necessary, and all equipment is tested continuously for errors. In this paper, spectrophotometric methods for nitrate, chloride and ammonium ions are described, but the system should also be able to accommodate many other flow methods with transient peaks. The spectrophotometric methods are all based on well established procedures.

EXPERIMENTAL

Apparatus

The PDP 11-03, LSI, 32K memory computer system was equipped with 2 inputs for DVM's, eight 12-bit ADC channels, two 12-bit DAC's, 15 output relays and 15 TTL inputs to control and check the status of instruments, buret interface and pulse counter [1].

Zeiss PM 2 ALC and Cenco Multichannel spectrophotometers were used. The pumps were Gilson minipuls 2 (8 channel), the sample changer was a Gilson escargot sc 6 (capacity 300 samples), and sample transfer was done pneumatically with 3 positions (only 2 are used in the flow system). The flow cells (Hellma) were of quartz (10-mm optical path) or glass (10- and 50-mm optical path) with debubblers.

Flow systems are built from 0.8-mm teflon tubing. All connectors (2-, 3- and 4-way) have a diameter of 0.8 mm (Flair-Fit). The sample valves are pneumatically actuated 4-way valves (Flair-Fit). The sample loops are connected in series (see Fig. 1). Solutions are heated or cooled in tubing coiled around thermostated copper holders (see Fig. 2).

The standard selection system (Fig. 3) comprises six bottles with standard solutions connected to a 6-way pneumatic valve (Cheminert U.K.). A 3-way pneumatic valve controls whether standards or samples are measured. Two microswitches are added to the 6-way valve: one indicates each turn of the valve, and the other gives a signal when a certain position of the valve is reached. This signal is used by the computer to identify the position of the valve.

The general arrangement of the system is shown in Fig. 4. The computer controls the sample changer, sample transfer system, injection valves and standard selection system and checks the performance of all these systems. The transmittance signal of the spectrophotometers is read by means of the 8-channel ADC.

All auxiliary apparatus is connected to the mains by means of a 220-V switch. The computer can thus switch off all systems when all analyses have been completed or if a system is malfunctioning.

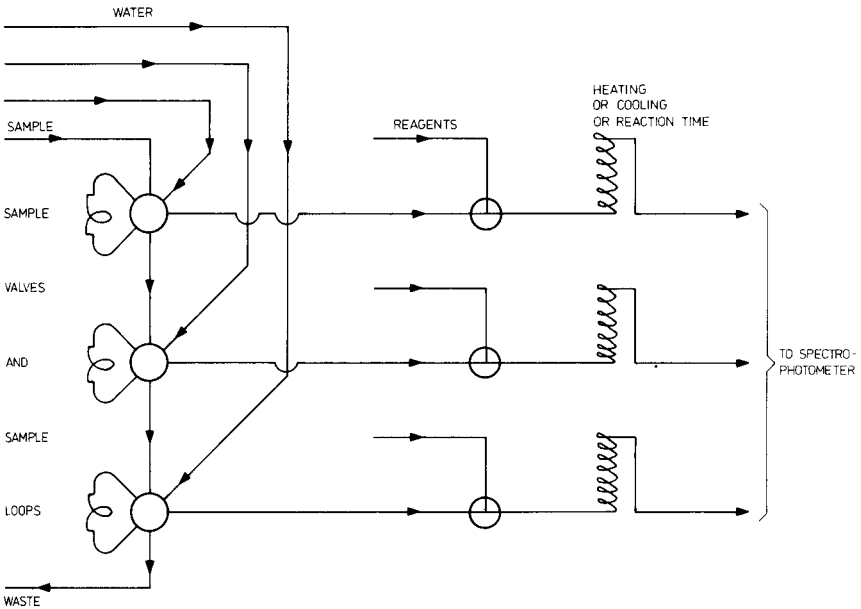

Fig. 1. Flow injection system.

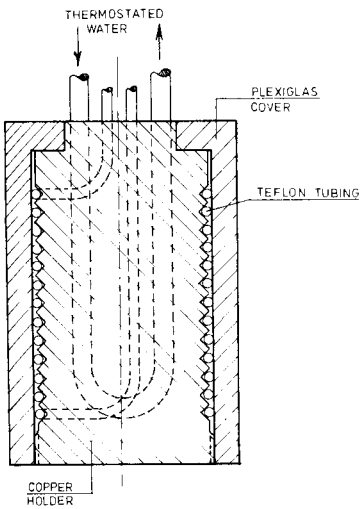

Fig. 2. Thermostating coils.

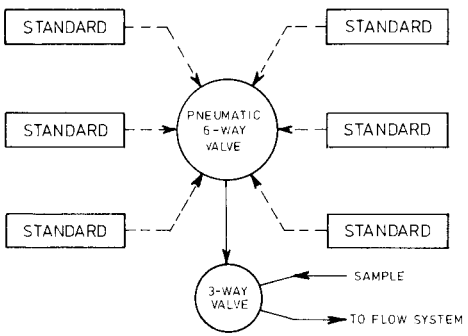

Fig. 3. Standard selection system.

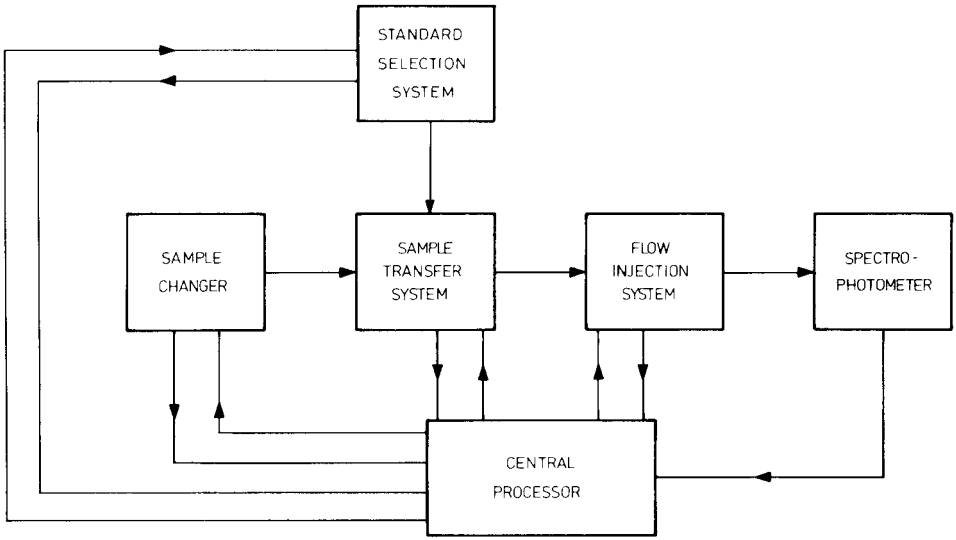

Fig. 4. Block diagram of the apparatus.

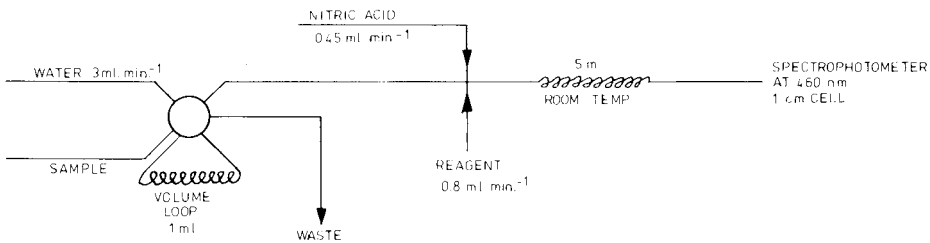

Fig. 5. Flow system for chloride.

Flow systems

The general arrangement of the flow system is given in Fig. 1. All sample loops are filled simultaneously by one sample stream.

Chloride. The flow diagram is shown in Fig. 5. The nitric acid solution is 0.4 M. For the reagent, first 220 g of $FeNO_3 \cdot 9H_2O$ is dissolved in 700 ml of water, 125 ml of concentrated nitric acid is added, and the mixture is diluted to 1 l with demineralized water and filtered. A mercury(II) thiocyanate solution is prepared by dissolving 4.17 g of $Hg(SCN)_2$ in 500 ml of methanol and diluting to 1 l with methanol; this solution is filtered after 3 h. For the actual reagent, 200 ml of water, 100 ml of the iron(III) nitrate solution and 100 ml of the mercury(II) thiocyanate solution are mixed.

Ammonium. The flow diagram is shown in Fig 6. For the phenolate

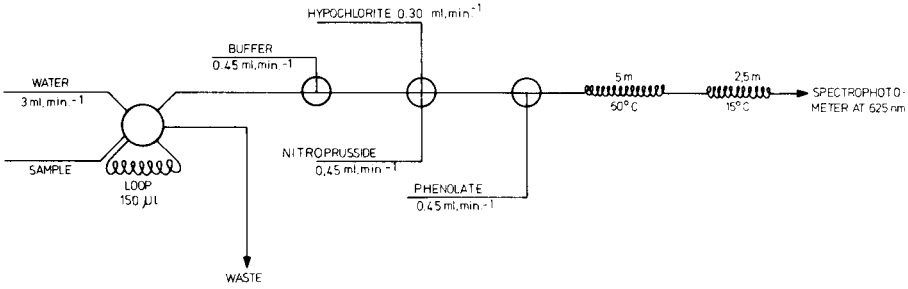

Fig. 6. Flow system for ammonia.

solution, 25 g of phenol in 50 ml of methanol is mixed with 45 ml of an aqueous solution of 20% (w/v) sodium hydroxide, the pH is adjusted to 11.6 and the solution is diluted to 500 ml with methanol. The hypochlorite solution is prepared by mixing 25 ml of 3 M sodium hypochlorite and 1 ml of 2 M sulphuric acid and diluting to 500 ml. For the sodium nitroprusside solution, 500 mg of $Na_2Fe(CN)_5NO$ is added to 250 ml of water and 18 ml of 0.1 M sodium hydroxide, which is then diluted to 500 ml. For the buffer, 450 g of $Na_2HPO_4 \cdot 12H_2O$, 60 g of sodium hydroxide, 10 g of EDTA and 2 g of sodium citrate are dissolved in 1900 ml of water and the pH is adjusted to 11.6.

Nitrate. The flow system is shown in Fig. 7. The reagent stream is simply 0.05 M perchloric acid containing 5 ppm NO_3^- (to avoid adsorption of nitrate in the sample on the Filopur filter). Activated carbon filters were from Filopur (Basel) or Schleicher and Schüll 3360.

Calibration (see Fig. 8).

First the computer asks for a number of parameters such as: (1) number of analyzed species, measurement of peak height or peak area, desired accuracy, number of standards, maximum time per sample; and (2) for each channel, species, concentration of standards, time between injection and highest point of the peak and parameters connected with the detection of

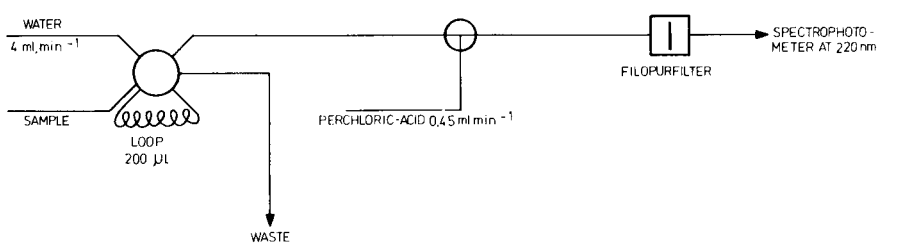

Fig. 7. Flow system for nitrate.

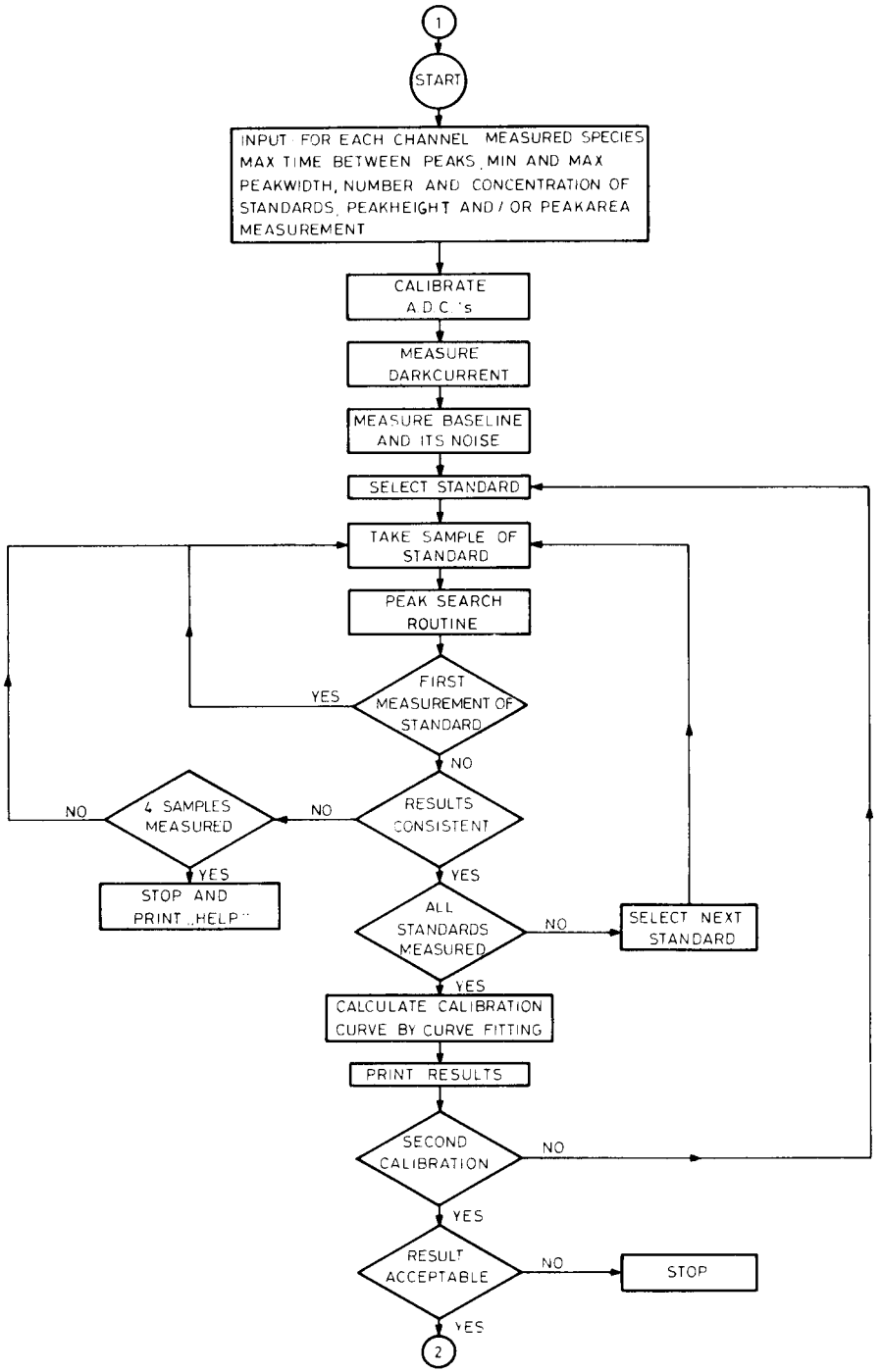

Fig. 8. Calibration.

the peak. The operator is asked to close the slits of the spectrophotometers and the dark current is measured. The slits are then opened and the 100% transmission signal is monitored. The computer starts the calibration procedure. A standard is selected and the sample loops are filled, while 100% transmission is measured for each channel by averaging 500 readings. The standard is then injected.

Two procedures have been developed for peak measurement. The simpler one determines peak height only, whereas the more complex one measures peak height and/or peak area. In the simpler procedure, which is outlined in Table 1, the background is measured at a fixed time, just before the peak arrives. The signal is monitored during a certain time after injection and the highest signal is accepted as the peak height. In this way, air bubbles can affect the result only if they appear within 10 s of the maximum signal of the peak.

In the more elaborate procedure (Fig. 9) the differences between 20 successive readings are computed. These differences are either positive, zero, or negative. The number of positive or negative signs in each group of 20 is used to detect a peak. If the number of positive signs of the 10 most recent values exceeds a preset limit, a peak is detected and from the 10 previous values the background signal is computed. The highest value is taken as peak height. A downward slope is detected if the number of negative signs exceeds a preset limit. The end of the peak is detected by testing if the number of negative signs of points 20 to 10 falls below a preset limit, and the 10 most recent points are used to calculate a second background signal. Peak area and peak height are corrected for background shift. Each standard is measured twice; if the difference exceeds the desired precision the measurement is repeated. If no acceptable results are obtained after 4 runs, the system will call for help.

Calibration curves are computed by fourth order fitting of all results for the standards and blanks and the calibration is repeated. If the second calibration is within the desired limits of precision, the calibration is accepted; if not a new calibration curve is measured and compared with the second calibration. If consistent results are not obtained after four calibrations the computer will switch off the system. Typical calibration curves between 0 and 20 ppm are given in Fig. 10; the lines for ammonium and chloride ions are quite curved above 8 ppm.

Analysis of samples

The flow chart is given in Fig. 11. After completion of calibration, the computer asks for the number and identification of samples. After each tenth sample a standard is analyzed. If the result is not within the set limit the measurement of the standard is repeated; if the result is again unsatisfactory, the system is recalibrated. The computer will switch off the system if: (a) all samples have been analyzed; (b) recalibration is unsuccessful; or (c) one of the connected systems is not functioning correctly.

TABLE 1

Simple peak height algorithm

Step 1 : Input.	For each channel : get set time for 100% transmittance measurement and for peak height measurement.
Step 2 : Wait 1.	If real time is less than set time for 100% transmittance measurement then go to Step 2.
Step 3 : Transmittance.	Acquire 100 data points and calculate average. Store an X_0 value.
Step 4 : Wait 2.	If real time is less than set time for peak height measurement, go to Step 4. Otherwise set X_{new} to zero.
Step 5 : Peak height.	Set X_{old} equal to X_{new}. Acquire 5 data points and calculate average. Store in X_{new}. If X_{new} is greater than X_{old}, go to Step 5.
Step 6 : Output.	Output X_0 as baseline value and X_{old} as peak height. END.

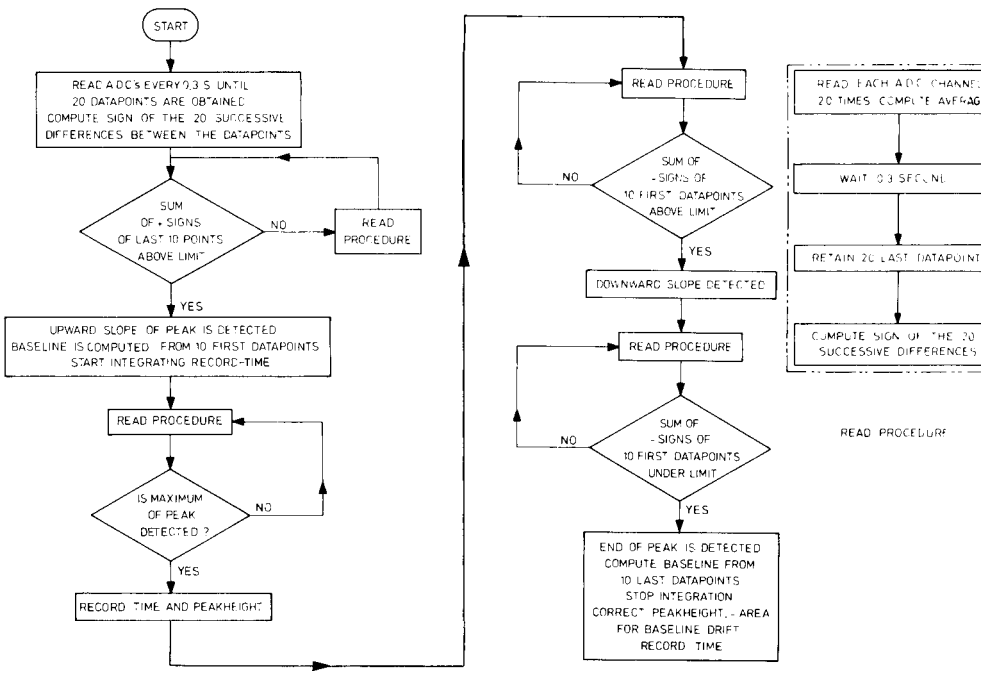

Fig. 9. Complex peak search routine.

RESULTS

The accuracy of the system was tested by measurements of standards. The system was calibrated with six standards containing 1, 4, 8, 12, 16 and 20 ppm of each ion. The results of the "complex" peak detection method

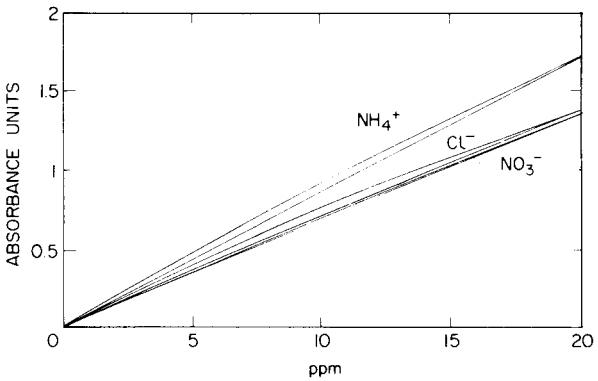

Fig. 10. Calibration graphs.

are given in Table 2. These results were obtained in three separate runs, each with its own calibration. The precision of the method was tested by repeated analysis of a rain-water sample (Table 3).

Generally, the same accuracy was found with peak height as with peak area measurements for moderate to high concentrations. Integration of very small peaks is a rather difficult matter. A small mistake in the baseline measurement can have serious effects; for example, 0.002 absorbance units gives an error of 3% in the peak height measurement of 1 ppm nitrate. The error in the measurement of the peak area can be as much as 25% in this case.

The accuracy of the "simple" peak detection procedure was also tested by repeated analysis of standards. The results (Table 4) were obtained in three runs. The precision of this technique was tested by repeated analysis of a rain-water sample (Table 5).

Eighteen samples per hour can be analyzed when the more elaborate peak detection procedure is used; with the simpler procedure, 35 samples per hour are possible. If the high precision considered essential for the present purpose is not necessary, the sampling rate can be much higher.

DISCUSSION

The system was tested in the range 0.2—20 ppm for ammonium, chloride and nitrate ions; this was the concentration range expected for the rain-water samples. The calibration curves of chloride and ammonium are quite curved even at moderate concentrations (see Fig. 10). Usually it is quite difficult to optimize the flow process in such a way that a straight calibration curve is obtained. Fortunately, the high reproducibility of the flow system together with computer curve fitting makes this quite unnecessary. An accuracy of better than 3% can be obtained even in the upper part of the

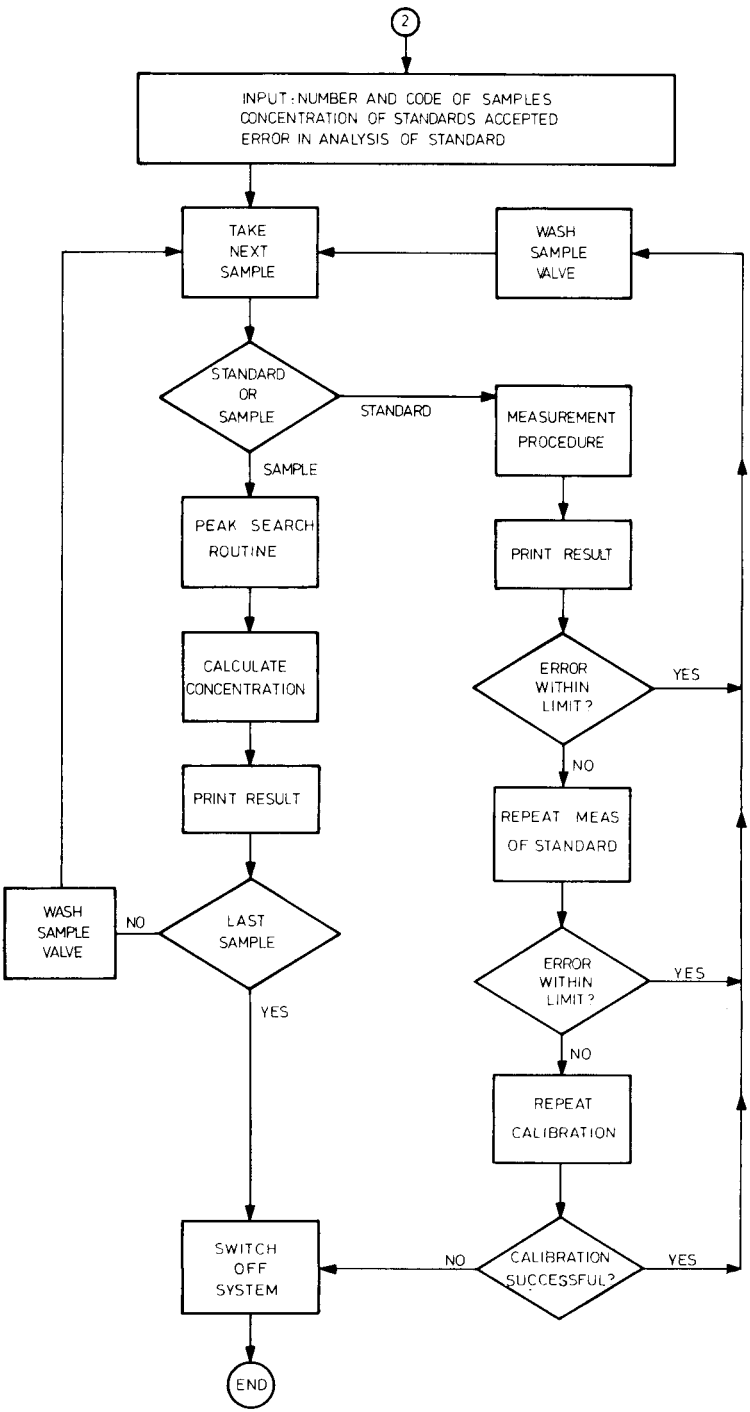

Fig. 11. Measurement of samples and standards.

TABLE 2

Analyses of standards by means of "complex" peak detection

Species	Conc. given (ppm)	Mean conc. found (ppm)	No. of detns.	R.s.d. (%)
Cl^-	0.2	0.23	16	5
	0.5	0.51	23	10
	1.0	0.97	30	4
	2.0	1.97	30	5
	5.0	4.99	28	2
	10.0	10.0	34	2
	15.0	15.2	21	1
NO_3^-	0.20	0.27	16	10
	0.50	0.57	25	10
	1.0	1.05	30	8
	2.0	2.05	30	3
	5.0	5.10	28	2
	10.0	10.2	34	2
	15.0	15.1	16	2
NH_4^+	0.20	0.20	16	5
	0.50	0.50	25	6
	1.0	1.00	30	5
	2.0	2.02	30	3
	5.0	5.06	28	2
	10.0	10.0	34	2
	15.0	15.3	21	2

TABLE 3

Repeated analysis of a rain-water sample by "complex" peak detection

Species	No. of detns.	Conc. found (ppm)	R.s.d. (%)
Cl^-	13	5.30	1
NO_3^-	13	1.80	3
NH_4^+	13	0.63	2

calibration curve. A very cheap multichannel spectrophotometer equipped with light detecting resistors (LDR's) as detectors proved to be adequate. The response of these instruments is not linear above 1 absorbance unit, but the curve-fitting procedure corrects for this error.

The calibration procedure is generally completed in 1—1.5 h so that 100—180 samples per day can be processed. The system is able to analyse very long series of samples and the recalibration procedure guarantees accurate results.

TABLE 4

Analysis of standards by "simple" peak detection

Species	Conc. given (ppm)	No. of detns.	Conc. found (ppm)	R.s.d. (%)
NO_3^-	0.20	12	0.23	10
	0.50	12	0.52	5
	1.00	12	1.00	4
	2.00	10	2.01	3
	5.00	10	4.97	1
	10.0	20	10.0	0.5
	15.0	15	15.1	0.8
Cl^-	0.20	10	0.23	8
	0.50	14	0.49	3
	1.00	12	1.01	3
	2.00	10	1.97	2
	5.00	10	5.08	1
	10.0	20	10.1	1
	15.0	14	15.2	0.5
NH_4^+	0.20	14	0.19	8
	0.50	10	0.48	3
	1.00	10	0.97	2
	2.00	10	1.97	1
	5.00	10	4.91	1
	10.00	20	10.0	0.5
	15.00	15	14.9	0.5

TABLE 5

Repeated analysis of a rain-water sample by the "simple" peak detection

Species	No. of detns.	Conc. found (ppm)	R.s.d. (%)
Cl^-	10	5.38	0.5
NO_3^-	10	1.63	1
NH_4^+	10	0.54	3

REFERENCES

1 J. Slanina, F. Bakker, J. J. Möls, J. E. Ordelman and A. G. M. Bruyn-Hes, Anal. Chim. Acta, 112 (1979) 45.
2 J. W. B. Stewart, J. Růžička, Anal. Chim. Acta, 83 (1976) 137.
3 D. Betteridge, Anal. Chem., 50 (1978) 832A.
4 J. Slanina, F. Bakker, A. G. M. Bruyn-Hes and J. J. Möls, Fresenius Z. Anal. Chem., 289 (1978) 38.

Analytica Chimica Acta, 113 (1980) 343—349

FLUORIMETRIC DETERMINATION OF TITANIUM WITH 2-METHYL-3-ETHYL-5-HYDROXYCHROMONE

TAKUSHI ITO*

Junior College of Engineering, Shizuoka University, 3-5-1, Johoku, Hamamatsu-shi, Shizuoka (Japan)

AKIRA MURATA

Faculty of Engineering, Shizuoka University, 3-5-1, Johoku, Hamamatsu-shi, Shizuoka (Japan)

(Received 9th August 1979)

SUMMARY

Titanium reacts with 5-hydroxychromone and eleven of its derivatives to form water-insoluble yellow complexes, which exhibit yellow-green fluorescence on extraction into carbon tetrachloride. An investigation of the substituent effect on the fluorescence intensity of the titanium complexes of these reagents showed that the best fluorescent reagent for the determination of titanium is 2-methyl-3-ethyl-5-hydroxychromone. The maximum wavelengths of the excitation and emission spectra of 2-methyl-3-ethyl-5-hydroxychromone complex are 395 nm and 513 nm, respectively. The titanium complex shows constant fluorescence intensity when extracted from a solution of pH 6.5—8.5. When extraction is done with 10ml of carbon tetrachloride, 0.5—5.0 μg of titanium can be determined. The effects of diverse ions and of substituent position in the reagents are discussed.

Various metal ions react with 5-hydroxychromone and its methyl, methoxyl and acetyl derivatives to form fluorescent complexes, the fluorescence intensities of which are strongly influenced by the insertion of the substituents into different positions of 5-hydroxychromone. In previous papers, the effects of substituents on the fluorescence intensity of the beryllium [1] and scandium [2] complexes of 5-hydroxychromone and some of its derivatives and the fluorimetric determination of these metals with 2-ethyl-3-methyl-5-hydroxychromone were reported. In the present paper, it is shown that titanium also reacts with these reagents to form water-insoluble complexes which exhibit yellow-green fluorescence when extracted into carbon tetrachloride. Fluorescent complexes of titanium do not seem to have been reported previously. Morin [3, 4], quercetin [5], rutin [6], galangin [7] and kaempferol [8], which are polyhydroxy derivatives of flavone, a 2-phenyl derivative of chromone, react with titanium to form complexes, but these complexes do not fluoresce and they cannot be extracted into organic solvents, probably because of their polyhydroxy groups. Accordingly, the fluorescent reactions of titanium with 5-hydroxychromone and eleven of its

derivatives were investigated in order to reveal any substituent effects. 2-Methyl-3-ethyl-5-hydroxychromone was found to be the most suitable reagent for the fluorimetric determination of titanium, providing a very sensitive determination.

EXPERIMENTAL

Reagents and apparatus

Titanium solutions. Fuse 0.4128 g of titanium dioxide with potassium pyrosulfate and dissolve in 500 ml of 0.5 M sulfuric acid (0.495 mg Ti ml^{-1}). Prepare more dilute solutions by suitable dilution with 0.5 M sulfuric acid.

2-Methyl-3-ethyl-5-hydroxychromone and the other 5-hydroxychromone derivatives listed in Table 1 were synthesized as described earlier [9—11]. These reagents were used as methanolic solutions.

All other chemicals were of analytical-reagent grade.

Fluorescence spectra were recorded with a Shimadzu Model 500 spectrofluorimeter equipped with a quantum counter; excitation spectra are corrected, but emission spectra are not. A Hitachi Model 203 spectrofluorimeter fitted with a 120-W medium-pressure mercury lamp was used for quantitative measurements. A Toadenpa pH meter, Model HM-5A, served for pH measurements.

TABLE 1

Fluorescent characteristics of titanium complexes of 5-hydroxychromone and its derivatives in carbon tetrachloride

Reagent	λ_{ex}(nm)	λ_{em}(nm)	Fluorescence intensity[a]	
			Complex	Reagent
5-Hydroxychromone	396	528	9.3	2.1
2-Methyl-	389	511	46.4	15.8
2-Ethyl-	392	509	57.8	25.0
3-Methyl-	397	530	20.7	3.1
3-Ethyl-	397	529	28.4	4.7
2,3-Dimethyl-	393	517	65.0	17.2
2-Methyl-3-ethyl-	395	513	100.0	23.6
2-Ethyl-3-methyl-	394	518	82.4	19.4
2,7-Dimethyl-3-ethyl-	393	509	71.6	21.8
2-Methyl-7-methoxy-	378	486	45.5	15.6
2,6-Dimethyl-7-methoxy-	386	515	11.4	3.2
2-Methyl-3-acetyl-	395	526	33.5	4.7

[a]Relative to the 2-methyl-3-ethyl derivative.

Procedure

To a sample solution containing 0.5—5.0 μg of titanium(IV) add 2.5 ml of a methanolic 2×10^{-2} M solution of 2-methyl-3-ethyl-5-hydroxychromone, 7.5 ml of methanol (the final content of methanol is 40% v/v) and sufficient 1 M ammonia solution to adjust the pH of the final solution to 6.5—8.5. Then dilute the mixture to 25 ml with water. After about 1 h, extract the titanium complex with 10 ml of carbon tetrachloride by shaking vigorously for 30 s. Separate the organic phase and dry over sodium sulfate. Measure the fluorescence intensity at an excitation wavelength of 405 nm (mercury line), using a secondary filter passing light at wavelengths above ca. 430 nm. Adust the sensitivity of the fluorimeter with an aqueous 0.5 μg ml^{-1} solution of sodium fluorescein.

RESULTS AND DISCUSSION

Titanium complex of 2-methyl-3-ethyl-5-hydroxychromone

Titanium reacts with 2-methyl-3-ethyl-5-hydroxychromone to form a water-insoluble yellow complex. This complex is soluble in aqueous solutions containing not less than 20% (v/v) methyl cellosolve, 4% (v/v) hydrogen peroxide (aqueous 3% solution), or 40% (v/v) methanol, but these solutions do not fluoresce at all. However the titanium complex extracted into some organic solvents exhibits a yellow-green fluorescence.

Organic solvents such as carbon tetrachloride, chloroform, benzene, chlorobenzene, toluene, isopropyl ether, butyl ether, amyl acetate, dichloroethane, amyl alcohol, and tributyl phosphate were examined for the extraction of titanium complex. Only carbon tetrachloride, toluene, and amyl alcohol were satisfactory. The fluorescence intensities of the complex and the reagent blank extracted into these organic solvents are shown in Table 2. Obviously, carbon tetrachloride is the most suitable.

Fluorescence spectra

The excitation and emission spectra of the titanium complex and the reagent in carbon tetrachloride are shown in Fig. 1. The excitation and emission spectra of the titanium complex have maxima at 395 and 513 nm, respectively.

TABLE 2

Effect of extracting solvents

Solvent	CCl_4	C_7H_8	$C_5H_{11}OH$
F.I.[a] (complex)	30.5	17.5	3.6
F.I. (reagent)	7.2	1.6	0.8

[a]Relative fluorescence intensity for 5×10^{-8} mol (2.40 μg) Ti with 5×10^{-5} mol of reagent.

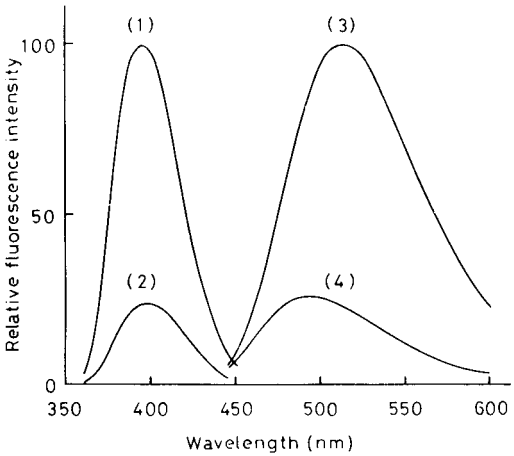

Fig. 1. Fluorescence spectra of titanium complex and reagent in carbon tetrachloride. (1) Excitation spectrum of titanium complex; (2) excitation spectrum of reagent blank; (3) and (4) corresponding emission spectra.

Effects of reaction variables

The effect of the pH of the aqueous phase on the extraction of the titanium complex into carbon tetrachloride is shown in Fig. 2. Maximum constant fluorescence intensity is obtained in the pH range 6.0—8.5, while the fluoresence of the blank becomes constant above pH 6.5. The recommended pH range is therefore 6.5—8.5.

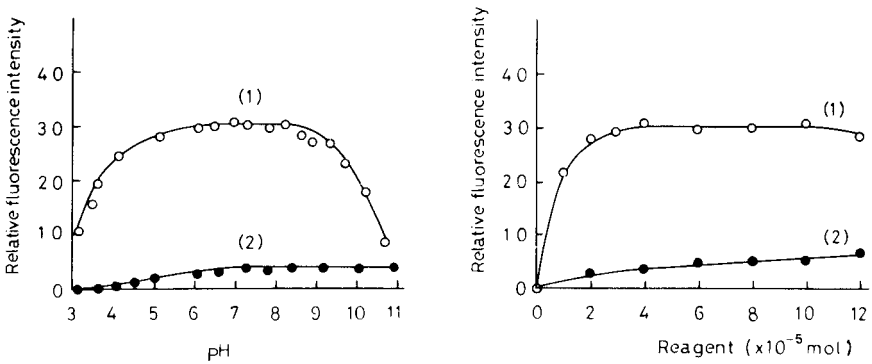

Fig. 2. Effect of pH on extraction of (1) the titanium complex and (2) the reagent into carbon tetrachloride (5×10^{-8} mol Ti, 2.40 μg) and 5×10^{-5} mol reagent.

Fig. 3. Effect of amount of reagent for (1) titanium complex (5×10^{-8} mol Ti, 2.40 μg); (2) reagent blank.

The optimum amount of the reagent is 4—10 × 10^{-5} mol for 5 × 10^{-8} mol of titanium (Fig. 3). The fluorescence intensity decreases gradually when more reagent is added probably because of inner filter effects. For general purposes, 2.5 ml of 2 × 10^{-2} M reagent solution (5 × 10^{-5} mol) was added.

A study of the effect of the methanol content of the aqueous phase on the extraction of the complex showed that the optimum content is 40% (v/v). Contents lower than about 30% gave an insoluble complex at the phase boundary whereas contents above 40% caused a steep decrease in the fluorescence, probably because of reduced extraction efficiency.

The titanium complex is readily extracted into carbon tetrachloride by shaking for 30 s. The fluorescence intensity remains constant for shaking times up to 30 min, after which it decreases gradually; for example, a fluorescence intensity of 31.0 immediately after the extraction became 27.2 after 30 min.

Calibration curve

Under the recommended conditions, the calibration graph was linear over the concentration range 0.5—5.0 μg of titanium per 10 ml of carbon tetrachloride. For titanium contents exceeding 7.2 μg, an insoluble complex formed at the interface probably owing to the poor solubility of the complex in carbon tetrachloride.

The coefficient of the variation obtained in five measurements was 2.8% for 2.40 μg of titanium.

Effect of diverse ions

The effect of 50 diverse ions on the determination of 2.40 μg of titanium was examined. Diverse ions which interfere below a concentration 100 times that of titanium are summarized in Table 3. EDTA, citrate, fluoride, phosphate and tartrate cause negative errors, whereas 400-fold amounts of oxalate, acetate, cyanide, sulfate, nitrate and chloride are without effect.

The positive interferences of beryllium, aluminium, scandium, zirconium, hafnium, gallium, antimony, indium, bismuth and yttrium can be attributed to the fact that these elements also form extractable fluorescent complexes. Platinum neither reacts with the reagent nor fluoresces, but causes positive errors at levels exceeding 200 μg. Various cations give negative errors probably by formation of non-fluorescing complexes or by adsorption of the titanium complex on colloidal hydrolysis products. Accordingly, for practical analyses, preliminary separations will be essential.

Composition of complex

The absorbances of the complexes formed in aqueous 40% (v/v) methanolic solutions containing 1 × 10^{-5} M titanium(IV) and 5—15 × 10^{-4} M concentrations of the reagent at pH 8.0 were measured, and the mole ratio of titanium to ligand was calculated [12, 13] to be 1:3. The spectrophotometric continuous variations method was attempted in this methanolic solution,

TABLE 3

Effect of diverse ions on the determination of 2.40 μg of titanium

Ion	Ion added (μg)	Ti found (μg)	Ion	Ion added (μg)	Ti found (μg)
EDTA	2	2.48	Y^{3+}	10	2.38
	10	1.75		50	2.66
Citrate	2	2.35	Pd^{2+}	10	2.35
	10	2.00		50	2.07
Fluoride	10	2.38	Th^{4+}	50	2.31
	50	1.92		100	1.96
Phosphate	10	2.35	Tl^{3+}	50	2.47
	50	2.19		100	1.40
Tartrate	100	2.38	U^{6+}	50	2.30
	250	2.01		100	1.77
Be^{2+}	2	142.7	Pb^{2+}	50	2.37
Al^{3+}	2	63.68		100	1.92
Sc^{3+}	2	32.14	Sn^{4+}	50	2.30
Zr^{4+}	2	10.46		100	2.15
Hf^{4+}	2	7.10	Pt^{4+}	100	2.47
Ga^{3+}	2	3.26		250	2.81
Sb^{3+}	2	2.87	Ce^{3+}	100	2.46
Cr^{3+}	2	1.51		250	1.63
Fe^{3+}	2	1.82	As^{5+}	100	2.36
In^{3+}	2	2.46		250	1.91
	10	3.26	La^{3+}	100	2.42
Bi^{3+}	2	2.38		250	1.92
	10	2.61	Zn^{2+}	100	2.45
Cu^{2+}	2	2.38		250	1.97
	10	2.25			

but the mole ratio could not be determined because the absorbance was extremely small at low concentrations and the reagent or the hydrolysis product of titanium deposited at high concentrations. The fluorimetric continuous variations method was attempted in carbon tetrachloride, but again the signal was extremely faint at low concentrations whereas extraction became incomplete at increased concentrations.

Comparison of substituent effects

The titanium complexes of 5-hydroxychromone and the eleven derivatives were all extracted into carbon tetrachloride, though the optimum pH ranges differed slightly. The maximum excitation and emission wavelengths of the titanium complexes are summarized in Table 1, along with the relative fluorescence intensities measured at the maximum wavelengths of the relevant spectrum. The absorption spectra could not be measured because of inadequate sensitivity under conditions of complete extraction. The fluorescence spectra of the titanium complexes are quite similar except for the titanium complex with 2-methyl-7-methoxy-5-hydroxychromone which shows a shift to shorter wavelengths.

The fluorescence intensity varies markedly with the insertion of some substituents. The insertion of an alkyl group (methyl < ethyl) into the 2- or 3-position, especially the 2-position, of 5-hydroxychromone increases the fluorescence intensity. The insertion of an alkyl group into both the 2- and 3-positions increases the fluorescence intensity even more. In contrast, the insertion of an alkyl group into the 6- or 7-position, or an acetyl group into the 3-position, or a methoxyl group into the 7-position tend to decrease the fluorescence intensity. However, the effects of independent insertion of these groups is still uncertain. Among these twelve reagents, the greatest fluorescence intensity was shown by 2-methyl-3-ethyl-5-hydroxychromone which was therefore selected for detailed study as described above.

REFERENCES

1 T. Ito and A. Murata, Bunseki Kagaku, 20 (1971) 1422.
2 M. Nakamura and A. Murata, Bunseki Kagaku, 22 (1973) 1474.
3 G. Almassy, Acta Chim. Acad. Sci. Hung., 6 (1955) 335.
4 A. Murata and F. Yamauchi, Bunseki Kagaku, 10 (1961) 379.
5 A. P. Golovina, I. P. Alimarin and N. F. Stepanov, Nauch. Dokl. Vyssh. Shk. Khim. Khim. Tekhnol., 2 (1958) 285; Chem. Abstr., 52 (1958) 16981.
6 B. Dev and B. D. Jain, Fresenius Z. Anal. Chem., 190 (1962) 316.
7 M. Katyal and R. P. Singh, J. Proc. Inst. Chemists (India), 35 (1963) 213.
8 B. S. Garg and R. P. Singh, J. Indian Chem. Soc., 45 (1968) 1047.
9 A. Murata, T. Ito and T. Suzuki, Bunseki Kagaku, 17 (1968) 1284.
10 A. Murata, T. Suzuki and T. Ito, Bunseki Kagaku, 14 (1965) 630.
11 A. Murata, F. Hirano and T. Suzuki, Bunseki Kagaku, 19 (1970) 1346.
12 H. A. Benesi and J. H. Hildebrand, J. Am. Chem. Soc., 71 (1949) 2703.
13 H. McConnell and N. Davidson, J. Am. Chem. Soc., 72 (1950) 3164.

Analytica Chimica Acta, 113 (1980) 351—354

Short Communication

DETERMINATION OF GLUTAMINE IN CEREBROSPINAL FLUID WITH A TISSUE-BASED MEMBRANE ELECTRODE

M. A. ARNOLD and G. A. RECHNITZ*

Department of Chemistry, University of Delaware, Newark, Delaware 19711 (U.S.A.)

(Received 11th September, 1979)

Summary. A glutamine-selective sensor consisting of porcine kidney tissue immobilized at an ammonia gas electrode is utilized. It yields good precision and accuracy over the clinically important range of glutamine concentrations (10^{-4}—10^{-2} M).

It has been shown that cells can be employed as bio-catalytic mediators for bio-selective probes. Examples include the use of living bacterial cells and intact tissue cells [1—3]. The first application of the tissue-based, glutamine-selective sensor [1] for the determination of glutamine in cerebrospinal fluid (CSF) is reported below. This sensor employs a slice of porcine kidney tissue immobilized at the surface of an ammonia gas-sensing electrode. The presence of a high activity of glutaminase in the kidney tissue allows the rapid deamination of glutamine to ammonia, which is sensed by the electrode. This probe exhibits excellent selectivity for glutamine over other amino acids, and has a lifetime of at least 30 d [1].

It has been reported that glutamine accounts for 67.4% of the total amino acid concentration in CSF [4]. Elevated concentrations of glutamine in human CSF have been shown to be related to hepatic coma [5] and Reye's syndrome in children [6]. These facts have stimulated research toward the development of analytical procedures to determine the glutamine concentration of CSF [5—12].

Elevated temperature ion-exchange chromatography methods for the determination of glutamine in CSF [9] involve long retention times and give nonquantitative recovery of glutamine [13]. Procedures which use isolated glutaminase followed by the detection of liberated ammonia have given favorable results [6, 7, 11], but these procedures require incubation periods and expensive reagents.

Experimental

Apparatus. All potentiometric measurements were made with a Corning Model 12 pH/mV meter and a Heath-Schlumberger SR-240 potentiometric recorder. All measurements were made in thermostatted cells at 30°C controlled with a Haake model FS bath. An Orion model 95—10 ammonia gas-sensing electrode was used.

Reagents. All solutions were prepared with distilled, deionized water. Analytical-grade reagents were used unless otherwise noted. L-glutamine, sodium azide, iodoacetamide, and glutaminase (EC 3.5.1.2; Grade V) were purchased from Sigma Chemical Co., St. Louis, Mo.

Two CSF controls were purchased. The CSF control obtained from Hyland Diagnostics (Deerfield, IL) is synthesized to simulate human CSF, and contains no amino acids. The CSF control obtained from Fisher Diagnostics (Orangeburg, NY) is freeze-dried pooled human CSF, which is spiked with glutamine by the manufacturer but not assayed for glutamine.

Porcine kidneys were obtained through a local abattoir from freshly killed animals and stored frozen until use.

Procedures. The glutamine-selective sensor was prepared as described previously [1], by using a mesh of monofilament nylon to immobilize the tissue slice at the ammonia gas-sensing electrode surface. The glutamine-selective sensor was stored between measurements at room temperature in a phosphate buffer (0.1 M, pH 7.8) containing 0.02% sodium azide.

Unless otherwise noted, all calibration curves were obtained in a phosphate buffer (0.1 M, pH 7.8) which was 0.02% in sodium azide and 1 mM in iodoacetamide. Standard glutamine solutions were also prepared in this buffer system.

Spiked synthetic and real CSF samples were assayed for glutamine by diluting 0.6 ml of the sample to 2.2 ml with the buffer. The potentiometric measurements were made directly in the resulting solution with the tissue-based, glutamine selective sensor, and the concentrations were read directly from a working calibration curve prepared with solutions made up in the buffer.

The real CSF samples were also assayed for glutamine by the method of Glasgow and Dhiensiri [6].

Results and discussion

A typical calibration curve obtained with the glutamine selective sensor is shown in Fig. 1. The limit of detection is 2.9×10^{-5} M and the linear range is 1.0×10^{-4}—1.1×10^{-2} M glutamine. This response is well suited for glutamine determinations in CSF, where the normal glutamine range is reported to be 3.3×10^{-4}—7.4×10^{-4} M [12]. Typically, the response time of the system falls within 4—6 min for each addition of glutamine.

The need for the presence of 1 mM iodoacetamide in the buffer system to suppress glycolysis [14] is shown in Fig. 2. Figure 2(a) shows the electrode response in the buffer and in diluted synthetic CSF control with no iodoacetamide added. In contrast, Fig. 2(b) shows the same conditions except for the presence of 1 mM iodoacetamide in each solution. It is clear that iodoacetamide is needed to obtain analytically useful results for the CSF samples.

Samples of synthetic CSF were spiked with known amounts of glutamine and analyzed with the glutamine-selective sensor. The results are shown in

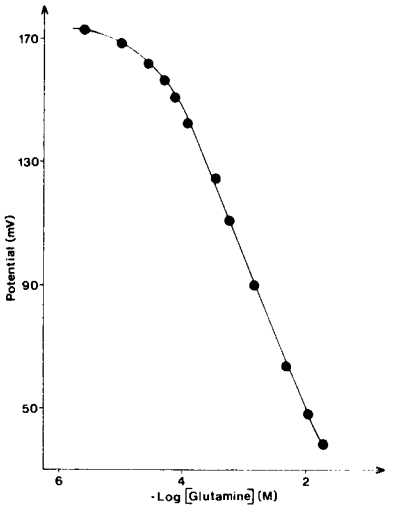

Fig. 1. Typical calibration curve for glutamine based on a tissue-based, glutamine-selective sensor.

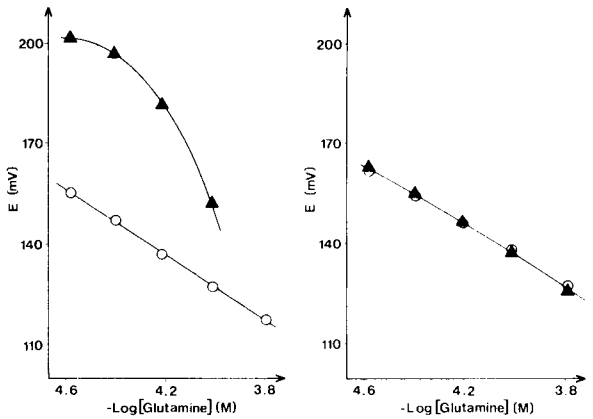

Fig. 2. (a) Calibration curves for glutamine with no iodoacetamide present, in buffer solution (○) and in diluted CSF control (▲). (b) As (a) but with iodoacetamide present at a final concentration of 1 mM.

Table 1. The amount of glutamine added to the samples covers both the normal range of glutamine concentration and the abnormal range expected for samples from patients suffering from hepatic coma [5] or Reye's syndrome [6]. The results indicate that acceptable accuracy and precision can be obtained with this method.

Finally, the proposed method was compared to a previously reported method [6] by analyzing the pooled human CSF control sample with both methods. Results from four measurements obtained by the present method

TABLE 1

Recovery of glutamine added to synthetic CSF control

Glutamine concentration ($\times 10^{-4}$ M)		Recovery (%)	n[a]
Added	Found		
0.79	0.82 ± 0.07	104	4
2.9	2.9 ± 0.2	100	4
7.9	7.8 ± 0.4	99	5
47.6	47.2 ± 0.9	98	4

[a]Number of determinations.

and by the previously reported method are $2.6 \pm 0.2 \times 10^{-3}$ and $2.4 \pm 0.1 \times 10^{-3}$ M, respectively, and are therefore in acceptable agreement.

The use of the glutamine-selective sensor offers the advantages of speed, convenience and low cost by eliminating the need for fresh enzyme for each measurement, as well as for other expensive reagents [11, 12]. The immobilization of the intact tissue cells at the surface of the electrode further eliminates the required incubation periods of conventional enzymatic assays.

We gratefully acknowledge support of this research by the National Science Foundation.

REFERENCES

1 G. A. Rechnitz, M. A. Arnold and M. E. Meyerhoff, Nature, 278 (1979) 466.
2 G. A. Rechnitz, T. L. Riechel, R. K. Kobos and M. E. Meyerhoff, Science, 199 (1978) 140.
3 G. A. Rechnitz, R. K. Kobos, T. L. Riechel and C. R. Gebauer, Anal. Chim. Acta, 94 (1977) 357.
4 E. H. F. McGale, I. F. Pye, C. Stonier, E. C. Hutchinson and G. M. Aber, J. Neurochem., 29 (1977) 291.
5 T. P. Whitehead and S. R. F. Whittaker, J. Clin. Pathol., 8 (1955) 81.
6 A. M. Glasgow and K. Dhiensiri, Clin. Chem., 20 (1974) 642.
7 S. R. Nahorski, Anal. Biochem., 42 (1971) 136.
8 I. Oreskes, F. Cantor and S. Kupfer, Anal. Chem., 37 (1965) 1720.
9 T. L. Perry, D. Stedman and S. Hansen, J. Chromatogr., 38 (1968) 460.
10 E. H. F. McGale and I. F. Pye, J. Chromatogr., 89 (1974) 350.
11 J. J. Moore, S. M. Sax and A. B. Blackburn, Jr., Clin. Chem., 24 (1978) 2213.
12 I. F. Pye, C. Stonier and E. H. F. McGale, Anal. Chem., 50 (1978) 951.
13 I. Oreskes and S. Kupfer, Anal. Chem., 39 (1967) 397.
14 M. Dixon and E. C. Webb, Enzymes, 2nd edn., Academic Press, New York, 1964, pp. 341—343.

Analytica Chimica Acta, 113 (1980) 355—359

Short Communication

DETERMINATION OF CHROMIUM IN HUMAN MILK AND URINE BY GRAPHITE-FURNACE ATOMIC ABSORPTION SPECTROMETRY

JORMA KUMPULAINEN

Department of Food Chemistry and Technology, University of Helsinki, 00710 Helsinki 71 (Finland)

(Received 11th September 1979)

Summary. Low-temperature ashing and dry ashing at 500°C are compared for the analysis of urine and human milk. Dry ashing gives superior accuracy. The importance of contamination control, background correction and temperature control are stressed. Both urine and human milk contain about 1 ng Cr ml^{-1}.

The trace element chromium is essential for normal glucose tolerance in man. About half the "typical U.S. diets" actually contain less chromium [1] than the lowest chromium intake proposed in 1979 for the Recommended Dietary Allowances. Chromium deficiency states have also been reported [2, 3]. In order to diagnose chromium nutritional states, sensitive, simple and reliable analytical methods are needed. The problem of reliability is critical for human serum, urine and milk, because at concentrations of 1 ng ml^{-1} there are no Standard Reference Materials for chromium.

In 1978, the concentration of chromium in urine of healthy subjects was shown [4, 5] to be about 1 ng ml^{-1}, and this level was recently confirmed [6]. Thus, the true concentration of chromium in urine is almost an order of magnitude less than was previously believed. In the case of human serum from healthy subjects the level of chromium was found by neutron activation analysis to be 0.1—0.2 ng ml^{-1} [7]; this level was confirmed by graphite-furnace atomic absorption spectrometry (a.a.s.) [5].

Much less attention has been given to the determination of chromium in human milk. In 1968, the milk from four women was reported to contain 40—80 ng Cr g^{-1} [8], whereas later the mean concentration in 14 samples of milk collected from five women was reported [9] to be 11.4 ng ml^{-1} (range 6.4—18.5 ng ml^{-1}).

Contamination appears to be the most important cause of erroneously high values for chromium in biological materials. When graphite-furnace a.a.s. is used, further problems arise from insufficient background correction, imprecise temperature control during atomization, as well as in the decomposition of organic matter [1, 10].

Experimental

Apparatus. The Perkin-Elmer 703 atomic absorption spectrometer used was equipped with a HGA 500 graphite furnace, a deuterium background corrector, and a Model 56 recorder. The instrumental settings were: 357.9-nm chromium line; 0.7-nm slit width; peak height mode; read-out signal on concentration; 5× scale expansion; 5-s integration time. The furnace program was as follows: (1) 150°C for 15 s (2-s ramp); (2) 300°C for 5 s (25-s ramp); (3) 1100°C for 10 s (10-s ramp); (4) 2650°C for 4 s. Argon purge gas was used at an internal flow rate of 50 ml min^{-1}. The automatic remote baseline correction was programmed 1 s prior to atomization. Pyrolytic graphite tubes were used to improve sensitivity.

Reagents. Deionized-distilled water was used throughout. Suprapur hydrochloric acid, and analytical-grade hydrogen peroxide, potassium dichromate and sulphuric acid (all Merck) were employed. A 1 g Cr l^{-1} stock standard prepared from $K_2Cr_2O_7$ was diluted daily to give working standards in the range 0.5—5.0 ng Cr ml^{-1} in 1 M HCl. The a.a.s. signals obtained from these standards were similar to those obtained from standards prepared from a $CrCl_3$ standard (Titrisol, Merck).

Sample preparation. A urine pool was prepared from 24-h urine samples collected from 4 healthy female and 5 healthy male adults aged 25—50 years. The urines were carefully shaken immediately after collection; the pool was prepared by pipetting equal volumes of each urine into a polyethylene bottle, and then frozen. The pooled urine was thawed immediately before use.

A frozen sample of pooled breast milk (from women in different stages of lactation) was obtained from the Milk Bank of the Children's Hospital, University of Helsinki. After thawing, the milk was heated to 40°C and carefully mixed before analysis.

Sample decomposition. Aliquots (1.0 ml) of urine or milk were transferred to 1.5-ml porcelain crucibles (Haldenwanger, Berlin). The milk samples were dried slowly on a hot plate in a Class 100 clean air hood (LIV 6016, Kojair, Tampere, Finland); urine samples were dried in a vacuum oven.

For dry ashing, the crucibles were placed in a covered aluminium container (2 cm high, 10 cm diameter) to avoid airborne contamination; this container was put into a cold oven, heated at 300°C for 3 h, and then ashed at 500°C overnight. After the samples had cooled, the ash was dissolved in 1.0 ml of 1 M HCl; this solution was analyzed after 30 min. If the ash was not white throughout, complete decomposition was achieved by using 5 µl of concentrated sulphuric acid and 20 µl of 30% H_2O_2 as described elsewhere [1].

For oxygen plasma ashing, the crucibles were treated for 3 h in a low-temperature asher (LTA 600, Tracerlab, Richmond, CA). The samples were then cooled, dried in a vacuum oven after addition of 100 µl of 30% H_2O_2, and ashed again in the LTA for 3 h. This ash was dissolved in 1.0 ml of 1 M HCl. In all cases, 20-µl samples were injected into the graphite furnace.

Results

The ability of most graphite-furnace atomic absorption spectrophotometers with deuterium background correction to measure chromium in ashed urine was recently questioned [4]. The ability of the instrument used here to cope with this problem was checked as follows: urine samples obtained from two healthy males, one high in salt (d. 1.023), and the other low in salt (d. 1.007), were ashed in the LTA and analyzed. The results obtained were 0.65 (± 0.04) and 0.60 (± 0.09) ng Cr ml^{-1}, respectively, when 10-μl samples were used; and 0.48 (± 0.04) and 0.50 (± 0.07) ng Cr ml^{-1} when 20-μl samples were used. The differences found do not seem significant.

The most suitable decomposition procedure for the milk and urine pools was ascertained by comparing the LTA and dry ashing methods. Wet ashing was not tested because of the difficulty of obtaining acids of sufficiently high purity for use at the 1 ng Cr ml^{-1} level. Table 1 shows the results of the comparison for pooled breast milk. The mean apparent chromium content after LTA was only 53% of the content obtained after dry ashing. The blanks were 0.10 ± 0.05 ng Cr ml^{-1} for LTA, and 0.18 ± 0.15 ng ml^{-1} for dry ashing. Day-to-day variation was 4.2% for dry ashing and 9.6% for LTA. Table 1 also shows the results of similar tests for pooled urine. The ratio between the mean chromium values after LTA and dry ashing was almost exactly the same for urine (0.56) as for breast milk (0.53). The blanks were 0.15 ± 0.12 ng Cr ml^{-1} for dry ashing and 0.1 ± 0.05 ng ml^{-1} for LTA. For urine, the day-to-day variation was 6.7% in dry ashing and 4.2% in LTA. The detection limits (signal/background = 2:1) for both the urine and milk were 0.20 ng ml^{-1} by the LTA method and 0.4 ng ml^{-1} by the dry ashing method.

To verify the accuracy of the methods, the National Bureau of Standards (NBS) Bovine Liver standard (SRM 1577) was analyzed. The sample sizes were chosen to match roughly the total amounts of chromium present in the urine or milk analyses. The results (Table 2) indicate a serious loss of chromium in the LTA procedure, and a smaller loss during dry ashing of small samples (ca. 15 mg); the latter loss was apparently due to absorption, as correct results were obtained with 150-mg samples. The ratio of the apparent chromium concentrations obtained after LTA and dry ashing for SRM 1577 corresponded almost exactly (0.57) to the ratios for milk and urine. The dry ashing procedure employed was exhaustively studied earlier and was found to give 95—100% yields for chromium in SRM 1577 [1].

Discussion

The above results indicate that analyses by the dry ashing method give correct or slightly low results for milk and urine, and that the normal level of chromium in breast milk is about 1 ng ml^{-1}, which is an order of magnitude lower than previously reported.

The causes of the losses of chromium in the LTA procedure are not clear. In a recent study [11], similar losses of chromium were found in the LTA procedure compared to the dry ashing procedure when chromium was

TABLE 1

Comparison of dry ashing and LTA in the determination of chromium in pooled breast milk and urine (Results are given as mean ± s.d. (in ng Cr ml^{-1}) with the number of crucibles used in parentheses)

	Day 1	Day 2	Day 3
Pooled breast milk			
Dry ashing	1.08 ± 0.23(5)	1.10 ± 0.30(5)	1.17 ± 0.16(7)
LTA	0.63 ± 0.17(4)	0.55 ± 0.13(7)	
Pooled urine			
Dry ashing	1.50 ± 0.08(4)	1.60 ± 0.20(5)	1.40 ± 0.16(5)
LTA	0.82 ± 0.14(6)	0.87 ± 0.10(5)	

TABLE 2

Comparison of dry ashing and LTA in the determination of chromium in NBS SRM 1577 (Bovine Liver)

	ng Cr g^{-1} ± s.d.	Mean sample size (dry wt.) (mg)
Dry ashing	61 ± 3(4)[a]	16.0
Dry ashing	88 ± 8(6)	150
LTA	35 ± 4(9)[b]	10.0

[a]NBS certified value 88 ± 12 ng g^{-1}. [b]Numbers in parentheses indicate the number of crucibles used.

determined in ethanol and ammonia extracts of SRMs; losses were greater at the 2—3 ng Cr ml^{-1} than at the 7—8 ng Cr ml^{-1} level in the extracts.

Recently, several problems were reported by Guthrie et al. [4] in the determination of chromium in urine using equipment similar to that employed here; particularly, the sample volume had a strong effect on the apparent chromium content, and peak shapes varied, including double peaks. None of these problems was encountered here. In addition to a new deuterium lamp, the better performance of the present instrumentation may have been due to the better temperature control system of the HGA-500 compared to the earlier HGA-2200.

The author thanks M. S. Jukka Kilpiö, Institute of Occupational Health, Helsinki, for providing the urine samples and M. D. Erkki Vuori, Department of Public Health Science, University of Helsinki, for donating the pooled milk sample.

REFERENCES

1 J. T. Kumpulainen, W. R. Wolf, C. Veillon and W. Mertz, J. Agric. Food Chem., 27 (1979) 490.
2 K. W. Jeejeebhoy, R. C. Chu, E. B. Marliss, S. R. Greenberg and A. Bruce-Robertson, Am. J. Clin. Nutr., 30 (1977) 531.
3 H. Freund, S. Atamian and J. E. Fischer, J. Am. Med. Assoc., 241 (1979) 496.
4 B. E. Guthrie, W. R. Wolf and C. Veillon, Anal. Chem., 50 (1978) 1900.
5 F. J. Kayne, G. Komar, H. Laboda and R. E. Vanderlinde, Clin. Chem., 24 (1978) 2151.
6 C. Veillon, W. R. Wolf and B. E. Guthrie, Anal. Chem., 51 (1979) 1022.
7 J. Versieck, J. Hoste, F. Barbier, H. Styaert, J. De Rudder and H. Michels, Clin. Chem., 51 (1979) 1022.
8 J. P. Carter, A. Cattab, K. A. Abd-al-Hadi, J. D. Davis, A. E. Gholmy and V. N. Padwardhan, Am. J. Clin. Nutr., 21 (1968) 195.
9 K. M. Hambidge, in W. Mertz and E. E. Cornatzer (Eds.), Newer Trace Elements in Nutrition, M. Dekker, New York, 1971, p. 169.
10 W. R. Wolf and F. E. Greene, in P. D. LaFleur (Ed.), Accuracy in Trace Analysis: Sampling, Sample Handling, Analysis I, NBS Publication No. 422, U.S. Government Printing Office, Washington, D.C., 1976, p. 605.
11 J. T. Kumpulainen, R. A. Anderson, M. M. Polansky and W. R. Wolf, Proc. Conf., Chromium in Nutrition and Metabolism, Sherbrooke, Quebec, Canada, June 1979, Elsevier/North Holland Biomedical Press, in press.

Analytica Chimica Acta, 113 (1980) 361—364

Short Communication

DISCRETE NEBULIZATION IN ATOMIC ABSORPTION SPECTROMETRY WITH A LONG ABSORPTION TUBE

TETSUO UCHIDA, CHUZO IIDA and ISAO KOJIMA

Laboratory of Analytical Chemistry, Department of Engineering Sciences, Nagoya Institute of Technology, Gokiso-cho, Showa-ku, Nagoya 466 (Japan)

(Received 9th July 1979)

Summary. The absolute detection limits obtained with 50 μl of sample solutions for 10 elements in an air—hydrogen flame are listed. The values for silver, cadmium, copper and manganese are of the same order of magnitude as those obtained by graphite furnace atomization. The method was satisfactorily applied to the determination of copper and zinc in Bovine Liver.

In flame atomic absorption spectrometry, the sensitivity and detection limits for some elements can be greatly improved by the use of a long absorption tube and an air—hydrogen flame [1—3]. Sample solutions are introduced into the flame by continuous nebulization and 0.5—2 ml of sample solution is needed for a single measurement. Recently, discrete nebulization techniques with conventional flame atomic absorption spectrometers have been reported [4—7] and applied to various samples [4—10]. Nebulization of about 100 μl of solution gives the same sensitivity as that obtained by continuous nebulization. The present communication deals with the combined use of the discrete nebulization and long tube techniques. The proposed method was successfully applied to the determination of copper and zinc in NBS-SRM 1577 Bovine Liver.

Experimental

The spectrometer used, operating conditions and preparation of standard solutions were as reported previously [3]. To introduce small amounts of sample solution to the nebulizer, a specially designed sampling cup was used (Fig. 1). This cup has four shallow holes (8 mm diam., 4 mm deep) of 200-μl volume, made by drilling the plane surface of a teflon rod (30 mm diam.). The 50-μl droplet of sample solution placed in a hole with a micropipette was completely aspirated through a capillary tube, as shown in Fig. 1.

Results and discussion

Spike-like signals similar to those observed in electrothermal atomization with a graphite furnace were obtained, by using the system described. The signal increased with the aspirated volume of sample solution to a saturation

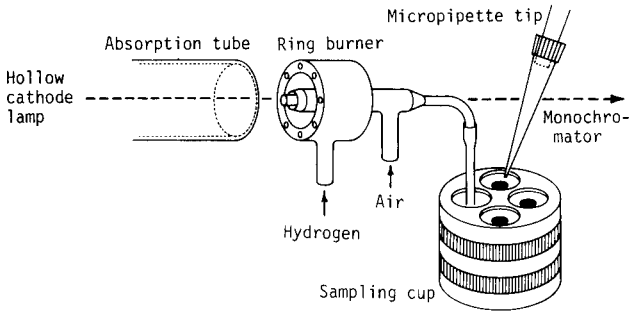

Fig. 1. Apparatus for nebulization of sample solution from cup.

value fixed by the uptake rate of the sample (Fig. 2). The peak height response became saturated for smaller volumes at lower flow rates. A sample flow rate of 2.7 ml min^{-1} was chosen for further study.

The calibration curves for copper (in 0.1 M nitric acid) obtained with various sample volumes are shown in Fig. 3. The curve obtained with 100 μl of solution was identical with that observed in continuous nebulization and was linear up to 120 ppb. With 50 μl, the responses were also identical up to 40 ppb, but discrete nebulization gave less response than continuous nebulization at higher concentrations. With 25 μl, the graph was slightly curved even at low concentrations and became parallel to the abscissa above 50 ppb. The differences were mainly due to the slow response of the instrument. With 0.1 M nitric acid as solvent, the calibration graphs for copper had an intercept as shown in Fig. 3. This intercept was probably due to the procedure used to set the baseline without nebulization of 0.1 M nitric acid. The relative standard deviations for peak height measurements were about 3% for 25-μl samples and less than 1% for 50- and 100-μl samples.

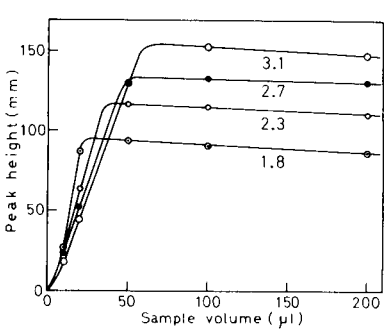

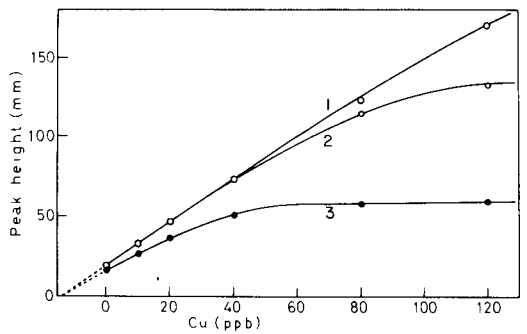

Fig. 2. Effect of sample volume and flow rate on peak height for an 80 ppb copper solution in 0.1 M HCl. The numbers on the curves are the sample flow rate in ml min^{-1}.

Fig. 3. Calibration curves for different volumes of copper solutions, 0.1 M in nitric acid. Sample volumes: (1) 100 μl; (2) 50 μl; (3) 25 μl.

Measurements were carried out with 50-μl samples to determine the detection limits for 10 elements. These limits are listed in Table 1. The detection limits are given both as the concentration (ppb) and the absolute amount (pg) dissolved in 50-μl sample solution giving a signal twice the noise. For comparison, the detection limits obtained with a conventional flame apparatus and a graphite furnace are included. More than 10 times enhancement in detectability was obtained for silver, cadmium, copper, and zinc and 1—6 times for the other elements by the present method compared to conventional flame atomic absorption spectrometry. The detection limits obtained for silver, cadmium, copper and manganese were of the same order of magnitude as those obtained with a graphite furnace. In practice, the present method was superior to electrothermal atomization in reproducibility, ease of use and rapidity of measurement.

Application to standard Bovine Liver. The technique was applied to the determination of copper and zinc in standard NBS-SRM 1577 Bovine Liver. The powdered sample (25 mg) was decomposed with 250 μl of nitric and 50 μl of perchloric acids in a sealed teflon vessel at 120°C for 3 h [12], and the digest was diluted to 250 ml with water. The results of six analyses were 184 ± 4 ppm (certified value 193 ± 10 ppm) for copper and 125 ± 3 ppm (certified value 130 ± 13 ppm) for zinc. Agreement is obviously good.

The technique is simple, accurate, rapid and reproducible, and could be quite useful for determination of trace metals in numerous fields, especially when only minute amounts of the original sample are available for analysis.

TABLE 1

Comparison of detection limits in concentration (ppb) and absolute amount (pg)

	Ag	Cd	Co	Cu	Fe	Mg	Mn	Ni	Pb	Zn
Present method (ppb)	0.16	0.16	7.2	0.73	9.7	0.45	1.3	12	5.5	0.49
Hitachi 518[a] (ppb)	3.8	11	20	8.1	13	0.52	3.7	20	31	14
Present method (pg)	8	8	360	37	490	23	65	600	280	25
Hitachi 518[a] (pg)	190	550	1000	410	650	26	190	1000	1600	700
Electrothermal[b] (pg)	0.02—20	0.2—2	2—30	5—10	2—20	0.1—1	1—20	9—100	5—10	0.1—1

[a]10-cm air—acetylene flame. [b]Ref. 11.

REFERENCES

1 K. Fuwa and B. L. Vallee, Anal. Chem., 35 (1963) 942.
2 See, e.g. I. Rubeska, Anal. Chim. Acta, 40 (1968) 187.
3 T. Uchida and C. Iida, Appl. Spectrosc., 29 (1975) 58.
4 E. Sebastiani, K. Ohls and G. Riemer, Fresenius Z. Anal. Chem., 264 (1973) 105.
5 D. C. Manning, At. Abs. Newsl., 14 (1975) 99.
6 H. Berndt and E. Jackwerth, Spectrochim. Acta, Part B, 30 (1975) 169.
7 T. Uchida, I. Kojima and C. Iida, Bunseki Kagaku, 27 (1978) T44.
8 K. C. Thompson and R. G. Godden, Analyst, 101 (1976) 174.

9 G. J. Ramelow and T. I. Balkas, Anal. Lett., 10 (1977) 733.
10 H. Berndt and W. Slavin, At. Abs. Newsl., 17 (1978) 109.
11 K. Yasuda and K. Hirokawa, High Sensitivity Atomic Absorption and Emission Spectrometry, Kodansha, 1976 (in Japanese).
12 C. Iida, T. Uchida and I. Kojima, Anal. Chim. Acta, 113 (1980) 365.

Analytica Chimica Acta, 113 (1980) 365—368

Short Communication

DECOMPOSITION OF BOVINE LIVER IN A SEALED TEFLON VESSEL FOR DETERMINATION OF METALS BY ATOMIC ABSORPTION SPECTROMETRY

CHUZO IIDA*, TETSUO UCHIDA and ISAO KOJIMA

Laboratory of Analytical Chemistry, Nagoya Institute of Technology, Gokiso-cho, Showa-ku, Nagoya 466 (Japan)

(Received 9th July 1979)

Summary. The teflon-lined bomb described is suitable for acid digestion of biological materials. Total decomposition time with nitric and perchloric acids is 6 h. Blanks are low and results agree well with certified values.

Biological materials normally have to be decomposed before trace elements can be determined by flame atomic absorption spectrometry; the metals must be completely dissolved without loss or contamination. Dry ashing in an electric furnace and wet digestion with oxidizing acids are commonly applied [1]. In the former, losses of metals or contamination can occur whereas the latter method requires careful manipulation when conventional apparatus is used. A sealed teflon vessel [2] has proved very useful for the decomposition of silicate samples with hydrofluoric and mineral acids in many investigations. In the present communication, the decomposition of bovine liver (NBS-SRM 1577) with small amounts of nitric and perchloric acids in a sealed teflon vessel at elevated temperature is described.

Experimental

Apparatus and reagents. The home-made decomposition vessel is shown in Fig. 1. The inner teflon vessel (ca. 23-ml capacity) is positioned in an outer jacket of stainless steel and is sealed tightly by tightening the stainless steel lid with an adjustable wrench while the bottom is held in a vise. A Hitachi atomic absorption spectrometer, Model 518, and Hitachi hollow-cathode lamps, HLA-3, were used under the normal operating conditions.

Standard stock solutions (1000 ppm in 0.5 M HCl) were prepared by dissolving high-purity metals (99.999% copper and zinc), Specpure oxides (iron, manganese, and magnesium), or Specpure calcium carbonate in hydrochloric acid. Mixed working solutions for constructing calibration curves were prepared by diluting the stock solutions appropriately and by adding the same amounts of nitric and perchloric acids as those used in sample decomposition.

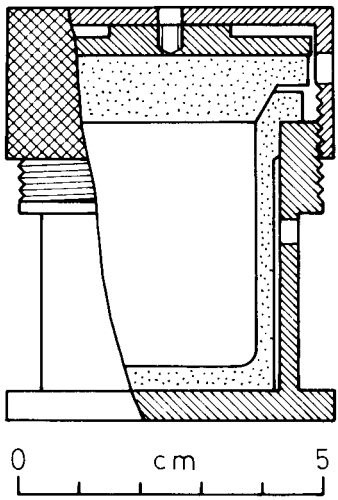

Fig. 1. Decomposition vessel.

Nitric and perchloric acids used were super-special grade (Wako Pure Chemical Industries, Ltd.) and the water used was twice-distilled.

Procedure. Powdered sample (250 mg) was placed in the inner teflon vessel. The vessel was cooled in a freezer (—20°C) for at least 30 min to insure a tight seal during the following heating steps, for the heat expansion coefficient of teflon is about 10 times larger than that of the stainless steel used as the jacket. To the sample were added 2.5 ml of nitric acid and 0.5 ml of perchloric acid. The decomposition vessel was sealed tightly and heated stepwise in a drying oven, first at 90°C for 3 h and next at 120°C for 3 h. The stepwise heating was preferred not only to decompose samples completely but also to avoid any explosive reaction of perchloric acid with organic matter. After cooling to room temperature, the contents were diluted to 25 ml with water. The concentrations of metals in the sample solution thus obtained were measured successively by atomic absorption spectrometry.

Results and discussion

Effect of perchloric acid on decomposition. In these tests, samples (500 mg) were decomposed with constant amounts of nitric acid (5 ml) and various amounts of perchloric acid (0—2 ml) by stepwise heating as described above. The sample solutions obtained became brownish yellow to pale yellow as the amounts of perchloric acid added were increased. A small amount of waxy residue was observed after decomposition without perchloric acid. The results obtained for six elements in these solutions are summarized in Table 1. Calcium was measured in the presence of 5000 ppm lanthanum; as is evident from the results for calcium, perchloric acid was

TABLE 1

Effect of perchloric acid on decomposition of NBS-SRM 1577 Bovine Liver

$HClO_4$ (ml)	Metal (ppm)					
	Cu	Zn	Mn	Fe	Ca	Mg
0.0	196	143	10.3	278	66	603
0.5	196	144	10.3	257	127	574
1.0	193	138	11.0	257	123	571
2.0	205	144	11.6	266	120	600
Certified value	193 ±10	130 ±13	10.3 ±1	268 ±8	124 ±6	604 ±9

essential for decomposition of bovine liver. Thus 1 ml of perchloric acid per 500 mg of sample was added for security.

Effect of temperature on decomposition. The decomposition of 500 mg of sample was tested with 5 ml of nitric acid and 1 ml of perchloric acid for 3 h at 90—150°C after the first heating step at 90°C for 3 h. The sample solution decomposed below 90°C was yellow, slightly opaque and a little viscous, and a small amount of waxy residue remained. Solutions decomposed above 110°C were clear and pale yellow. Despite the different color and viscosity of the solutions decomposed at different temperatures, the results for the six elements agreed well with each other and also with the certified values. However, the capillary of the nebulizer clogged occasionally, when sample solutions decomposed below 90°C were aspirated; thus decomposition below 90°C is unsuitable for routine analysis. Because of the probability of leakage at high temperatures, decomposition at 120°C is recommended.

Reproducibilty and accuracy. The recommended procedure was applied to eight samples (250 mg) of bovine liver. As can be seen from Table 2, the relative standard deviation and the accuracy are satisfactory.

Comparison of the present method with other methods

In preliminary experiments, dry ashing and wet digestion methods were also tried with 500-mg samples of bovine liver. Dry ashing was done at 450°C in an electric furnace fully lined with quartz plates after charring of the sample under an infra-red lamp. The time necessary for complete decomposition was about 3 days. Wet digestions were done with 5 ml of nitric acid and 1.5 ml of perchloric acid in 50-ml flasks fitted with reflux condensers; after standing at room temperature overnight, the flask was gradually heated with a micro-burner for about 2 h until a clear solution was obtained.

No significant differences in the analytical results obtained by the three methods were observed. Generally, however, the total blank in dry ashing tended to be high and variable; this was also a problem, though less severe, with

TABLE 2

Reproducibility and accuracy of the recommended method (n = 8)

	Cu	Zn	Mn	Fe	Ca[a]	Mg
Average (ppm)	189	132	10.2	256	116	593
S. d.	2	7	0.1	3	2	10
R.s.d. (%)	1.1	5.4	1.3	1.1	3.3	1.7
Certified value (ppm)	193 ±10	130 ±13	10.3 ±1	268 ±8	124 ±6	604 ±9
Recovery (%)[b]	98	102	99	96	94	98

[a]5000 ppm La added. [b]Compared to the certified value.

the wet digestion method. The proposed method gave either the lowest or an intermediate total blank depending on the metal, i.e. below 0.2 μg for manganese, below 0.5 μg for copper, iron, calcium and magnesium, and 0.7 μg for zinc. These values were essentially constant in every test.

The proposed method is as simple as dry ashing and is preferable to wet digestion for the simultaneous decomposition of many samples. It is free from sporadic contamination such as can be encountered in the wet digestion method. The method was satisfactorily applied to the decomposition of micro amounts of various biological samples [3].

REFERENCES

1 T. T. Gorsuch, The Destruction of Organic Matter, Pergamon Press, 1970.
2 B. Bernas, Anal. Chem., 40 (1968) 1682.
3 T. Uchida, C. Iida and I. Kojima, Anal. Chim. Acta, 113 (1980) 361.

Analytica Chimica Acta, 113 (1980) 369—373

Short Communication

CONCENTRATION OF TRACE METALS FROM NATURAL WATERS BY FREEZE-DRYING PRIOR TO FLAME ATOMIC ABSORPTION SPECTROMETRY

ARISTIDES HALL* and MANUEL CASIMIRO GODINHO

Department of Chemistry, University of Aveiro, 3.800 Aveiro (Portugal)

(Received 20th July 1979)

Summary. Freeze-drying is shown to be as effective as solvent extraction or chelating ion exchange for concentration of Fe, Mn, Ni, Al, Cr, Cu and Cd from fresh-water samples.

Several methods can be used for concentrating trace metals before flame atomic spectroscopic measurements. Those most frequently reported [1] are electrodeposition, carbon adsorption, ion exchange, coprecipitation, solvent extraction, evaporation and freeze-drying. None is of general applicability, the method selected depending on the nature of the sample and on the analytes of interest. Of these techniques, ion exchange and carbon adsorption are convenient when analysis is done by neutron activation [2] or x-ray fluorescence [3] since the concentration medium can be used as matrix, but for atomic absorption elution is normally required. Collection on chelating resins is particularly suitable for concentrating metals from sea water [4, 5] since it preferentially concentrates some trace elements. Coprecipitation is normally suitable only for a few elements. Solvent extraction is probably most often used [6], and specific procedures have been recommended by national bodies for water analysis [7, 8]. Extraction methods, nevertheless, are prone to difficulties [8, 9] related to pH adjustments, phase equilibration and separation and stability of complexes.

An advantage of evaporation methods over those referred to above is that there is no limit to the number of metals that can simultaneously be concentrated. In addition, both dissolved and colloidal material is retained. This feature is particularly attractive in dealing with fresh-water samples where the major components exist at relatively low concentrations. Of the two existing evaporation techniques, evaporation by heat and freeze-drying (lyophilization), the latter offers the biggest advantages. By working well below 0°C, freeze-drying minimizes losses even of the more volatile elements such as mercury [10]. Losses of pesticides [11] from water and essential oils [12] from model solutions have been reported during lyophilization, but those losses could be minimized by proper pH adjustment. No losses of metals were reported during the freeze-drying of river water with sodium

carbonate added as a carrier for trace metal analysis by neutron activation [13].

In the study reported here the potential of freeze-drying for the concentration of trace metals in river water prior to flame atomic absorption spectrometry was explored by comparing recoveries of known concentrations of Al, Cd, Cr(VI), Cu, Fe, Mn and Ni by freeze-drying with those obtained by solvent extraction and chelating ion-exchange techniques.

Experimental

Apparatus. All atomic absorption measurements were made with a Perkin-Elmer model 400 spectrometer connected to a Perkin-Elmer model 56 recorder. Scale expansion and the integration time facilities were used as required. Hollow-cathode lamps (Al, Cr, Cu, Fe, Mn, Ni) and electrodeless discharge lamps (Cd, Pb) were operated as recommended by Perkin-Elmer.

Freeze-drying was done in pear-shaped, long-necked, 250-ml borosilicate flasks with a Vir-Tis automatic freeze-dryer, model 10-100. Ion exchange was done in polyethylene siphons (7 mm i.d., 10-cm long) fed from 1-l borosilicate extraction funnels.

Reagents. The water used for preparing solutions and final rinsing of vessels was distilled and passed through an Elgastat model B104 HR mixed-bed ion exchanger. The water conductivity, as measured by the deionizer meter, never exceeded 0.2 μmho cm^{-1}, and is referred to hereafter as pure water. Chelex 100 chelating resin was slurried with water into polyethylene siphons, conditioned by passing two 25-ml portions of 2 M nitric acid and washed with pure water until the effluent pH was above 5. After use the resin was converted to the H^+- form with the nitric acid, washed as above and left immersed in water. Standard solutions were prepared by appropriate dilution of BDH or J. T. Baker atomic absorption standards. Pyrrolidine-dithiocarbamic acid (PDCA) in chloroform was prepared as prescribed by the E.P.A. [8]. All reagents used were of analytical-reagent grade. Nitric and hydrochloric acids were twice-distilled; the other reagents were used without further purification.

Materials. Only borosilicate glassware, greaseless joints, polyethylene and PTFE were allowed to contact the solutions and the natural water used. Both the glass and plastic ware were cleaned by soaking in a 2% RBS35 detergent solution for not less than 24 h, rinsing with tap water, soaking in 1 M nitric acid for at least 3 h, rinsing with tap water and then three times with pure water, and finally drying in an oven.

Samples and standards. Natural water collected at Pateira de Fermentelos was filtered under pressure through 0.45-μm membrane filters mounted on a Sartorius all-plastic filtration apparatus, preserved with 5 ml of nitric acid per liter and kept in polyethylene flasks. The chemical content (in mg l^{-1}) of the natural water was alkalinity (120), Cl^- (0.06), NH_3-N (0.09), NO_2^--N (0.009), NO_3^--N (0.48), total N (0.89), total P (0.64), SO_4^{2-} (58.2), SiO_2 (1.9), Ca (14.9), K (2.49), Mg (8.9), Na (15.6), Fe (0.045), Mn (0.012),

non-filterable residue (34.2). The concentration range used for each element in the standard solutions was chosen after selective sampling and analysis of local surface waters so as to span all the concentrations likely to be found.

Chelation. Appropriate volumes of the standard solutions were diluted to 500 ml with pure water. Portions of natural water were spiked with the mixed standard and their volume made up to 500 ml. Three increments of standard were used. The solutions were adjusted to pH 7.6 (pH meter) with hydrochloric acid or sodium hydroxide, and transferred to glass ampoules mounted on Chelex-100 columns, and the flow rates were regulated at 1.5 ml min^{-1}. Elution was carried out with 25 ml of 2 M nitric acid. Atomic absorption analysis was performed immediately after elution, with 2 M nitric acid used as a blank.

Extraction. Standard solutions and spiked natural water samples, 200 ml each, were prepared in quadruplicate as described above. Extractions were done with PDCA as proposed by the E.P.A. [8] and the final volumes were adjusted to 10 ml with water. Atomic absorption readings were taken immediately using 0.5 M nitric acid as a blank.

Freeze-drying. Four replicate 100-ml samples of standard solutions and spiked natural water were prepared as described above, transferred to long-neck pear-shaped flasks, frozen in a deep freezer and connected to the freeze-dryer. About 24 h were necessary for the sublimation of water to be complete. To each flask was added 2 ml of 1 M hydrochloric acid; after mechanical shaking for 5 min, the solutions were gently refluxed on a water bath for 10 min. This process left a small amount of whitish scales in suspension; x-ray diffraction spectrometry showed this fraction to be hydrated calcium sulphate. The supernatant solution was decanted into a vial for immediate analysis by atomic absorption spectrometry.

Calibration curves. Calibration curves for each concentration technique were drawn from the readings obtained with freshly prepared mixed standards that were made 2 M in nitric acid for chelation, 0.5 M in nitric acid for extraction and 1 M in hydrochloric acid for freeze-drying.

Results and discussion

The recoveries achieved by the three methods tested are shown in Table 1. Aluminium and chromium were not used in the ion-exchange experiments because they are not quantitatively retained by Chelex-100 [4]. Similarly, aluminium and nickel were not used for the extraction procedure [8]. Lead is not removed with hydrochloric acid from the residue left after freeze-drying. Acid concentrations from 0.1 M upwards and aqua regia were tried without success; apparently the formation of chloroplumbate ions is inhibited by the sulphate present in the precipitate. Lead is easily and quantitatively removed with nitric acid from the residue of spiked pure water samples, but residues from natural waters still gave erratic results (though much of the lead was recovered) probably because of the effect of different particle sizes on the solubility of lead sulphate. Of the elements of

TABLE 1

Comparison of recoveries from spiked pure water and natural water samples

Metal	Concentration range ($\mu g\ l^{-1}$)	Ion exchange[a]	Recoveries (%)	
			Extraction	Freeze-drying
Al	0—250	—	—	109
Cd	0—16	104	106	90
Cr(VI)	0—40	—	73	110
Cu	0—100	99	99	114
Fe	0—250	59	75	101
Mn	0—100	85	98	99
Ni	0—150	75	—	104
Pb	0—400	89	99	102[b]

[a]Calculated after elimination of results more than twice the standard deviation from the mean (see text). [b]For spiked pure water only (see text).

interest only lead could not be recovered from the residue with hydrochloric acid. In general, measurements on hydrochloric acid extracts were higher than those obtained with nitric acid, thus hydrochloric acid is recommended for the dissolution.

As all spike additions were prepared in quadruplicate, it was possible to estimate the precision associated with each procedure. Ion exchange was the least precise procedure; scatter of the readings about the mean was sometimes in excess of 50%. Reconditioning of the resin as recommended by the manufacturer, changing and fixing the pH with buffers and measures to avoid contamination by atmospheric dust did not improve the precision. Although no reference to this difficulty could be found in the literature, it has also been experienced elsewhere [14]. Recoveries are lower than those reported in the literature [5], except for cadmium and copper, possibly because the resin was rather old.

The average precisions for the extraction and freeze-drying procedures were 7% and 6%, respectively. Extraction gave virtually complete recoveries of Cd, Cu, Mn and Pb but recoveries of only about 75% for Fe and Cr(VI). Recoveries by freeze-drying are nearly 100% for Fe, Mn and Ni, only 90% for Cd and higher than 100% for Al, Cr and Cu. Cadmium tends to give low recoveries whatever the concentration technique used [9, 15, 16]. Adsorption or complexing has been held responsible [16], but in the proposed method, the formation of mixed sulphates with calcium may be the reason. The high recoveries observed for Al, Cu and Cr seem to be associated with the very low concentrations present in the samples. A similar enhancement in the recovery of mercury from biological samples has been observed for concentrations below 100 $\mu g\ kg^{-1}$ but not for concentrations above that limit [10].

The results show that the use of freeze-drying for concentrating trace elements from fresh waters can be valuable. In terms of precision and recovery, it can match other techniques and has the advantage of being free of some of their shortcomings. Thus there is no limit to the number of elements concentrated, the procedure is extremely simple and economical in reagents and operator time and opportunities for contamination are reduced.

We are grateful to Ms. Adelinda Alves of the Department of Geosciences, University of Aveiro, for the x-ray analyses.

REFERENCES

1 See, e.g., B. Orpwood, Concentration Techniques for Trace Elements: A Review, Water Research Centre and Technical Report TR 102, Medmenham, 1979, 32 pp.
2 See, e.g., A. Hirose, K. Kobors and D. Ishii, Anal. Chim. Acta, 97 (1978) 303.
3 See, e.g., S. L. Law and W. J. Campbell, Adv. X-Ray Anal., 17 (1974) 279.
4 J. P. Riley and D. Taylor, Anal. Chim. Acta, 40 (1968) 479; 41 (1968) 175.
5 E. W. Davey and A. E. Soper, Limnol. Oceanogr., 20 (1975) 1019.
6 M. J. Cresser, Solvent Extraction in Flame Spectroscopic Analysis, Butterworths, London, 1978.
7 A. R. Cockcroft, D. Nield and L. Ranson, Water Research Centre, Technical Report TR59, Medmenham, 1977.
8 Environmental Protection Agency, Manual of Methods for the Chemical Analysis of Water and Wastes, Cincinnati, 1974, pp. 85, 89.
9 T. N. Tweeten and J. W. Knoeck, Anal. Chem., 48 (1976) 64.
10 G. Ramelow and H. Hornung, At. Abs. Newsl., 17 (1978) 59.
11 H. Bargnoox, D. Pepin, J. L. Chabard, F. Verdrine, H. Petit and J. A. Berger, Analusis, 6 (1978) 107.
12 T. G. Smyrl and M. Lemaguer, J. Food Sci., 43 (1978) 1357.
13 D. P. Kharkar and K. K. Bertine, Geochim. Cosmochim. Acta, 32 (1968) 285.
14 M. Del Negro, personal communication.
15 B. M. Vanderborght and R. E. Van Grieken, Anal. Chem., 49 (1977) 311.
16 K. V. Krishnamurty and M. M. Reddy, Anal. Chem., 49 (1977) 222.

Analytica Chimica Acta, 113 (1980) 375—381

Short Communication

IDENTIFICATION OF CYCLOHEXAMINE, PHENCYCLIDINE AND SIMPLE ANALOGUES BY CARBON-13 NUCLEAR MAGNETIC RESONANCE SPECTROSCOPY

KEITH BAILEY* and DONALD LEGAULT

Drug Research Laboratories, Health Protection Branch, Tunney's Pasture, Ottawa KIA OL2 (Canada)

(Received 22nd June 1979)

Summary. The ^{13}C-nuclear magnetic resonance spectra are reported for phencyclidine and ten analogues, five of which are drugs of abuse. Data from the spectra of the bases and hydrochloride salts are presented with signal assignments, and are interpreted in terms of the structural differences between series of primary, secondary, and tertiary amines, phenyl and thienyl moieties, and free-base and protonated forms in chloroform and aqueous solutions. The spectra are suitable for identification and authentication purposes.

The increasing number and variety of illicit street drugs have required the preparation and authentication of numerous reference materials for analytical purposes. Procedures for identification and purity determination are frequently developed from the authentication methods. Carbon-13 nuclear magnetic resonance (n.m.r.) spectra form part of the authentication process for in-house reference materials employed in these laboratories. However, although ^{13}C-n.m.r. spectra appear to fingerprint organic molecules [1], they do not form part of the routine examination of forensic drug exhibits. There are several reasons for this: few forensic laboratories have ^{13}C-n.m.r. spectrometers because they are expensive; the technique is still relatively insensitive; and the well established colour tests, thin-layer and gas chromatography (with or without mass spectrometry), ultraviolet and infrared spectrophotometry when judiciously applied are held to be entirely adequate for identification purposes.

^{13}C-n.m.r. spectral data have been published for several groups of abused substances: barbiturates [2], cannabinoids [3], cocaine and derivatives [4], and opiates [5]. ^{13}C-n.m.r. data are presented here for eleven structurally similar 1-arylcyclohexylamine analogues (I—XI). Five of these have appeared on the street: cyclohexamine (PCE, III), the propyl homologue (IV), phencyclidine (PCP, VII) and the pyrrolidine and thienyl analogues (VI and X). Examination and assignment of the spectral data confirm the authenticity of the materials and provide valuable reference data in addition to those recently published for these substances [6, 7].

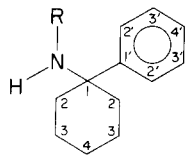

I ; R=H
II ; R=CH_3
III ; R=CH_2CH_3
IV ; R=$CH_2CH_2CH_3$
V , R=$CH(CH_3)_2$

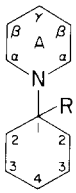

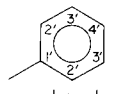

phenyl

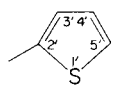

2-thienyl

VI ; ring A = pyrrolidine, R = phenyl
VII ; ring A = piperidine, R = phenyl
VIII ; ring A = morpholine, R = phenyl
IX ; ring A = pyrrolidine, R = 2-thienyl
X ; ring A = piperidine, R = 2-thienyl
XI ; ring A = morpholine, R = 2-thienyl

Experimental

Compounds I—XI and their hydrochlorides were obtained as described previously [6, 7]. ^{13}C-n.m.r. spectra were determined at 20.1 MHz on a Brüker WP80 Fourier-transform spectrometer. Spectra were recorded at ambient temperature by using the deuterium resonance of the solvent as the internal lock. Hydrochlorides were examined in D_2O and $CDCl_3$ and free bases in $CDCl_3$; δ values were measured in ppm downfield from TMS in $CDCl_3$ solution. Solution concentrations were about 150 mg in 2 ml of solvent in 10-mm tubes. Protons were decoupled by broad-band irradiation (4—5 W, offset 6,000 Hz) except in single-frequency off-resonance decoupling (s.f.o.r.d.) experiments (4 W, offset 4,700 Hz) [8]. Protons were selectively decoupled by applying a series of low-power irradiations (ca 0.02 W) at increments of 0.06 ppm across the proton region of interest. Normally about 5000 interferograms of 5000-Hz sweepwidth were stored for output in 4 K data points following transform (δ precision ± 0.03 ppm). Pulse widths were 1.5 μs (19.2° flip angle) with no pulse delay following data acquisition. For convenience in comparison, stick diagrams (not shown here) of the spectra were prepared by expressing the strengths of the resonance lines as relative percentages of the most intense signal observed.

Results and discussion

The ^{13}C-n.m.r. spectra of the analogues are easily distinguishable from one another. The designation of carbons is shown in the structural formulae to simplify the numbering of equivalent nuclei. The rules of ^{13}C-n.m.r. spectra, in particular relative intensities, chemical shift effects and carbon-proton coupling revealed by s.f.o.r.d. experiments [8] enabled self-consistent assignments to be made by comparative examination of the data; these are presented in Tables 1 and 2. No internal standard was added to the D_2O solutions and chemical shift measurements were made relative to C-4 which was assigned the value determined in $CDCl_3$.

TABLE 1

Data from the ^{13}C-n.m.r. spectra of phencyclidine analogues I-VIII and their hydrochlorides[a]

Compound	1	2	3	4	1′	2′	3′	4′	α	β	γ
I.	53.81 w	39.48 vs	22.65 vs	25.93 s	150.40 w	125.47 s	128.63 s	126.56 m			
I. HCl	58.67 m	34.80 s	21.62 s	24.96 m	139.26 m	126.93 vs	128.99 vs	128.51 s			
I. HCl (D_2O)	58.97 m	34.68 vs	22.11 vs	24.96 s	138.83 m	127.23 s	130.21 s	129.90 s			
II.	57.24 w	35.83 vs	22.29 vs	26.11 s	146.70 w	126.69 vs	128.45 vs	126.44 s	28.42 m		
II. HCl	63.77 m	33.34 vs	22.17 s	25.14 m	135.67 m	129.60 vs	128.39 vs	129.24 s	26.24 m		
II. HCl (D_2O)	64.01 w	32.86 s	22.17 s	25.14 m	134.82 w	130.21 vs	128.63 s	130.21 vs	26.48 m		
III.	57.51 w	36.38 vs	22.29 vs	26.05 m	147.25 w	126.56 vs	128.39 vs	126.32 s	35.95 s	15.91 m	
III. HCl	64.44 m	33.46 vs	22.35 vs	25.20 m	135.67 m	129.54 vs	128.69 vs	129.12 s	36.99 m	12.09 m	
III. HCl (D_2O)	64.19 m	33.16 vs	22.23 vs	25.20 m	134.88 m	130.15 vs	128.69 s	130.15 vs	36.99 m	11.42 m	
IV.	57.33 w	36.44 vs	22.35 vs	26.11 m	148.00 w	126.62 vs	128.39 vs	126.32 s	43.73 m	24.11 m	11.96 m
IV. HCl	64.56 m	33.46 s	22.41 vs	25.20 m	135.67 m	129.54 vs	128.69 vs	129.12 s	43.61 m	20.10 m	11.48 m
IV. HCl (D_2O)	64.50 w	33.22 s	22.29 s	25.20 m	134.95 w	130.15 vs	128.81 s	130.15 vs	43.42 m	20.10 m	10.69 m
V.	57.76 w	37.29 vs	22.59 vs	26.24 m	147.69 w	126.99 vs	128.26 vs	126.38 s	43.00 m	25.75 vs	
V. HCl	65.83 w	33.83 s	22.35 s	25.14 m	135.98 m	129.48 m	129.12 vs	129.12 vs	47.67 m	22.53 s	
V. HCl (D_2O)	65.35 w	33.65 s	22.23 s	25.14 m	134.95 w	130.21 vs	128.87 s	130.21 vs	47.61 m	21.44 s	
VI.	60.06 w	34.98 vs	22.65 vs	26.48 m	138.36 w	127.84 vs	128.26 vs	126.44 s	44.82 vs	23.08 vs	
VI. HCl	68.38 w	32.43 s	22.41 s	24.84 m	131.24 w	129.72 vs	129.72 vs	129.97 m	47.07 s	22.84 s	
VI. HCl (D_2O)	68.69 w	32.31 s	22.29 vs	24.84 w	131.67 w	130.03 s	129.78 s	130.15 m	47.92 s	22.29 vs	
VII.	61.28 w	33.77 s	22.53 s	26.60 m	140.80 w	127.72 vs	127.72 vs	126.32 m	46.70 s	27.27 s	25.14 m
VII. HCl	71.36 m	30.73 s	22.90 m	24.78 m	131.00 w	129.90 vs	129.54 vs	129.90 vs	47.37 s	23.02 vs	22.65 m
VII. HCl (D_2O)	71.72 m	31.28 vs	22.65 s	24.78 s	131.12 w	130.27 vs	129.60 vs	130.27 vs	47.67 vs	25.56 m	21.68 m
VIII.	60.97 w	33.04 vs	22.41 vs	26.48 s	140.05 w	127.66 vs	128.02 vs	126.66 s	46.16 vs	68.14 vs	
VIII. HCl	71.72 w	30.37 s	22.71 s	24.78 m	130.27 s	129.84 vs	129.72 vs	130.27 s	45.85 vs	63.83 s	
VIII. HCl (D_2O)	72.57 w	30.85 s	22.59 s	24.78 m	130.57 m	130.33 vs	129.84 vs	130.57 m	46.34 s	64.31 s	

[a]Measured in $CDCl_3$ containing TMS except where indicated (D_2O); δ values in ppm from TMS except for hydrochlorides in D_2O in which the chemical shift of C-4 was assigned the same value as that determined in $CDCl_3$; vs, s, m, and w refer to the relative intensities of the resonance lines (100—75, 74—50, 49—25, and 24—0%, respectively) compared to the most intense line observed for the particular compound.

TABLE 2

Data from the ^{13}C-n.m.r. spectra of thiophencyclidine analogues IX—XI and their hydrochlorides[a]

Compound	1	2	3	4	2′	3′	4′	5′	α	β	γ
IX.	59.18 w	37.71 vs	22.59 vs	26.05 m	145.60 w	124.80 s	126.32 s	123.28 s	45.00 vs	23.50 vs	
IX. HCl	67.11 w	34.92 vs	22.65 vs	24.23 m	136.59 w	130.51 m	128.63 s	128.26 s	47.19 vs	23.26 vs	
IX. HCl (D_2O)	67.47 w	34.74 vs	22.41 vs	24.23 m	136.34 w	131.48 m	128.45 m	129.30 m	48.04 vs	22.53 vs	
X.	60.00 w	36.32 vs	22.35 vs	26.24 s	147.31 w	124.16 m	126.32 m	122.92 m	46.25 vs	27.21 vs	25.08 s
X. HCl	69.72 m	33.22 s	23.08 vs	24.17 m	136.89 w	130.45 m	128.57 m	128.20 m	47.25 s	23.08 vs	22.65 m
X. HCl (D_2O)	70.08 m	33.46 vs	22.90 vs	24.17 m	136.34 m	131.61 m	128.39 m	129.30 m	47.61 vs	23.56 vs	21.56 m
XI.	59.94 w	35.53 vs	22.23 vs	26.11 m	146.34 w	124.56 m	126.44 m	123.47 m	45.91 vs	68.02 vs	
XI. HCl	70.08 m	32.80 vs	23.02 vs	24.17 m	136.04 w	130.69 s	128.99 s	128.39 m	45.67 vs	63.83 vs	
XI. HCl (D_2O)	70.87 m	32.98 vs	22.77 vs	24.17 m	135.27 w	131.97 m	128.57 m	129.78 m	46.10 vs	64.19 vs	

[a]See footnote, Table 1.

The signals from C-4 were readily identified in all the spectra. They appear upfield from all except the nearby C-3 signals which have about twice the relative intensity, and some C-β and C-γ resonances. The chemical shifts fall in the range 25.93—26.60 ppm for the bases and 24.17—25.20 ppm for the hydrochlorides in $CDCl_3$.

The signals from C-1 have an intensity similar to that of C-4 and appear within the range 53—73 ppm for salts and bases. Signals from C-β of the morpholine analogues VIII and XI are the only intruders in this region and are easily distinguished by virtue of relative intensity and chemical shift comparisons. The C-2 signals of salts and bases appear between 30 and 40 ppm. The α-carbon of cyclohexamine (III) is the only other signal to appear here, having half the relative intensity of C-2.

The assignment of C-3 was somewhat complicated in the pyrrolidine and piperidine compounds VI, VII, IX, and X by the equally intense nearby signal from C-β. In the case of the bases, the remaining seven compounds cover the very narrow range of 22.23—22.65 ppm for C-3 which identifies the signal in the remaining spectra and shows that C-β is at lower field than C-3 in these four heterocyclic analogues. In the case of the hydrochlorides, C-3 may be located as the signal with the best fit to the limits determined for the remaining seven salts (21.62—23.02 and 22.11—22.77 in $CDCl_3$ and D_2O, respectively). The C-3 and C-β signals coincide for VI.HCl in D_2O and X.HCl in $CDCl_3$. The distinction of the equally intense C-3 and C-β signals of V.HCl was easily accomplished by the s.f.o.r.d. experiment. These assignments of signals for the cyclohexyl moiety are in agreement with those assigned for cyclohexylamine [9].

The C-α, β, γ signals are thus distinguished from one another and from the C-2, 3, 4 signals and identified as presented in the Tables. The identification of the phenyl carbons (Table 1) was straightforward for the bases; the signals from C-2′ and C-3′ of the salts were assigned on the basis that the chemical shift of the *meta* (C-3′) carbon would be much the less affected by protonation [8].

The thienyl carbon signals were assigned for the bases (Table 2) by comparison with the chemical shifts reported for 2-methylthiophene [9]. Selective decoupling of the thienyl protons of IX, employing the assignment H-5′, H-4′, H-3′ successively from low to high field, which applies to 2-methylthiophene and the similar furfuryl amine [10], confirmed the sequence C-4′, C-3′, C-5′ from low to high field.

The signal from H-4′ in the p.m.r. spectra of IX.HCl in $CDCl_3$ and D_2O was identified as the double-doublet [J (1st order) 2.7 and 3.6 Hz and 3.8 and 5.0 Hz, respectively] appearing at lowest and highest field, respectively, of the aromatic proton region. The signal from C-4′ was then identified in both solvents (Table 2) from the results of selective decoupling of H-4′. Signals from H-3′ and H-5′ were separated by 0.3 ppm in the spectrum of IX.HCl in D_2O and are believed to be those at higher and lower field, respectively, on the basis of the previous spectra [10] and similar (1st order) J values (3.8

and 1.0 Hz and 5.0 and 1.0 Hz, respectively) to those in the base (H-3′, 3.4 and 1.2 Hz; H-5′, 5.0 and 1.2 Hz, respectively). Hence, selective decoupling indicated the assignments C-3′, C-5′, C-4′ from lower to higher field for IX.HCl in D_2O. Protons 3′ and 5′ of IX.HCl were separated by only about 0.05 ppm in $CDCl_3$ and could not be confidently assigned, rendering the decoupling technique ambiguous. (Selective decoupling showed that the lower-field signal of C-3′ and C-5′ was associated with the lower-field region of the overlapping proton signals.) If the change in solvent does not reverse the positions of the C-5′ and C-3′, the assignments are C-3′, C-4′, C-5′ from low to higher field for IX.HCl in $CDCl_3$. It also seems reasonable that the C-4′ signal would be the least affected by protonation. The signals from X.HCl and XI.HCl have been tentatively assigned (Table 2) consistently with the foregoing deductions for IX.HCl.

The series of compounds show several interesting effects of structural variation on chemical shifts.

(1) Changing the amino function in the sequence primary—secondary—tertiary amine of the phenyl series I—VIII results in downfield shifts of the ranges of C-1 for both bases and salts but the ranges of the adjacent C-2 and C-1′ shift upfield (Table 1); there are small downfield shifts at C-2′, C-3′ (salts) and C-4.

(2) Substitution of thiophene for benzene (compounds IX—XI vs VI—VIII) results in shifts of C-1 upfield by about 1 ppm, C-2 downfield by about 2.5 ppm and apparently small upfield shifts of C-3 and C-4 except for C-3 of the salts which are shifted slightly downfield. The α- and β-carbon signals were not shifted in a consistent manner.

(3) Protonation shifts C-1 of all compounds downfield by some 5—11 ppm; the adjacent C-2 and C-1′ (C-2′ of the thienyl analogues) shift upfield by about 2.5—4 and 7—13 ppm, respectively; the next adjacent C-3 undergoes small, inconsistent shifts but C-2′ (compounds I—VIII) shifts downfield by 1.5—3 ppm; the next adjacent C-4 shifts upfield by 1—2 ppm and C-3′ downfield by as much as 1.8 ppm; C-4′ is consistently shifted downfield by 2—3.5 ppm. Protonation shifts the α-carbons downfield except for the two morpholine derivatives and the methyl and n-propyl analogues (II and IV); the β- and γ-carbons are all shifted upfield. The results for the aliphatic carbons are in contrast to those for cyclohexylamine, piperidine and *N*-methylpiperidine [9] in which all affected signals shifted upfield on protonation.

(4) The effect of changing the solvent from $CDCl_3$ to D_2O on the chemical shifts of the salts can be determined from Tables 1 and 2, relative to the effect at C-4. The C-1 signals are shifted downfield except for the ethyl, propyl, and isopropyl analogues (III—V). The C-2 signals are shifted relatively upfield except for the two piperidine and two morpholine analogues, whereas the C-3 signals are shifted upfield except for the amino analogue I and possibly the methylamino analogue (II). Effects on the α-, β-, and γ-carbon signals are consistent in the phenyl and thienyl series. With

respect to the aromatic carbon signals of the phenyl analogues (I—VIII), there is a relative upfield shift of C-1′ for all except the three tertiary amine salts. (The equivalent C-2′ of the thienyl analogues is also shifted relatively upfield). The effects at C-3′ are smaller than those at C-2′ and C-4′, and the signals are shifted relatively downfield. The general trend of changes in shifts spanning the arylcyclohexane moiety suggests that solvation of the salts by water rather than chloroform has an effect equivalent to a decrease in the shielding constant in the aromatic portion relative to the effect in the alicyclic portion.

(5) Consistent chemical shift effects on changing the heterocyclic moiety are clear from compounds VI—XI. Substitution in the sequence pyrrolidine—piperidine—morpholine results in downfield shifts of C-1 (salts), upfield shifts of C-2 (salts and bases) and upfield shifts of C-3 (bases). The sequence pyrrolidine—morpholine—piperidine applies to consistent shifts of other carbons: downfield shifts of C-1 (bases), C-3 (salts) and C-4 (bases). These effects are evidently complex.

The assignments are in agreement with those proposed previously for phencyclidine itself [11]. A review of these interpretations of the spectra and the changes produced by structural variations indicates that complex interactions occur. These can result in such effects as alternating upfield-downfield shift sequences along the carbon chain progressing from the site of change as described in paragraphs (1) and (3) above.

It is apparent that the ^{13}C-n.m.r. spectra of cyclohexamine, phencyclidine and their simple analogues can be used for their unambiguous identification and authentication.

REFERENCES

1 H. L. Surprenant and C. N. Reilley, Anal. Chem., 49 (1977) 1134.
2 S. Asada and J. Nishijo, Bull. Chem. Soc. Jpn., 51 (1978) 3379.
3 R. A. Archer, D. W. Johnson, E. W. Hagaman, L. N. Moreno and E. Wenkert, J. Org. Chem., 42 (1977) 490.
4 J. K. Baker and R. F. Borne, J. Heterocyclic Chem., 15 (1978) 165.
5 F. I. Carroll, C. G. Moreland, G. A. Brine and J. A. Kepler, J. Org. Chem., 41 (1976) 996.
6 K. Bailey, D. R. Gagne and R. K. Pike, J. Assoc. Off. Anal. Chem., 59 (1976) 81.
7 K. Bailey and D. Legault, J. Assoc. Off. Anal. Chem., 62 (1979) 1124.
8 F. W. Wehrli and T. Wirthlin, Interpretation of Carbon-13 NMR Spectra, Heyden, London, 1976, pp. 66, 47.
9 J. B. Stothers, Carbon-13 NMR Spectroscopy, Academic Press, New York, 1972, pp. 153, 253, 256, 272.
10 NMR Spectra Catalog, Varian Associates, Palo Alto, 1962, Spectra 103 and 104.
11 P. Geneste and J. M. Kamenka, Org. Magn. Reson., 7 (1975) 579.

Analytica Chimica Acta, 113 (1980) 383—387

Short Communication

RECOVERY OF NICKEL FROM AMMONIACAL MEDIA WITH DIOXIME-LOADED OPEN-PORE POLYURETHANE FOAMS

M. HALMANN*
Isotope Department, Weizmann Institute of Science, Rehovot (Israel)
D.-W. LEE
Department of Chemistry, Yonsei University, Seoul (Korea)
(Received 25th July 1979)

Summary. Best recovery of nickel was obtained with dimethylglyoxime-loaded polyurethane foam, but the most stable foam for repeated absorption and recovery of nickel was found to be polyurethane loaded with α-benzildioxime dissolved in tributyl phosphate. Applications to the removal of nickel from industrial effluents are described.

Open-pore polyurethane foams have found increasing application for the separation of a wide range of mixtures [1—3]. The use of dimethylglyoxime (DMG) physically immobilized on polyurethane foam was recently reported for the selective extraction of nickel(II) from aqueous solutions [4]. The advantage of the DMG-treated foam with high capacity, selectivity and rapidity of adsorption of nickel, even down to 0.5 ppm. Nickel was optimally absorbed from solutions of pH 7—10, and could be completely eluted by 1—2 M hydrochloric acid. The drawback of this foam, however, was that elution also removed 90% of the DMG from the foam. Thus, before each recycling step, it was necessary to reload the foam with DMG.

The purpose of the present study was to develop dioxime-foam systems stable to acid leaching, and to study the effect of plasticizers such as tri-n-butyl phosphate (TBP) on the performance of the foams.

Experimental

α-Benzildioxime, dimethylglyoxime and 1,2-cyclohexanedione dioxime (nioxime; all Fluka, puriss) and tri-n-butyl phosphate (TBP; Merck) were used as received.

Nickel was determined by atomic absorption spectrometry or spectrophotometrically with nioxime [5].

Dimethylglyoxime-loaded polyurethane was prepared as previously described [4]. Benzildioxime-loaded foam was prepared by shaking the foam cubes with a saturated solution of the reagent in dimethylsulfoxide (DMSO) for 4 h. DMG—TBP-loaded foam was prepared by shaking the polyurethane (1 g) for 10—30 min with a solution of 3% DMG in TBP

(20 ml). After squeezing out the excess of TBP-DMG and washing with water, the dried foam contained ca. 70% (w/w) of TBP. Benzildioxime—TBP loaded foam was prepared by shaking the polyurethane (1.5 g) with benzildioxime (1.5 g) and TBP (100 ml) for 1 h, squeezing out the excess solvent, rinsing with distilled water until the washings were clear, and then bringing the foam to pH 9.2.

Nickel was absorbed on the dioxime-loaded foams by the batch method, by shaking glass or plastic bottles containing aqueous nickel solutions (shaker speed, ca. 180 rpm) with weighed amounts of foam cubes (about 100 mg, each cube about 5 mm edge) at 20—25°C.

Columns (10 cm long, 1 cm diameter) were prepared by packing cylindrical plugs of the treated polyurethane foams into glass columns. Column elution experiments were carried out by passing 100-ml aliquots of solutions through the columns.

Results and discussion

In order to evaluate the time required for adequate absorption of nickel on the various dioxime-loaded foams the effect of shaking time was determined. As shown in Fig. 1 (A), the fastest approach to equilibrium was achieved with the DMG—TBP-treated foam; absorption was complete well within 30 min. Slowest equilibration (incomplete even after 3 h) was obtained with a foam loaded with only benzildioxime. Here, too, the addition of the TBP plasticizer improved the performance considerably. The role of the plasticizer may be to increase the mobility of nickel ions in the foam, thus enhancing the rate of extraction of nickel. Plasticizers such as TBP are known generally to enhance the mobility of metal ions and thus facilitate the reaction of metal ions with dissolved agents [2].

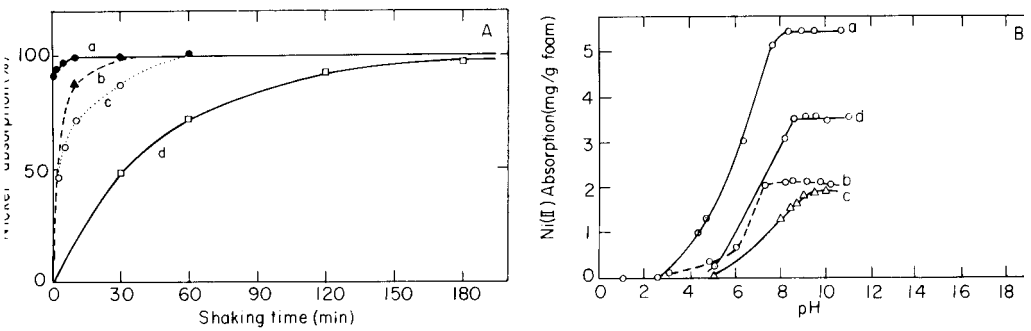

Fig. 1. (A). Effect of time on the absorption of nickel on loaded polyurethane foams at room temperature. (B). Effect of pH on nickel absorption. (a) DMG—TBP: 3% DMG—TBP foam (100 mg), 900 μg Ni/15 ml solution. (b) DMG: 9.3×10^{-5} mmol DMG/g foam taken, 200 μg Ni/13 ml solution. (c) Benzildioxime—TBP: 1.5% benzildioxime—TBP foam (100 mg), 900 μg Ni/15 ml solution. (d) Benzildioxime: 1.2×10^{-4} mmol benzildioxime/g foam (60 mg), 400 μg Ni/20 ml solution.

The effect of pH on the absorption of nickel by the various foams is presented in Fig. 1 (B). All foams reach a plateau in the alkaline region and are most efficient at pH 9—10, as expected for the reaction between nickel(II) and dioximes in aqueous solution. The comparison was carried out only for determining the effect of pH, and not at the maximum absorption capacity.

The dependence of the nickel capacity of TBP-plasticized foam on the DMG content is shown in Table 1, which indicates that with increasing DMG-loading, the absorption capacity levels off at about 3% DMG. Thus 3% DMG was chosen as the best loading. The lack of further absorption with the higher amount of DMG may be due to the amount of reagent leached out at this higher initial DMG concentration.

The decrease in the efficiency of nickel absorption with increasing dilution of the nickel solution is shown in Table 2. At the lowest concentrations tested (0.4—0.5 ppm) the foam loaded only with benzildioxime was most efficient (77%).

A comparison of the capability of the various foams to withstand repeated cycles of nickel absorption from ammoniacal media and acid elution (Table 3) showed that polyurethane loaded only with DMG lost all its reagent content after one cycle. Best results were obtained with TBP-plasticized foam loaded with benzildioxime (BDO), which gave stable nickel absorption through 5 cycles. This resistance of benzildioxime to leaching is probably due to its low solubility in aqueous solutions.

The effect of foreign ions on the absorption capacity for 2.3×10^{-4} M nickel was tested. Copper, cadmium and iron(II) ($2.1—4.8 \times 10^{-4}$ M) gave 100% nickel recoveries with both TBP foams. Cobalt (2.3×10^{-4} M) did not affect the DMG—TBP foam, but reduced nickel recovery to 94% with the benzildioxime—TBP foam. The latter recovery was decreased to 64% by 4.5×10^{-4} M cobalt. A mixture of copper (2.1×10^{-4} M), cobalt (2.3×10^{-4} M), iron(II) (2.4×10^{-4} M) and cadmium (1.2×10^{-4} M) allowed a 98%

TABLE 1

Effect of DMG content of DMG—TBP-loaded foam on the nickel absorption capacity[a]

DMG in foam (%)	Nickel absorbed (mg g^{-1}) foam		
	Calc.[b]	Obs.	Ratio
0.5	0.9	0.9	1.0
1.0	1.8	1.6	0.9
2.0	3.5	3.1	0.9
3.0	5.5	5.0	0.9
4.0	7.6	5.7	0.8

[a]100 mg of loaded foam taken, 70 ± 1.5% TBP. 67 ppm Ni^{2+}, pH 9.0 buffer, 60 min shaking. [b]On the basis of a 1:2 nickel—ligand chelate. [c]Average capacity of 3% DMG—TBP foam, 5.3 ± 0.1 mg Ni g^{-1}.

TABLE 2

Effect of nickel concentration on absorption

Volume (ml)	Initial Ni(II) conc. (ppm)	Absorption (%)	Volume (ml)	Initial Ni(II) conc. (ppm)	Absorption (%)
DMG—TBP foam (110 mg)[a]*			*Benzildioxime foam (60 mg)*[b]*		
15	33.3	98.9 + 0.5	10	12.0	97.7 + 0.5
100	5.0	96.0 + 0.6	20	6.0	92.3 + 0.3
250	2.0	60.0 + 0.2	50	2.4	87.0 + 0.5
500	1.0	40.0 + 0.5	100	1.2	77.0 + 0.5
			100[a]	0.5	77.1 + 0.7
Benzildioxime—TBP foam (150 mg)[c]*					
20	10.0	99.5 + 0.5			
100	2.0	91.5 + 0.4			
250	0.8	66.0 + 0.5			
500	0.4	42.0 + 0.6			

*Nickel added (μg): a, 50; b, 120; c, 200.

TABLE 3

Recycling of the loaded foams

Cycle	Nickel absorbed (mg g^{-1} foam)			
	DMG	DMG—TBP	BDO	BDO—TBP
1	15.4	4.8	3.5	1.3
2	0.0	3.3	2.3	1.3
3	0.0	2.8	1.5	1.3
4	0.0	1.7	0.8	1.3
5	0.0	1.1	0.0	1.3
6	0.0	0.5	0.0	0.0

nickel recovery with the DMG—TBP foam. Citrate (5.7×10^{-4} M) allowed a 99% recovery from the DMG—TBP foam and 96% from the benzildioxime—TBP foam. The corresponding results for tartrate (5.2×10^{-4} M) were 99% and 98.5%, for EDTA (1.5×10^{-4} M) were 94% and 51%, and for potassium cyanide (1.5×10^{-4} M) were 86% and 56%. Thus the nickel absorption capacity of the DMG—TBP-loaded foam was excellent in the presence of most of these ions. The only real interference was by cyanide ion. Obviously, metal ions which do not form precipitates with DMG or benzildioxime will not be absorbed by the treated foam. After the absorption process, very small nickel/foreign ion ratios were obtained in the effluent solutions; the nickel concentrations were close to the limit of detection.

A comparison of the various foams for nickel absorption is given in Table 4.

TABLE 4

Summary of the properties of the loaded foams investigated

	DMG	DMG—TBP	BDO	BDO—TBP
Capacity of foam (mg Ni g^{-1} foam)	15.4	5.3 ± 0.1	3.4	1.9 ± 0.05
Optimum pH range	8—10	8—10	8—11	9—10
Recommended shaking time (min)	60	30	240	60
50% absorption (min)[a]	3	0.3	30	3
90% absorption (min)[a]	13	1	110	33
Chelate agent loading capacity (mmol g^{-1} foam)	0.68	0.18 (3% DMG)	0.12	0.065 (1.5% BDO)
Solvent for oxime (recommended)	Acetone	TBP	DMSO	TBP
Elution	1.2 M HCl	1 M HCl	3—5 M HCl	1 M HCl
Recycle	No	somewhat	somewhat	yes

[a]Time required to achieve 50% or 90% absorption.

Several applications to the removal of nickel from industrial waste waters were devised. A column packed with DMG—TBP polyurethane foam was brought to pH 8—9. Waste-water from a nickel plating plant (100 ml, 7 ppm nickel, pH 8.5) was passed through the column at 5 ml min^{-1}. The effluent contained less than 0.05 ppm nickel, and thus the retention was better than 99%. When a column of benzildioxime—TBP was used for passing through waste-water from a nickel—cadmium battery plant (diluted 1000 times to 15 ppm nickel, 100 ml, pH 9), the effluent contained 0.3 ppm nickel. The low volume capacity of the dioxime-loaded polyurethane foams relative to liquid extraction methods seems to restrict their practical applications in hydrometallurgical recovery of nickel. On the other hand, the capacity to strip nickel to very low concentrations may be applicable to the treatment of nickel-polluted industrial effluents [6].

The authors thank Ms. V. Katzir and Mr. Y. H. Kim for help in some of the experiments, and Ziklag Chemicals, Haifa, Israel, for the donation of the polyurethane foam.

REFERENCES

1 H. J. M. Bowen, J. Chem. Soc., (1970) 1082.
2 T. Braun and A. B. Farag, Talanta, 22 (1975) 699.
3 T. Braun and A. B. Farag, Anal. Chim. Acta, 99 (1978) 1.
4 D.-W. Lee and M. Halmann, Anal. Chem., 48 (1976) 2214.
5 R. C. Ferguson and C. V. Banks, Anal. Chem., 23 (1951) 448.
6 M. M. Halmann and D.-W. Lee, U. S. Patent, Ser. No. 845, 236; Oct. 25, 1977.

Analytica Chimica Acta, 113 (1980) 389—392

Short Communication

SPECTROPHOTOMETRIC DETERMINATION OF MOLYBDENUM WITH THIOCYANATE AND NITRON

THOMAS J. KORALEWSKI** and GORDON A. PARKER*

Department of Chemistry, University of Toledo, Toledo, Ohio 43606 (U.S.A.)

(Received 2nd August 1979)

Summary. The ternary complex molybdenum(V)—thiocyanate—nitron exhibits an apparent molar absorptivity of 15,200 l mol^{-1} cm^{-1} when extracted by chloroform from aqueous 3 M hydrochloric acid solutions. Beer's law is followed for solutions containing 1.2—12 μg Mo ml^{-1}. The effects of diverse ions and application to determination of molybdenum in steels are described.

Molybdenum(VI) is frequently determined spectrophotometrically with the aid of thiocyanate ion in the presence of a reducing agent forming a molybdenum(V)—thiocyanate complex [1, 2]. Various auxiliary ligands allow extraction of this complex into chloroform or other immiscible solvents. Numerous ternary complexes containing molybdenum, thiocyanate ion and different auxiliary ligands have been proposed for colorimetric determinations of molybdenum [3—6] and applied to the determination of molybdenum steels [7—12].

Nitron (3,5,6-triphenyl-2,3,5,6-tetraazabicyclo[2.1.1]hex-1-ene) is known to form mixed thiocyanate complexes with several metals, including molybdenum, and absorption spectra for many of these have been reported [13]. This communication describes optimum experimental conditions for formation of the ion pair of nitron with the anionic molybdenum—thiocyanate complex and its application to determination of molybdenum in various steels.

Experimental

Apparatus and reagents. All absorbances were measured with a Cary Model 14 spectrophotometer with 1.00-cm cells. A standard molybdenum solution (100 μg Mo ml^{-1}) was prepared by dissolving reagent-grade sodium molybdate, $Na_2MoO_4 \cdot 2H_2O$, in distilled deionized water.

Nitron was purified and converted to its sulfate salt [13] by dissolving 10 g of nitron in 100 ml of 0.5 M sulfuric acid. After cooling, the solution was extracted with successive 20-ml portions of diethyl ether until the ether layer was colorless. The sample was then boiled to remove excess of ether,

**Present address: Libbey-Owens-Ford Technical Center, Toledo, Ohio 43605, U.S.A.

25 ml of 3 M sulfuric acid was added, and the solution was cooled until crystallization occurred. The crystals were filtered through a sintered glass crucible, washed once with 25 ml of 0.5 M sulfuric acid, twice with ice water, and three times with ether. The dried crystals were then recrystallized from 200 ml of 0.05 M sulfuric acid, filtered and dried at 50°C. A 0.5 $g\,l^{-1}$ solution was then prepared.

All other chemicals were of reagent-grade quality.

Recommended procedure. Transfer a sample aliquot, less than 10 ml, containing up to 0.3 mg of molybdenum to a separatory funnel. Add sufficient 12 M hydrochloric acid, less than 10 ml, to make the final concentration 3—4 M. Add, in order, 1 ml of 10% (w/v) iron(II) sulfate, 10 ml of 10% (w/v) ascorbic acid (see Discussion), 2 ml of 10% (w/v) potassium thiocyanate, and 10 ml of nitron sulfate solution. Add 10 ml of chloroform and shake vigorously for 1 min. Transfer the organic layer to a 25-ml volumetric flask. Repeat the extraction with 5 ml of chloroform. Combine the extracts and dilute to exactly 25 ml with chloroform. Measure the absorbance of this solution 20—40 min after dilution at 465 nm against a reagent blank prepared in the same manner but containing no molybdenum.

Results and discussion

The absorbance spectrum of the molybdenum—thiocyanate—nitron complex shows a fairly broad peak with its maximum at 465 nm; the molar absorptivity at this wavelength is 15,200 l mol^{-1} cm^{-1}. Beer's law is obeyed in the range 1.2—12 μg Mo ml^{-1}. Optimum concentration for molybdenum, as determined by Ringbom's method [14], is 3.6—9.6 μg Mo ml^{-1}. Repetitive measurement, at 465 nm, of fifteen samples each containing 5.6 μg Mo ml^{-1}, resulted in a mean absorbance reading and standard deviation of 0.890 ± 0.005.

Optimum conditions for extraction and measurement. Ideal conditions for color development of the molybdenum—thiocyanate complex include a strong acid solution. Optimum color occurs when the aqueous phase is 2.5—6.0 M in acid, either hydrochloric or sulfuric. The presence of iron(II) is necessary to insure full color development; iron(II) is said to catalyze formation of the molybdenum(V)—thiocyanate complex [15]. Here 1 ml of 10% (w/v) iron(II) sulfate is incorporated.

The thiocyanate concentration chosen assures an approximately 500-fold excess of thiocyanate ion to molybdenum. Increasing nitron concentration, after the minimum excess necessary for color development, results in slowly increasing absorbance values for a fixed amount of molybdenum. The presence of excessive amounts of nitron is undesirable because of possible precipitate formation. The amount recommended is a reasonable compromise.

Absorbance readings for this complex reach a stable value about 20 min after extraction and remain stable until at least 1 h after extraction. Samples, after extraction, maintained at 30°C for 20 min showed a decrease in absorbance of about 1% compared with those maintained at ambient temperature. Heating at 40°C caused a decrease of about 6%.

Two extractions with chloroform suffice for quantitative removal of the molybdenum-containing complex. No red-orange color from the complex was observed in the aqueous phase during 2 h after two extractions with chloroform.

Colorimetric procedures for molybdenum with thiocyanate, and perhaps an auxiliary ligand, frequently employ an additional reducing agent to facilitate reduction of molybdenum(VI) to molybdenum(V) [16, 17]. Usually tin(II) or ascorbic acid is used although some modifications omit the reducing agent entirely [18]. It was found here that an additional reducing agent is unnecessary unless a large excess of iron(III) is present, e.g., Fe:Mo $\geqslant$ 100:1. When molybdenum in steel is to be determined, the presence of ascorbic acid is necessary, otherwise it can usually be omitted.

Interferences. Various diverse ions were added separately to a solution containing 5.6 μg Mo ml^{-1} and the proposed determination performed. Interference was considered to occur if the absorbance observed differed from the expected value (0.890) by more than 0.015 absorbance unit, i.e. three times the standard deviation at this level. Only manganese(VII), titanium(IV), and peroxide ion must be completely absent from solution. Tungsten is acceptable in a 2-fold amount relative to molybdenum. Chromium(VI), copper(II), iron(III), platinum(IV), uranium(VI), and vanadium(V) are acceptable up to a 20-fold amount. A 200-fold amount of each of the following ions caused no interference: ammonium, aluminum, barium, bismuthyl, cadmium, calcium, cobalt, iron(II), lead, lithium, magnesium, mercury(II), nickel, potassium, sodium, strontium, thallium(III), zinc, zirconyl, acetate, bromide, cyanide, EDTA, fluoride, iodide, nitrate, oxalate, phosphate, sulfate, and tartrate.

Composition of the complex. Both Job's method of continuous variations [19] and the slope ratio method [20] were applied to determine the composition of the complex. In the presence of a constant amount of thiocyanate ion, variations between molybdenum and nitron concentrations led to a Mo:nitron ratio of 2:3 by both methods. In the presence of a fixed nitron concentration, however, variations between molybdenum and thiocyanate ion concentration produced inconsistent results from those expected partly because of precipitation of nitron molybdate. It appears that the Mo:SCN ratio is 1:5. Thus the postulated composition for the ternary Mo—SCN—nitron complex is 2:10:3, which is in agreement with other reports that the molybdenum(V) ion is dimeric [21]. Various other ratios for the ratio Mo:SCN:auxiliary ligand have been reported [3, 5—7, 10, 12] and there is no agreement regarding ratios for complexes of this type.

Analysis of standard steel samples. National Bureau of Standards steel samples were analyzed by the proposed colorimetric procedure. Results are shown in Table 1. It appears that steels with higher percentages of molybdenum give the best results when this method is used. Titanium was absent from the steels used, and according to the standard dissolution processes, neither manganese(VII) nor hydrogen peroxide would be present.

TABLE 1

Standard steel analyses

NBS Number	Type	Molybdenum (%)	
		Certified value	This work[a]
153	Co-Mo (Tool steel)	8.38	8.38 (8.00—8.90)
111B	Ni-Mo (SAE 4620)	0.255	0.279 (0.220—0.310)
139	Cr-Ni-Mo (AISI 8640)	0.178	0.191 (0.150—0.230)

[a]Mean of three determinations; range in parentheses.

REFERENCES

1 E. B. Sandell, Colorimetric Determination of Trace Metals, Interscience, New York, 1959, p. 648.
2 Z. Marczenko, Spectrophotometric Determination of Elements, Halsted Press, New York, 1976, p. 358.
3 L. I. Ganago and I. F. Ivanova, Zh. Anal. Khim., 27 (1972) 713.
4 R. Neeb, Fresenius Z. Anal. Chem., 182 (1961) 10.
5 V. Pandre Ranga Rao, Y. Anjaneyulu and A. S. R. Krishna Murty, Mikrochim. Acta, (1975) 265.
6 H. Puzanowska-Tarasiewicz, A. Grudniewska and M. Tarasiewicz, Anal. Chim. Acta, 94 (1977) 435.
7 M. K. Arunachalam and M. K. Kumaran, Talanta, 21 (1974) 355.
8 A. S. Babenko, L. A. Mineeva and K. I. Godovskaya, Zavod. Lab., 42 (1976) 1035.
9 A. V. Dolgorev and I. D. Gushchina, Zavod. Lab., 40 (1974) 26.
10 A. T. Pilipenko and Z. G. Solomeina, Ukr. Khim. Zh., 39 (1973) 1169.
11 C. P. Savariar, M. K. Arunachalam and T. R. Hariharan, Anal. Chim. Acta, 69 (1974) 305.
12 A. M. Wilson and O. K. McFarland, Anal. Chem., 36 (1964) 2488.
13 A. S. Babenko and V. M. Tolmachev, Ukr. Khim. Zh., 27 (1961) 732.
14 A. Ringbom, Fresenius Z. Anal. Chem., 115 (1939) 332.
15 A. T. Dick and J. B. Bingley, Nature, 158 (1946) 516.
16 A. I. Busev, Analytical Chemistry of Molybdenum, Ann Arbor-Humphrey Science Publishers, Ann Arbor, 1969, p. 181.
17 A. G. Fogg, J. L. Kumar and D. T. Burns, Analyst, 100 (1975) 311.
18 M. Mitra and E. K. Mitra, Talanta, 24 (1977) 698.
19 P. Job, Ann. Chim., 9 (1928) 113.
20 A. E. Harvey and D. L. Manning, J. Am. Chem. Soc., 72 (1950) 4488.
21 P. C. H. Mitchell and R. J. P. Williams, J. Chem. Soc., (1962) 4570.

Analytica Chimica Acta, 113 (1980) 393—394

Short Communication

ADSORPTION AND CONTINUOUS EXTRACTION OF RESIN WITHOUT DRYING IN A MODIFIED SOXHLET APPARATUS

BJØRN OLUFSEN

Central Institute for Industrial Research, Blindern, Oslo 3 (Norway)

(Received 16th July 1979)

Summary. The design allows adsorption of trace organic materials from waters and their extraction with small solvent volumes without drying-out of the resin used.

Analyses for trace organic constituents in aqueous samples often include adsorption on a resin such as Amberlite XAD-2 or Tenax [1, 2], the adsorbed organics being later suitably eluted. During both adsorption and elution, care must be taken to prevent air from entering the column, to avoid air pockets which would cause irreproducible results. One of the main drawbacks with most of the existing systems is that the elution often requires relatively large solvent volumes. The apparatus described here for continuous extraction of the resin obviates this problem. To reduce the possibilities of sample contamination, the apparatus has been designed so that it can be used throughout the sampling procedure and subsequent extraction. The resin can be cleaned prior to use, and regenerated, in the same apparatus.

Originally made for the adsorption of polynuclear aromatic hydrocarbons (PAH) in drinking water, the apparatus shown in Fig. 1 has been used with XAD-2 resins. The polymer suspended in methanol is added to the column. The glass wool is cleaned and evaporated ("degassed") under solvent before use. Prior to adsorption the methanol in the column is replaced by water; internal standards may be added on top of the resin, and the space above the resin is filled with water. Stopcocks a and b in Fig. 1 are closed during adsorption. Sampling may be done on location (Fig. 2, left) or in the laboratory (Fig. 2, centre). In the latter case either nitrogen pressure applied at point d or a peristaltic pump sucking at point e may be used to achieve a flow of water through the column. Stopcock c in Fig. 2 is open. The only critical point is during laboratory sampling where the flow has to be stopped before gas enters the resin. The sample water in the 5- or 20-l flask is degassed except when low boiling compounds are of interest (but then the stripping technique described by Grob [3] is usually preferred).

During extraction (Fig. 2, right) both stopcocks a and b are open. The inner tube in b (Fig. 1) prevents the liquid level from dropping below the

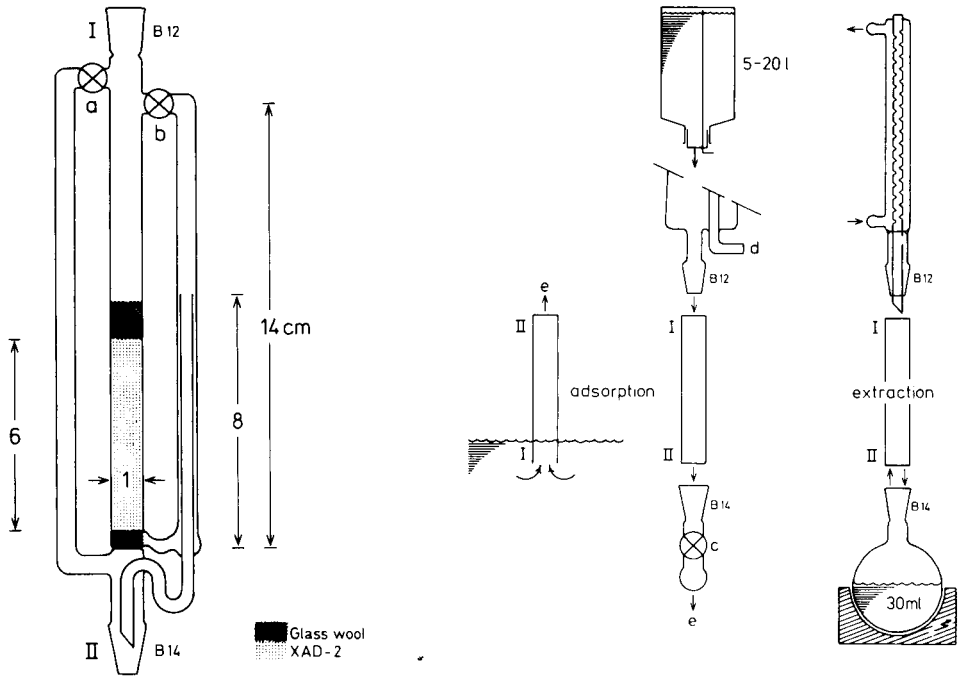

Fig. 1. Modified Soxhlet apparatus used as an adsorption column for organic compounds in water allowing continuous extraction of resin without entry of air.

Fig. 2. Set-up for the adsorption of organic compounds in water (on location, left, and in the laboratory, centre) and continuous extraction (right). The adsorption column described in Fig. 2 is shown schematically with Roman numbers referring to Fig. 1. Further lettering is described in the text.

upper glass wool plug. Thus, no air is sucked into the resin which would have happened during a normal Soxhlet extraction. As water still remains in the column, a water-miscible solvent must be applied for the extraction. For PAH, methanol is suitable as it is a good solvent for those tar compounds which are easily extracted into a less polar solvent such as cyclohexane after the addition of more water to the methanol.

The author thanks V. Sletner for the glass work and G. Carlberg for reading the manuscript.

REFERENCES

1 G. A. Junk, J. J. Richard, M. D. Grieser, D. Witiak, J. L. Witiak, M. D. Arguello, R. Vick, H. J. Svec, J. S. Fritz and G. V. Calder, J. Chromatogr., 99 (1974) 745.
2 V. Leoni, G. Puccetti and A. Grella, J. Chromatogr., 106 (1975) 119.
3 K. Grob, J. Chromatogr., 84 (1973) 255.

Analytica Chimica Acta, 113 (1980) 395—397

Short Communication

ORGANIC-FREE WATER FOR TOTAL ORGANIC CARBON DETERMINATION[‡]

GARY N. PETERSON and JOHN R. MONTGOMERY*

Harbor Branch Foundation Inc., RR 1, Box 196, Fort Pierce, FL 33450 (U.S.A.)

(Received 7th August 1979)

Summary. Commercially available "organic-free" water is compared with water cleaned by ultraviolet (u.v.) radiation for applicability to total organic carbon determinations. The u.v.-treated water contains an organic carbon concentration less than the detection limit of the method used (0.056 mg C l^{-1}). The commercially processed water lacks the consistently low blank level required for use in TOC determinations.

One of the major difficulties in the determination of total organic carbon (TOC) is the removal of organic carbon from the reagents and water used in the analysis. Various techniques to lower the organic carbon concentration in water have been examined to optimize the TOC analysis. Distillation is too slow and expensive for production of the required amounts of "clean" water. Activated charcoal lacks the efficiency required for optimum results. Photo-oxidation with intense ultraviolet (u.v.) light has been found to be an excellent cleaning technique [1]. After an irradiation period of 2 h, the organic carbon in the water is substantially oxidized to carbon dioxide, which can be removed by bubbling with an inert gas. This cleaning technique is capable of producing large volumes of water with undetectable levels of organic carbon. Unfortunately, the method is both time-consuming and expensive.

Recently, the J. T. Baker Chemical Co. has developed water ("Baker Analyzed" reagent) for use in high-performance liquid chromatography (h.p.l.c.) which is advertised as "free from organic impurities". The applicability of this ultrapure water to TOC work is discussed in the present communication. TOC determinations were done on representative samples from two different lots of the "Baker Analyzed" water. The results were compared to organic carbon levels found in water cleaned by ultraviolet oxidation.

Experimental

Equipment. An Oceanography International Total Carbon System was used; the instrument consists of a sealing unit for sample vial preparation, a digestion bomb, and an infrared analyzer. The u.v. source used for the photo-oxidation process was a Hanovia high-intensity (450 W) u.v. lamp. Quartz sample tubes were used.

[‡]Harbor Branch Foundation, Inc. Contribution No. 151.

Reagents. The oxidizing solution contained potassium persulfate (50 g l^{-1}), which oxidizes organic carbon to carbon dioxide on heating. A 6% phosphoric acid solution was used to remove inorganic carbonates.

The various waters studied were as follows: ordinary laboratory deionized water treated by reverse osmosis, henceforth referred to as R.O. water; R.O. water exposed to u.v. radiation; "Baker Analyzed" h.p.l.c. water, lots 8208J and 838101; and lot 838101 exposed to u.v. radiation.

Procedure. Samples were prepared with each of the five sources of water; 1.0 ml of oxidizing solution and 0.25 ml of 6% phosphoric acid were added to 10.0 ml of the water to be tested. The blank for TOC determinations can be divided into the reagent blank and the blank arising from organic carbon in the diluent water. The amount of organic carbon in the reagents alone was estimated by preparing reagent blanks with 2, 4, 6, 8, and 10 ml of u.v. cleaned R.O. water. After extrapolation to 0.0 ml of water, the concentration of organic carbon in the reagents was determined by comparing the remaining signal to the standard curve. The samples and blanks were purged with CO_2-free oxygen and sealed in vials. After oxidation at 175°C for 16 h, the resulting carbon dioxide was measured by using a non-dispersive infrared analyzer. The procedure is based on a technique described by Menzel and Vaccaro [2].

Results and discussion

The concentrations of organic carbon, expressed as mg C l^{-1}, found in the various sources of water are summarized in Table 1. The approximate concentration of the reagent blank (oxidant and phosphoric acid) was lower than the detection limit of the procedure but was estimated to be 0.026 mg C l^{-1}. The detection limit of the technique, defined as twice the standard deviation of five reagent blanks prepared with the standard curve, was 0.056 mg C l^{-1} [3]. The merit of u.v. irradiation as a cleaning technique is clearly evident.

Several bottles of "Baker Analyzed" h.p.l.c. water lot 8208J exhibited an undetectable level of organic carbon with no treatment necessary. In contrast, lot 838101 contained a high concentration of organic carbon, 0.380 mg C l^{-1}. The actual lot analysis showed this water to contain 23.3 times more particulate matter and 2.8 times more residue after evaporation than lot 8208J, although the chromatogram provided with the lot showed no significant absorbance at 254 nm.

Thus, although the h.p.l.c. water is free of the organic materials which typically interfere with h.p.l.c. work, the product is not consistently well suited for TOC determinations. The cleaning technique used is efficient for removing organic material which absorbs at 254 nm, but the non-dispersive infrared analyzer applied for detection of CO_2 is sensitive to a broad range of the infrared spectrum. Apparently, lot 838101 contained organic materials not present in lot 8208J, which were probably associated with the high levels of particulate matter. This organic material, when oxidized to carbon dioxide, produces unacceptably high i.r. absorbance. The organic carbon in lot 838101 was susceptible to oxidation by u.v. light; after irradiation, the organic carbon level was also below the level of detection.

TABLE 1

Organic carbon (mg C l^{-1}) determined in five sources of water

Water	mg C l^{-1}
R.O. water	0.260
R.O. water after u.v. treatment	<0.056
H.p.l.c. water, lot 8208J	<0.056
H.p.l.c. water, lot 838101	0.380
H.p.l.c. water, lot 838101 after u.v. treatment	<0.056

The "Baker Analyzed" water is well suited for its intended h.p.l.c. use, but without further treatment is not necessarily applicable for use in TOC determination.

REFERENCES

1 A. J. Armstrong, P. M. Williams and J. D. H. Strickland, Nature, 211 (1966) 481.
2 D. W. Menzel and R. F. Vaccaro, Limnol. Oceanogr., 9 (1964) 138.
3 R. K. Skogerboe, Accuracy and Precision, in J. A. Dean and T. C. Rains (Eds.), Flame Emission and Atomic Absorption Spectrometry, Vol. 1, M. Dekker, New York, 1969, p. 407.

ANALYTICA CHIMICA ACTA, Vol. 113 (1980)

AUTHOR INDEX

ACA announcements

CHEMVIRON AWARD 1980

Chemviron, Europe's leading manufacturer of granular activated carbons, has created the Chemviron Award for outstanding contributions to the study of water treatment as it relates to environmental health. The prize — a cash award of $10.000 plus a commemorative medal and certificate — is awarded every second year.

The Chemviron Award is given in recognition of outstanding work in the area of physical-chemical treatment of potable and waste water (not restricted to adsorption). However, it does not exclude any association with biological treatment schemes. Candidature is open to virtually anyone from universities, municipal authorities or industry. Candidates may be individuals or groups. Applications are, however, limited to papers originating in Europe.

Major criteria of evaluation will include the scientific value of the work, its originality, and especially its practical application and potential for industrial use. A significant contribution of original experimental work and its interpretation will be expected. Papers will be evaluated by the Chemviron Award Committee, a distinguished body representing many European countries. The Award Committee will evaluate and judge the papers entirely independently of the Chemviron organisation; all submitted applications will be kept in strict confidence.

Papers should be received by the Committee before March 1, 1980. They will only be accepted in a format which could allow immediate publication; e.g. they should consist of 10 to 15 typewritten pages plus supporting documentation. Detailed abstracts about 400 words of the submitted work should be supplied in all of the three more common European languages — English, French and German. The paper itself may be submitted in any one of these three languages, whilst supporting documentation should be added as a technical appendix in their original languages. Each paper should be accompanied by a complete list of all literature references, a short description of the state-of-the-art in the field related to the subject of the submitted paper and a brief curriculum vitae of the author(s).

All submissions and correspondence regarding applications for the Chemviron Award should be directed to the Secretary of the Chemviron Award 1980 Committee: Professor J. Bourne, c/o Chemviron, Chaussée de Waterloo 1135, B-1180 Brussels, Belgium. Tel.: (02) 375.24.20, ext. 212.

10th ANNUAL SYMPOSIUM ON THE ANALYTICAL CHEMISTRY OF POLLUTANTS

The 10th Annual Symposium on the Analytical Chemistry of Pollutants, organized jointly by the International Association of Environmental Analytical Chemistry and by the Gesellschaft Deutscher Chemiker, Fachgruppe Analytische Chemie, will be held in Dortmund (Federal Republic of Germany), from May 28—30, 1980.

The scientific programme will contain: Invited plenary lectures, invited and submitted research lectures and poster-presentations covering the whole field of environmental analytical chemistry. One day is dedicated to the following interdisciplinary topics: Analytical Chemistry and Air Chemistry, and Analytical Chemistry and Mutagenicity.

Plenary lectures will be given by:

- Dr. K. Cantor, Cancer Epidemiology as Related to Chemicals in Drinking Water.
- Dr. B. Commoner, Mutagenicity; some Test Results.
- Prof. Dr. D.H. Enhalt, Measurement of Stratospheric Trace Constituents.
- Dr. S.A. Penkett, The Application of Analytical Techniques to the Understanding of Chemical Processes Occurring in the Atmosphere.
- Prof. Dr. F.K. Zimmermann, Biological Analytical Tests for the Detection of Mutagenic Chemicals.
- Prof. Dr. Yu.A. Zolotov, Preconcentration of Trace Metals from Water.

Information can be obtained from: Dr. J. Wendenburg, Gesellschaft Deutscher Chemiker, P.O. Box 90 04 40, D-6000 Frankfurt am Main 90, FRG. Phone: (0611) 7917366 Telex: 412526 gmeli d.f. gdch.

SAC 80

The Fifth International Conference on ANALYTICAL CHEMISTRY, SAC 80, will be held from July 20—26, 1980 at the Lancaster University, England.

SAC 80 is the 6th triennial International Conference organised by the Analytical Division of the Chemical Society and will be held at the University of Lancaster from July 20th to 26th, 1980. The Conference is sponsored by the International Union of Pure and Applied Chemistry (IUPAC).

The scientific programme will follow the successful pattern of previous Conferences held at the Universities of Nottingham, Durham and Birmingham, and will include sessions of specialized interest, bringing the most recent developments in analytical chemistry to the attention of delegates. This will be coupled with a range of workshop sessions, an extensive trade exhibition, and specialist discussions, with, of course, the traditional programme of social events.

Information can be obtained from: The Secretary, Analytical Division, The Chemical Society, Burlington House, London W1V 0BN, England.

J. HEYROVSKY MEMORIAL CONGRESS ON POLAROGRAPHY

The J. Heyrovský memorial congress on polarography will be held in Prague, (Czechoslovakia) from August 25—29, 1980. The congress will be concerned with recent development of polarography and related techniques with emphasis on

- basic problems including thermodynamic and kinetic studies, solvent interactions, adsorption effects and electrocatalysis, photoelectrochemical phenomena, etc.
- instrumentation (especially recent techniques with high sensitivity both for theoretical and analytical applications and utilization of computers),
- analysis (trace analysis of organic and inorganic materials, stripping techniques, new electrochemical sensors, continuous analyzers, etc.)
- applications in industry, biology, pharmacology, medicine and environmental science.

The J. Heyrovský Memorial Congress on Polarography continues in the series of International Polarographic Congresses started in Prague in 1951. It is organized on the occasions of the 90th anniversary of the birth of Professor Jaroslav Heyrovský, Nobel Prize Laureate in Chemistry 1959 and of 30 years since the foundation of the former Polarographic Institute. The classical form of plenary and section lectures will be maintained. To give equal chance to the largest possible number of the participants for presentation and mutual communication the poster sessions have been chosen as the main form of presenting new results and data. The most immediate problems will be discussed in several microsymposia and panel discussions organized by invited conveners and in special sessions.

Further information can be obtained from: Secretariat of the J. Heyrovský Memorial Congress on Polarography, J. Heyrovský Institute of Physical Chemistry and Electrochemistry, Czechoslovak Academy of Sciences, Vlašská 9, CS 118 40 Praha 1, Czechoslovakia.

CALENDAR OF FORTHCOMING MEETINGS

Feb. 6, 1980 London, Great Britain	**Chemical Society/Analytical Division – Recent Advances in Organic Mass Spectrometry in Analytical Chemistry** Contact: The Secretary, Analytical Division, The Chemical Society, Burlington House, London W1V 0BN, Great Britain.
Feb. 13, 1980 London, Great Britain	**Chemical Society/Analytical Division – Sophistication in Instrumentation – has it gone too far?** Contact: Miss P.E. Hutchinson, Southside Senior Common Room, Imperial College of Science and Technology, Princes Gardens, London W.S. 7, Great Britain.
March 10—14, 1980 Atlantic City, N.J., U.S.A.	**(31st Annual) Pittsburgh Conference on Analytical Chemistry and Applied Spectroscopy** Contact: Mrs. Linda Briggs, Program Secretary, 437 Donald Road, Pittsburgh, Pa. 15235, U.S.A.

March 23–28, 1980 Houston, Texas, U.S.A.	**ACS 179th National Meeting** Contact: A.T. Winstead, 1155 16th Street, N.W., Washington, D.C. 20036, U.S.A.
March 24–28, 1980 York, Great Britain	**International Conference on ESR of Organic and Bio-organic Radicals** Contact: Dr. J.B. Raynor, Chemistry Department, The University, Leicester LE1 7RH, Great Britain.
April 1–2, 1980 Canterbury, Great Britain	**Chemical Society/Analytical Division – Research and Development Topics in Analytical Chemistry** Contact: The Secretary, Analytical Division, The Chemical Society, Burlington House, London W1V 0BN, Great Britain.
April 9–11, 1980 Durham, Great Britain	**Chemical Society/Analytical Division – CS/RIC Annual Congress; Modern Techniques for Surface Characterization** Contact: The Secretary, Analytical Division, The Chemical Society, Burlington House, London W1V 0BN, Great Britain.
April 23–25, 1980 King of Prissia, Pa., U.S.A.	**ACS – 14th Middle Atlantic Regional Meeting** Contact: Henry C. Beck, P.O. Box 133, Swarthmore, Pa. 19081, U.S.A. Tel. (215) 387-2255.
April 27–29, 1980 Neuherberg/Munich, F.R.G.	**First International Workshop on Trace Element Analytical Chemistry in Medicine and Biology** Contact: Dr. P. Schramel, Gesellschaft für Strahlen- und Umweltforschung, Physikalisch-Technische Abteilung, Ingolstädter Landstrasse 1, D-8042 Neuherberg, F.R.G.
April 29–May 2, 1980 Munich, F.R.G.	**Biochemische Analytik 80** (7th European Conference on Biochemical and Instrumental Analysis) Contact: Dr. Rosmarie Vogel, Nussbaumstr. 20, P.O. Box 200324, D-8000 Munich 2, F.R.G. Tel. (089) 15 14 19.
May 5–8, 1980 Brussels, Belgium	**XXXVIIIth Annual Colloquium on Protides of the Biological Fluids** Contact: Colloquium "Protides of the Biological Fluids", Secretariat, c/o Lipid and Protein Department, Institute for Medical Biology, Alsembergsesteenweg 196, B-1180 Brussels, Belgium. Tel. 02-3441950.
May 25–30, 1980 New York, N.Y., U.S.A.	**28th Annual Conference of the Amer. Soc. for Mass Spectrometry** Contact: Dr. H.M. Fales, c/o NIH Building 10, Room 7N 322, Bethesda, Md. 20014, U.S.A.
May 27–30, 1980 Balaton Lake, Hungary	**4th Symposium on Ion Exchange** Contact: Professor J. Inczédy, Organizing Committee, 4th Int. Symposium on Ion Exch., P.O. Box 28, Veszprém, H-8201 Hungary.
May 28–30, 1980 Dortmund, F.R.G.	**10th Annual Symposium on the Analytical Chemistry of Pollutants** Contact: J. Wendenburg, Gesellschaft Deutscher Chemiker, P.O. Box 900440, D-6000 Frankfurt/Main, F.R.G. Tel. (0611) 791 73 66.

June 8–11, 1980 Ottawa, Ontario, Canada	**63rd Canadian Chemical Conference and Exhibition** Contact: Don Emmerson, 151 Slater St., Suite 906, Ottawa, Ontario, Canada K1P 5H3, Tel. 613-233-5623.
June 10–13, 1980 Ghent, Belgium	**3rd International Symposium on Quantitative Mass Spectrometry in Life Science** Contact: Professor A.P. de Leenheer, Laboratoria voor Medische Biochemie en Klinische Analyse, de Pintelaan 135, B-9000 Ghent, Belgium.
June 16–18, 1980 Milan, Italy	**7th International Symposium on Mass Spectrometry in Biochemistry, Medicine and Environmental Research** Contact: Dr. A. Frigerio, Istituto di Ricerche Farmacologiche "Mario Negri", Via Eritrea 62, 20157 Milan, Italy.
June 18–19, 1980 London, Great Britain	**Nuclear Magnetic Resonance Spectroscopy in Solids** Contact: The Executive Secretary, The Royal Society, 6 Carlton House Terrace, London SW1Y 5AG, Great Britain.
June 30–July 4, 1980 Cannes, France	**13th International Symposium on Chromatography** Contact: GAMS, 88 Boulevard Malesherbes, 75008 Paris, France.
July 7–11, 1980 Brussels, Belgium	**2nd International Congress on Toxicology** Contact: Secretariat, SdR Associated, 16 Avenue des Abeilles, B-1050 Brussels, Belgium.
July 20–26, 1980 Lancaster, Great Britain	**SAC 80** Contact: The Secretary, Analytical Division, The Chemical Society, Burlington House, London W1V 0BN, Great Britain. (Further details published in Vol. 106, No. 2).
Aug. 4–8, 1980 Denver, U.S.A.	**Conference on Applications of X-Ray Analysis.** Contact: Mrs. Mildred Cain, Denver Research Institute, University of Denver, Denver, Colorado 80208, U.S.A. Tel. 303/753-2141
Aug. 4–9, 1980 Ottawa, Canada	**7th International Conference on Raman Spectroscopy** Contact: Mr. Ken Charbonneau, Conference Services, National Research Council of Canada, Ottawa, Ontario, Canada K1A OR6.
Aug. 17–23, 1980 Wolfeboro, N.H., U.S.A.	**Gordon Research Conference on Vibrational Spectroscopy** Contact: Dr. Erich Ipsen, Bell Laboratories, Holmdel, N.J. 07733, U.S.A.
Aug. 24–28, 1980 Espoo, Finland	**Euroanalysis IV** (Conf. Fed. of European Chemical Societies) Contact: Prof. L. Niinistoe, University of Technology, Dept. of Chemistry, 62150 Espoo 15, Finland. (Further details published in Vol. 109, No. 1)
Aug. 24–29, 1980 San Francisco, U.S.A.	**ACS 180th National Conference/2nd Chemical Congress of the North Amer. Continent** Contact: A.T. Winstead, 1155 16th Street, N.W. Washington, D.C. 20036, U.S.A.

Aug. 24–31, 1980 Rzeszów, Poland	**2nd International Summer School on Data Processing in Chemistry DPC '80** Contact: Prof. Dr. Z. Hippe, Dept. of Physical Chemistry, Technical University, 35-959 Rzeszów, Poland
Aug. 25–29, 1980 Prague, Czechoslovakia	**J. Heyrovský Memorial Congress on Polarography** Contact: Czechoslovak Academy of Sciences, J. Heyrovský Institute of Physical Chemistry and Electrochemistry, Vlasská 9, CS118 40 Praha 1, Czechoslovakia.
Aug. 25–30, 1980 Delft, The Netherlands	**Joint ISMAR–Ampère International Conference on Magnetic Resonance** Contact: ISMAR-Ampère 1980, Postbus 30424, NL.2500 GK Den Haag, The Netherlands.
Aug. 25–30, 1980 Graz, Austria	**8th International Microchemical Symposium** Contact: Prof. Dr. A. Holasek, Institut für Medizinische Biochemie, Universität Graz, Harrachgasse 21, A-8010 Graz, Austria. (Further details published in Vol. 109, No. 1 and Vol. 110, No. 2).
Sep. 2–5, 1980 Prague, Czechoslovakia	**VII European Symposium on Connective Tissue Research** Contact: Dr. Z. Deyl, Physiological Institute Czechoslovak Academy of Sciences, 142 20 Budejovická 1083, Prague 4, Czechoslovakia.
Sep. 6–12, 1980 Liège, Belgium	**International Solvent Extraction Conference 1980 (ISEC '80)** Contact: Conference Secretariat ISEC '80, Department of Chemistry, University of Liège, Sart Tilman, B-4000 Liège, Belgium. (Further details published in Vol. 107).
Sep. 7–12, 1980 Florence, Italy	**IUPAC International Symposium on Macromolecules** (Structural Order in Polymers) Contact: Macro IUPAC 80, Fondazione Giovanni Lorenzini, Via Monte Napoleone 23, 20121 Milan, Italy.
Sep. 9–12, 1980 Eindhoven, The Netherlands	**2nd International Symposium on Isotachophoresis** Contact: ITP 80, Afd. Instrumentele Analyse, Technische Hogeschool, Eindhoven, Postbus 513, 5600 MB Eindhoven, The Netherlands.
Sep. 16–19, 1980 Bratislava, Czechoslovakia	**6th International Symposium on Advances and Application of Chromatography in Industry** Contact: Dr. Ján Remeň, Analytical Section ČS VTS, pri n.p. Slovnaft, 82300 Bratislava, Czechoslovakia.
Sep. 22–26, 1980 Cannes, France	**8th International Vacuum Congress – 4th International Conference on Solid Surfaces – 3rd European Conference on Surface Science** Contact: Société Française du Vide, 19 Rue Renard, F-75004 Paris, France.

Sep. 22–26, 1980 Paris, France	**European Conference on Chemical Pathways in the Environment** Contact: Dr. C. Troyanowsky, Société de Chimie physique, 10, rue Vauquelin, F-75005 Paris, France. Tel. 707-54-48.
Sep. 23–25, 1980 Cardiff, Great Britain	**Chemical Society/Analytical Division – CS Autumn meeting: Trace and Ultratrace Analysis** Contact: The Secretary, Analytical Division, The Chemical Society, Burlington House, London W1V 0BN, Great Britain.
Sep. 28–3 Oct. 1980 Philadelphia, Penn., U.S.A.	**7th Annual Meeting of Federation of Analytical Chemistry and Spectroscopy Societies (FACSS)** Contact: Mrs. J.G. Graselli, c/o Standard Oil Co., 4440 Warrensville Road, Cleveland, Ohio 44128, U.S.A.
Sep. 29–Oct. 3, 1980 York, Great Britain	**Modern Radiochemical Practice** Contact: The Secretary, Analytical Division, Chemical Society, Burlington House, London W1V 0BN, Great Britain.
Oct. 6–9, 1979 Houston, U.S.A.	**EXPOCHEM '80** Contact: Professor A. Zlatkis, Chemistry Department, University of Houston, Houston, Texas 77004, U.S.A. Tel. (713) 749 - 2623.
Oct. 19–23, 1980 Washington, D.C., U.S.A.	**Ann. Meeting of Assoc. of Official Analytical Chemists** Contact: K.M. Fominaya, Box 540, Benjamin Franklin Station, Washington, 20044 D.C., U.S.A.
Nov. 19–21, 1980 New York, N.Y., U.S.A.	**19th Eastern Analytical Symposium** Contact: Norman Gardner, Exposition Manager, 73 Ethel Street, Methuchen, N.J. 08840, U.S.A. Tel. (201) 548 7377.
Dec. 16–17, 1980 Brighton, Great Britain	**Chromatography, Equilibria and Kinetics** Contact: Mrs. Y.A. Fish, The Chemical Society, Burlington House, London W1V 0BN, Great Britain. Tel. 01-7349971.
Aug. 16–22, 1981 Vancouver, Canada	**28th Congress International Union of Pure and Applied Chemistry** Contact: Congress Secretariat, 28th IUPAC Congress, c/o The Chemical Institute of Canada, 151, Slater Street, Suite 906, Ottawa, Ontario – Canada K1P 5H3.
Aug. 23–28, 1981 University of Auckland, New Zealand	**Golden Jubilee Conference "Chemistry in the Service of Man"** Contact: Dr. D.J. McLennan, Chemistry Dept., Univ. of Auckland, Auckland, New Zealand.
Aug. 30–Sep. 5, 1981 Vienna, Austria	**XI International Congress of Clinical Chemistry – IV European Congress of Clinical Chemistry** Contact: Congress Secretariat, Interconvention, P.O. Box 35, A-1095 Vienna, Austria. Tel. (0222) 42 13 52.

Evaluation and Optimization of Laboratory Methods and Analytical Procedures

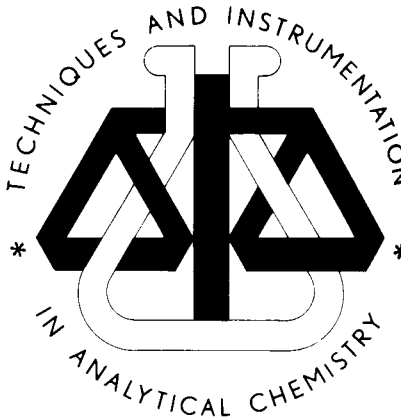

A Survey of Statistical and Mathematical Techniques

D.L. MASSART, A. DIJKSTRA *and* L. KAUFMAN.

with contributions by S. Wold, B. Vandeginste *and* Y. Michotte

Techniques and Instrumentation in Analytical Chemistry - Volume 1

This book provides detailed treatment, in a single volume, of formal methods fo optimization in analytical chemistry. It is a comprehensive and practical handbool which no analytical laboratory will want to be without.

All aspects of optimization are discussed, from the simple evaluation of procedure to the organization of laboratories or the selection of optimal complex analytica programmes. Quantitative discrete analysis as well as qualitative and continuou measurement techniques are evaluated.

The book consists of 30 chapters divided into 5 main parts.The main sections are Evaluation of the Performance of Analytical Procedures, Experimental Optimizatior Combinatorial Problems, Requirements for Analytical Procedures, and System Approach in Analytical Chemistry.

This work will be of practical value not only to those involved with optimizatio problems in analytical chemistry, but also to those in related fields such a clinical chemistry or specialized fields such as chromatography. Because i discusses the application of many mathematical techniques in analytical chemistry this book will also serve as a general introduction to the new field of Chemometrics

1978 1st Reprint 1979 xvi + 596 pages US $68.25 / Dfl. 140.0
ISBN 0-444-41743-5

ELSEVIER

P.O. Box 211,
1000 AE Amsterdam
The Netherlands

52 Vanderbilt Ave
New York, N.Y. 10017

The Dutch guilder price is definitive. US $ prices are subject to exchange rate fluctuations.

Recent Developments in Chromatography and Electrophoresis

Proceedings of the 9th International Symposium on Chromatography and Electrophoresis, Riva del Garda, 15-17 May, 1978

edited by **A. FRIGERIO** and **L. RENOZ**

ANALYTICAL CHEMISTRY SYMPOSIA SERIES, Volume 1

The symposium was organized by the Italian Group for Mass Spectrometry in Biochemistry and Medicine and the Belgian and Italian Societies for Pharmaceutical Sciences. This volume, as a result, comprises 34 papers presented at the symposium by specialists in various branches of chromatography and electrophoresis.

The proceedings, providing general reviews on chromatography and electrophoresis, cover a wide range of potential applications of these techniques. Of particular interest are the studies concerning identification of drugs, drug metabolites and pollutants, whilst other investigations are concerned with the identification of endogenous metabolites in living organisms. In addition, the medical applications of chromatography and electrophoresis for diagnostic purposes are presented. These techniques will undoubtedly become a necessary tool in every major hospital.

This work, reflecting current developments in the use of chromatography and electrophoresis, will be of value to research workers in chemistry, biochemistry, medicine, toxicology, drug metabolism, forensic science, clinical chemistry and pollution studies.

March 1979 x + 358 pages US $58.50/Dfl. 120.00 ISBN 0-444-41785-0

ELSEVIER

P.O. Box 211,
1000 AE Amsterdam
The Netherlands

52 Vanderbilt Ave
New York, N.Y. 10017

The Dutch guilder price is definitive. US $ prices are subject to exchange rate fluctuations.

7135

ELECTROANALYSIS IN HYGIENE ENVIRONMENTAL, CLINICAL and PHARMACEUTICAL CHEMISTRY

Proceedings of a Conference organised by t Electroanalytical Group of the Chemical Socie London, held at Chelsea College, University London, U.K., 17-20 April, 1979.

edited by W. FRANKLIN SMYTH, Chels College, University of London, U.K.

ANALYTICAL CHEMISTRY SYMPOSIA SERIES 2

The proceedings of this international conference comprise 39 papers, principally concerned wi how potentiometric and voltammetric methods of electroanalysis are used to solve a wide ran of analytical problems in the fields of clinical chemistry, hygiene, pharmacy, pharmacology a environmental chemistry.

Although the papers reflect the many topics under discussion certain themes predominate. The include investigation of the actual electrochemical techniques and instrumentation, the importan of the mechanism of the electrochemical reaction at the chosen indicator electrode in optimisi the electroanalytical 'finish', and direct, rapid and sensitive measurement in complex biologic matrices. The results on the determination of inorganic, organic and organometallic substanc in complex matrices such as body fluids, factory air and the aqueous environment are also d cussed. On-line analysis with and without a prior separation process, speciation studies by t application of 'cold' electroanalytical methods and details of novel electrode construction, instr mental design and analytical methods complete the discussion.

SELECTED CONTENTS: **Plenary Lectures.** New Ion Selective Electrodes and Their Clinical and Biological Application *(D. Amman, H.-B. Jenny, P. C. Meier and W. Simon)*. Polarographic Analysis of Nucleic Acids *(E. Palaček)*. Electrochemical Gas Monitors in Occupational Hygiene *(I. Bergman)*. Electroanalytical Applications in Pharmacy and Pharmacology *(G. J. Patriarche and J.-C. Vire)*. Stripping Voltammetry of Molecules of Pharmaceutical Importance *(W. Franklin Smyth)*. A Critical Assessment of the Voltammetric Approach for the Study of Toxic Trace Metals in Biological Specimens *(H. W. Nürnberg)*. Polarographic Analysis of Pesticides in Food Products *(J. Davidék)*. **Keynote Lectures.** Design Principles and Behaviour of Sensitive Calcium Ion-Selective Electrodes *(G. J. Moody and J. D. R. Thomas)*. The Determination of Radiation Damages in Native DNA by Single Sweep Voltammetry *(J. M. Sequaris and P. Valenta)*. The Importance of Measuring Oxidation-Reduction Systems in Clinical Research *(J. Chayen)*. Determination of Mercury in Urine by Potentiometric Stripping Analysis *(D. Jagner and K. Ärén)*. Differential Pulse Polarographic Determination of Drugs in Pharmaceutical Formulations *(E. Jacobsen)*. Trace Level Polarographic Analysis of Drugs in Body Fluids *(M. A. Brooks)*. Electrochemical Approaches to Environmental Pollution Control *(S. das Gupta, B. Fleet and I. F. T. Kennedy)*. Electroanalysis of Economic Poisons *(J. Osteryoung, J. W. Whittaker and M. R. Smyth)*.

CONTRIBUTORS OF OTHER PAPERS:

A. Apoteker, C. H. P. Bruins, K. Brunt, J. S. Burnicz, A. Catterall, I. E. Davidson, D. A. Doornbos, N. M. Fayad, Zs. Feher, A. G. Fogg, J. P. Hart, A. Ivaska, V. J. Jennings, D. B. Kell, V. R. Krishnan, H. P. van Leeuwen, K. Ohzeki, E. Pungor, S. Jayarama Reddy, R. C. Rooney, T. Rydström, R. Samuelsson, E. Schumacher, W. James Scott, R. J. Simpson, R. Sternberg, G. Svehla, Y. M. Temerk, D. R. Thévenot, K. Toth, F. Umland, Y. Vaneesorn, A. Watson, P. D. J. Weitzman.

1979 xii + 464 pages US $ 70.75 / Dfl. 145.00 ISBN 0-444-41850-4

ELSEVIER

P.O. Box 211, Amsterdam
The Netherlands
52 Vanderbilt Ave
New York, N.Y. 10017

The Dutch guilder price is definitive. US $ prices are subject to exchange rate fluctuations.

(continued from outside of cover)

Short Communications

VOL. 113 No. 2 ANALYTICA CHIMICA ACTA JANUARY 15, 1980

CONTENTS

(continued on inside page of cover)

Printed in The Netherlands.